ZooKeys 899: 1–36 (2019)
doi: 10.3897/zookeys.899.46779
http://zookeys.pensoft.net

RESEARCH ARTICLE

A peer-reviewed open-access journal
ZooKeys
Launched to accelerate biodiversity research

DNA barcoding reveals a species group of the genus *Campiglossa* (Diptera, Tephritidae, Tephritinae) with recognition of a new species from East Asia and previously unknown females of *Campiglossa coei* (Hardy)

Ho-Yeon Han[1], Kyung-Eui Ro[1]

1 *Division of Biological Science and Technology, College of Science and Technology, Yonsei University, 1 Yonsei-dae-gil, Wonju-si, Gangwon-do 26493, South Korea*

Corresponding author: *Ho-Yeon Han* (hyhan@yonsei.ac.kr)

Academic editor: *M. De Meyer* | Received 23 September 2019 | Accepted 14 November 2019 | Published 12 December 2019

http://zoobank.org/C2944B70-E212-421A-94A9-B0AB70B991C0

Citation: Han H-Y, Ro K-E (2019) DNA barcoding reveals a species group of the genus *Campiglossa* (Diptera, Tephritidae, Tephritinae) with recognition of a new species from East Asia and previously unknown females of *Campiglossa coei* (Hardy). ZooKeys 899: 1–36. https://doi.org/10.3897/zookeys.899.46779

Abstract

While analyzing DNA barcodes of all the Korean and some East Asian tephritid species in conjunction with the barcode sequences available from BOLD Systems (www.boldsystems.org), the large and taxonomically enigmatic genus *Campiglossa* was recovered as a monophyletic clade, together with the genera *Dioxyna* and *Homoeotricha*, which are here synonymized for that reason. Ten major lineages are also recognized within the *Campiglossa* clade: *producta* group, *loewiana* group, *sororcula* group, *irrorata* group, *achyrophori* group, *difficilis* group, *luxorientis* group, *magniceps* group, *arisanica* group, and *misella* group. Here, more detailed taxonomic accounts are provided for the *misella* group, including four DNA analysis-recovered members: *C. coei*, *C. misella*, *C. paramelaena* **sp. nov.**, and *C. melaena*. A single morphological synapomorphy is proposed for this species group: the presence of a large mid-anterior dark wing marking in males with associated structural modification (more apically positioned crossvein R-M than in females). Based on the morphological characteristics, two presumptive members that are only known from male specimens are further recognized: *C. pishanica* and *C. propria* from China. A full description of *C. paramelaena* **sp. nov.**, and a redescription of *C. coei*, for which only males were previously known, are provided. For all the included species, a taxonomic key, diagnoses, and photographs to aid their accurate identification are given. Finally, *C. favillacea* is synonymized with *C. coei* and *C. roscida* with *C. misella*, and *C. coei* and *C. pishanica* resurrected from the synonymy of *C. misella*.

Keywords
Campiglossa, *Dioxyna*, *Homoeotricha*, *misella* group, Tephritini

Introduction

Tephritidae is a relatively recently diverged fly family that might have arisen around the Late Eocene (~36 mya; Han and Ro 2016). Currently, this family includes approximately 4,700 valid species under ca. 500 genera, seven of which are species-rich (i.e., over 100 species) genera (Norrbom et al. 1999; Catalogue of Life as of Aug. 2019 – http://www.catalogueoflife.org). These highly diverged genera are notorious for harboring a number of species complexes that are taxonomically difficult to deal with (White 2006; Drew and Romig 2013).

The genus *Campiglossa* Rondani, 1870, is one of those species-rich genera, and is estimated to have approximately 200 described species (White 1988; Norrbom et al. 1999; Catalogue of Life as of Aug. 2019). *Campiglossa* is a predominantly Palaearctic genus but a significant number of representative species occur in all the other zoogeographical regions. The majority of species of known biology are associated with the capitula of composite plants (family Asteraceae) (White 1988). The members of this genus have often been treated either as *Campiglossa* or *Paroxyna* in the past, but Norrbom et al. (1999) did not find any clear distinction between these two genera and, thus, regarded them as a single genus, *Campiglossa*. In the present study, we also synonymize the genera *Dioxyna* Frey, 1945, and *Homoeotricha* Hering, 1944, with the genus *Campiglossa*.

Due to their high intra-specific variation, low inter-specific variation, sexual dimorphism and seasonal variation, systematic investigation of *Campiglossa* is considered very difficult (A. Freidberg, V. Korneyev, S. Masahiro, B. Merz, pers. comm.). Examination of their male and female postabdominal structure has been somewhat helpful for defining species and species groups (White 1988; Korneyev 1990, 1997; Merz 1994; Korneyev and Ovchinnikova 2004). Obtaining host associated specimens has also been useful for understanding their intra- and interspecific variation (Merz 1994; Han 2019). Most recently, DNA barcoding has proven useful for identifying tephritid species and species groups, as well as confirming generic limits (Smit et al. 2013, Barr et al. 2018).

In the process of analyzing DNA barcodes of all the Korean and some East Asian tephritid species in conjunction with the barcode sequences available from BOLD Systems (www.boldsystems.org), we recovered the genus *Campiglossa* as a monophyletic clade together with the genera *Dioxyna* and *Homoeotricha*. We also recognized ten major lineages within the *Campiglossa* clade, each of which can be regarded as a monophyletic species group. In this study, we provide more detailed taxonomic accounts for the *misella* group, including four DNA analysis-recovered members: *C. coei* (Hardy, 1964), *C. misella* (Loew, 1869), *C. paramelaena* sp. nov., and *C. melaena* (Hering, 1941). Based on the morphological characteristics, we further recognize two presumptive members that are only known from male specimens: *C. pishanica* (Wang, 1996) and *C. propria* (Chen, 1938) from China. We provide a full description of *C. paramelaena*

sp. nov., and a redescription of *C. coei*, for which only males were previously known. For all included species, we provide a taxonomic key, diagnoses, and photographs to aid their accurate identification.

Materials and methods

The terminology and morphological interpretations used in this study follow the glossary of White et al. (1999). A total of 12 ratios are used in the descriptions: head ratio (head length excluding the antennae in lateral view/head height); frons-head ratio (narrowest width of frons in dorsal view/width of head); eye ratio (shortest eye diameter/longest eye diameter); gena-eye ratio (genal height/longest eye diameter) - genal height is the distance between ventral eye margin and ventral genal margin anterior to genal seta (gena measured with head tilted slightly dorsally so that gena is at its broadest); antenna-head ratio (antenna length measured from scape to flagellomere 1/head height); arista-antenna ratio (arista length/antenna length); wing-thorax ratio (wing length from tegula to apex of vein R_{4+5}/thorax length in dorsal view); wing ratio (wing length/wing width); vein M ratio (distance along vein M between crossveins R-M and DM-Cu/distance between crossveins R-M and BM-Cu); subcosta-costa ratio (distance along vein C of subcostal cell/costal cell); cell r_1-r_{2+3} ratio (distance along vein C of cell r_1/cell r_{2+3}); cell r_{4+5}-r_{2+3} ratio (distance along vein C of cell r_{4+5}/cell r_{2+3}).

The molecular methods follow Han and Ro (2016, 2018). For our analysis, 765 base pair fragments of the mitochondrial COI gene sequences (the DNA barcode region) were newly obtained from 55 specimens representing 26 species of the genus *Campiglossa*. The collection and voucher data, and GenBank accession numbers (MN445522–MN445576) are presented in Table 1. We used the same PCR and sequencing primers listed in Han and Ro (2016). We analyzed these sequences plus a number of the sequences downloaded from BOLD Systems (www.boldsystems.org, as of Jan. 2019). A neighbor-joining (NJ) analysis (Saitou and Nei 1987) was performed in MEGA version X (Kumar et al. 2018) using the Kimura 2-parameter model of nucleotide substitution (Kimura 1980). A maximum-likelihood (ML) analysis was also performed in MEGA X using the general time reversible model (Nei and Kumar 2000). The reliability of clustering patterns in the ML tree was determined by the bootstrap test (Felsenstein 1985; 2,000 replications). Bayesian inferences (BI) were conducted using MrBayes v3.0b4 (Huelsenbeck and Ronquist 2001) by Markov chain Monte Carlo (MCMC) sampling for two million generations, with tree sampling every 100 generations and a burn-in of 1,000 trees. The BI analyses were run twice using different random starting trees to evaluate the congruence of the likelihood values and posterior clade probabilities (Huelsenbeck et al. 2002). Additional details of the molecular analyses are mentioned in the appropriate section.

Photographs of pinned specimens were captured with a Panasonic (Osaka, Japan) DMC G5 camera with a Panasonic Lumix 45–175 mm lens and a Raynox (Yoshida Inc., Tokyo, Japan) MSN-202 macro conversion lens. The consecutive digital images in different focal planes (usually 50–100 shots per a single figure) were Z-stacked us-

Table 1. The collection and voucher information for the *Campiglossa* flies sequenced for the DNA barcoding analysis. The status of the voucher specimens and the GenBank accession numbers are indicated in parentheses.

C. absinthii (Fabricius, 1805)	1. ♂, KOREA: Gangwon-do, Jeongseon-gun, Nam-myeon, Mt. Mindungsan, from Yupyeong-ri to 1,119 m peak, 37°16'15"N, 128°46'30"E, 4.VIII.2005, H.-Y. Han et al. (both wings glued on a rectangular card; YSUW090915027; GenBank Acc. Nr. MN445522).
	2. ♀, KOREA: Gangwon-do, Jeongseon-gun, Nam-myeon, Mt. Mindungsan, from Yupyeong-ri to 1,119 m peak, 37°16'15"N, 128°46'30"E, 24.VII.2005, H.-Y. Han et al. (both wings glued on a rectangular card; YSUW090915028; GenBank Acc. Nr. MN445523).
	3. ♀, RUSSIA: Primorsky-Krai, Khasansky-District, Barabash, 43°10'46.9"N, 131°28'20.0"E, 22.VI.2008, H.Y. Han & H.S. Lee (specimen with the abdomen detached; YSUW140201102; GenBank Acc. Nr. MN445524).
C. achyrophori (Loew, 1869)	1. ♀, SWITZERLAND: Valais 1787–2041 m, Pointe de Bellevue, Morgins, 28.VII.2004, H.-Y. Han & K.-E. Ro (specimen with the abdomen detached; YSUW140201037; GenBank Acc. Nr. MN445525).
C. albiceps (Loew, 1873)	1. ♂, USA: North Carolina, Haywood Co, Great Smoky Mountains National Park, in meadow 250 m N of house at Purchase Knob, 1444 m (both wings glued on a rectangular card; YSUW090915005; GenBank Acc. Nr. MN445526).
C. bidentis (Robineau-Desvoidy, 1830), comb. nov. from *Dioxyna*	2. ♂, KOREA: Gangwondo, Jeongseon, Nammyeon, Mt. Mindungsan, from Yupyeongri to 1,119 m peak, 37°16'15"N, 128°46'30"E, 16.VII.2005, H.-Y. Han et al. (specimen with the abdomen detached; YSUW130901095; GenBank Acc. Nr. MN445527).
	3. ♀, KOREA: Gyeongsangbuk-do, Bonghwa Myeongho-myeon, Mt. Cheongnyangsan, 29.IX.2007, Coll. H.-S. Lee et al., ex *Bidens biternata* (Lour.) flower, em. 3–12.X.2007 (specimen with the abdomen detached; YSUW130901096; GenBank Acc. Nr. MN445528).
C. coei (Hardy, 1964)	1. ♂, CHINA: Yunnan, Mengsong, Manlvcunhanzudazhai, small hilltop, 22°07'44.0"N, 100°28'51.7"E, 1690 m, 12.VII.2011, H.-Y. Han & S.-W. Suk (specimen with the abdomen detached; YSUW 130901058; GenBank Acc. Nr. MN445530).
	2. ♀, CHINA: Yunnan, Mengsong, Bengangxizhai, in forest, 22°10'34.5"N, 100°35'06.8"E, 1725 m, 11.VII.2011, H.-Y. Han & S.-W. Suk (specimen with the abdomen detached; YSUW 130901059; GenBank Acc. Nr. MN445531).
	3. ♂, CHINA: Yunnan, Mengsong, Manlvcunhanzudazhai, small hilltop, 22°07'44.0"N, 100°28'51.7"E, 1690 m, 12.VII.2011, H.-Y. Han & S.-W. Suk (specimen with the abdomen detached; YSUW YSUW140201034; GenBank Acc. Nr. MN445532).
	4. ♀, CHINA: Yunnan, Mengsong, Manlvcunhanzudazhai, small hilltop, 22°07'44.0"N, 100°28'51.7"E, 1690 m, 12.VII.2011, H.-Y. Han & S.-W. Suk (specimen with the abdomen detached; YSUW 140201035 6; GenBank Acc. Nr. MN445533).
C. deserta (Hering, 1939)	1. ♂, KOREA: Gangwon-do, Pyeongchang-gun, Doam-myeon, Hoenggye-ri, Daegwallyeong Samyang pasture, col. 7.X.2004, em. 1–21.VI.2005, ex *Aster* sp., flower, H.-Y. Han & H.-W. Byun (both wings glued on a rectangular card; YSUW090915029; GenBank Acc. Nr. MN445534).
	2. ♀, KOREA: Gangwon-do, Jeongseon-gun, Gohan-eup, Mt. Hambaeksan, Recreation forest to Manhang-jae, col. 10.X.2003, em. 24–31.V.2004, ex *Aster ciliosus* Kitamura ?, flower, H.-Y. Han & K.-E. Ro (both wings glued on a rectangular card; YSUW090915030; GenBank Acc. Nr. MN445535).
	3. ♀, RUSSIA: Primorsky-Krai, Nadezhdinsky-District, Vol'no-Nadezhdinskoye, 43°22'31.6"N, 132°01'43.1"E, 22.VI.2008, Coll. H.-Y. Han & H.-S. Lee (specimen with the abdomen detached; YSUW140201103; GenBank Acc. Nr. MN445536).
	1. ♀, KOREA: Gangwon-do, Jeongseon-gun, Nam-myeon, Mt. Mindungsan, from Yupyeong-ri to 1,119 m peak, 37°16'15"N, 128°46'30"E, col. 6.X.2001, em. 24–26.X.2001, ex *Lactuca indica* var. *laciniata* flower, H.-Y. Han et al. (both wings glued on a rectangular card; YSUW08100129; GenBank Acc. Nr. MN445537).
	2. ♀, KOREA: Jeju-do, Jeju-si, Aewol-eup, along rt 1117, col 19.X.2005, em. 23–31.X.2005, ex *Lactuca indica* var. *laciniata* flower, H.-Y. Han et al. (both wings glued on a rectangular card; YSUW08100130; GenBank Acc. Nr. MN445538).
C. difficilis (Hendel, 1927)	1. ♂, SWITZERLAND: Valais 1689–1950 m, Portes du Soleil, Morgins, 27.VII.2004, H.-Y. Han & K.-E. Ro. (specimen with the abdomen detached; YSUW140201038; GenBank Acc. Nr. MN445539).
C. guttella (Rondani, 1870)	1. ♀, SWITZERLAND: Valais 1787–2041 m, Pointe de Bellevue, Morgins, 28.VII.2004, H.-Y. Han & K.-E. Ro (specimen with the abdomen detached; YSUW140201039; GenBank Acc. Nr. MN445540).

C. hirayamae (Matsumura, 1916)	1. ♀, KOREA: Gangwon-do, Jeongseon-gun, Nam-myeon, Mt. Mindungsan, from Yupyeong-ri to 1,119 m peak, 37°16'15"N, 128°46'30"E, 24.VI.2005, Han et al. (both wings glued on a rectangular card; YSUW06010914; GenBank Acc. Nr. MN445541).
	2. ♂, KOREA: Gangwon-do, Pyeongchang-gun, Yongpyeon-myeon, S. Valley of Mt. Gyebangsan, 3.X.2003, H.-Y. Han et al. (both wings glued on a rectangular card; YSUW08100131; GenBank Acc. Nr. MN445542).
	3. ♀, KOREA: Gyeongsangbuk-do, Yeongju-si, Sunheung-myeon, Mt. Sobaeksan, Choamsa to Gukmangbong (1421 m), 27.V.2005, H.-W. Byun (both wings glued on a rectangular card; YSUW08100132; GenBank Acc. Nr. MN445543).
C. loewiana (Hendel, 1927)	1. ♀, MONGOLIA: Tuv Prov., Tusgalt Valley, Forestry Research-Training Center, Ntn. Univ. of Mongolia, 48°15'37"N 106°51'11"E, 1277 m, 4.VII.2013, H.Y. Han & H.S. Lee (specimen with the abdomen detached; YSUW140201075; GenBank Acc. Nr. MN445544).
	2. ♂, MONGOLIA: Tuv Prov., Tusgalt Valley, Forestry Research-Training Center, Ntn. Univ. of Mongolia, 48°15'37"N 106°51'11"E, 1277 m, 4.VII.2013, H.Y. Han & H.S. Lee (specimen with the abdomen detached; YSUW140201076; GenBank Acc. Nr. MN445545).
	3. ♂, MONGOLIA: Tuv Prov., Tusgalt Valley, Forestry Research-Training Center, Ntn. Univ. of Mongolia, 48°15'23"N, 106°50'23"E, 1522 m, 5.VII.2013, H.Y. Han & H.S. Lee (specimen with the abdomen detached; YSUW140201081; GenBank Acc. Nr. MN445546).
C. longipennis Shiraki, 1933, comb. nov. from *Homoeotricha*	1. ♂, RUSSIA: Sakhalin, Yuzhno-Sakhalinsk Vestochka, 46°51'58.3"N, 142°50'54.9"E, 18.VII.2008, H.Y. Han & H.S. Lee (specimen with the abdomen detached; YSUW090915062; GenBank Acc. Nr. MN445547).
C. luxorientis (Hering, 1940)	1. ♀, KOREA: Gangwon-do, Jeongseon-gun, Nam-myeon, Mt. Mindungsan, from Yupyeong-ri to 1,119 m peak, 37°16'15"N, 128°46'30"E, 29.VIII.2005, H.-Y. Han et al. (both wings glued on a rectangular card; YSUW090915035; GenBank Acc. Nr. MN445548).
	2. ♂, KOREA: Gangwon-do, Jeongseon-gun, Nam-myeon, Mt. Mindungsan, from Yupyeong-ri to 1,119 m peak, 37°16'15"N, 128°46'30"E, 29.VIII.2005, H.-Y. Han et al. (both wings glued on a rectangular card; YSUW090915036; GenBank Acc. Nr. MN445549).
C. melaena (Hering, 1941)	1. ♂, RUSSIA: Primorsky-Krai, Khasansky-District, Barabash, 43°10'46.9"N, 131°28'20.0"E, 22.VI.2008, H.Y. Han & H.S. Lee (specimen with the abdomen detached; YSUW140201105; GenBank Acc. Nr. MN445560).
	2. ♂, RUSSIA: Primorsky-Krai, Nadezhdinsky-District, Vol'no-Nadezhdinskoye, N43°22'31.6", E132°01'43.1", 22.VI.2008, H.-Y. Han & H.-S. Lee (specimen with the abdomen detached; YSUW140201106; GenBank Acc. Nr. MN445561).
C. melanochroa (Hering, 1941)	1. ♀, KOREA: Gangwon-do, Jeongseon-gun, Nam-myeon, Mt. Mindungsan, from Yupyeong-ri to 1,119 m peak, 37°16'15"N, 128°46'30"E, col. 6.X.2001, em. 26–30.X.2001, ex *Aster ageratoides* Turcz. flower, H.-Y. Han et al. (both wings glued on a rectangular card; YSUW090915039; GenBank Acc. Nr. MN445554).
	2. ♂, KOREA: Gangwon-do, Jeongseon-gun, Nam-myeon, Mt. Mindungsan, from Yupyeong-ri to 1,119m peak, 37°16'15"N, 128°46'30"E, col. 25.IX.2003, em. 13–20.IX.2003, ex *Aster tataricus* L. flower, H.-Y. Han et al. (both wings glued on a rectangular card; YSUW090915040; GenBank Acc. Nr. MN445555).
C. messalina (Hering, 1937)	A1. ♂, KOREA: Gangwon-do, Pyeongchang-gun, Yongpyeon-myeon, S. Valley of Mt. Gyebangsan, 5.VIII.2005, H.-Y. Han & H.-S. Lee (both wings glued on a rectangular card; YSUW08100133; GenBank Acc. Nr. MN445550).
	A2. ♀, KOREA: Gangwon-do, Jeongseon-gun, Gohan-eup, Mt.Hambaeksan, Recreation Forest to Manhang-jae, col. 10.X.2003, em 3–6.V.2004 ex *Artemisia* sp. flower, H.-Y. Han & K.-E. Ro (both wings glued on a rectangular card; YSUW08100134; GenBank Acc. Nr. MN445551).
	B1. ♂, KOREA: Gangwon-do, Jeongseon-gun, Gohan-eup, Mt.Hambaeksan, Recreation forest to Manhang-jae, col.10.X.2003, em. 3–6.V.2004, ex *Artemisia* sp. flower, H.-Y. Han & K.-E. Ro (both wings glued on a rectangular card; YSUW090915037; GenBank Acc. Nr. MN445552).
	B2. ♀, KOREA: Gangwondo, Jeongseon, Nammyeon, Mt. Mindungsan, from Yupyeongri to 1,119 m peak, 37°16'15"N, 128°46'30"E, 29.VIII.2005, H.-Y. Han et al. (both wings glued on a rectangular card; YSUW090915038; GenBank Acc. Nr. MN445553).
C. misella (Loew, 1869)	1. ♀, HUNGARY: Bdaors, Odvas hg., 18.VI.1991, Merz & Adams (both wings glued on a rectangular card; YSUW94082638; GenBank Acc. Nr. MN445556).

C. misella (Loew, 1869)	2. ♀, SWITZERLAND: Valais, Leuk-Rotafen, 46°18'59"N, 7°40'18"E, 640 m, 22.VII.2004, H.-Y. Han & K.-E. Ro (specimen with the abdomen detached; YSUW130901215; GenBank Acc. Nr. MN445557).
	3. ♂, SWITZERLAND: Valais, Leuk-Rotafen, 46°18'59"N, 7°40'18"E, 640 m, 22.VII.2004, H.-Y. Han & K.-E. Ro (specimen with the abdomen detached; YSUW140201041; GenBank Acc. Nr. MN445558
	4. ♀, SWITZERLAND: Valais, Visperterminen-Kreuz, 46°15'17"N, 7°53'52"E, 1500 m, 21.VII.2004, H.-Y. Han & K.-E. Ro (specimen with the abdomen detached; YSUW140201042; GenBank Acc. Nr. MN445559).
C. paramelaena sp. nov.	1. Holotype ♂, KOREA: Gyeongsangbuk-do, Bonghwa-gun, Myeongho-myeon, Mt. Cheongnyangsan, 36°46'43.6"N, 128°55"30.8'E, 600 m, 30.VI.2007, H.Y. Han et al. (specimen with the abdomen detached; YSUW090915094; GenBank Acc. Nr. MN445564).
	2. Paratype ♀, RUSSIA: Primorsky-Krai: between Chernyatino and Pokrovk, 43°57'32.7"N, 131°32'24.1"E, 55 m, 26.VI.2008, H.Y. Han & H.S. Lee (both wings glued on a rectangular card; YSUW090915019; GenBank Acc. Nr. MN445565).
	3. Paratype ♂, RUSSIA: Khasansky-District, Kedrovaya Pad, 43°05'09.4"N, 131°35'06.0"E, 22m, 23.VI.2008, H.Y. Han & H.S. Lee (specimen with the abdomen detached; YSUW140201108; GenBank Acc. Nr. MN445566). Paratype.
	4. Paratype ♀, RUSSIA: Khasansky-District, Barabash, 43°10'46.9"N 131°28'20.0"E, 61m, 22.VI.2008, H.Y. Han & H.S. Lee (specimen with the abdomen detached; YSUW090915068; GenBank Acc. Nr. MN445567). Paratype.
C. producta (Loew, 1844)	1. ♀, ISRAEL, Golan Heights, Mt. Hermon, 2000 m, 29.V.2000, H.-Y. Han & K.-E. Ro (specimen with the abdomen detached; YSUW130901194; GenBank Acc. Nr. MN445568).
C. quadriguttata (Hendel, 1927)	1. ♂, KOREA: Gangwon-do, Jeongseon-gun, Nam-myeon, Mt. Mindungsan, from Yupyeongri to 1,119 m peak, 37°16'15"N, 128°46'30"E, 19.VII.2005, H.-Y. Han et al. (specimen with the abdomen detached; YSUW090915089; GenBank Acc. Nr. MN445569).
	2. ♀, KOREA: Gangwon-do, Pyeongchang-gun, Yongpyeon-myeon, S. Valley of Mt. Gyebangsan, 3.X.2003, H.-Y. Han et al. (specimen with the abdomen detached; YSUW090915090; GenBank Acc. Nr. MN445570).
C. sabroskyi (Novak, 1974)	1. ♂, USA: Utah: Grand Co., La Sal Mt. Warner Lake, 7.IX.1992, A.L. Norrbom, ex flower of *Senecio* sp. (1♂, 1♀ from same collecting lot; HAN115; GenBank Acc. Nr. MN445529).
C. shensiana (Chen, 1938)	1. ♂, KOREA: Gangwon-do, Wonju-si, Gwirae-myeon, Unnam-ri, col. 13.X.2001, em. 2–16.V.2002, ex *Chrysanthemum boreale*, flower, D.-S. Choi et al. (both wings glued on a rectangular card; YSUW090915041; GenBank Acc. Nr. MN445571).
	2. ♀, KOREA: Gangwondo, Jeongseon, Nammyeon, Mt. Mindungsan, from Yupyeongri to 1,119m peak, 37°16'15"N, 128°46'30"E, col. 6.X.2001, em 9.V.2002, ex *Chrysanthemum makinoi*, flower, H.-Y. Han et al. (both wings glued on a rectangular card; YSUW090915042; GenBank Acc. Nr. MN445572).
	3. ♀, KOREA: Gangwon-do, Samcheok-si, Geunsan-dong, Mt. Geunsan, 37°24'28"N, 129°8'9"E, 4.V.2012, H.-Y. Han et al. (specimen with the abdomen detached; YSUW130901200; GenBank Acc. Nr. MN445573).
C. sororcula (Wiedemann, 1830), comb. nov. from *Dioxyna*	4. ♀, JAPAN: Kyushu, Kagoshima-shi, Hirakawa-cho, Goino, 31°27'53"N 130°30'01"E, 66 m, 10.VII.2010 H.-Y. Han & S.-W. Suk (specimen with the abdomen detached; YSUW130901083; GenBank Acc. Nr. MN445574).
	5. ♀, MALAWI: Nyika National Park, Chelinda, 15kmW, 10°35.036'S 33°44.096'E, 2234 m, 31.XII.2009, H.-Y. Han (specimen with the abdomen detached; YSUW130901145; GenBank Acc. Nr. MN445575).
C. sp. near *guttella*	1. ♀, MONGOLIA: Tuv Prov., Tusgalt Valley, Forestry Research-Training Center, Ntn. Univ. of Mongolia, 48°15'23"N, 106°50'23"E, 1522 m, 5.VII.2013, H.Y. Han & H.S. Lee (specimen with the abdomen detached; YSUW140201077; GenBank Acc. Nr. MN445562).
	2. ♂, MONGOLIA: Tuv Prov., Tusgalt Valley, Forestry Research-Training Center, Ntn. Univ. of Mongolia, 48°15'23"N, 106°50'23"E, 1522 m, 5.VII.2013, H.Y. Han & H.S. Lee (specimen with the abdomen detached; YSUW140201082; GenBank Acc. Nr. MN445563).
C. spenceri (Hardy, 1973)	1. ♂, VIETNAM: Lam Dong Prov., Mt. Lang Biang, N of DaLat, 12°02'50.1"N 108°26'26.5"E, 12.XII.2013, H.Y. Han et al. (specimen with the abdomen detached; YSUW140201110; GenBank Acc. Nr. MN445576).

ing Helicon Focus software (Helicon Soft, Ltd., Kharkov, Ukraine). Photographs of live specimens (kept in a glass cage) were taken with a Nikon (Tokyo, Japan) D7000 camera with a macro lens and extension tubes. Photographs of postabdominal structures were taken with a Nikon (Tokyo, Japan) D90 camera mounted on an Olympus (Tokyo, Japan) CX41 compound microscope.

Most of the specimens used in this study are deposited in the Division of Biological Science and Technology, Yonsei University, Wonju, Korea (**YSUW**), and some in the National Institute of Biological Resources, Incheon, Korea (**NIBR**). Abbreviations of the other institutions mentioned in the text are as follows:

NHMUK The Natural History Museum, Department of Entomology, London, England, UK;
IZAS Institute of Zoology, Academia Sinica, Insect Collection, Beijing, China;
NIAS Laboratory of Insect Systematics, National Institute of Agro-Environmental Sciences, Tsukuba, Japan;
UOPJ Entomological Laboratory, University of Osaka Prefecture, Osaka, Japan;
ZMHU Museum fur Naturkunde der Humboldt Universitat zu Berlin, Bereich Zoologisches Museum, Berlin, Germany.

Results and discussion

DNA barcoding and species group recognition

The genus *Campiglossa* is a morphologically homogeneous taxon, and their monophyly has been suggested based on at least two possible synapomorphies: the elongated proboscis and the spinulose phallic preglans area (Korneyev 1999). The published and our present DNA barcoding analyses also indicate that they form a monophyletic group, but together with at least two other genera, *Dioxyna* and *Homoeotricha*.

Smit et al. (2013) performed a DNA barcoding analysis of approximately half of the European tephritids species (42 genera, 135 species, 555 specimens), of which 12 *Campiglossa* and a single *Dioxyna* species were included. In their neighbor-joining tree, five sequences of *Dioxyna bidentis* (Robineau-Desvoidy, 1830) were strongly clustered (90 % bootstrap support) with all other *Campiglossa* sequences, indicating that the genus *Campiglossa* is monophyletic and that *Dioxyna* is merely an aberrant member of *Campiglossa*.

As a result of our ongoing DNA barcoding study of the family Tephritidae, we assembled a large dataset of 7,223 individuals, 543 species, and 80 genera publicly available from BOLD systems (www.boldsystems.org), as well as our own dataset of 55 individuals and 26 *Campiglossa* species. The combined dataset contained 7,278 individuals, 543 species and 80 genera. Our simple neighbor-joining analysis recovered a monophyletic cluster of the genera *Campiglossa*, *Dioxyna*, and *Homoeotricha* together (only this portion of the tree is shown in Fig. 1), indicating that the latter two genera

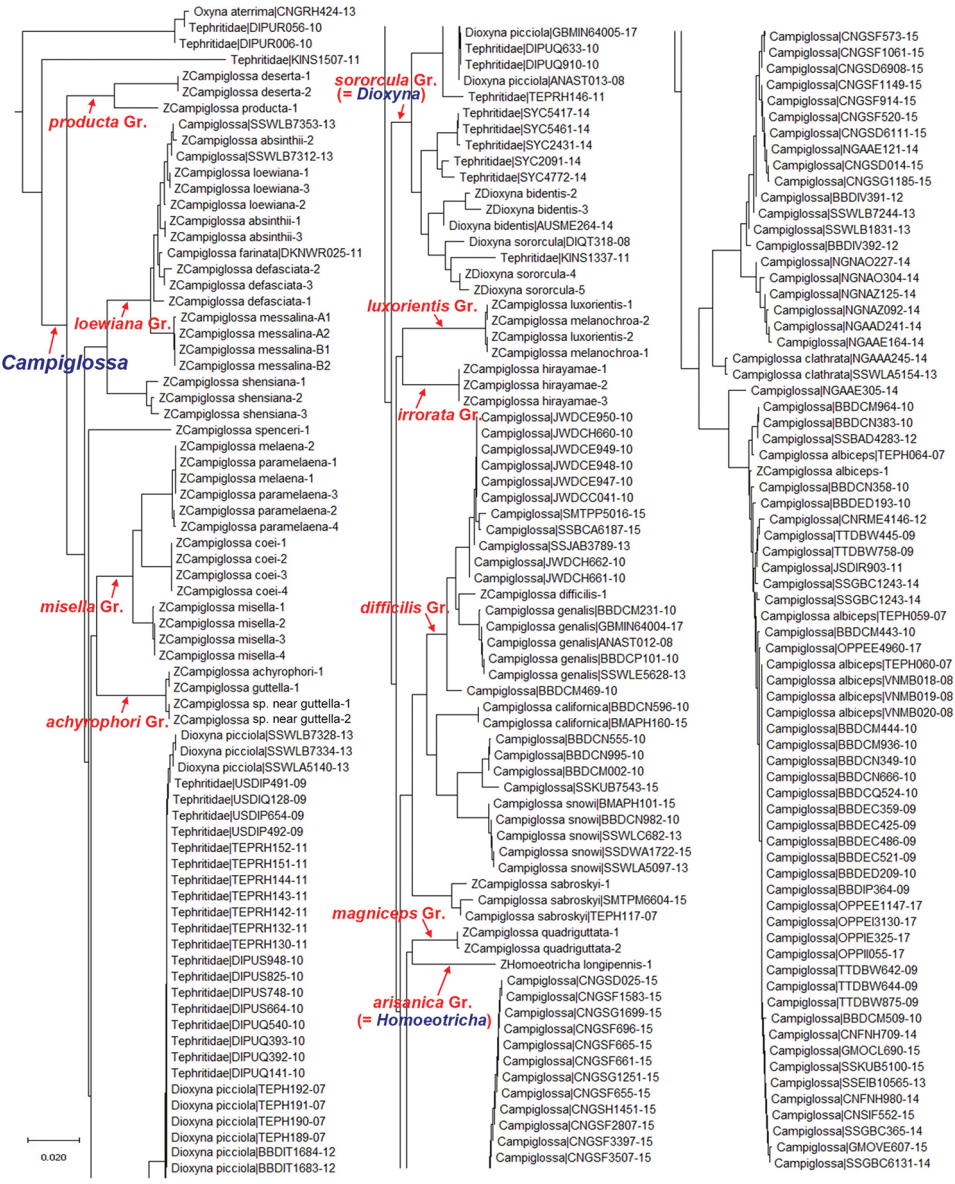

Figure 1. The genus *Campiglossa* portion of the neighbor-joining tree based on the Kimura 2-parameter distances of 7,223 tephritid DNA barcode sequences mostly extracted from BOLD Systems (www.boldsystems.org, as of Jan 2019), including 55 newly obtained *Campiglossa* sequences (names prefixed with Z). All 211 *Campiglossa*, *Homoeotricha*, and *Dioxyna* (regarded to be the genus *Campiglossa*, *sensu lato*, in this study) sequences were recovered as a monophyletic clade in this analysis. Putative species group names (in red) are marked on the respective branches.

should be merged within the genus *Campiglossa*, which has a nomenclatorial seniority. For an updated analysis (Han and Ro, in preparation) of our earlier molecular phylogenetic study of the subfamily Tephritinae (Han et al. 2006), we greatly increased our

taxon sampling to include the majority of the *Campiglossa* genus group genera (sensu Norrbom et al. 1999). Our unpublished preliminary molecular analysis grouped the above three genera together, separated from the other closely related genera (i.e., *Desmella* Munro, 1957; *Mesoclanis* Munro, 1938; *Oxyna* Robineau-Desvoidy, 1830; *Scedella* Munro, 1957; and *Tanaica* Munro, 1957), again supporting the expanded concept of the genus *Campiglossa*.

We also analyzed a scale-down dataset of 32 species and 76 individuals of the genus *Campiglossa* as well as four species and ten individuals of the genus *Tephritis* that is known to be closely related to *Campiglossa* (Norrbom et al. 1999; Korneyev 1999; Merz 1999; Han et al. 2006). These *Tephritis* sequences were used as an outgroup to root the ingroup taxa. Our maximum-likelihood tree (Fig. 2), even though lacking high statistical support on deeper phyletic branches, recognized the following ten major lineages within the *Campiglossa* clade, each of which can be regarded as a monophyletic species group. Recognizing such a group would be an initial step toward establishing a sound classification of this large and confusing genus of Tephritidae.

The *producta* group was originally recognized by Merz (1994) including the western and eastern Palaearctic species, *C. producta* (Loew, 1844), and *C. deserta* (Hering, 1939), plus 20 Afrotropical species without listing their specific names. He defined this species group based on the more or less flattened head (approx. as long as wide) and the dark paravertical setae. Our analysis, including the above two species, recovered this group as the basal-most lineage within the *Campiglossa* clade. This result is consistent with Smit et al. (2013) who analyzed DNA barcodes from approximately half of the European tephritid species. *Campiglossa producta* has been reared from the capitula of a wide range of composites, most of which belong to the subfamily Cichorioideae (White 1988). *Campiglossa deserta* was reared by us from the capitula of *Lactuca indica* in Korea (new record).

The *loewiana* group includes ca. 30 Holarctic species that have white frontal setulae, and white postocular and posterior notopleural setae (Merz 1994). In our analysis, the five selected species of this group were clearly recovered as a monophyletic group (Fig. 2; pb/pp = 99/1.00).

The *sororcula* group was previously known as the genus *Dioxyna*, which is synonymized here with *Campiglossa.* Both our analysis, as well as Smit at al.'s (2013) analysis clearly recovered this group within the *Campiglossa* clade. The only significant morphological differences of *Dioxyna* are their dorsoventrally flattened head as well as rather short apical scutellar setae (not more than 0.25× as long as basal scutellar setae). They are superficially similar to the *producta* group species, especially in having the dorsoventrally flattened head, but the *sororcula* group can be distinguished by their whitish paravertical setae.

The *irrorata* group, sensu stricto. In our dataset, this group is only represented by a single species, *C. hirayamae* (Matsumura, 1916), which has a peculiar wing pattern, including the pterostigma with two hyaline spots and the wing margin between apices of veins R_1 and Cu_1 with rather regularly arranged nine or ten round hyaline spots. These characteristics seem to be shared by at least the following four species: *C. amurensis* Hendel, 1927; *C. grandinata* (Rondani, 1870); *C. irrorata* (Fallén, 1814); and *C.*

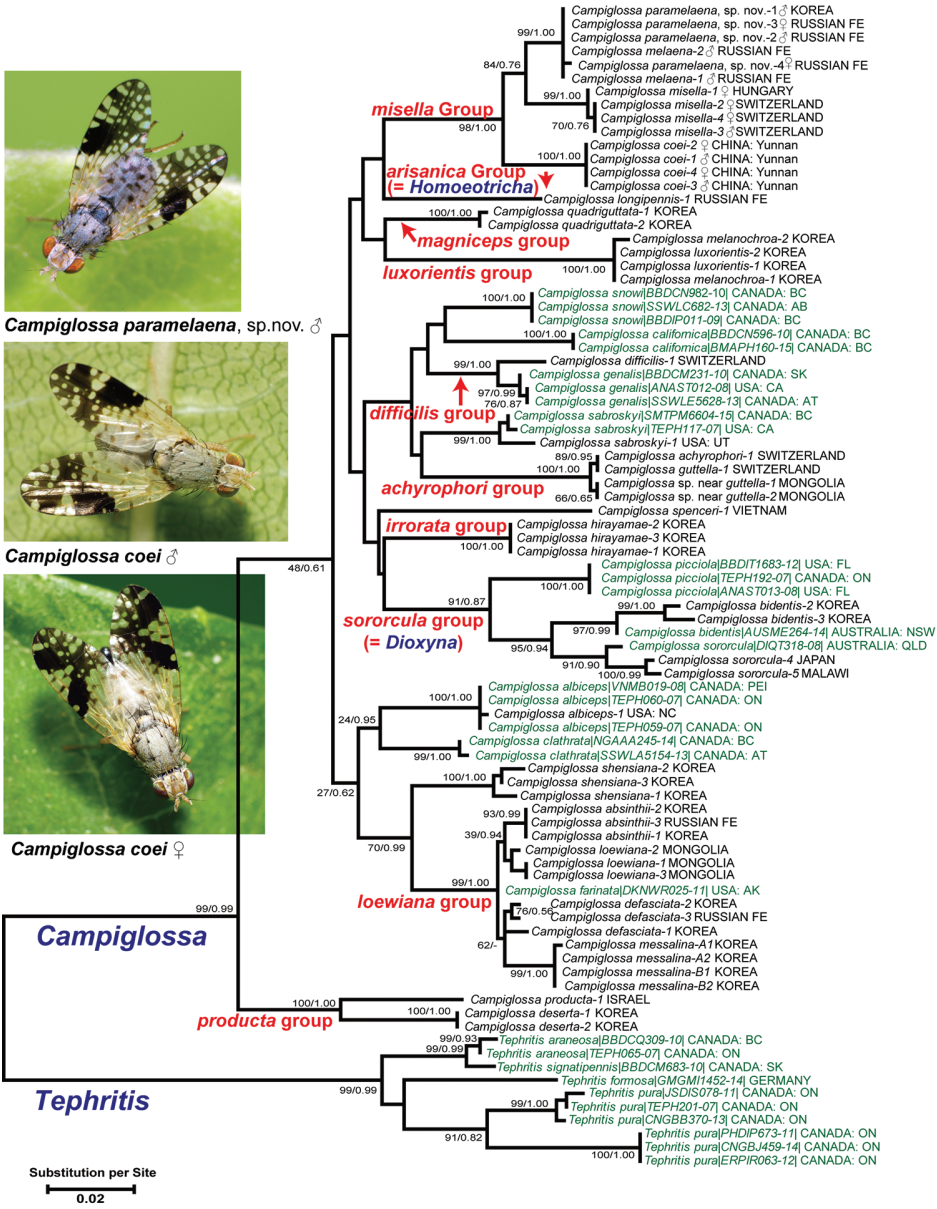

Figure 2. MEGA X analysis produced a maximum-likelihood (ML) phylogram of the 76 selected *Campiglossa* (ingroup) and ten *Tephritis* (outgroup) DNA barcode sequences using the general time reversible model. The first number on each branch is the bootstrap support from ML analysis (pb); the second number represents posterior probability (pp) from Bayesian inference (BI). Samples in green letters were extracted from BOLD systems (www.boldsystems.org).

venusta Dirlbek & Dirlbeková, 1971. In BOLD Systems (boldsystems.org), our identification attempt using a *C. hirayamae* sequence indeed recovered two closely related species, *C. irrorata* (1.84–2.00 % barcode distance) and *C. grandinata* (1.83–2.15 %).

The sequences of these two species were not included in our phylogenetic analyses because they were not open for public download. The name, *irrorata* group, was originally used by Merz (1994), and included a number of distantly related species, but we refined the group more narrowly to include the above species recognized both by DNA barcodes as well as morphology.

The *achyrophori* group was originally recognized by Korneyev (1990), listing eight species defined using an identification key. Merz (1994) loosely defined them based on their superficial morphological similarity including the wing with numerous hyaline spots. In our results (Fig. 2), *C. achyrophori* (Loew, 1869), *C. guttella* (Rondani, 1870), and an unidentified species from Mongolia (as *C.* sp. near *guttella*) were grouped together as a clear monophyletic clade (Fig. 2; pb/pp = 100/1.00). They are indistinguishable by DNA barcode sequences (0.00–0.26 % barcode distance) but the former two species can only be separated by the relative length of their oviscapes and their host plants (Merz 1994). The unidentified Mongolian species seems to be close to the European *C. guttella* in having a short oviscape, but does have five more distinct longitudinal stripes on the scutum. Since both longer and shorter oviscape individuals exist in the Mongolian specimens roughly sorted as *C. guttella* (Han, personal observation), further study including the female terminalia as well as host relationships is required to clarify their species status.

The *difficilis* group was defined by Merz (1992, 1994) based on male genitalic characteristics. He mentioned that there were five species from Palaearctic, Nearctic, and Afrotropical regions without listing their names. Our data at least grouped Palaearctic *C. difficilis* (Hendel, 1927) and Nearctic *C. genalis* (Thomson, 1869) (Fig. 2; pb/pp = 99/1.00). It is interesting to note that *C. difficilis* females are difficult to distinguish from those of *C. misella* (Merz 1994) of the sexually dimorphic *misella* group, which includes six morphologically distinct species (see the next section). Our data indicates that the average barcode distance between the similar looking *C. difficilis* and *C. misella* is 6.27 %, while the average distance among the four morphologically distinct *misella* group species is only 1.64 % (0–2.86 %). Therefore, these observations prove that looks can be deceptive in *Campiglossa*.

The *luxorientis* group was originally named by Korneyev (1990) based on *C. luxorientis* (Hering, 1940) and *C. melanochroa* (Hering, 1941) [as *C. dorema* (Hering, 1941)]. Both species show high intraspecific morphological variation as well as remarkable sexual dimorphism in wing patterns (Han 2019). These species could not be separated by DNA barcode sequences, but can easily be distinguished by their morphological characteristics (Fig. 2; Han 2019). They appear to be recently diverged sister species.

The *magniceps* group was defined as such by Korneyev (1997) as three species with distinct sexual wing dimorphism [*C. festiva* (Chen, 1938); *C. magniceps* (Hendel, 1927); *C. quadriguttata* (Hendel, 1927)], and were previously transferred by him (Korneyev 1990) to *Campiglossa* from the genus *Gonioxyna* Hendel, 1927. Though only *C. quadriguttata* is included in our analysis, this group appears to be monophyletic based on the long acrophallus of the male glans [illustrated by Korneyev (1990)], which is posited to be a synapomorphy of this group. Their sexually dimorphic male wings appear similar to those of the *arisanica* group (= *Homoeotricha*; see also the next

paragraph) especially in having the rounded to angulated anterior wing margin as well as more numerous hyaline spots (Korneyev 1997). The neighbor-joining tree included 7,278 barcode sequences (Fig. 1) clustered these two species groups together, but the maximum likelihood tree, including the selected 76 sequences (Fig. 2) did not group them. Additional genetic markers are needed to test their relationships (Han and Ro, in preparation).

The *arisanica* group was previously known as the genus *Homoeotricha*, which is here synonymized with *Campiglossa.* Our DNA barcoding analyses recovered *C. longipennis* Shiraki, 1933, within the *Campiglossa* clade. This species closely resembles *C. arisanica* (Shiraki, 1933), which is the type species of the East Asian genus *Homoeotricha* (the senior author examined the holotype ♀ of *C. longipennis* and the syntype ♂♀ of *C. arisanica* in NIAS). In addition to these two species, four other species are currently listed under this genus (Norrbom et al. 1999). They appear similar to the *magniceps* group species in having sexually dimorphic male wings (see the above paragraph), but the following possible synapomorphies (extracted from Korneyev 1993) differentiate the *arisanica* group: 1) vein R_{2+3} undulate; 2) labella longer than peristomal cavity, expanded in a leaf-like fashion in males; and 3) male genitalia with short and flattened sclerite around opening of acrophallus.

The *misella* group is named and reviewed in detail below.

The *misella* group of the genus *Campiglossa*

Our DNA barcoding analyses (Figs 1, 2) recovered a closely related group of four species (*C. coei*, *C. misella*, *C. paramelaena* sp. nov., and *C. melaena*; average DNA barcode distance 1.64 %, range 0.00–2.86 %), all of which show close morphological resemblance each other. Based on their morphological characteristics, especially the large dark mid-anterior wing marking in males, we recognized two further members, *C. pishanica* and *C. propria* from China, both of which are only known from male specimens.

Merz (1994) previously placed *C. misella* in the *irrorata* group, sensu lato, based on a few male genitalic characteristics, but this species group was not supported in Smit et al.'s (2013) barcoding analysis, which included both *C. misella* and *C. irrorata* (barcode distance approximately 5 %). Our analysis, including the *misella* group and the *irrorata* group, sensu stricto (represented by *C. hirayamae*) did not support their close relationship either (Figs 1, 2; barcode distance of 4.74 %).

Diagnosis. Members of the *misella* group can be diagnosed as follows, including the remarkable sexually dimorphic wing pattern: ***Head*** with paravertical and genal setae whitish. ***Thorax*** with both notopleural setae dark; apical scutellar setae at most half as long as basal setae; anepisternum with upper seta strong, dark, but lower seta approx. half as long, whitish; katepisternal seta strong, dark; anepimeral seta strong, whitish. ***Legs*** with both mid and hind coxal setae whitish. ***Male wing*** (except for some European populations of *C. misella* that show small sexual wing dimorphism)

with large dark mid-anterior marking (roughly elliptic to inverted triangular shape; e.g., Fig. 4A, C, G) usually covering mid-anterior 1/3 to center of wing. ***Abdominal tergites*** 3–5 in male and 3–6 in female each with pair of brown to dark brown submedian spots (e.g., Fig. 4I, K). ***Male genitalia*** with short proctiger; epandrium plus surstyli oval in caudal view, with posteriorly serrate lateral surstylar flange; preglans area of phallus strongly spinulose; glans without subapical lobe; tube-like acrophallus highly pronounced with apicodorsal opening, approx. half as long as glans; ejaculatory apodeme large, fan-shaped. ***Female postabdomen*** with oviscape cone shaped, dorsoventrally flattened; posterior 3/4 area of eversible membrane densely covered with anteriorly directed triangular spinules; aculeus elongated, dorsoventrally flattened, apically gradually pointed, apex with pair of tiny subapical teeth; two similar sized dark brown spermathecae, each with elliptical apical receptacle with transverse papillae and narrow basal neck; spermathecal duct transparent.

Distribution. All the recognized species of the *misella* group are distributed in East Asia including Nepal, China, the Russian Far East, and Korea, but the widespread *C. misella* extends its distribution to Central Asia and to Europe.

Biology. *Campiglossa misella* is the only species with known biology. White (1988) reported that they usually attack the flowering spikes of *Artemisia vulgaris*, inducing a stem gall in the first generation and developing in the capitula in the second generation in the U.K. (see the Biology section of *C. misella*).

Remarks. In addition to the large mid-anterior wing marking, the position of the crossvein R-M is more apically placed in males of all three species measured both sexes (male vs. female vein M ratios of *C. coei* 0.4–0.45 vs. 0.62–0.76; *C. misella*, 0.26–0.28 vs. 0.4–0.49; *C. paramelaena* sp. nov., 0.29–0.43 vs. 0.41–0.53). Such a structural modification seems to be associated with the male wing pattern modification of the *misella* group. We posit that the large mid-anterior dark marking with associated structural modification present only in males is a good candidate for a morphological synapomorphy of this species group. Interestingly, the wing cell r_1 of *C. propria* (Chen, 1938) male is further modified (see the Diagnosis of *C. propria* and Fig. 10F).

Since the females of the *misella* group do have more typical *Campiglossa* wing patterns and there are a good number of *Campiglossa* species currently known only by females, there might be some more species of the *misella* group not recognized in this study. A further survey of East Asian *Campiglossa* species in conjunction with DNA barcoding analyses is required.

Key to the species of the *misella* group of the genus *Campiglossa* (an asterisk (*) denotes likely members)

1 Legs entirely yellow-brown (Fig. 4A) **2**
– Legs dark (Fig. 7G) or at least with dark femora (Fig. 4H) **3**
2 Width of cell r_1 measured on axis of crossvein R-M as wide as or slightly wider than cell r_{2+3} (as in Fig. 10E-a) ..... ***C. coei***

– Width of cell r_1 measured on axis of crossvein R-M approx. twice as wide as cell r_{2+3} (Fig. 10F-a) ..... ***C. propria**** ♂

3 Scutum dark brown (Fig. 7H); wing cell r_{2+3} with posteroapical hyaline spot (Fig. 7I-a) ..... ***C. melaena***

– Scutum ash-grey (Fig. 7B); wing cell r_{2+3} without posteroapical hyaline spot (Fig. 7D-a) **4**

4 Cell br posterior to fork of vein Rs hyaline (Fig. 7C-a) ..... ***C. paramelaena* sp. nov.**

– Cell br posterior to fork of vein Rs with dark area (Fig. 4G-a, J-a) **5**

5 Cell r_1 posterior to pterostigma with two hyaline spots (Fig. 10E-b); apical 1/4 of cell dm with only posterior hyaline spot (Fig. 10E-c) basal 3/4 of cell dm almost entirely hyaline ..... ***C. pishanica**** ♂

– Cell r_1 posterior to pterostigma with three hyaline spots (Fig. 4G-b); apical 1/4 of cell dm with anterior and posterior hyaline spots (Fig. 4J-b); basal 3/4 of cell dm with dark background and 2–3 large hyaline spots ..... ***C. misella***

***Campiglossa coei* (Hardy)**
Figs 2, 4A–E, 5A–G, 10A, B

Tephritis coei Hardy, 1964: 164 (Type-locality: NEPAL, Taplejung Dist., N of Sangu, above river bank, ca. 5000 ft, holotype ♂, NHMUK); Wang 1998: 291, 294 (in the East Asian *Tephritis* key; diagnosis, new Chinese record – 2♂ from Yunnan Province).

Campiglossa coei: Korneyev 1990: 444 (new combination), 2004: 8 (erroneous synonymy with *C. misella*); Norrbom et al. 1999: 109 (in the world tephritid catalog); Korneyev and Ovchinnikova 2004: 546 (erroneous synonymy with *C. misella*).

Campiglossa favillacea Ito, 2011: 29 (Type-locality: NEPAL, Taplejung Dist., Kharu Pokhar, 3,000 m, holotype ♂, UOPJ – examined, Fig. 10A, B), syn. nov.

Material examined. Type series of *C. favillacea* Ito, 2011 (UOPJ; Fig. 10A, B): NEPAL: Taplejung: Kharu Pokhar, 3,000 m, 17.VII.1962, T. Yasuda, holotype ♂ of *C. favillacea*; Ilam: Phikol, 1,460 m, 19.IV.1962, T. Yasuda paratype 2♀, of *C. favillacea*. CHINA: Yunnan, Mengsong, Manlvcunhanzudazhai, small hilltop, 22°07'44.0"N, 100°28'51.7"E, 1690 m, 12.VII.2011, H.Y. Han and S.W. Suk, 72♂, 42♀ (YSUW); Yunnan, Mengsong, Bengangxizhai, in forest, 22°10'34.5"N, 100°35'06.8"E, 1725 m, 11.VII.2011, H.Y. Han and S.W. Suk, 1♀ (YSUW).

Diagnosis. This light-colored species can be diagnosed by the following characteristics. ***Head*** largely yellow-brown with grey upper occiput. ***Thorax*** with scutum entirely matte whitish grey without any outstanding dark spots or stripes; scutellum mostly matte whitish grey but ca. apical 1/3 yellow-brown. ***Legs*** entirely yellowish brown without any dark marking; fore femur with six or seven strong, brown posteroventral setae. ***Wing*** with basal area (basal 1/3 anteriorly and basal 1/2 posteriorly)

Figure 3. The habitat of *Campiglossa coei*. CHINA: Yunnan, Mengsong, Manlvcunhanzudazhai, small hilltop, 22°07'44.0"N, 100°28'51.7"E, 1,690 m, 12 July 2011. Many more than 100 individuals of *C. coei* were collected along with at least ten other species of the subfamily Tephritinae.

largely hyaline with only few small dark spots, especially cell br with area posterior to fork of vein Rs completely hyaline (Fig. 4A-a); male with large dark mid-anterior marking covering from mid-anterior 1/3 to posterior end of crossvein R-M; pterostigma dark brown with large round hyaline spot in both sexes (Fig. 4A-b; in the other *misella* group species this spot tends to be smaller or missing in male); cell r_1 posterior to pterostigma with two large hyaline spots (sometimes with tiny additional basal spot, Fig. 4A-c) in male and three large hyaline spots in female; cell r_{2+3} without posteroapical hyaline spot. ***Abdomen*** matte whitish grey with tergites 3–5 in male and 3–6 in female each with pair of pale brown submedian spots; oviscape shiny dark brown, as long as three preceding segments.

This species appears similar to *C. pishanica* (with only males known) but the latter species can be readily separated by the dark femora and more extensive mid-anterior wing marking with pterostigma completely dark (Figs 4A, C vs. 10E).

Description. ***Body*** (Fig 4A–E) predominantly matte whitish grey; setae mostly brown to dark brown but some white; setulae mostly white but some brown to dark brown; wing length 4.0–4.3 mm; thorax length 1.5–1.8 mm.

Head yellow-brown with whitish pruinosity except for dark brown ocellar triangle and grey upper occiput; head ratio 0.78–0.90, frons-head ratio 0.46–0.50, eye ratio 0.71–0.77, gena-eye ratio 0.17–0.23, antenna-head ratio 0.40–0.44, arista-antenna ratio 1.3–1.6; vertex yellow-brown; dark brown inner vertical seta approx. as long as

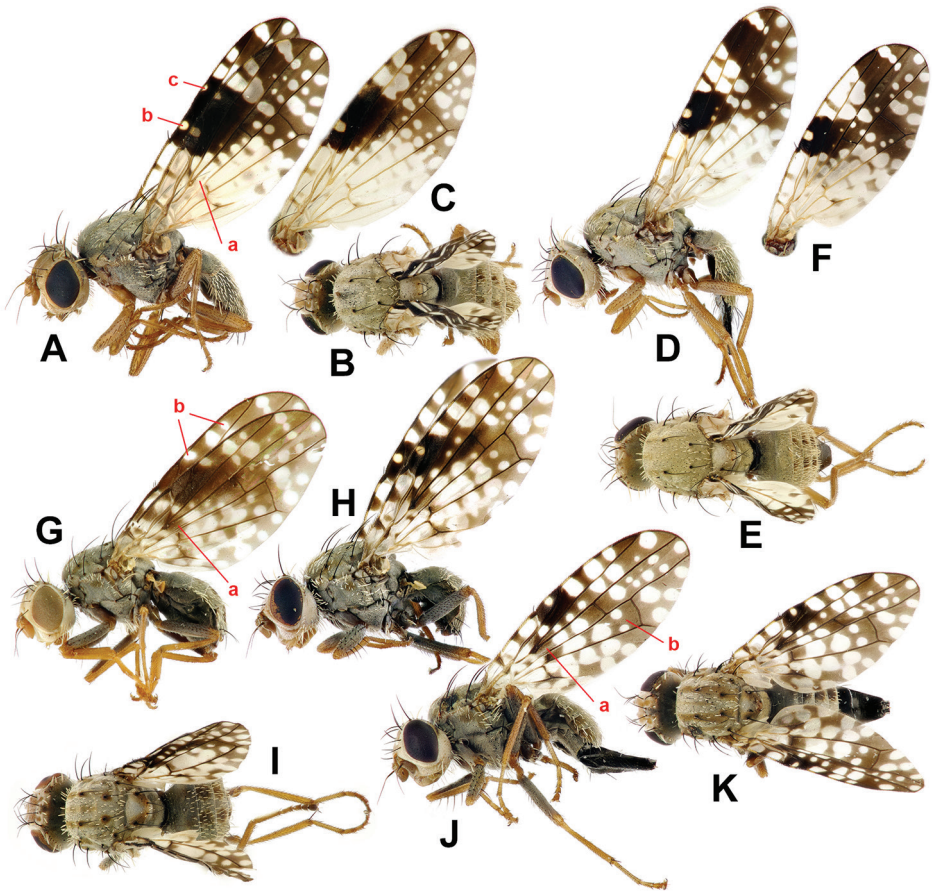

Figure 4. A–F *Campiglossa coei* **A** male, lateral view **B** male, dorsal view **C** male wing **D** female, lateral view **E** female, dorsal view **F** female wing **G–K** *C. misella* **G** male, lateral view **H** male, lateral view **I** male, dorsal view **J** female, lateral view **K** female, dorsal view.

longest diameter of eye; outer vertical seta white, 0.4× inner vertical seta; post ocellar seta white, 0.4× post ocellar seta; paravertical seta white, 0.7–0.8× post ocellar seta; ocellar seta dark brown, 3.3–4.0× ocellar triangle length; frons almost bare with frontal angle ca. 115 degree; with two dark brown frontal setae; white posterior orbital seta 0.6× dark brown anterior orbital seta; scape and pedicel yellow-brown with short brown setulae; first flagellomere 1.4–1.8× pedicel length, apically rounded, yellow-brown; arista entirely short pubescent, brown except yellow-brown basal area; face yellow-brown without distinct antennal groove; parafacial 0.4× as wide as first flagellomere; facial ridge with fine pale yellow setulae; gena with strong white genal seta and relatively long white setulae; postgena swollen with strong white postgenal seta and relatively long white setulae; postocular setae with two thick white setulae plus over ten shorter brown setulae, extended 0.5× distance from upper eye margin to lower eye margin; supracervical setae white; mouthparts geniculated with yellow-brown setulose labella; palpus with brown setulae apically and white setulae on remaining area.

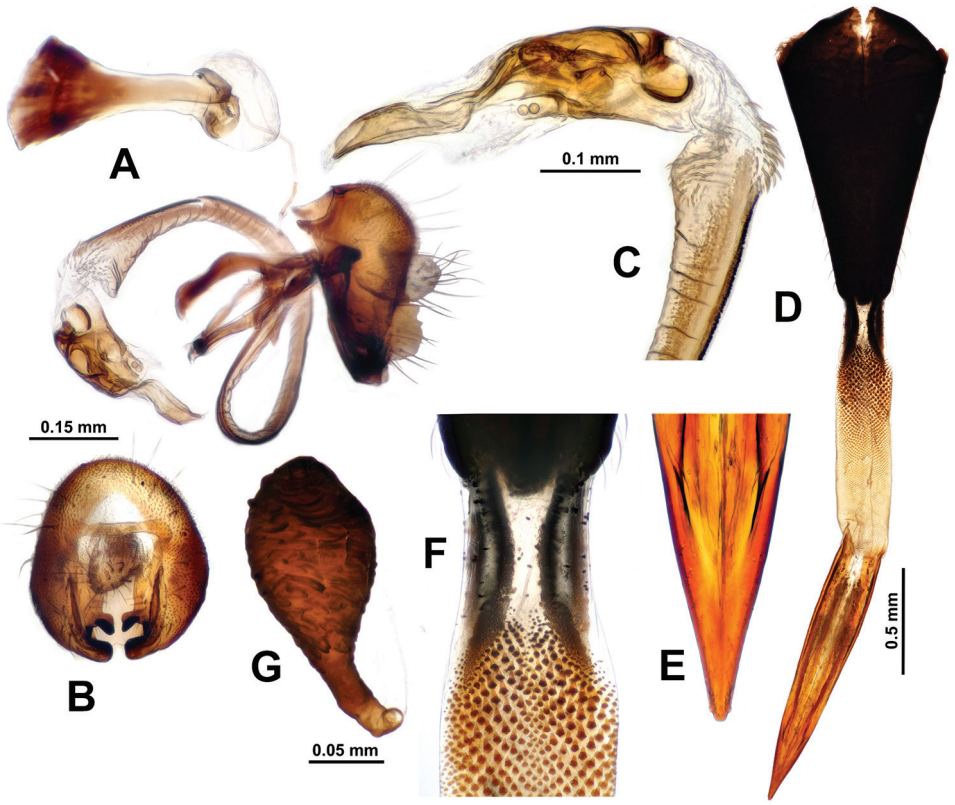

Figure 5. Genitalia of *Campiglossa coei* **A** epandrial complex, lateral view **B** epandrial complex, caudal view **C** glans and preglans of distiphallus **D** female postabdomen with aculeus and eversible membrane pulled out, ventral view **E** magnified view of aculeus tip **F** magnified view of oviscape and eversible membrane **G** spermatheca.

Thorax largely dark brown ground color with very heavy whitish pruinosity, generally appearing matte whitish grey; postpronotal lobe with single dark brown seta, yellow-brown in ground color, but appearing similar color as nearby areas due to heavy whitish pruinosity; scutum matte whitish grey with five faint brownish longitudinal bands traceable in clean specimens; two pairs of white scapular setae; acrostical setae widely separated each other, situated midway between levels of intra-alar setae and postsutural supra-alar setae; post-alar setae same level as intra-alar setae; dorsocentral setae same level as or slightly lower than transverse suture; presutural supra-alar setae approximately the same level as anterior notopleural setae; two notopleural setae dark brown with posterior seta0.5× anterior seta; scutellum mostly matte whitish grey but ca. apical 1/3 yellow-brown, slightly convex, almost bare except marginal tiny white setulae; basal scutellar setae more or less parallel, 2.3–3.5× as long as scutellum; apical scutellar setae crossed near apex, 0.9–1.3 as long as scutellum; pleura largely matte whitish grey; proepisternum with 3–5 white setulae; anepisternum matte grey with posterior 2/3 white setulose, with one strong dark brown seta and one half as long white seta ventral to it; katepisternum matte grey with a strong dark brown seta, upper

area sparsely with short white setulae and lower area with long white setulae; mediotergite matte grey.

Legs entirely yellow-brown with slight grey pruinosity and brown to dark brown setae and setulae; fore coxa anteriorly with white setulae, posteriorly bare; mid coxa anteriorly with few long white setulae, posteriorly bare; hind coxa with strong white lateral seta, posteriorly largely membranous; front femur with six or seven strong brown posteroventral setae; tibiae and tarsi entirely yellow-brown; midtibial spur dark brown, 1.2–1.4 as long as tibial width.

Wing (Fig. 4A, C, D, F) hyaline with brown to dark brown pattern; area around pterostigma with sexual dimorphism (see next paragraph); cells bc, bm, bcu, alula, anal lobe almost entirely hyaline; cell c mostly hyaline with narrow brown to faint brown medial longitudinal band; pterostigma with distinct hyaline spot in both sexes (Fig. 4A-b); cell r_{2+3} mostly without apical hyaline spot but with two large subapical spots often coalesced, one or two large hyaline spots posterior to two large r_1 spots; cell br with basal 3/5 area almost hyaline, apically dark brown with two or three hyaline spots posteriorly coalesced; cell r_{4+5} with single large apical spot and 8–12 variably sized hyaline spots; cell dm with basal 2/3 almost hyaline, apically dark brown with 4–7 variably shaped hyaline spots; cell m with basal 3/4 almost hyaline, apically dark brown with 1–3 variably shaped hyaline spots. Wing-thorax ratio 2.4–2.5; subcostal to costa ratio 0.43–0.53; cell r_1-r_{2+3} ratio 2.7–3.3; cell r_{4+5}-r_{2+3} ratio 0.58–0.73. R_{4+5} bare.

Wing dimorphism. Male (Fig. 4A, C) with cell r_1 with two large hyaline spots apical to pterostigma (rarely tiny additional spot anteriorly; Fig. 4A-c); large, more or less elliptic dark brown mid-anterior marking traceable covering pterostigma, cell r_1 well beyond pterostigma, approx. basal 1/3 to 2/3 of cell r_{2+3}, and anterior areas of cells br and r_{4+5} near crossvein R-M; vein M ratio 0.40–0.45. Female (Fig. 4D, F) – cell r_1 with three large hyaline spots apical to pterostigma; dark brown mid-anterior marking, if traceable, much smaller, or not wider than pterostigma; vein M ratio 0.62–0.76.

Male abdomen. Preabdomen slightly longer than wide, almost entirely matte pale grey; tergites 2–5 with white setulae, but tergite 5 also with 4–7 dark brown marginal setae; tergites 3–5 each with pair of pale brown submedian spots. Postabdomen (Fig. 6A–C) with proctiger short, 0.4× as long as epandrium in lateral view, microtrichosae, lower half with numerous yellow-brown setae; epandrium plus surstyli oval in caudal view; epandrium dark brown with long yellow-brown to brown setae, microtrichosae; lateral surstylar flange posteriorly serrate, with its basal width approx.1/3 as long as epandrial complex height; medial surstylus with lateral prensiseta approx.2/3 as long as medial prensiseta; preglans area of phallus strongly spinulose; glans without subapical lobe; tube-like acrophallus highly pronounced with apicodorsal opening, approx. half as long as glans; ejaculatory apodeme large, fan-shaped.

Female abdomen. Preabdomen slightly longer than wide, almost entirely matte grey; tergites 2–6 with white setulae, and tergite 6 especially with 4–7 dark brown marginal setae; tergites 3–6 each with pair of pale brown submedial spots. Postabdomen (Fig. 6D–G) with shiny dark brown oviscape approx. as long as three preceding segments; oviscape densely with dark brown setulae but without any macrosetae,

1.8× longer than wide, cone shaped, dorsoventrally flattened; eversible membrane with taeniae approx.1/4 as long as total length of membrane; posterior 3/4 area of eversible membrane densely covered with anteriorly directed triangular spinules; spinules largest in area behind taeniae; aculeus elongated, dorsoventrally flattened, 5.5× longer than wide with apical 1/3 gradually pointed, apex with pair of tiny subapical teeth; two similar sized dark brown spermathecae, each with elliptical apical receptacle with transverse papillae and 3/5 as long narrow basal neck; spermathecal duct transparent.

Distribution. Nepal, China (Yunnan).

Remarks. The male wing pattern of *C. coei* is atypical for the genus *Campiglossa* (Fig. 4A, C), and that is probably why this species, based on a single male specimen, was originally classified as *Tephritis* by Hardy (1964). Since then, Wang (1998), under this name, recorded two males from Yunnan, China. More recently, Ito (2011) described a new species (*C. favillacea* syn. nov.) based on the male holotype (from the type locality of *C. coei*) and two female paratypes (Fig. 10A, B), but he did not mention their wing dimorphism in the description. We, fortunately, were able to collect over a hundred male and female specimens from China, showing a remarkable sexual wing dimorphism (Fig. 4A, C vs. Fig. 4D, F). Most of the specimens were collected along with at least ten other species of the subfamily Tephritinae from a small hilltop in Yunnan, China (Fig. 3; Mengsong, Manlvcunhanzudazhai, 22°07'44.0"N, 100°28'51.7"E, 1690 m, 12 July 2011). This hilltop appears to be a temporary Tephritinae hot spot due to the clearing of a small forest patch.

***Campiglossa misella* (Loew)**

Figs 4G–K, 6A–G

Oxyna misella Loew, 1869: 19 (Type-locality: RUSSIA, Sarepta [Volgograd Region]. Syntype ♂♀, ZMHU. Inference of holotype by White 1986: 152, invalid; l.c. Norrbom et al. 1999: 112).

Tephritis lusoria Nowicky, 1869: 145 (Type-locality: UKRAINE, "Podolu, Sinkowie"; and Skale [Skala Podilska]. Syntype ♂, ZMHU, inference of holotype by White 1986: 152 (invalid; depository of other syntypes unknown); l.c. Norrbom et al. 1999: 112).

Paroxyna kunlunica Wang, 1996: 185 (Type-locality: CHINA, Yecheng, Xinjiang. Holotype ♂, IZAS); Wang 1998: 267 (new synonym of *C. misella*).

Campiglossa roscida Ito, 2011: 28 (Type-locality: NEPAL, Taplejung Dist., Walungchung Gola, 3,350 m. Holotype ♀, UOPJ – examined, Fig. 10C, D), syn. nov.

Campiglossa misella: Korneyev 1990: 443 (new combination, redescription); Norrbom et al. 1999: 112 (in the world Tephritidae catalog); Korneyev and Kameneva 1993: 44 (host plants); Wang 1998: 255, 267 (in the East Asian *Campiglossa* key, diagnosis); Korneyev 2004: 8 (taxonomic notes and erroneous synonymy of *Tephritis coei* and *T. pishanica* – see Remarks); Korneyev and Ovchinnikova 2004 (in the Russian Far East Tephritidae key); Smit et al. 2013: 297 (DNA barcoding analysis).

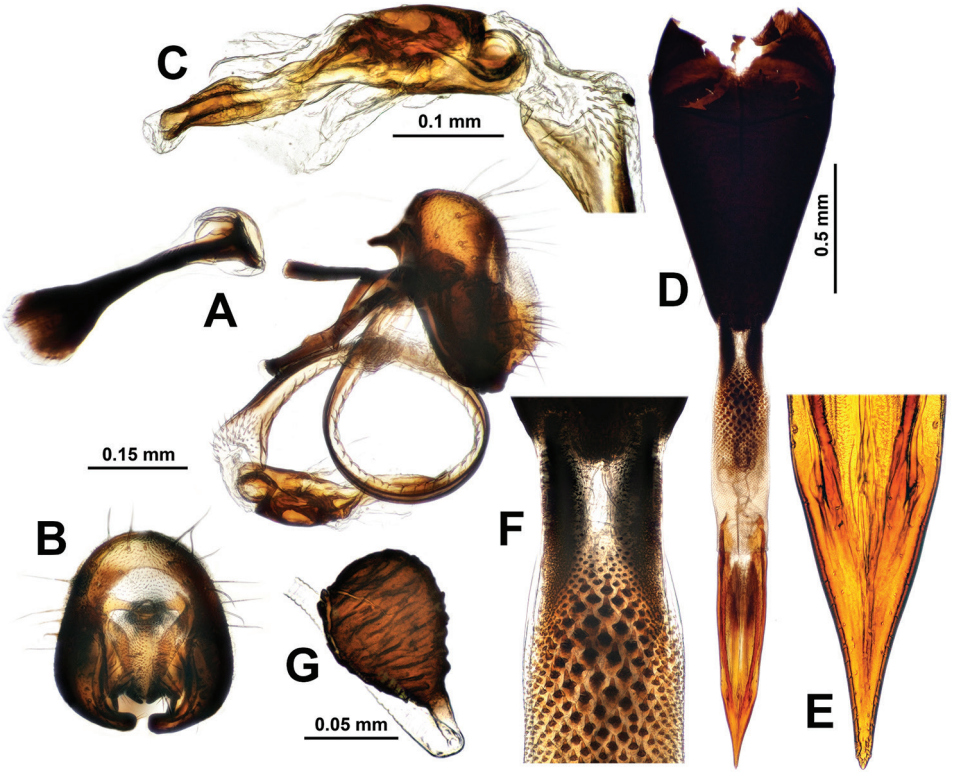

Figure 6. Genitalia of *Campiglossa misella* **A** epandrial complex, lateral view **B** epandrial complex, caudal view **C** glans and preglans of distiphallus **D** female postabdomen with aculeus and eversible membrane pulled out, ventral view **E** magnified view of aculeus tip **F** magnified view of oviscape and eversible membrane **G** Spermatheca.

Paroxyna misella: Hendel 1927: 155, X-2 (description, wing photograph of a syntype male); White, 1988: 5, 50 (biology, diagnosis, in the British *Paroxyna* key).

Material examined. HUNGARY: Bdaors, Odvas hg., 18.VI.1991, B. Merz and Adams, 1♀ (YSUW). ITALY: Aosta, St. Pierre, M. Torrette, 800–850 m, 22.IV.2003, B. Merz and F. Amiet, 1♂ (YSUW). NEPAL: Taplejung: Walungchung Gola, 3,350 m, 14.VI.1962, T. Yasuda, holotype ♂ of *C. roscida* (UOPJ; Fig. 10C, D). SWITZERLAND: Valais 642 m, St. German/Brüke, 3.VIII.1998, B. Merz and G. Bächli, 1♀; Valais, Leuk-Rotafen, 46°18'59"N, 7°40'18"E, 640 m, 22.VII.2004, H.Y. Han and K.E. Ro, 1♂ 1♀ (YSUW); Valais, Visperterminen-Kreuz, 46°15'17"N, 7°53'52"E, 1500 m, 21.VII.2004, H.Y. Han and K.E. Ro, 2♀ (YSUW). KYRGYZSTAN: S-Issik-Kul nr. Barskaun vill., 31.VII.1995, S.V. Ovchinnikov, 1♀ (YSUW); Telash Mt. r./N slope, Ara-Bijik rav, 2300 m, 4.VII.1998, D. Milko, 1♂ (YSUW).

Diagnosis. Males of *C. misella* usually have distinct sexually dimorphic wing patterns [e.g., Fig. 4G from Kyrgyzstan is almost identical to the male syntype photograph by Hendel (1927)] but some European populations seem to show slight sexual

dimorphism (e.g., Fig. 4H from Switzerland). More extensive survey is required to understand their variation, but they could still be readily diagnosed even based on our limited samples. ***Head*** largely yellowish brown with grey upper occiput. ***Thorax*** with scutum entirely ash-grey with five brownish longitudinal stripes (Fig. 4I, K); bases of acrostichal, dorsocentral, intra-alar, basal scutellar setae dark brown; scutellum ash-grey with lateral margins brown, apex yellowish brown; ***Legs*** with femora largely dark grey except for yellowish brown apices (Fig. 4G, H, J), but tibiae and tarsi yellowish brown; fore femur with six or seven dark brown posteroventral setae. ***Wing*** with basal half largely with dark spots, especially cell br posteroapical to fork of vein Rs with dark brown rectangular area (approx. twice as wide as long; Fig. 4G-a, J-a); male often with large dark mid-anterior marking covering from mid-anterior 1/3 to posterior end of crossvein R-M (Fig. 4G); pterostigma almost completely dark brown in such sexually dimorphic male (Fig. G), but with large hyaline spot in minimally dimorphic male (Fig. 4H), and female (Fig. 4J); cell r_1 apical to pterostigma with three large hyaline spots with 1st and 3rd spots much smaller than middle one in dimorphic male (Fig. 4G-b), but with three large similarly sized hyaline spots in female (Fig. 4J) or minimally dimorphic male (Fig. 4H); cell r_{2+3} without posteroapical hyaline spot. ***Abdomen*** ash-grey with tergites 3–5 in male and 3–6 in female each with pair of brown submedian spots; oviscape shiny dark brown, as long as four preceding segments.

Distribution. Europe, Central Asia, China (Xinjian, Shanxi, Sichuan, Xizang, Yunnan), Nepal.

Biology. This is the only species of the *misella* group with host feeding biology known. Interestingly, White (1988) reported that this species usually attacks the flowering spike of *Artemisia vulgaris*, inducing a stem gall in the first generation and developing in the capitula in the second generation in the UK. In addition to *Ar. vulgaris*, Korneyev and Kameneva (1993) listed *Ar. santolinifoliae and Ar. dracunculus* as their host plants in Central Asia (Kazakhstan).

Remarks. We resurrected *C. coei* and *C. pishanica* from the synonymy of *C. misella* by Korneyev (2014). Our study indicates that *C. coei* is a valid species (Figs 1, 2). *Campiglossa pishanica* is somewhat similar to *C. misella* in having the dark femora and the large mid-anterior wing marking, but *C. pishanica* has the following characteristics that, we posit, are beyond the variation range of the *C. misella* wing pattern (Figs 4G vs. 10E): cell r_1 apical to pterostigma with two hyaline spots instead of 3, basal 3/4 of cell dm almost hyaline, and anal lobe hyaline. See also the Remarks of *C. pishanica* for further discussion.

Campiglossa paramelaena **sp. nov.**
http://zoobank.org/0B2A4DE8-E854-4722-8AB8-374B36D68E12
Figs 5A–F, 8A–G

Type material. ***Holotype*** ♂: KOREA: Gyeongsangbuk-do, Bonghwa-gun, Myeongho-myeon, Mt. Cheongnyangsan, 36°46'43.6"N, 128°55'0.8"E, 600 m, 30.VI.2007,

H.Y. Han et al. (NIBR). ***Paratypes***: RUSSIA: Primorsky-Krai: between Chernyatino and Pokrovk, 43°57'32.7"N, 131°32'24.1"E, 55 m, 26.VI.2008, H.Y. Han and H.S. Lee, 3♂ 3♀; Khasansky-District, Kedrovaya Pad, 43°05'09.4"N, 131°35'06.0"E, 22 m, 23.VI.2008, H.Y. Han and H.S. Lee, 1♂; Khasansky-District, Barabash, 43°10'46.9"N, 131°28'20.0"E, 61 m, 22.VI.2008, H.Y. Han and H.S. Lee, 1♀; Ussuriysk, 43°47'05.4"N, 132°01'37.8"E, 19 m, 26.VI.2008, H.Y. Han and H.S. Lee, 1♀. All paratypes in YSUW.

Etymology. The specific epithet is derived from the closely related species *melaena* prefixed with *para*.

Diagnosis. This new species can be diagnosed by the following characteristics. ***Head*** largely yellowish brown with grey upper occiput. ***Thorax*** with scutum entirely ash-grey with five faint brownish longitudinal stripes (Fig. 7B, E); bases of acrostichal, dorsocentral, intra-alar, basal scutellar setae dark brown; scutellum ash-grey with apex yellowish brown; ***Legs*** with femora largely dark grey except for yellowish brown apices (Fig. 4G, H, J), but tibiae and tarsi yellowish brown; fore femur with six or seven dark brown posteroventral setae. ***Wing*** with basal area (basal 1/3 anteriorly and basal 1/2 posteriorly) largely hyaline with only few small dark spots, especially cell br with area posterior to fork of vein Rs completely hyaline (Fig. 7C-a); male with large dark mid-anterior marking covering from pterostigma to posterior end of crossvein R-M; male pterostigma almost completely dark brown, at most with tiny hyaline spot (Fig. 7C-b); female pterostigma with large round hyaline spot (Fig. 7D-a); cell r_1 posterior to pterostigma with three large hyaline spots in both sexes; cell r_{2+3} without posteroapical hyaline spot (Fig. 7C-c, D-a). ***Abdomen*** ash-grey with tergites 3–5 in male and 3–6 in female each with pair of brown submedian spots; oviscape shiny dark brown, as long as three preceding segments.

Campiglossa paramelaena sp. nov., appears similar to *C. misella* but the former species can be readily separated by the almost hyaline basal area of the wing, and the area posterior to the fork of vein Rs in particular is completely hyaline while the latter species has a distinctly dark spot on that area (Fig. 7C-a vs. Fig. 4G-a, J-a).

Description. ***Body*** (Fig. 7A–F) predominantly ash-grey; setae mostly dark brown but some white; setulae mostly white but some dark brown; wing length 3.0–3.8 mm; thorax length 1.2–1.5 mm.

Head yellow-brown with whitish pruinosity except for dark grey ocellar triangle and upper occiput; head ratio 0.85–0.92, frons-head ratio 0.47–0.53, eye ratio 0.75–0.83, gena to eye ratio 0.17–0.22, antenna-head ratio 0.41–0.46, arista-antenna ratio 1.3–1.7; vertex yellow-brown; dark brown inner vertical seta approximately as long as longest diameter of eye; outer vertical seta white, 0.4× inner vertical seta; post ocellar seta white, 0.3–0.4× post ocellar seta; paravertical seta white, 0.7–0.9× post ocellar seta; ocellar seta dark brown, 3.0–3.5× ocellar triangle length; frons almost bare with frontal angle 110–115 degree; with two dark brown frontal setae; white posterior orbital seta 0.6–0.8× dark brown anterior orbital seta; scape and pedicel yellow-brown with short dark brown setulae; first flagellomere 1.5–2.1× pedicel length, apically rounded, yellow-brown but with greyish tinge in some individuals; arista entirely short pubescent, dark brown except yellow-brown basal area; face yellow-brown without dis-

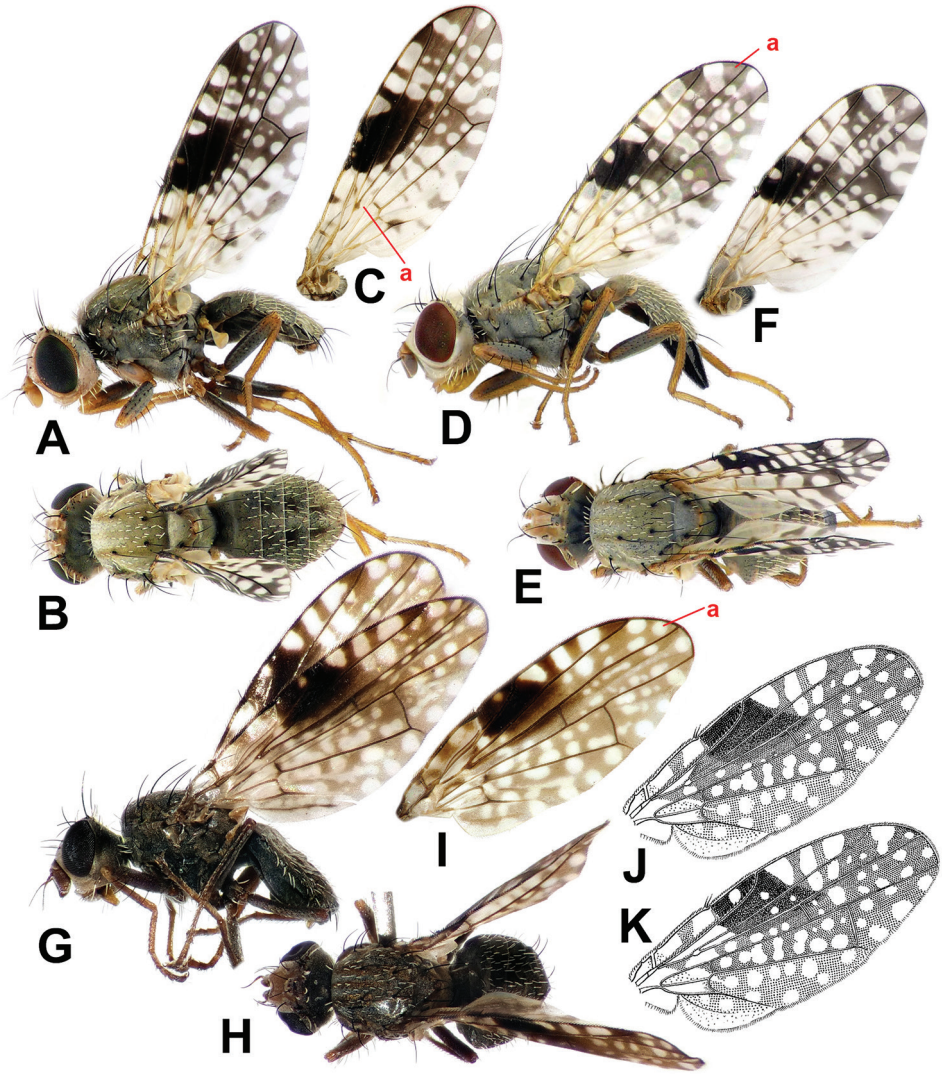

Figure 7. A–E *Campiglossa paramelaena* sp. nov. **A** male, lateral view **B** male, dorsal view **C** male wing **D** female, lateral view **E** female, dorsal view **F** female, wing **G–K** *C. melaena* **G** male, lateral view **H** male, dorsal view **I** male, wing **J** holotype male, wing **K** female, wing **J, K** Reproduced from Korneyev and Ovchinnikova (2004) with permission from Valery Korneyev.

tinct antennal groove; parafacial 0.4–0.5× as wide as first flagellomere; facial ridge with fine pale yellow setulae; gena with strong white genal seta and relatively long white setulae; postgena swollen with strong white postgenal seta and relatively long white setulae; postocular setae with two thick white setulae plus ten or more shorter dark brown setulae, extended 0.6× distance from upper eye margin to lower eye margin; supracervical setae white; mouthparts geniculated with labella yellow-brown setulose; palpus with brown setulae apically, white setulae on remaining area.

Thorax largely dark brown in ground color with heavy whitish grey pruinosity, generally appearing ash-grey; postpronotal lobe with single dark brown seta, yellow-brown in ground color, therefore, appearing paler than nearby areas; scutum ash-grey with five faint brownish longitudinal bands traceable in clean specimens; two pairs of white scapular setae; acrostical setae widely separated, situated midway between levels of intra-alar setae and postsutural supra-alar setae; post-alar setae same level as intra-alar setae; dorsocentral setae approximately same level as transverse suture; presutural supra-alar setae slightly above level of anterior notopleural setae; two notopleural setae dark brown with posterior seta 0.5× anterior seta; bases of acrostichal, dorsocentral, intra-alar, basal scutellar setae dark brown; scutellum mostly ash-grey but ca. apical 1/5 yellow-brown, slightly convex, almost bare except marginal tiny white setulae; basal scutellar setae more or less parallel, 3.1–3.6× (in males) and 2.4–3.0× (in females) as long as scutellum; apical scutellar setae crossed near apex, 1.1–1.4× (in males) and 0.9–1.1× (in females) as long as scutellum; pleura largely ash-grey; proepisternum with 3–5 white setulae; anepisternum ash-grey with posterior 2/3 white setulose, with single strong dark brown seta and one seta half as long and white ventral to it; katepisternum ash-grey with a strong seta, upper area sparsely covered with short white setulae and lower area with long white setulae; mediotergite ash-grey. Legs yellow-brown ground color with ash-grey pattern and brown to dark brown setae and setulae; fore coxa yellow-brown with posterobasal 1/3 grey, anteriorly with white setulae, posteriorly bare; midcoxa yellow-brown, anteriorly with few long white setulae, posteriorly bare; hind coxa greyish yellow-brown, with white lateral seta, posteriorly largely membranous; femora largely ash-grey except yellow-brown apices; tibiae and tarsi entirely yellow-brown; midtibial spur dark brown, 1.0–1.3× as long as wide.

Wing (Fig. 5A, C, D, F) hyaline with brown to dark brown pattern; area around pterostigma with distinct sexual dimorphism (see next paragraph); cells bc, bm, bcu, alula, anal lobe almost entirely hyaline; cell c mostly hyaline with narrow brown to faint brown medial longitudinal band; cell r_1 with basal 1/4 hyaline, apical 3/4 dark brown with three large hyaline spots apical to pterostigma; cell r_{2+3} without apical hyaline spot but with two large subapical spots often coalesced, two large hyaline spots posterior to three r_1 spots, two or three tiny spots apical to them; cell br with basal 2/3 almost hyaline, apically dark brown with 1–3 hyaline spot; cell r_{4+5} with single apical spot and 8–12 variably shaped hyaline spots; cell dm with basal 2/5 almost hyaline, apically dark brown with 4–7 variably shaped hyaline spots; cell m with 5–7 hyaline spots; cell cu_2 with six or seven large hyaline spots coalesced each other resulting in largely hyaline background with few small brown spots. Wing-thorax ratio 2.4–2.6, subcosta-costa ratio 0.53–0.64, cell r_1-r_{2+3} ratio 2.2–2.7, cell r_{4+5}-r_{2+3} ratio 0.54–0.67. R_{4+5} bare.

Wing dimorphism. Male (Fig. 7A, C) with pterostigma entirely dark brown or at most with tiny hyaline spot; large, more or less elliptic dark brown mid-anterior marking traceable covering pterostigma, cell r_1 adjacent to pterostigma, basal 1/4 to 3/5 of cell r_{2+3}, and anterior areas of cells br and r_{4+5} near crossvein r-m; vein M ratio 0.29–0.43. Female (Fig. 5D, E) with pterostigma dark brown with distinct round hyaline spot; large mid-anterior marking not traceable; such marking interrupted by distinct round hyaline spot on pterostigma and 2–4 small round spots on cell br posterior to it; vein M ratio 0.41–0.53.

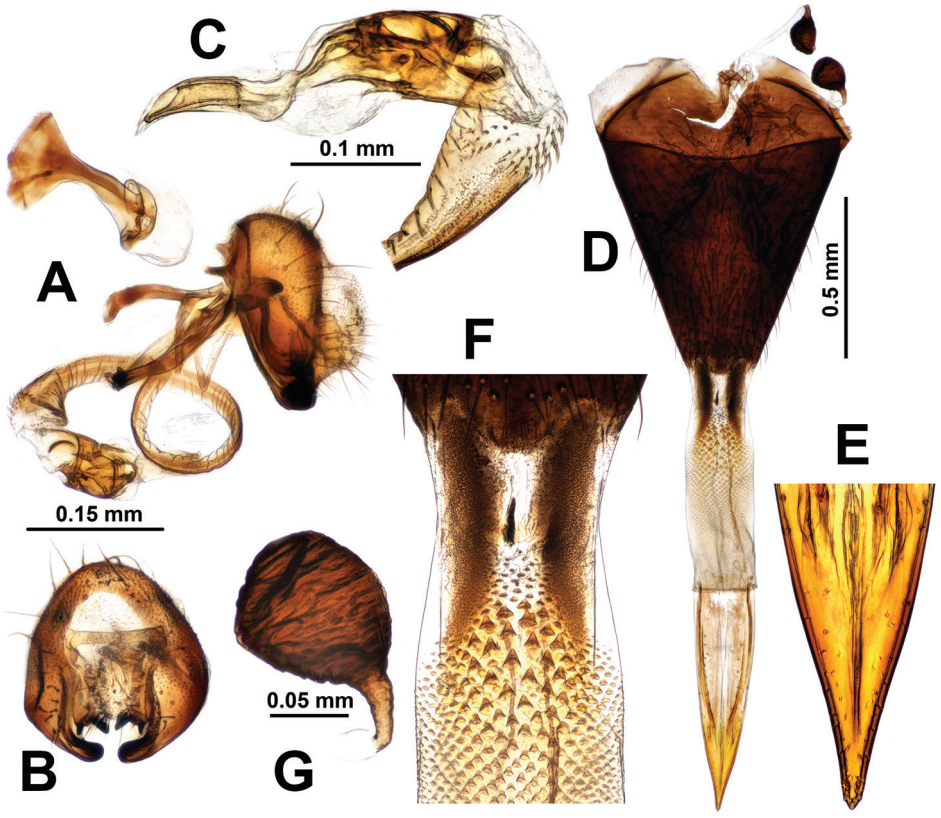

Figure 8. Genitalia of *Campiglossa paramelaena* sp. nov. **A** epandrial complex, lateral view **B** epandrial complex, caudal view **C** glans and preglans of distiphallus **D** female postabdomen with aculeus and eversible membrane pulled out, ventral view **E** magnified view of aculeus tip **F** magnified view of oviscape and eversible membrane **G** spermatheca.

Male abdomen. Preabdomen slightly longer than wide, almost entirely ash-grey; tergites 2–5 with white setulae, but tergite 5 also with 5–7 dark brown marginal setae; tergites 3–5 each with pair of brown submedian spots. Postabdomen (Fig. 8A–C) with proctiger short, 0.4× as long as epandrium in lateral view, microtrichosae, lower half with numerous yellow-brown setae; epandrium plus surstyli oval in caudal view; epandrium dark brown with long yellow-brown to brown setae, microtrichosae; lateral surstylar flange posteriorly serrate, with its basal width approx.1/3 as long as epandrial complex height; medial surstylus with lateral prensiseta approx.2/3 as long as medial prensiseta; preglans area of phallus strongly spinulose; glans without subapical lobe; tube-like acrophallus highly pronounced with apicodorsal opening, approx. half as long as glans; ejaculatory apodeme large, fan-shaped.

Female abdomen. Preabdomen slightly longer than wide, almost entirely ash-grey; tergites 2–6 with white setulae, tergite 6 especially with dark brown marginal setae; tergites 3–6 each with pair of brown submedial spots. Postabdomen (Fig. 8D–G) with shiny dark brown oviscape approx. as long as three preceding tergites; oviscape densely

covered by dark brown setulae but without any macrosetae, 1.3× longer than wide, cone shaped, dorsoventrally flattened; eversible membrane with taeniae approx. 1/3 as long as total length of membrane; posterior 2/3 area of eversible membrane densely covered with anteriorly directed triangular spinules; spinules largest in area behind taeniae; aculeus elongated, dorsoventrally flattened, approx. 4× longer than wide with apical 2/5 gradually pointed, apex with pair of tiny subapical teeth; two similar sized dark brown spermathecae, each with pear-shaped apical receptacle with transverse wrinkles and half as long narrow basal neck; spermathecal duct transparent.

Distribution. Korea, the Russian Far East.

Remarks. Individuals of *C. paramelaena* sp. nov., have DNA barcodes (Figs 1, 2) indistinguishable from those of *C. melaena*, which is a distinctly darker species with a more extensive wing pattern (Fig. 7G–I). Superficially, *C. paramelaena* sp. nov., more closely resembles *C. misella* (see Diagnosis), while the average barcode distance between these two species is 1.9 % (range 1.7–2.1 %). We postulate that *C. paramelaena* sp. nov., is not a light-colored seasonal form of *C. melaena*, because both species are from the same collecting lot in the Russian Far East (see Type material). Moreover, this species not only has a lighter body coloration but also has a much sparser wing pattern on the anal area then in *C. melaena*. In addition, the male surstylar flange of *C. melaena* is relatively larger (the base of the flange is approx. half as long as the height of the epandrial complex in the lateral view) than that of *C. paramelaena* sp. nov. (the base of the flange is distinctly shorter than half the height of the epandrial complex) (Fig. 9A vs. Fig. 8A).

Campiglossa melaena (Hering)

Figs 5G–K, 9A–C

Sinotephritis melaena Hering, 1941: 27 (Type-locality: China: Manchuria, Sjaolin. Holotype ♂, allotype ♀, NHMUK).

Campiglossa melaena: Korneyev 1990: 443 (new combination); Wang 1998: 255, 265 (in the East Asian *Campiglossa* key, diagnosis); Norrbom et al., 1999: 112 (in world Tephritidae catalog); Korneyev and Ovchinnikova 2004: 545 (in the Russian Far East Tephritidae key).

Material examined. Russia: Primorsky-Krai: Khasansky-District, Barabash, 43°10'46.9"N, 131°28'20.0"E, 61m, 22.VI.2008, H.Y. Han and H.S. Lee, 3♂ (YSUW); Nadezhdinsky-District, Vol'no-Nadezhdinskoye, grassland near restaurant, 43°22'31.6"N, 132°01'43.1"E, 61m, 22.VI.2008, H.Y. Han and H.S. Lee, 3♂ (YSUW).

Diagnosis. This is the darkest species of the *misella* group, showing the least wing dimorphism (Fig. 7G, I, J vs. K). ***Head*** largely brown with dark grey upper occiput. ***Thorax*** with dark grey scutum with five brownish longitudinal stripes (Fig. 7H); scutellum dark grey; ***Legs*** with coxae and femora largely dark grey but tibiae and tarsi brown;

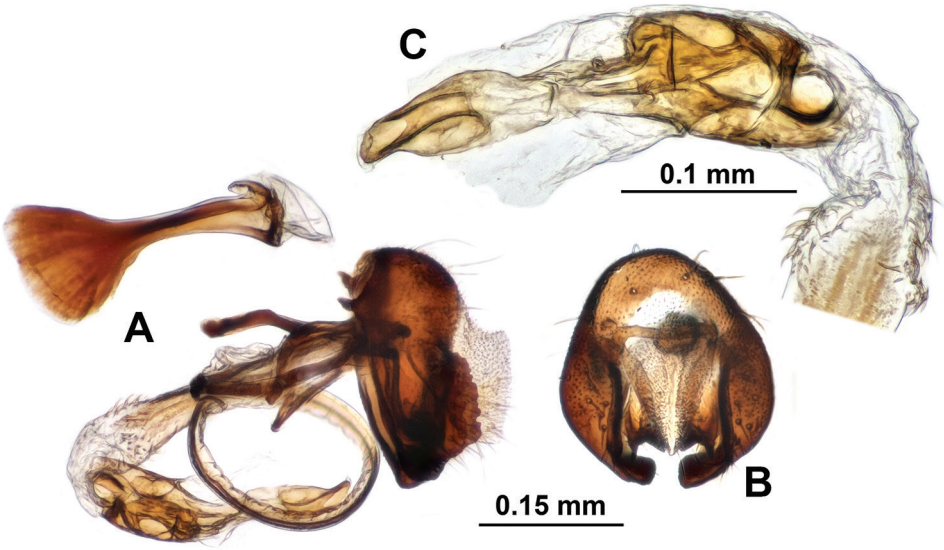

Figure 9. Male genitalia of *Campiglossa melaena* **A** epandrial complex, lateral view **B** epandrial complex, caudal view **C** glans and preglans of distiphallus.

fore femur with 5–7 dark brown posteroventral setae. ***Wing*** almost entirely brown to dark brown with numerous hyaline spots; male with large dark mid-anterior marking covering from pterostigma to posterior end of crossvein R-M; male pterostigma almost completely dark brown, at most with tiny hyaline spot (Fig. 7I-a); female pterostigma with larger hyaline spot (Fig. 7K-a); cell r_1 posterior to pterostigma with three large hyaline spots in both sexes; cell r_{2+3} with posteroapical hyaline spot (Fig. 7I-b). ***Abdomen*** almost entirely dark grey.

Distribution. North east China, the Russian Far East.

Remarks. Hering's (1941) original description and wing drawing of the holotype from north east China fall clearly within the variation range of the specimens we obtained from the Russian Far East. Unfortunately, we were not able to collect any female specimens, but Korneyev and Ovchinnikova's (2004) illustrations (Fig. 7J, K) show a similar sexual dimorphism of the wing pattern as in the other *misella* group species. Individuals of *C. melaena* have DNA barcodes (Figs 1, 2) indistinguishable from those of *C. paramelaena* sp. nov. (see the Remarks of the latter species for further discussion).

Presumed members of the *misella* group

The following two species are tentatively placed in the *misella* group based only on the superficial male characters available from the original and subsequent descriptions. In the future, their memberships should be confirmed by the female characters as well as a DNA barcoding analysis.

***Campiglossa pishanica* (Wang, 1996)**
Fig. 10E

Tephritis pishanica Wang, 1996: 188 (Type-locality: CHINA, Xinjian Province, Pishan, holotype ♂, paratype 2♂, IZAS); Wang 1998: 291, 300 (in the East Asian Tephritis key, diagnosis); Korneyev 2004: 8 (erroneous synonymy with *C. misella*); Korneyev and Ovchinnikova 2004; 546 (erroneous synonymy with *C. misella*).

Diagnosis. This is an interesting species showing the characteristics of both *C. coei* and *C. misella*. The only known *C. pishanica* male wing pattern is very similar to that of *C. coei* (Fig. 10E vs. Fig. 4A, C), but Fig. 10E shows the following differences: pterostigma almost completely dark with very tiny hyaline spot (Fig. 10E-a; *C. coei* male consistently has a much larger spot, Fig. 4A-a), and fork of vein Rs and area posterior to it with dark spot. Except for the much lighter basal wing area, *C. pishanica* body appears very similar to that of *C. misella*, which also has dark femora and a scutum with five stripes.

Distribution. Only three males (the type series) known from China (Xinjian).

***Campiglossa propria* (Chen, 1938)**
Fig. 10F

Sinotephritis propria Chen, 1938: 149 (Type-locality: China, s.e. Gansu, Mi-tching-ngai, holotype ♂, IZAS).

Campiglossa propria: Korneyev 1990: 454 (new combination); Wang 1998: 254, 268 (in the East Asian *Campiglossa* key, diagnosis); Norrbom et al. 1999: 113 (in the world Tephritidae catalog); Korneyev and Ovchinnikova 2004: 544 (in the Russian Far East Tephritidae key).

Diagnosis. We are not sure if this species actually belongs to the *misella* group, because the only known male (holotype) does not show close similarity to any known member of the group except for its large mid-anterior dark wing marking (Fig. 10F). This male also shows an unusual enlargement of cell r_1 resulting in a distinctly more rounded anterior wing margin than other species (Fig. 10F-a vs. Fig. 10E-a). In addition to this peculiar enlarged cell r_1, *C. propria* male can also be diagnosed based on the following characteristics: scutum ash-grey with five brownish longitudinal stripes; legs entirely yellowish; cell r_1 apical to pterostigma with three tiny hyaline spots plus a large subapical hyaline spot; cell r_{2+3} basal to crossvein R-M dark without any spot, apical to R-M with six hyaline spots including posteroapical spot; abdominal tergite 3–5 each with pair of large brown submedian spots.

Distribution. Only known from the type locality (Gansu, China).

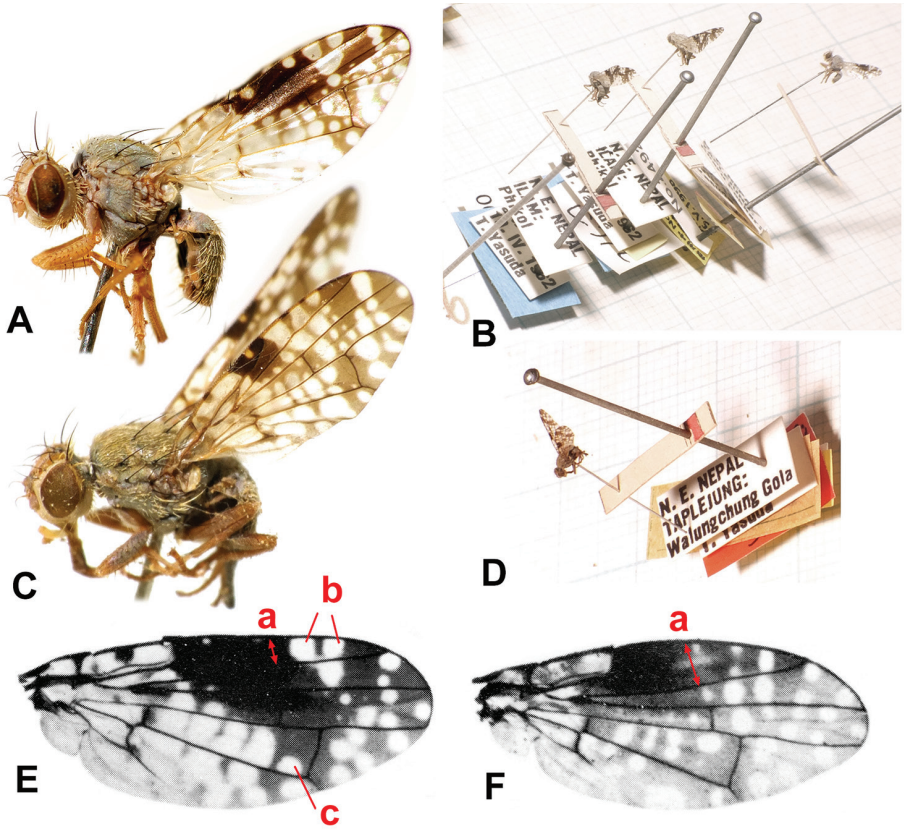

Figure 10. A Holotype male of *Campiglossa favillacea* Ito, 2011 (new synonym of *C. coei*, UOPJ) **B** from left, two paratype females and holotype of *C. favillacea* [UOPJ] **C** holotype female of *C. roscida* Ito, 2011 (new synonym of *C. misella*) **D** ditto **E** holotype or paratype male wing of *C. pishanica* **F** holotype male wing of *C. propria* **E, F** reproduced from Wang (1998) with permission from Xing-Jian Wang.

Conclusions

The genus *Campiglossa* currently includes ca. 200 similar looking species with their larvae usually feeding in the capitula of Asteraceae plants (White 1988). Unlike other species-rich pest tephritid genera such as *Bactrocera* Macquart, 1835, and *Anastrepha* Schiner, 1868, most *Camiglossa* species have been considered to be non- or minor economic pests. Therefore, relatively less research effort has been made to investigate *Campiglossa*. Furthermore, their unusually high intraspecific and low interspecific variation (Han 2019) has been a hurdle against establishing a sound classification of the genus *Campiglossa*. We found that the combination of the following taxonomic procedures is useful to investigate this enigmatic genus of the family Tephritidae.

Collecting and preservation

The male and female flies of most *Campiglossa* species seem to stay close to their host plants (White 1988; pers. obs.), unlike many other lek-mating tephritid taxa whose females only briefly visit their host plants for oviposition (White 1988; Díaz-Fleischer and Aluja 1999; Han 1999). According to our experience, sweep-netting through the area of suspected host plants has been the most productive way of obtaining diverse *Campiglossa* species; the Malaise and lure traps have not been effective methods for collecting this group of flies. Pinned specimens (usually double-mounted) are best for examining external morphological characteristics of *Campiglossa*, because it is difficult to observe the pattern of pruinosity in alcohol-preserved specimens. Postmortem changes can often be a problem as in other tephritids. For example, the brilliant coloration of the eyes disappears quickly in dried or alcohol specimens. In pinned *Campiglossa* specimens, some oily body fluid often oozes out and ruins specimens. In such specimens, observation of the color pattern becomes increasingly difficult. Freeze drying (simply by keeping specimens in a freezer for a few months) can alleviate this problem to some extent, but there seems to be no complete solution.

Host rearing

Capitula infesting tephritids including *Campiglossa* are the easiest tephritids to rear. Mature flower heads of Asteraceae plants should be collected and kept in mesh bags (similar to insect net bags). These bags should be stored in a sheltered area which maintains an approximate outdoor temperature, and examined for emerging flies. Once the plant materials dry, proper moisture should be maintained by misting with sterile water once or twice a week. In Korea, fall-collected flower heads, after harvesting fall-emerged tephritids, are kept in a 4 °C refrigerator between early December and early April. Overwintered flower heads, if infested by overwintering immature tephritids, usually yield adult flies until early June. Emerged flies should always be kept alive for a few days for hardening and coloring of their cuticles. Each puparium may be separated and kept in a gelatin capsule to match the emerged adult and its own puparium (see White 1988, for more detail). The host-associated *Campiglossa* specimens obtained in this manner have been extremely useful in understanding their inter- and intraspecific variations as well as sexual dimorphism and seasonal variations (Han 2019).

Photography

Due to the postmortem deterioration of the *Campiglossa* specimens, it is desirable to take high resolution photographs while they are still alive or just after euthanasia. Most of the figures presented in this study have been made in this manner. A collapsible glass

Figure 11. Macro photography setups for multi-day collecting trips. **A** A simple handmade collapsible macro-photography unit for focus stacking **B** A setup for photographing live tephritid flies. Please see the Materials and methods for details of the camera setups.

cage and a simple hand-made macro-photography stacking station are useful for taking such pictures during a multi-day collecting trip (Fig. 11). Male and female terminalia can also be photographed using the focus stacking method.

DNA barcoding

As demonstrated in this study, DNA barcode sequences of the genus *Campiglossa* form a strong monophyletic clade when analyzed phylogenetically. Therefore, any tephritids of uncertain identity clustering together within this clade should be regarded as *Campiglossa*. For this reason, we synonymize the genera *Dioxyna* and *Homoeotricha*, which were clearly placed within this clade (Figs 1, 2). We also found at least ten major monophyletic lineages within the *Campiglossa* clade and recognize them as ten putative species groups, among which the *misella* group is taxonomically revised here. We postulate that more species groups could be discovered as our DNA barcode dataset increases. Recognizing such a group would be an initial step toward establishing a sound classification of this enigmatic genus of Tephritidae. For the *misella* group, DNA barcoding has also been useful for clarifying their inter- and intraspecific morphological variation, as well as their sexual dimorphism.

Acknowledgments

This work could not have been possible without the generous assistance from Drs. Bernhard Merz and Valery Korneyev, who are the world authorities of the *Campiglossa* taxonomy. Dr. Bernhard Merz provided many reference specimens of a number

of European *Campiglossa* species. He also kindly identified many Korean and exotic *Campiglossa* species in our possession when he visited our laboratory in 2005. Dr. Valery Korneyev kindly reviewed the initial draft of our manuscript and made some important comments that helped us improve our manuscript. He also permitted us to use his published illustrations of *C. melaena* wings, and provided high quality scanned files of the original drawings. We are thankful to Dr. Xiaolin Chen, who invited the senior author for a collecting trip in 2011 in Yunnan Province, China, where we found a series of *C. coei* used in this study. We thank Dr. Xing-Jian Wang for permitting us to use his published wing pictures of *C. pishanica* and *C. propria*. We also thank professor Minoru Ishii for allowing us to examine the late Dr. Syusiro Ito's tephritid collection housed in the Osaka Prefecture University (UOPJ). We greatly appreciate Dr. Shinichi Yoshimatsu of the National Institute for Agro-Environmental Science (NIAS) for allowing us to access the late Dr. Tokuichi Shiraki's collection of Tephritidae, from which we were able to examine a number of primary types of tephritid species described in the early part of the 20th century. We sincerely thank Hye-Woo Byun, Sam-Kyu Kim, Chan-Hee Park, Hyun-Suk Lee, O-Young Lim, Sang-Wook Suk, Jong-Su Lim, Yong-Bong Lee, Dong-Jun Cha, Seulmaro Hwang, Jong-Mee Jung, Hak-Seon Lee, Dong-Han Kim, Han-Saem Lee, Seung-Su Euo, Soo-Hyun Jeong, Chan-Ouk Kim, and Jung-Whan Choi for their help in collecting and curating the tephritid specimens deposited in Yonsei University, Mirae Campus (YSUW). We wish to thank Drs. Marc De Meyer, Severyn Korneyev, and Massimiliano Vergilio, who rigorously reviewed our manuscript as subject editor and reviewers for ZooKeys. This work was supported by the Korea Institute of Planning and Evaluation for Technology in Food Agriculture, Forestry and Fisheries (IPET) through the Export Promotion Technology Development Program, funded by the Ministry of Agriculture, Food and Rural Affairs (MAFRA) (316015-04-2-HD030). This work was supported in part by the Basic Science Research Program through the National Research Foundation of Korea (NRF) funded by the Ministry of Education (2012R1A2042975), and also by a grant from the National Institute of Biological Resources (NIBR), funded by the Ministry of Environment (MOE) of the Republic of Korea (NIBR201902205).

References

Barr NB, Ruiz-Arce R, Farris RE, Silva JG, Lima KM, Dutra VS, Ronchi-Teles B, Kerr PH, Norrbom AL, Nolazco N, Thomas DB (2018) Identifying *Anastrepha* (Diptera; Tephritidae) species using DNA barcodes. Journal of Economic Entomology 111: 405–421. https://doi.org/10.1093/jee/tox300

Chen SH (1938) Subfamily Tephritinae. In: Zia Y, Chen SH (Eds) Trypetidae of North China. Sinensia 9: 57–172.

Díaz-Fleischer F, Aluja M (1999) Behavior of tephritid flies: a historical perspective. In: Aluja M, Norrbom AL (Eds) Fruit Flies (Tephritidae): Phylogeny and Evolution of Behavior. CRC Press: Boca Raton, Florida, 39–69. https://doi.org/10.1201/9781420074468.ch3

Dirlbek J, Dirlbeková O (1971) Ergebnisse der mongolisch-tschechoslowakischen etomologische-botanischen Expeditionen (1965, 1966) in die Mongolei. Nr. 26: Diptera, Trypetidae, 2 Teil. Acta faunistica entomologica Musei Nationalis Pragae 14: 165–172.

Drew RAI, Romig M (2013) Tropical Fruit Flies of South-East Asia (Tephritidae: Dacinae): Indomalaya to North-West Australasia. CABI, Wallingford, 653 pp. https://doi.org/10.1079/9781780640358.0000

Fabricius JC (1805) Systema antliatorum secundum ordines, genera, species, adiectis synonymis, locis, observationibus, descriptionibus. Reichard, Brunsvigae [= Brunswick]. 1 + 373 + 30 pp. https://doi.org/10.5962/bhl.title.15806

Fallén CF (1814) Beskrifning of ver de i sverige funna tistel-flugor, horande till dipter-slagtet *Tephritis*. Kungl. Svenska Vetenskapsakademiens Handlingar 35: 156–177.

Felsenstein J (1985) Confidence limits on phylogenies: an approach using the bootstrap. Evolution 39: 783–791. https://doi.org/10.1111/j.1558-5646.1985.tb00420.x

Frey R (1945) Tiergeographische Studien über die Dipteren fauna der Azoren. 1. Verzeichnis der bisher von den Azoren bekannten Dipteren. Commentationes Biologicae Societas Scientiarum Fennicae 8: 1–114.

Han HY (1999) Chapter 11. Phylogeny and behavior of flies in the tribe Trypetini (Trypetinae). In: Aluja M, Norrbom AL (Eds) Fruit Flies (Tephritidae): Phylogeny and Evolution of Behavior. CRC Press: Boca Raton, Florida, 253–297. https://doi.org/10.1201/9781420074468.ch11

Han HY (2019) Ten species of the subfamily Tephritidae (Insecta: Diptera: Tephritidae) newly recorded in Korea. Journal of Species Research 8: 294–312.

Han HY, Ro KE (2016) Molecular phylogeny of the superfamily Tephritoidea (Insecta: Diptera) reanalyzed based on expanded taxon sampling and sequence data. Journal of Zoological Systematics and Evolutionary Research 54: 276–288. https://doi.org/10.1111/jzs.12139

Han HY, Ro KE (2018) Discovery of a naturally occurring individual of *Acanthiophilus helianthi* (Rossi) (Diptera: Tephritidae) in Korea, a managed quarantine pest by the Korean Animal and Plant Quarantine Agency. Journal of Asia-Pacific Entomology 21: 1262–1267. https://doi.org/10.1016/j.aspen.2018.09.011

Han HY, Ro KE, McPheron BA (2006) Molecular phylogeny of the subfamily Tephritinae (Diptera: Tephritidae) based on mitochondrial 16S rDNA sequences. Molecules and Cells 22: 78–88. http://www.molcells.org/journal/list.html?pn=search&s_t=&s_a=&s_k=Tephritinae&s_v=&s_n=&x=58&y=14

Hardy DE (1964) Diptera from Nepal. The fruit flies (Diptera: Tephritidae). Bulletin of the British Museum (Natural History). Entomology 15: 147–169. https://doi.org/10.5962/bhl.part.20538

Hardy DE (1973) The fruit flies (Tephritidae – Diptera) of Thailand and bordering countries. Pacific Insects Monograph 31, 353 pp.

Hendel FG (1927) 49. Trypetidae. In: Lindner E (Ed.) Die Fliegen der palaearktischen Region 5. Stuttgart, lfg. 16–19, 1–221. [pls 1–17]

Hering EM (1936) Bohrfliegen aus der Mandschurei. 11. Beitrag zur Kenntnis der Trypetidae. Konowia 15: 180–189.

Hering EM (1937) Weitere Bohrfliegen aus der Mandschurei. 19. Beitrag zur Kenntnis der Trypetidae. Mitteilungen der Münchner Entomologischen Gesellschaft 8: 52–62.

Hering EM (1939) Neue Trypetiden der Erde (25. Beitrag zur Kenntnis der Trypetiden). Verhandlungen der Internationaler Kongress für Entomologie (1938) (7th) 1: 165–190.

Hering EM (1940) Kleiner Bemerkungen und Namensanderunge. Siruna Seva 1: 16.

Hering EM (1941) Neue ostasiatische Fruchtfliegen. Siruna Seva 3: 26–32.

Hering EM (1944) Neue Gattungen und Arten von Fruchtfliegen der Erde. Siruna Seva 5: 1–17.

Huelsenbeck JP, Ronquist FR (2001) MrBayes: Bayesian inference of phylogeny. Bioinformatics 17: 754. https://doi.org/10.1093/bioinformatics/17.8.754

Huelsenbeck JP, Larget B, Miller RE, Ronquist F (2002) Potential applications and pitfalls of Bayesian inference of phylogeny. Systematic Biology 51: 673–688. https://doi.org/10.1080/10635150290102366

Ito S (2011) Die Bohrfliegen aus Nordost-Nepal (Diptera, Tephritidae). Esakia (51): 1–45. https://catalog.lib.kyushu-u.ac.jp/opac_detail_md/?reqCode=fromlist&lang=1&amode=MD100000&bibid=19908&opkey=B157491498534277&start=1&listnum=14&place=&totalnum=15&list_disp=20&list_sort=0&fc_val=yearkey%23%40%23%5B2010+TO+2019%5D&fc_val=yearkey%23%40%232011&cmode=0&chk_st=0&check=000000000000000

Kimura M (1980) A simple method for estimating evolutionary rate of base substitutions through comparative studies of nucleotide sequences. Journal of Molecular Evolution 16: 111–120. https://doi.org/10.1007/BF01731581

Korneyev VA (1990) A review of *Sphenella* and *Paroxyna* series of genera (Diptera, Tephritidae, Tephritinae) of eastern Palaearctic. Nasekomye Mongolii 11: 395–470.

Korneyev VA (1993) A revision of Palaearctic fruit flies of the genus *Homoeotricha* Hering (Diptera Tephritidae Tephritinae). Russian Entomological Journal 2: 119–128.

Korneyev VA (1997) A revision of Palaearctic *Campiglossa* species assigned to *Gonioxyna* (Diptera: Tephritidae). Journal of Ukraine Entomological Society 3: 19–28.

Korneyev VA (1999) Phylogeny of the subfamily Tephritinae: relationships of the tribes and subtribes. In: Aluja M, Norrbom AL (Eds) Fruit Flies (Tephritidae): Phylogeny and Evolution of Behavior. CRC Press, Boca Raton, Florida, 549–580. https://doi.org/10.1201/9781420074468.sec6

Korneyev VA (2004) A new species and new synonymy of fruit flies (Diptera, Tephritidae) from Palaeactic region. Far Eastern Entomologist 140: 1–16.

Korneyev VA, Kameneva EP (1993) On the consortial associations of Asteraceae in western Tien-Shang. Ukrainian Botanical Journal 50: 39–51.

Korneyev VA, Ovchinnikova OG (2004) 79. Tephritidae-pestrokrylki [fruit flies]. In: Lehr PA (Ed.) Key to the Insects of Russian Far East. Vol. VI, Diptera and Siphonaptera. Pt. 3: 456–565. Dal'nauka, Vladivostok. [In Russian]

Kumar S, Stecher G, Li M, Knyaz C, Tamura K (2018) MEGA X: Molecular Evolutionary Genetics Analysis across computing platforms. Molecular Biology and Evolution 35: 1547–1549. https://doi.org/10.1093/molbev/msy096

Loew H (1844) Kritische Untersuchung der europaischen Arten des Genus *Trypeta* Meigen. Zeitschrift für die Entomologie 5: 312–437.

Loew H (1869) Revision der europaischen Trypetina. Zeitschrift für die gesammten Naturwissenschaft 34(7/8): 1–24.

Loew H (1873) Monographs of the Diptera of North America. Part III. Smithsonian Miscellaneous Collections 11 (3 [= pub. 256]), vii + 351+ XIII pp.

Macquart JPM (1835) Histoire naturelle des Insectes. Diptères. Tome deuxième. Ouvrage accompagne de planches., IV + 703 or 710 p. In: Roret NE (Ed.) Nouvelles suites a Buffon, formant, avec les œuvres de cet auteur, un cours complet d'histoire naturelle. Collection accompagnée de planches. Paris, 82 vols. + 11 atlases.

Matsumura S (1916) Thousand insects of Japan, Additamenta, Vol. 2 (Diptera). Keisei-sha, Tokyo, 413–424. [in Japanese]

Merz B (1992) Revision der west palaearktischen Gattungen und Arten der *Paroxyna*-Gruppe und Revision der Fruchtfliegen der Schweiz (Diptera, Tephritidae). Ph.D. thesis, Zürich Switzerland: Eidgenössischen Technischen Hochschule Zürich, 341 pp.

Merz B (1994) Diptera, Tephritidae. Insecta Helvetica Fauna 10, 198 pp.

Merz B (1999) Phylogeny of the Palearctic and Afropical genera of the *Tephritis* Group (Tephritinae: Tephritini). In: Aluja M, Norrbom AL (Eds) Fruit Flies (Tephritidae): Phylogeny and Evolution of Behavior. CRC Press: Boca Raton, Florida, 629–669. https://doi.org/10.1201/9781420074468.ch24

Munro HK (1938) New genera of African Trypetidae (Dipt.). Proceedings of the Royal Entomological Society of London. Series B, Taxonomy 7: 117–120. https://doi.org/10.1111/j.1365-3113.1938.tb01257.x

Munro HK (1957) Trypetidae. In: Ruwenzori Expedition, 1934–1935. Vol. 2, No. 9. British Museum (Natural History), 853–1054.

Nei M, Kumar S (2000) Molecular Evolution and Phylogenetics. Oxford University Press, 333 pp.

Norrbom AL, Carroll LE, Thompson FC, White IM, Freidberg A (1999) Systematic database of names. In: Thompson FC (Ed.) Fruit Fly Expert System and Systematic Information Database, Diptera Data Dissemination Disk 1 and Myia, 65–251.

Novak JA (1974) A taxonomic revision of *Dioxyna* and *Paroxyna* (Diptera: Tephritidae) for America north of Mexico. Melanderia 16: 1–53.

Nowicky M (1869) Zapiski faunicze. Dwuskrzydle (Diptera). Sprawozdanie Komisyi Fizyograficznej, Krakow 3: 145–152.

Robineau-Desvoidy JB (1830) Essai sur les Myodaires. Mémoires presentés a L'Institut des Sciences, Lettres et Arts, par divers savants èt lus dans ses assemblées: Sciences, Mathématiques et Physiques [ser. 2] 2: 813 pp.

Rondani C (1870) Ortalidinae Italicae collectae, distinctae et in ordinum dispositae. Dipterologiae Italicae prodromus. Pars VII. Fasc. 4 (sect. 1) [concl.]. Bollettino della Societa Entomologica Italiana 2: 105–133.

Saitou N, Nei M (1987) The neighbor-joining method: A new method for reconstructing phylogenetic trees. Molecular Biology and Evolution 4: 406–425. https://doi.org/10.1093/oxfordjournals.molbev.a040454

Schiner IR (1868) Diptera, vi + 388 pp. In: Reise der osterreichischen Fregatte Novara um die Erde in den Jahren 1857, 1858, 1859, unter den Befehlen des Commodore B. von Wullerstorf-Urbair. Zoologischer Theil. Zweiter Band. 1. Abtheilung, [Sect.] B, [Art. I]. B. K. Gerold's Sohn, Wien [= Vienna].

Shiraki T (1933) A systematic study of Trypetidae in the Japanese Empire. Memoirs of the Faculty of Science and Agriculture, Taihoku Imperial University 8 (Entomol. 2), 509 pp.

Smit J, Reijnen B, Stokvis F (2013) Half of the European fruit fly species barcoded (Diptera, Tephritidae); a feasibility test for molecular identification. In: Nagy ZT, Backeljau T, De Meyer M, Jordaens K (Eds) DNA barcoding: a practical tool for fundamental and applied biodiversity research. ZooKeys 365: 279–305. https://doi.org/10.3897/zookeys.365.5819

Thomson CG (1869) Diptera. Species nova descripsit. In: Svenska K (Ed.) Vetenskaps-Akademien, Kongliga svenska fregatten Eugenies resa omkring Jorden under befal af C. A. Virgin, aren 1851–1853. Pt. 2: Zoologie, [Sect.] 1. Insecta. PA Norstedt & Soner, Stockholm, 443–614 pp, pl. 9 (1868).

Wang XJ (1996) New genus and species of Tephritinae (Diptera: Tephritidae) from Inner Mongolia, China. Entomotaxonomia 12: 291–304.

Wang XJ (1998) The fruit flies (Diptera: Tephritidae) of the East Asia Region. Acta Zootaxonomica Sinica (1996) 21 (Supplement), 419 pp.

White IM (1986) A new species of *Paroxyna* Hendel and notes on the nomenclature of other British Tephritidae (Diptera). Entomologist's Monthly Magazine 122: 145–163.

White IM (1988) Tephritid flies (Diptera: Tephritidae). Handbook for the Identification of Insects 10(5a), 134 pp.

White IM (2006) Taxonomy of the Dacina (Diptera: Tephritidae) of Africa and the Middle East. African Entomology. Memoir No. 2, 156 pp.

White IM, Headrick DH, Norrbom AL, Carroll LE (1999) Glossary. In: Aluja M, Norrbom AL (Eds) Fruit Flies (Tephritidae): Phylogeny and Evolution of Behavior. CRC Press: Boca Raton, Florida, 881–924. https://doi.org/10.1201/9781420074468.sec8

Wiedemann CRW (1830) Aussereuropaische zweiflugelige Insekten. Vol. 2. Schulz, Hamm. 684 pp.

ZooKeys 899: 37–45 (2019)
doi: 10.3897/zookeys.899.47030
http://zookeys.pensoft.net

RESEARCH ARTICLE

A peer-reviewed open-access journal
ZooKeys
Launched to accelerate biodiversity research

Nienna chukotka sp. nov. (Protura, Acerentomidae, Nipponentominae) from the Arctic region, with a key to species of the genus

Julia Shrubovych[1,2,3]

1 *Institute of Soil Biology, Biology Centre, Czech Academy of Sciences, Na Sádkách 7, 370 05 České Budějovice, Czech Republic* **2** *Institute of Systematics and Evolution of Animals, Polish Academy of Science, Sławkowska 17, Pl 31-016 Krakow, Poland* **3** *State Museum of Natural History, Ukrainian Academy of Sciences, Teatral'na St. 18, UA 79008 Lviv, Ukraine*

Corresponding author: *Julia Shrubovych* (shrubovych@gmail.com)

Academic editor: *W. M. Weiner* | Received 3 October 2019 | Accepted 26 November 2019 | Published 12 December 2019

http://zoobank.org/0EDFAA7D-133C-462D-BDB3-B38A228FFE57

Citation: Shrubovych J (2019) *Nienna chukotka* sp. nov. (Protura, Acerentomidae, Nipponentominae) from the Arctic region, with a key to species of the genus. ZooKeys 899: 37–45. https://doi.org/10.3897/zookeys.899.47030

Abstract

A new species of *Nienna* was collected in the most northern part of the Palearctic, inside the Arctic Circle. In possessing seta *Pc* on tergite VII and sternites VI–VII and a very long foretarsal sensillum *a*, *Nienna chukotka* **sp. nov.** is more similar to *Alaskaentomon* species than to the other *Nienna* species distributed in southern Siberia and northern China. The new species differs from nearly all other members of Nipponentominae in possessing five anterior setae on tergite VII and in the presence of posterolateral pores on tergite I, as in members of *Hesperentomon* (Hesperentomidae). An identification key to *Nienna* species is provided.

Keywords

Chaetotaxy, Chukotka, identification key, northern Palearctic, porotaxy

Introduction

The proturan genus *Nienna* Szeptycki, 1988 was created for *Nienna parvula* Szeptycki, 1988, described from the Altai mountains in southern Siberia (Szeptycki 1988). The genus differs from the 12 other genera of Nipponentominae Yin, 1983 in possessing a small, indistinctly granulated calyx and a short posterior filament on the maxillary

gland, and in the small, nearly globular foretarsal sensillum *t3*. A second species, *Nienna quinghaiensis* Bu & Yin, 2008, was described from northern China. The diagnosis of the genus was recently updated (Galli et al. 2018). In the current paper, the description of a third species of *Nienna* is given. The type specimens, collected from the Arctic region, are the northernmost records for any Protura. A key to the species of *Nienna* is given.

Materials and methods

Protura specimens collected from western Chukotka in 2018 were extracted from soil samples with Berlese-Tullgren funnels into 95% ethanol. The specimens were mounted on glass slides in Faure's medium (Dunger and Fiedler 1989).

The classification system of Protura follows Szeptycki (2007). Terminology for body chaetotaxy and porotaxy follows Szeptycki (1988) and Shrubovych (2014); head seta designations follows Rusek et al. (2012).

Abbreviations

Abd.	abdominal segments,	***sal***	sternal anterolateral,
Th.	thoracic segments,	***psm***	posterosubmedial,
***A*-setae**	anterior setae,	***psl***	posterosublateral,
***P*-setae**	posterior setae,	***pl***	posterolateral,
fp	frontal,	***spm***	sternal posteromedial,
cp	clypeal,	***spsm***	sternal posterosubmedial cuticular pore.
al	anterolateral,		
sl	sublateral,		

Results

The genus *Nienna* is characterized by three pairs of *A*-setae on the mesonotum and metanotum, small, indistinctly granulated appendices on the calyx and a short posterior filament on the maxillary gland. The foretarsal sensillum *t1* is filiform, sensillum *t3* is small and globular (lanceolate in *N. quinghaiensis* Bu &Yin, 2008), the position of sensillum *d* is close to the base of *e*, and seta *β1* is setiform. Sensillum *a'* is distal to the base of *t2*. Sensillum *b'* is missing. The genus is similar to twelve other genera from the subfamily Nipponentominae in having abdominal legs with 2 nearly equal setae, 5 pairs of *A*-setae on tergites II–VI (except for *Alaskaentomon* Nosek, 1977 and *Nanshanentulus* Bu & Yin, 2007) and by the posterior position of seta *P3* on abdominal tergites II–VI (except for *A. fjellbergi* Nosek, 1977) (Bu and Yin 2007; Bu et. al. 2013; Galli et al. 2018; Nosek 1977, 1981; Shrubovych 2009, 2011, 2014; Shrubovych and Smykla 2012; Shrubovych et al. 2012; Shrubovych et al. 2014a, b, c).

***Nienna chukotka* sp. nov.**
http://zoobank.org/2FEE913F-CC4C-445A-869E-F25B7267F644
Figs 1, 2, Table 1

Material examined. Holotype (ISEA 6650): female, Russia, Chukotka Autonomous Okrug, Chaunskiy district, 2 kilometers from Apapelgino village, hill Akanotenmeem, in dry locality with *Dryas* sp., elev. 20 m, 69°48'40"N, 170°35'51"E, 24-VII-2018, coll. Makarov K. and Makarova O. Paratype (ISEA 6651): female, same data as holotype. The holotype and paratype are deposited in the collection of the Institute of Systematics and Evolution of Animals, Krakow, Poland (ISEA).

Diagnosis. *Nienna chukotka* is characterized by 3 pairs of *A*-setae on the mesonotum, metanotum and tergite VIII, 3 *A*-setae on sternites I–VII, absence of *P1a* setae on tergites I–VI, 5 pairs of *A*-setae on tergites II–VII, absence of *A2* on prosternum, presence of seta *Pc* on tergite VII and sternites VI–VII, and presence of additional *d6* setae on head. Foretarsal sensillum *a* is broadened, very long, surpassing the base of sensillum *e*. Posterolateral pores (*pl*) present on tergite I, *psl* pores present on tergites VI and VII, asymmetrical *spsm* pores present on sternites IV–VII.

Description. Head setae *l3*, *sd4* and *sd5* long, setiform, additional seta *d6* present, length ratio of posterior setae *d7*:*sd7*:*l5* as 2.4:2.5:1.0; frontal pore (*fp*) and a pair of clypeal (*cp*) pores present (Fig. 1A). Pseudoculus circular, with short posterior extension, PR = 12 (Fig. 1B). Sensilla of maxillary palps slender, pointed apically, equal in length (Fig. 1C). Labial palps with four-branched tuft of apical setae and broadened sensillum (Fig. 1D). Maxillary gland with small, indistinctly granulated calyx, short posterior filament and trilobed posterior dilation (Fig. 1E), CF = 6.0.

Foretarsus (Fig. 1J, H) without sensillum *b*'; *t1* filiform, *t3* small and globular; *a* broad, very long, evidently surpassing base of seta *γ3*, nearly reaching base of sensillum *f*; other sensilla parallel-sided. Sensillum *b* slightly longer than *c*. Sensillum *d* situated nearer to *e* than to *c*; *a*' distal to level of *t2* insertion. Length formula of sensilla: *t3* < *t1* < *t2* < (*c* = *e*) < *b* < (*g* = *a*' = *c*') < (*d* = *f*) < *a*. Setae *β1* and *δ4* long and setiform, about twice as long as other *δ*-setae (Fig. 1H). Single pores situated near bases of sensilla *t1* (Fig. 1J) and *t3* (pore not visible on Fig. 1J because closed by sensillum *e*). Claw short, without inner tooth, empodial appendage short. BS = 0.4, TR = 2.7, EU = 0.3.

Formula of chaetotaxy given in Table 1. Setae on nota differing in length (Fig. 2A, B). Pronotal seta *1* 1.6 times longer than seta *2* (Fig. 1A). Meso- and metanota with setae *P1a* and *P2a* setiform, lengths 7 and 5 μm, respectively; *P2a* situated nearly midway between *P2* and *P3* (Fig. 2A, B). Length ratio of mesonotal setae *P1*: *P1a*: *P2* as 2.7: 1: 3.6. Meso- and metanota with *sl* and *al* pores (Fig. 2B). Pro-, meso- and metasterna without pores (Fig. 2E, F).

Accessory setae on tergites and sternites I–VII setiform, those of tergite VII significantly longer than those on I–VI. (Fig. 2C, D, G, H, K, L). Pores *pl* present on tergite I, *psm* on tergites I–VII, *psl* on tergites VI–VII, *al* on tergites II–VII (Fig. 2C, D, H).

Abdominal legs with 4, 2, 2 setae. Subapical and lateral apical setae on second and third pairs of abdominal legs nearly equal in length, 15 and 14 μm, respectively

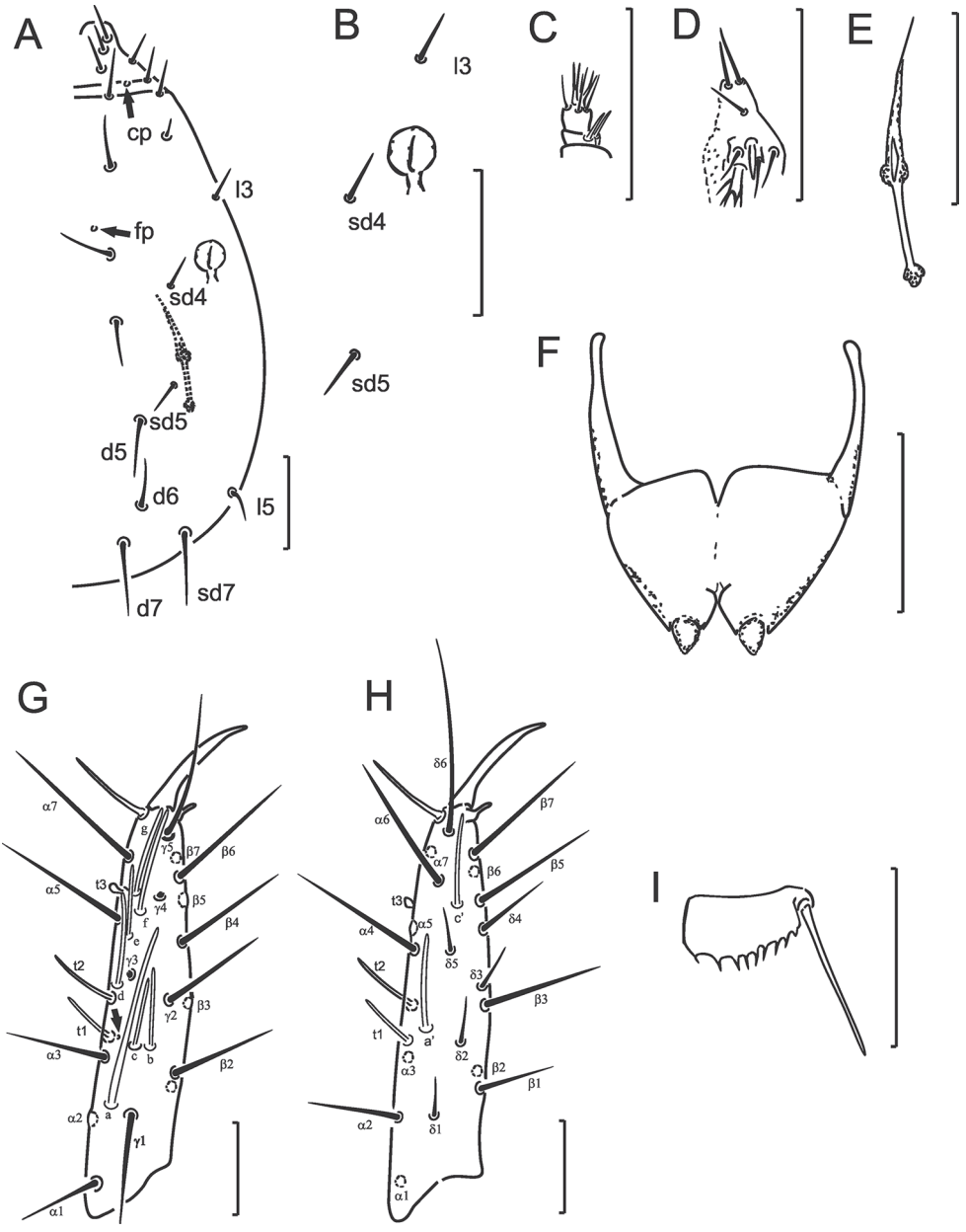

Figure 1. *Nienna chukotka* sp. nov. holotype. **A** Part of head **B** pseudoculus with setae *sd4*, *sd5* and *l3* **C** maxillary palpus **D** labial palpus **E** maxillary gland **F** female squama genitalis **G** exterior view of foretarsus **H** interior view of foretarsus **I** comb. Arrows show pores. Scale bars: 20 μm.

(Fig. 2J). Sternites I–III without pores (Fig. 2G). Sternites IV–VII with asymmetrical *spsm* pore, with short anterolateral lines and sternite VII with a connecting line on anterior part (Figs 2K, L).

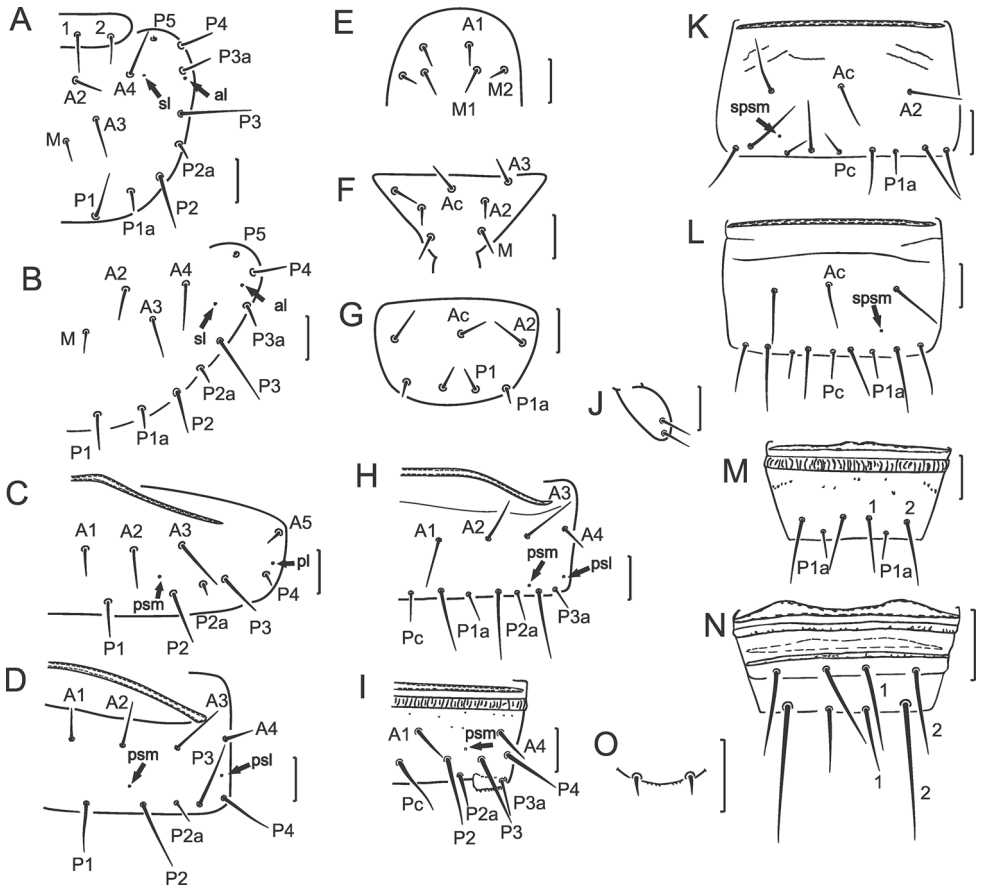

Figure 2. *Nienna chukotka* sp. nov. holotype. **A** Part of pro- and mesonotum **B** part of metanotum **C** part of tergite I **D** part of tergite VI **E** anterior part of prosternum **F** anterior part of mesosternum **G** sternite I **H** part of tergite VII **I** part of tergite VIII **J** abdominal leg of segment II **K** sternite VI **L** sternite VII **M** sternite VIII **N** sternites IX–X **O** hind margin of sternite XII. Arrows show pores. Scale bars: 20 μm.

Abdominal segment VIII with distinct striate band; tergite and sternite anteriorly with irregular small teeth (Figs 2 I, M). Pore *psm* without accompanying teeth. Posterior margin of sternite VIII and laterotergites smooth. Comb VIII with 9–10 small teeth (Fig. 1I). Seta *1a* on tergite IX half the length of seta *1*. Seta *2a* on tergites IX and X shorter than other setae. Sternites IX–X with traces of striate band (Fig. 2N). Setae *1* and *2* on sternite IX of equal length, on sternite X seta *1* about half the length of seta *2* (Fig. 2N). Medial pore on dorsal lobe of segment XII and pair of *sal* pores on ventral lobe. Hind margin of dorsal lobe smooth, ventral lobe with fine serrations (Fig. 2O).

Female squama genitalis with short, pointed acrostyli (Fig. 1F).

Body measurements (2 females) (in μm): maximum body length 1004, head 115, pseudoculus 8, lever 3, posterior part of maxillary gland 12; pronotal setae *1* 18, *2* 11; mesonotal setae *P1* 19, *P1a* 7, *P2* 25, *M* 10, foretarsus 94–95, claw 30, empodial appendage 4.

Table 1. Body chaetotaxy of *Nienna chukotka* sp. nov.

	Dorsal		Ventral	
Segment	**Formula**	**Setal composition**	**Formula**	**Setal composition**
Th. I	4	1, 2	(2+4)/6	A1, M1, 2, P1, 2, 3
Th. II	8/16	A2, 3, 4, M P1, 1a, 2, 2a, 3, 3a, 4, 5	(5+2)/4	Ac, 2, 3, M P1, 3
Th. III	8/16	A2, 3, 4, M P1, 1a, 2, 2a, 3, 3a, 4, 5	(7+2)/4	Ac, 2, 3, 4, M P1, 3
Abd. I	8(6)/10	A1, 2, (3), 5 P1, 2, 2a, 3, 4	3/4	Ac, 2 P1, 1a
Abd. II-III	10/14	A1, 2, 3, 4, 5 P1, 2, 2a, 3, 4, 4a, 5	3/5	Ac, 2 Pc, 1a, 2
Abd. IV-V	10/14	A1, 2, 3, 4, 5 P1, 2, 2a, 3, 4, 4a, 5	3/8	Ac, 2 P1, 1a, 2, 3
Abd. VI	10/14	A1, 2, 3, 4, 5 P1, 2, 2a, 3, 4, 4a, 5	3/9	Ac, 2 Pc, 1, 1a, 2, 3
Abd. VII	10/19	A1, 2, 3, 4, 5 Pc, 1, 1a, 2, 2a, 3, 3a, 4, 4a, 5	3/9	Ac, 2 Pc, 1, 1a, 2, 3
Abd. VIII	6/15	A1, 4, 5 Pc, 2, 2a, 3, 3a, 4, 4a, 5	4/2	1, 2 P1a
Abd. IX	12	1, 1a, 2, 2a, 3, 4	4	1, 2
Abd. X	10	1, 2, 2a, 3, 4	4	1, 2
Abd. XI	6	1, 3, 4	6	
Abd. XII	9		6	

(3) – setae *A3* absent in paratype. Tergite I with 6 *A*-setae.

Chaetal variability. In the holotype, seta *P4* is doubled asymmetrically on the mesonotum; in the paratype, seta *A3* is absent symmetrically on tergite I and seta *P2a* is doubled on tergite VII.

Etymology. The species name is taken from the general locality where the specimens were collected.

Remarks. *Nienna chukotka* sp. nov. differs from *N. parvula* and *N. quinghaiensis* in the presence of seta *Pc* on tergite VII and sternites VI–VII (in *N. quinghaiensis* seta *Pc* is present on sternite VII only), the presence of 5 pairs of *A*-setae (4 pairs in the other two species) and *P3a* on tergite VII, the shape of the accessory setae on tergites and sternites I–VI (setiform in the new species, sensilliform in the other two species) and the shape of foretarsal sensilla *a*, *c* and *e* (in the other species sensillum *a* is shorter, reaching base of sensillum *t2*, sensilla *c* and *e* short and broad). The porotaxy of meso- and metanota and abdominal sternites also differs: *Nienna chukotka* has two pairs of *sl* and *al* pores on the meso- and metanota, and asymmetrical *spsm* pores on sternites IV–VII;], whereas *N. parvula* has a pair of *sl* pores on the meso- and metanota, and a simple *spm* pore on sternites VI–VII. *Nienna quinghaiensis* has *al* and *l* pores on the mesonotum, *l* pores on the metanotum, and an *spm* pore on sternite VII. The new species is more similar to *N. parvula* in possessing traces of a striate band on sternites IX–X and in the globular foretarsal sensillum *t3*. *Nienna chukotka* is characterized by the presence of *pl* on tergite I, which is the first report of posterolateral pores in Acerentomidae. Szeptycki (1988) previously described *pl* pores on *Hesperentomon martynovae*

Szeptycki, 1988 (Hesperentomidae) collected in the Altai Mts. These *pl* pores have also been recorded in other *Hesperentomon* species: *H. fopingense* Bu, Shrubovych & Yin, 2011, *H. nanshanensis* Bu & Yin, 2007, *H. xiningense* Bu & Yin, 2007 distributed in China, and *H. tianshanicum* Martynova, 1970 (Shrubovych 2010).

Discussion

The foretarsus of *N. chukotka* sp. nov. has a very long sensillum *a*, surpassing the base of sensillum *e*, and filiform foretarsal sensillum *t1*, characters shared with two species of *Alaskaentomon* (*A. fjellbergi*, *A. condei*). These two *Alaskaentomon* species possess seta *Pc* on tergite VII and sternites VI–VII. *Alaskaentomon* spp. differ from *N. chukotka* sp. nov. in having two pairs of *A*-setae on the meso- and metanota and large granulated appendices on the calyx of the maxillary gland (Shrubovych et al. 2014c). In notal chaetotaxy (three pairs of *A*-setae) and the filiform sensillum *t1*, the genus *Nienna* is similar to the genera *Callientomon* Yin, 1980, *Noldo* Szeptycki, 1988, *Paracerella* Imadaté, 1980 and *Verrucoentomon* Rusek, 1974. However, *Nienna* differs from all of them in possessing small, indistinctly granulated appendices on the calyx of the maxillary gland and in the small, nearly globular foretarsal sensillum *t3* (Shrubovych et al. 2014a). The new species differs from nearly all species of Nipponentominae in possessing a pair of *A1* setae on tergite VII (five pairs of *A*-setae), while nearly all other nipponentomines have four pairs of *A*-setae (except *Nipponentomon macleani* Nosek, 1977 from Alaska, which also has 5 pairs of *A*-setae). Therefore, *N. chukotka* sp. nov. from Chukotka is more similar in body chaetotaxy and in foretarsal sensilla pattern to members of other genera distributed in Alaska than to the other *Nienna* species distributed in more southern regions of the Palearctic. This peculiarity could be an effect of subsequent allopatric speciation resulting from successive closings of the Bering Strait and cooling of the Arctic Ocean during the Pliocene-Pleistocene. Another interesting fact is that species recorded on the northern edge of proturan distribution (only a few Protura species are known from the Arctic region) possess a larger number of setae on the body than species with a more southern distribution.

Key to *Nienna* species

1 Foretarsal sensillum *a* very long, surpassing base of sensillum *e*, tergite VII with 5 pairs of *A*-setae and with *Pc*, *P3a* present, sternites VI–VII with *Pc*.... ..... ***Nienna chukotka* sp. nov.**

– Foretarsal sensillum *a* short, nearly reaching base of sensillum *t2*, tergite VII with 4 pairs of *A*-setae and without *Pc*, *P3a* absent, sternite VI without *Pc*, sternite VII with or without *Pc* **2**

2 Foretarsal sensilla *b* and *c* nearly equal in length, seta *δ4* setiform, sternite VII without *Pc* ..... ***N. parvula* Szeptycki, 1988**

– Foretarsal sensillum *c* half the length of *b*, seta *δ4* sensilliform, sternite VII with *Pc*..... ***N. quinghaiensis* Bu & Yin, 2008**

Acknowledgements

The author is very grateful to Kirill Makarov (Moscow State Pedagogical University) and Olga Makarova (Severtsov Institute of Ecology and Evolution) for Protura material from the western Chukotka, to Anatoly Babenko (Severtsov Institute of Ecology and Evolution) for valuable comments, to Ernest C. Bernard (University of Tennessee) for English corrections and remarks, to Osami Nakamura for the review and to the editor Wanda M. Weiner for her constructive comments.

References

Bu Y, Yin WY (2007) Two new species of *Hesperentomon* Price, 1960 from Qinghai Province, Northwestern China (Protura: Hesperentomidae). Acta Zootaxonomica Sinica 32(3): 508–514.

Bu Y, Yin WY (2008) Occurrence of *Nosekiella* Rusek 1974 and *Nienna* Szeptycki 1988 (Protura: Nipponentomidae: Verrucoentominae) in China. Annales de la Société Entomologique de France 44(2): 201–207. https://doi.org/10.1080/00379271.2008.10697556

Bu Y, Shrubovych J, Yin WY (2011) Two new species of genus *Hesperentomon* Price, 1960 (Protura, Hesperentomidae) from Northern China. Zootaxa 2885: 55–64. https://doi.org/10.11646/zootaxa.2885.1.6

Bu Y, Wu D, Shrubovych J, Yin WY (2013) New *Nipponentomon* species from northern Asia (Protura: Acerentomata, Nipponentomidae). Zootaxa 3636(4): 525–546. https://doi.org/10.11646/zootaxa.3636.4.2

Dunger W, Fiedler HJ (1989) Methoden der Bodenbiologie. Gustav Fischer, Jena, 432 pp.

Galli L, Shrubovych J, Bu Y, Zinni M (2018) Genera of the Protura of the World: diagnosis, distribution, and key. ZooKeys 772: 1–45. https://doi.org/10.3897/zookeys.772.24410

Imadaté G (1980) A new genus of Acerentomidae (Protura) from Japan and North America. Kontyû 48: 278–290.

Martynova EF (1970) New species of Protura from the High Mountain Region of Tian Shan. Zoologicheskii Zhurnal 49: 236–240. [in Russian]

Nosek J (1977) A new genus and six new species of Protura from Alaska (Protura: Acerentomidae, Eosentomidae). Entomologica Scandinavica 8(4): 271–284. https://doi.org/10.1163/187631277X00378

Nosek J (1981) Three new Protura from Alaska with key to known Alaskan species (Insecta: Protura). Entomologica Scandinavica 12(2): 158–162. https://doi.org/10.1163/187631281794709827

Rusek J (1974) Zur Taxonomie einiger Gattungen der Familie Acerentomidae (Insecta, Protura). Acta entomologica bohemoslovaca 71: 260–281.

Rusek J, Shrubovych J, Szeptycki A (2012) Head porotaxy and chaetotaxy of order Acerentomata (Protura). Zootaxa 3262: 54–61. https://doi.org/10.11646/zootaxa.3262.1.5

Shrubovych J (2009) *Nipponentomon jaceki* sp. nov. from the Russian Far East (Protura: Acerentomidae, Nipponentominae). Zootaxa 2231: 55–61. https://doi.org/10.11646/zootaxa.2231.1.4

Shrubovych J (2010) Redescription of *Hesperentomon tianshanicum* Martynova, 1970 (Protura: Acerentomata, Hesperentomidae) and key to *Hesperentomon* species. Zootaxa 2720: 28–34. https://doi.org/10.11646/zootaxa.2720.1.2

Shrubovych J (2011) Redescription of *Verrucoentomon montanum* new status (= *Acerella montana* Martynova) (Protura: Acerentomidae, Nipponentominae). Zootaxa 2743: 63–67. https://doi.org/10.1603/AN12135

Shrubovych J (2014) Identification and character analysis of the Acerentomidae (Protura) of the northeastern Palearctic (Protura: Acerentomidae). Zootaxa 3755(2): 136–164. https://doi.org/10.11646/zootaxa.3755.2.2

Shrubovych J, Bernard EC (2012) Two new species of *Verrucoentomon* Rusek (Protura: Acerentomidae, Nipponentominae) and a key to species. Annals of the Entomological Society of America 105(5): 628–637. https://doi.org/10.1603/AN11175

Shrubovych J, Smykla J (2012) Review of the genus *Paracerella* Imadaté (Protura: Acerentomidae, Nipponentominae) with identification key and description of a new species. Zootaxa 3509: 69–76. https://doi.org/10.11646/zootaxa.3509.1.4

Shrubovych J, Rusek J, Bernard EC (2012) Redefinition and four new species of *Yavanna* Szeptycki and comparison with *Nosekiella* Rusek (Protura: Acerentomidae: Nipponentominae). Annals of the Entomological Society of America 105(1): 3–19. https://doi.org/10.1603/AN11119

Shrubovych J, Rusek J, Bernard EC (2014a) Revision of *Vesiculentomon*, *Nosekientomon* n. g. (Protura: Acerentomidae, Nipponentominae) with a key to genera of Nipponentominae. Annals of the Entomological Society of America 107(1): 74–80. https://doi.org/10.1603/AN12135

Shrubovych J, Rusek J, Bernard EC (2014b) Revision of *Nosekiella* (Protura: Acerentomidae, Nipponentominae). Annals of the Entomological Society of America 107(4): 721–727. https://doi.org/10.1603/AN13160

Shrubovych J, Rusek J, Smykla J, Bernard EC (2014c) Revision of *Alaskaentomon* Rusek (Protura: Acerentomidae: Nipponentominae). Annals of the Entomological Society of America 107(4): 728–733. https://doi.org/10.1603/AN13160

Szeptycki A (1988) New genera and species of Protura from the Altai Mts. Acta Zoologica Cracoviensa 31: 297–362.

Szeptycki A (2007) Catalogue of the world Protura. Acta Zoologica Cracoviensa 50B(1): 1–210.

Yin WY (1980) Studies on Chinese Protura: Description of new species and new genera of the family Acerentomidae with discussions on their phylogenetic significance. Contributions from Shanghai Institute of Entomology 1980: 135–156. [In Chinese with English summary]

Yin WY (1983) Grouping the known genera of Protura under eight families with keys for determination. Contributions from Shanghai Institute of Entomology 3(1982–1983): 151–163. [In Chinese with English summary]

ZooKeys 899: 47–58 (2019)
doi: 10.3897/zookeys.899.39638
http://zookeys.pensoft.net

RESEARCH ARTICLE

A peer-reviewed open-access journal
ZooKeys
Launched to accelerate biodiversity research

A study of the endohelminths of the European perch *Perca fluviatilis* L. from the central region of the Danube river basin in Slovakia

Ľudmila Juhásová[1], Alžbeta Radačovská[1], Eva Bazsalovicsová[1], Dana Miklisová[1], Marcela Bindzárová-Gereľová[2], Ivica Králová-Hromadová[1]

1 *Institute of Parasitology, Slovak Academy of Sciences, Hlinkova 3, 040 01 Košice, Slovakia* **2** *Institute of Geodesy, Cartography and Geographical Information Systems, Technical University of Košice, Faculty of Mining, Ecology, Process Control and Geotechnologies, PK 19, 04120 Košice, Slovakia*

Corresponding author: *Ivica Králová-Hromadová* (hromadova@saske.sk)

Academic editor: *D. Gibson* | Received 2 September 2019 | Accepted 26 November 2019 | Published 12 December 2019

http://zoobank.org/AE5CC6F3-D5FD-472F-AAC9-2BC6A145A5BC

Citation: Juhásová Ľ, Radačovská A, Bazsalovicsová E, Miklisová D, Bindzárová-Gergeľová M, Králová-Hromadová I (2019) A study of the endohelminths of the European perch *Perca fluviatilis* L. from the central region of the Danube river basin in Slovakia. ZooKeys 899: 47–58. https://doi.org/10.3897/zookeys.899.39638

Abstract

The European perch *Perca fluviatilis* L. serves as a host of different endohelminths of Trematoda, Cestoda, Nematoda, and Acanthocephala. Its natural range covers freshwater basins throughout much of Europe, including the Danube. Since information about endohelminths of European perch from this international river basin has been rather sporadic, the parasitological examinations of 700 perch from the central region of the Danube river basin in Slovakia were performed in October 2017 and April 2018. The larval stages of *Triaenophorus nodulosus* (Cestoda) were found in cysts located in the perch liver and adults of *Proteocephalus percae* (Cestoda) were isolated from the intestine. The larval stages of *Eustrongylides* sp. (Nematoda) and metacercariae of *Clinostomum complanatum* (Trematoda), both potential causative agents of fish-borne zoonoses, were found in the musculature. Spatial and seasonal differences in the occurrence of currently detected helminths were discussed with data on biological and environmental conditions of particular sampling site.

Keywords

endoparasites, *Clinostomum complanatum*, *Eustrongylides* sp., Percidae, *Proteocephalus percae*, *Triaenophorus nodulosus*

Introduction

The Danube is the second longest river in Europe shared by 10 European countries, including Germany, Austria, Slovakia, Hungary, Croatia, Serbia, Romania, Bulgaria, Moldova, and Ukraine. The Danube river basin, one of the most international river basins in the world (Liska 2015), is divided into Upper, Middle, and Lower basins (Liška et al. 2008). The largest part is the Middle Basin, which includes the area from Bratislava in Slovakia to the Iron Gate dams at the border of Serbia and Romania (Paunovic et al. 2007).

The Danube represents an important ecosystem with a high biodiversity of aquatic organisms (Tockner et al. 1998). A study on the fish fauna of the entire course of the Danube revealed the presence a high diversity of some 100 fish species, including cyprinids, silurids, esocids, percids, anguillids, and salmonids (Schiemer et al. 2004). Due to its international character and rich fish fauna, the Danube also plays a notable role in the spreading of various parasitic and infectious fish diseases.

Percids represent a so-called promising fish species for a fishery and aquaculture (Kestemont et al. 2015). The European perch, *Perca fluviatilis* Linnaeus, 1758, is an ecologically significant predator and popular sport fish noted for its fighting qualities and taste (Popova and Sytina 1977). It is among the most common and widely distributed members of the Percidae throughout Europe (Giannetto et al. 2012), including the Danube.

The European perch serves as a host for different endohelminths (Trematoda, Cestoda, Nematoda, and Acanthocephala). However, only a few parasitological studies have been conducted on the European perch from the Danube since the 1980s. All of them were in the Lower Basin, in particular in Srebarna Lake (north-eastern Bulgaria), which is connected via an artificial canal to the Bulgarian part of the Danube (Kakacheva-Avramova 1983; Shukerova et al. 2010; Atanasov 2012; Kirin et al. 2013). Since no recent information about endohelminths of the European perch from the Middle Danube is available, parasitological examinations of perch from five selected localities in the Slovak part of the river were performed in two periods of the year. The spatial and seasonal differences in the occurrence of detected endohelminths were discussed with data on biological and environmental conditions of particular sampling site.

Material and methods

Material

The European perch were collected from the central region of the Danube, in particular from four river branches (RB) located next to the main stream and from Šulianske Lake, a gravel pit permanently flooded with water and near the Danube (Fig. 1).

In total, 700 individuals of European perch (length 107–165 mm; 71.4% females and 28.6% males) from all localities were caught by professional fishermen in October 2017 and April 2018. The number of fish obtained during both seasons was approximately equal (October 49.4%; April 50.6%; for more details see Table 2). Incomplete

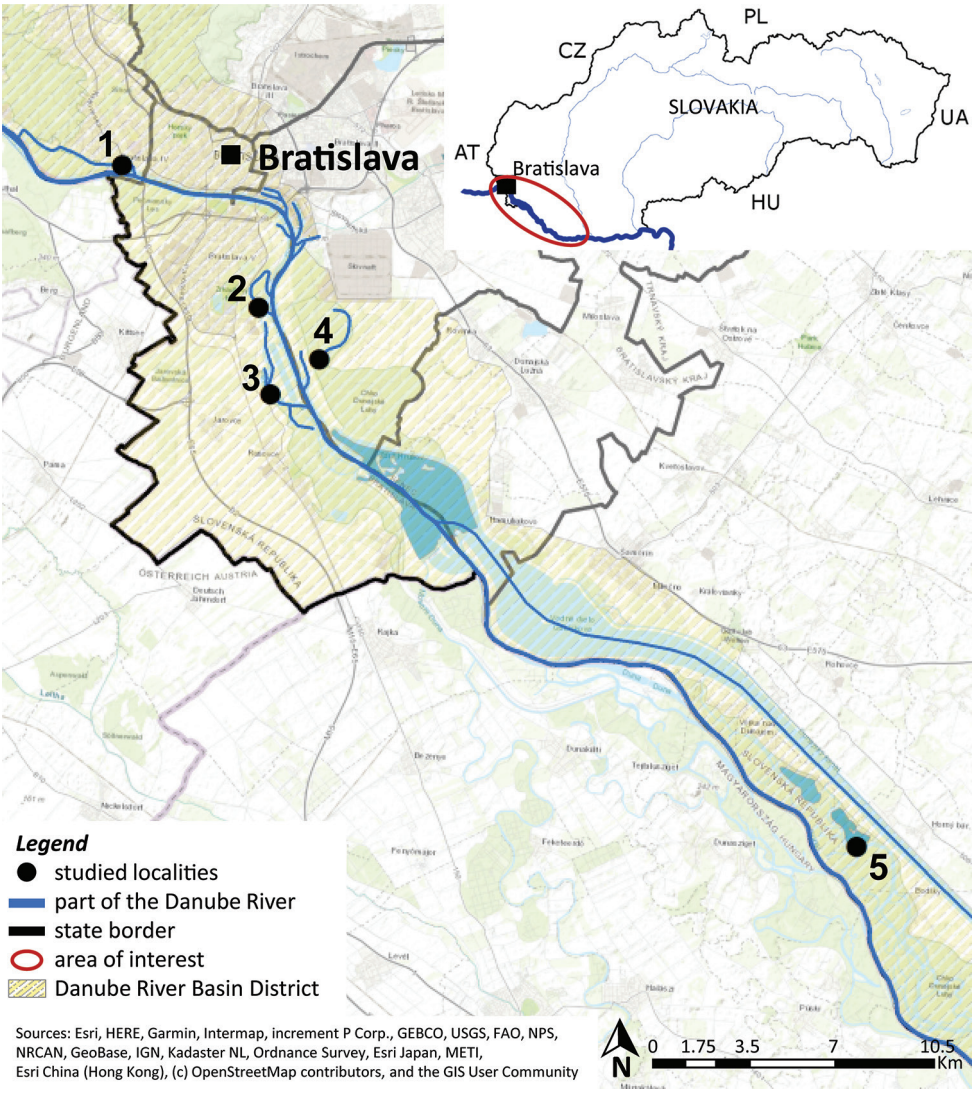

Figure 1. The schematic presentation of sampling sites in Slovak part of the Danube. 1, Karloveské river branch (48°8'46.08"N, 17°3'50.33"E); 2, Starohájske river branch (48°6'11.50"N, 17°7'56.19"E); 3, Jarovecké river branch (48°4'32.34"N, 17°8'23.90"E); 4, Biskupické river branch (48°5'15.45"N, 17°9'44.21"E); 5, Šulianske Lake (47°56'26.66"N, 17°25'42.55"E).

parasitological necropsy included a detailed examination of the peritoneal cavity, intestine, liver and other abdominal organs. In order to examine the musculature of perch, thin (approximately 5 mm) slices of fillets of whole fish were examined. The skin, gills, and eyes were not investigated. The parasites were washed in a physiological solution and observed under a stereoscopic microscope for morphological identification to genus and/or species level using taxonomic keys (Moravec 1994; Scholz and Hanzelová 1998; Gibson et al. 2002; Kuchta et al. 2008).

Molecular genotyping

The parasites were rinsed in physiological solution and fixed in 96% ethanol immediately after dissection. Taxonomic identification of the parasites to the species level was performed by molecular genotyping using a partial small subunit of the nuclear ribosomal RNA gene (ssrDNA) as a molecular marker. For PCR amplification and sequencing of ssrDNA, the following universal primers were applied: WormA (5'–GCGAATGGCTCATTAAATCAG–3') and WormB (5'–CTTGTTACGACTTTTACTTCC–3') (Littlewood and Olson 2001). Details on PCR amplification, sequencing and sequence analysis were published in Bazsalovicsová et al. (2018). The data obtained were compared with sequences deposited in the GenBank database (https://www.ncbi.nlm.nih.gov/).

Statistical tests

Fisher's exact test was used to compare the prevalence of endohelminths from the five studied localities between the two seasons. The samples were initially analysed as separate observations of the locality per season for each parasite species, then consequently evaluated independently to the examination timing for each locality. A p value under 0.05 was considered to be significant. Moreover, 95% confidence intervals (CI) were calculated individually for each proportion. The statistical analyses were performed by the Quantitative Parasitology on the Web (Reiczigel et al. 2019).

Results

Of the 700 European perch examined from five sampling sites in the Middle Danube river basin in Slovakia in October 2017 and April 2018, 176 were found to be infected (prevalence 25.1%; CI 22.0–28.5%). Endohelminths were determined in all the studied localities; however, species composition and prevalence varied between different sampling sites and/or examination timing.

Two tapeworms were found in European perch; larval stages of *Triaenophorus nodulosus* (Pallas, 1781) Rudolphi, 1793 (Bothriocephalidea) were found in cysts localized in the liver, and juveniles to adults (at different stages of maturity) of *Proteocephalus percae* (Müller, 1780) (Proteocephalidea) were isolated from the pyloric caeca. In the musculature, the larval stages of the nematodes of the genus *Eustrongylides* Jägerskiöld, 1909 (Dioctophymatoidea) and metacercariae of the fluke *Clinostomum complanatum* (Rudolphi, 1814) Braun, 1899 (Diplostomida) were detected.

To confirm the taxonomic status of all detected species, ssrDNA was applied as the molecular marker for genotyping. After PCR amplification, a 730 bp fragment was obtained, sequenced and compared with sequences of respective species deposited in the GenBank. The ssrDNA sequence of *T. nodulosus* from our study was 100% identical with *T. nodulosus* from pike (*Esox lucius*) from Scotland (GenBank Accession number KR780923; Bra-

bec et al. 2015), and the one of *P. percae* was 100% identical with *P. percae* from European perch from Switzerland (KX768934; Scholz et al. 2017). The nematode *C. complanatum* corresponded (100% identity) with *C. complanatum* from Italy (FJ609420; Gustinelli et al. 2010). The sequence of *Eustrongylides* sp. was 99.1% identical with *Eustrongylides* sp. from dwarf snakehead (*Channa gachua*) from India (MG696298; unpublished).

Note: Although more than 20 species of the genus *Eustrongylides* were originally described, the validity of many of them is disputable (Eberhard and Ruiz-Tiben 2014). A revision of the genus revealed that there are three valid species: the type species *Eustrongylides tubifex* (Nitzsch & Rudolphi, 1819) Jägerskiöld, 1909; *Eustrongylides ignotus* Jägerskiöld, 1909; and *Eustrongylides excisus* Jägerskiöld, 1909 (Measures 1988). Although *E. excisus* and *E. tubifex* have previously been reported from perch in the Lower Danube (Table 1), there are no data on any DNA region of both nematodes available in the GenBank database. The sequences obtained in the current study corresponded to the sequence data on species assigned as *Eustrongylides* sp.

Triaenophorus nodulosus (larvae)

The mean intensity of infection (MI) for *T. nodulosus* from all five localities ranged between 1.0 and 9.5 (Table 2). The overall highest prevalence was observed for *T. nodulosus* in perch from the Biskupické RB, with higher values in October (P = 49%) than in April (P = 23%). On the contrary, larvae of this tapeworm were not detected in Šulianske Lake irrespective of the season (Fig. 2; Table 2). There were no statistically significant differences between sampling periods in all studied localities, except for the Biskupické RB ($p < 0.05$) (Table 2).

Proteocephalus percae (adult)

The MI for this intestinal tapeworm was 2.3 and 4.0 (Table 2). It was detected in two out of five localities, in particular in the Karloveské RB (P = 7.0%) and Starohájske RB (P = 11.1%); at both localities *P. percae* was present only in spring (Fig. 2, Table 2).

Clinostomum complanatum (metacercariae)

The mean intensity of infection ranged between 1.0–3.4 (Table 2). The highest prevalence (45%) was detected in the Biskupické RB in October and markedly lower values (P = 10%) were recorded in April (Fig. 2; Table 2). A similar seasonal pattern was observed in Šulianske Lake (October, P = 14%; April, P = 6%). While there was high statistical support for the results in the Biskupické RB ($p < 0.001$), data detected in Šulianske Lake were statistically nonsignificant (Table 2). Opposite results were observed in the three remaining localities, where metacercariae of *C. complanatum* were not detected in October but were present in April (Fig. 2; Table 2).

Table 1. Summary of the literature data (1980–2019) of endohelminths detected in European perch *Perca fluviatilis* L. in the Danube.

Parasite	Locality	Season	No.	P (%)	Dev. stage	References
CESTODA						
Proteocephalus percae	Srebarna Lake, NE Bulgaria	autumn	60	3.3	A	Shukerova et al. 2010
		spring	60	1.7	A	Shukerova et al. 2010
TREMATODA						
Bolboforus confusus	Srebarna Lake, NE Bulgaria	spring	60	3.3	M	Shukerova et al. 2010
		summer	60	10.0	M	Shukerova et al. 2010
		autumn	60	1.7	M	Shukerova et al. 2010
Diplostomum pseudospathaceum	Srebarna Lake, NE Bulgaria	autumn	60	1.1	M	Shukerova et al. 2010
	River Danube, Bulgaria	n.a.	40	20.0	M	Atanasov 2012
Diplostomum spathaceum	Srebarna Lake, NE Bulgaria	spring	60	3.3	M	Shukerova et al. 2010
		summer	60	1.7	M	Shukerova et al. 2010
Ichthyocotylurus pileatus	Srebarna Lake, NE Bulgaria	summer	60	3.3	M	Shukerova et al. 2010
Posthodiplostomum cuticola	Srebarna Lake, NE Bulgaria	summer	60	1.7	M	Shukerova et al. 2010
Tylodelphys clavata	Srebarna Lake, NE Bulgaria	spring	60	56.7	M	Shukerova et al. 2010
		summer	60	81.7	M	Shukerova et al. 2010
		autumn	60	86.7	M	Shukerova et al. 2010
NEMATODA						
Contracaecum microcephalum	Srebarna Lake, NE Bulgaria	autumn	60	3.3	L	Shukerova et al. 2010
Eustrongylides excisus	Srebarna Lake, NE Bulgaria	spring	60	8.3	L	Shukerova et al. 2010
		summer	60	10.0	L	Shukerova et al. 2010
		autumn	60	23.3	L	Shukerova et al. 2010
	River Danube, Bulgaria	n.a.	40	7.5	L	Atanasov 2012
	Srebarna Lake, NE Bulgaria	summer	n.a.	100	L	Kirin et al. 2013
	River Danube, Bulgaria	summer	n.a.	100	L	Kirin et al. 2013
Eustrongylides tubifex	Srebarna Lake, NE Bulgaria	autumn	60	1.7	L	Shukerova et al. 2010
Rhaphidascaris acus	Srebarna Lake, NE Bulgaria	summer	60	10.0	L	Shukerova et al. 2010
ACANTHOCEPHALA						
Acanthocephalus lucii	River Danube, Bulgaria	n.a.	n.a.	n.a.	n.a.	Kakacheva-Avramova 1983
	Srebarna Lake, NE Bulgaria	spring	60	1.7	A	Shukerova et al. 2010
Acanthocephalus anguillae	Srebarna Lake, NE Bulgaria	spring	60	1.7	A	Shukerova et al. 2010

No. number of fish examined, P prevalence, Dev. stage developmental stage, NE north-eastern, n.a. not available, A adults, L larvae, M metacercariae.

Eustrongylides sp. (larvae)

The MI values ranged between 1.0–2.8 (Table 2). The larvae of *Eustrongylides* sp. were detected in perch musculature at the highest prevalence in the Jarovecké RB, where no striking differences were detected between October (P = 26%) and April (P = 24%) (Fig. 2; Table 2). A similar prevalence (P = 22%) was detected in Šulianske Lake in spring, while lower prevalence (P = 5%) was recorded in October (Fig. 2; Table 2). Larvae of *Eustrongylides* sp. were not detected in the Karloveské RB (Fig. 2; Table 2).

Table 2. Statistical data on detected endohelminths of European perch *Perca fluviatilis* L. from studied localities in the Danube river basin, Slovakia.

Locality	TE	No.	*Triaenophorus nodulosus* (Cestoda)					*Proteocephalus percae* (Cestoda)				
			IF	MI (max)	P (%)	FET	95% CI	IF	MI (max)	P (%)	FET	95% CI
Karloveské RB	Oct/17	29	2	9.5 (15)	7	ns	1–23	0	–	–	–	–
	Apr/18	57	3	1.0 (1)	5	ns	1–15	4	4.0 (4)	7	ns	2–17
Starohájske RB	Oct/17	143	3	3.0 (4)	2.1	ns	0.4–6.0	0	–	–	–	–
	Apr/18	171	10	2.8 (12)	5.8	ns	2.8–10.5	19	2.3 (8)	11.1	***	6.8–16.8
Jarovecké RB	Oct/17	70	3	1.3 (2)	4	ns	1–12	0	–	–	–	–
	Apr/18	49	2	5.0 (9)	4	ns	5–14	0	–	–	–	–
Biskupické RB	Oct/17	67	33	7.1 (20)	49	*	37–62	0	–	–	–	–
	Apr/18	31	7	6.4 (12)	23	*	10–41	0	–	–	–	–
Šulianske Lake	Oct/17	37	0	–	–	–	–	0	–	–	–	–
	Apr/18	46	0	–	–	–	–	0	–	–	–	–
In total		**700**	**63**	**5.6 (20)**	**9.0**	**–**	**7.0–11.4**	**23**	**2.3 (8)**	**3.3**	**–**	**2.1–4.9**
			***Clinostomum complanatum* (Trematoda)**					***Eustrongylides* sp. (Nematoda)**				
			IF	MI (max)	P (%)	FET	95% CI	IF	MI (max)	P (%)	FET	95% CI
Karloveské RB	Oct/17	29	0	–	–	–	–	0	–	–	–	–
	Apr/18	57	2	2.0 (2)	4	ns	1–12	0	–	–	–	–
Starohájske RB	Oct/17	143	0	–	–	–	–	6	1.3 (2)	4.2	ns	1.6–8.9
	Apr/18	171	5	1.0 (1)	2.9	ns	1.0–6.7	11	1.9 (10)	6.4	ns	3.3–11.2
Jarovecké RB	Oct/17	70	0	–	–	–	–	18	1.4 (5)	26	ns	16–38
	Apr/18	49	6	2.0 (6)	12	**	5–25	12	2.2 (7)	24	ns	13–39
Biskupické RB	Oct/17	67	30	3.4 (23)	45	***	33–57	5	1.0 (1)	8	ns	2–17
	Apr/18	31	3	2.0 (2)	10	***	2–26	1	1.0 (1)	3	ns	0–17
Šulianske Lake	Oct/17	37	5	1.6 (4)	14	ns	4–28	2	1.0 (1)	5	ns	7–18
	Apr/18	46	3	1.0 (1)	6	ns	1–18	10	2.8 (7)	22	ns	11–36
In total		**700**	**54**	**2.6 (23)**	**7.7**	**–**	**5.8–9.9**	**65**	**1.8 (10)**	**9.3**	**–**	**7.2–11.7**

RB river branch, TE timing of examination, Oct/17 October 2017, Apr/18 April 2018, No. number of fish examined, IF number of infected fish, MI mean intensity of infection, max maximum number of parasites, P prevalence, FET Fisher's exact test of seasonal differences in prevalence for each locality separately, 95% CI confidence interval, ns nonsignificant, * $p < 0.05$, ** $p < 0.01$, *** $p < 0.001$

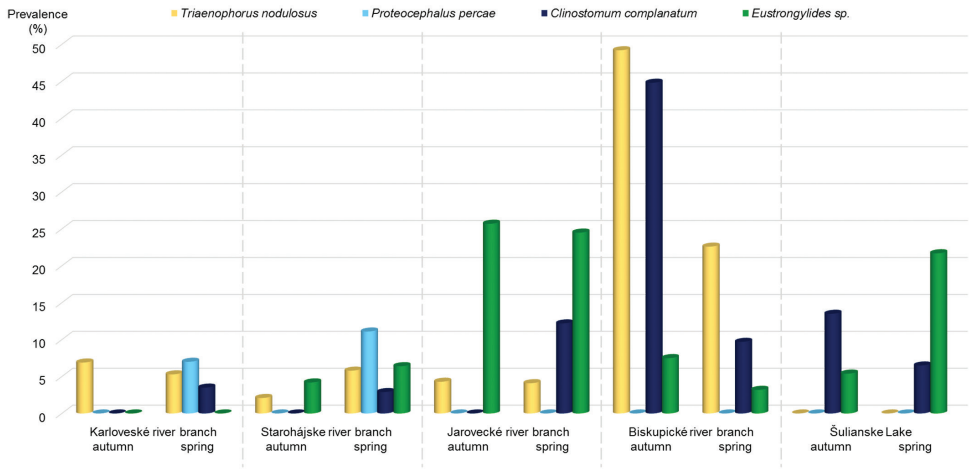

Figure 2. Schematic presentation of prevalence of the parasites found in the five studied localities in autumn and spring.

Discussion

Over the last four decades, several species of flukes and nematodes, two species of thorny-headed worms and single tapeworm have been found in European perch from the Danube (for details, see Table 1 and references therein). In the current study, only four endohelmints were detected in perch from the central region of the river. Metacercariae of *C. complanatum* were detected for the first time, while *P. percae* and *Eustrongylides* sp. were previously found in Srebarna Lake in north-eastern Bulgaria (Shukerova et al. 2010; Kirin et al. 2013). The only record of the presence of *T. nodulosus* in perch from the Danube was published more than 60 years ago (Dyk 1955). Spatial and seasonal differences in the occurrence of currently detected helminths could be explained by diverse environmental conditions of particular sampling site and by an availability of suitable definitive hosts.

The occurrence of *T. nodulosus* in the studied localities was rather diverse; it was absent in Šulianske Lake, while low values of prevalence were documented in Karloveské, Starohájske and Jarovecké RB. The highest prevalence was detected in the Biskupické RB, a branch of the river about 20 m wide and connected to the Danube by an artificial channel (Jursa 2003). Water in the stream branch has rich fish diversity, and it is regularly restocked with various fish species, including perch (second intermediate host) and pike (definitive host of *T. nodulosus*). The high prevalence of *T. nodulosus* in this particular RB may be related to the fact that 5000 individuals of pike were restocked in the Biskupické RB in December 2015 (http://cokdezakolko.sk/category/zarybnenie/; in Slovak).

The prevalence of *T. nodulosus* in the Biskupické RB was significantly higher in autumn. On the contrary, no evident seasonal variation was detected in three other stud-

ied localities. Since plerocercoids can live in the intermediate fish host up to three years, little or no seasonal variations have been previously detected in periodicity of *T. nodulosus* in perch. Besides, the dynamics of infections and maintenance of plerocercoids in fish may vary considerably from water to water (Chubb 1980 and references therein).

The second tapeworm detected in the current work, *P. percae*, was present in Karloveské and Starohájske RB only in spring (April). Similar seasonal dynamics with the maximum values of prevalence in March and April were also observed by Scholz (1986) and Chubb (1982), respectively.

The two remaining helminths, *C. complanatum* and *Eustrongylides* sp., utilize birds as definitive hosts. The Protected Bird Area of the Danube floodplain is a refuge for tens of thousands of birds; it is an internationally important breeding area, nesting site, migration corridor, and wintering place of migratory and resident birds, such as mallard, great crested grebe, cormorant, black stork and other long-necked wading birds, which serve as definitive host of the above species. This has evidently played an important role in a broad spatial distribution of both endohelminths; while *C. complanatum* was detected in all five studied localities, *Eustrongylides* sp. was absent only in Karloveské RB.

Whereas birds are preferable hosts of *C. complanatum*, humans can be incidentally infected by eating raw or undercooked freshwater fish infected by *C. complanatum* metacercariae (Soylu 2013), causing parasitic pharyngitis and laryngitis (Gaglio et al. 2016). Human infections are rather rare and have occurred mainly in Asian countries (e.g. Korea) with a tradition of eating raw fish (Kim et al. 2019).

Eustrongylides sp. may also pose a public health risk to consumers of raw or undercooked fish, such as perch (Branciari et al. 2016). Human infections have been recorded mainly in Asia (Ljubojevic et al. 2015) or Africa (Eberhard and Ruiz-Tiben 2014). Although humans are not frequent hosts for species of *Eustrongylides*, it is known that this fish-borne zoonosis can cause gastritis and intestinal perforation in occasionally infected human. According to the recommendations of the European Commission, food producers should visually examine fish products before their release to the market (Branciari et al. 2016). Since larvae of species of *Eustrongylides* are typically large and are conspicuously red, they are easily differentiated from the fish tissue, even by visual inspection.

A potential risk of transmission of *C. complanatum* and *Eustrongylides* sp. from perch to humans in Europe is very limited, although it can not be absolutely excluded. A good example is diphyllobothriosis, fish-borne zoonosis, which re-emergence in the subalpine region was due to increased popularity of raw perch dishes (Wicht et al. 2009).

The Danube and its adjacent floodplain forests are characterized by rich aquatic and terrestrial faunas. However, anthropogenic activities, such as hydropower dams (Schiemer et al. 2004) may influence diversity and number of aquatic species (Guti 1992). The data on fish parasites from the Danube are, in general, scarce. Since some information are rather old and require updates, up-to-date surveys are necessary for accurate knowledge on fish parasites from this dynamically changing aquatic environment.

Acknowledgements

The work was financially supported by the Slovak Research and Development Agency under contract APVV-15-0004, the Slovak Grant Agency VEGA no. 2/0134/17, and by the Research and Development Operational Programme funded by the ERDF: Environmental protection against parasitozoonoses under the influence of global climate and social changes (code ITMS: 26220220116; rate 0.2). The authors would like to acknowledge Dr Daniel Gruľa for his help and assistance during fieldwork.

References

Atanasov G (2012) Fauna, morphology and biology on the endohelminths of fish from Bulgarian part of the Danube river. PhD thesis, Sofia, Bulgaria, Bulgarian Academy of Science. [In Bulgarian]

Bazsalovicsová E, Králová-Hromadová I, Xi BW, Štefka J (2018) Tour around the globe: the case of invasive tapeworm *Atractolytocestus huronensis* (Cestoda: Caryophyllidea), a parasite of common carp. Parasitology International 67: 366–374. https://doi.org/10.1016/j.parint.2018.02.004

Brabec J, Waeschenbach A, Scholz T, Littlewood DTJ, Kuchta R (2015) Molecular phylogeny of the Bothriocephalidea (Cestoda): molecular data challenge morphological classification. International Journal for Parasitology 45: 761–771. https://doi.org/10.1016/j.ijpara.2015.05.006

Branciari R, Ranucci D, Miraglia D, Valiani A, Veronesi F, Urbani E, Lo Vaglio G, Pascucci L, Franceschini R (2016) Occurrence of parasites of the genus *Eustrongylides* spp. (Nematoda: Dioctophymatidae) in fish caught in Trasimeno Lake, Italy. Italian Journal of Food Safety 5: 206–209. https://doi.org/10.4081/ijfs.2016.6130

Chubb JC (1980) Seasonal occurrence of helminths in freshwater fishes. Part III. Larval Cestoda and Nematoda. In: Lumsden WHR, Müller R, Baker JR (Eds) Advances in Parasitology 18. Academic Press, London, 1–120. https://doi.org/10.1016/S0065-308X(08)60398-X

Chubb JC (1982) Seasonal occurrence of helminths in freshwater fishes. Part IV. Adult Cestoda, Nematoda and Acanthocephala In: Lumsden WHR, Müller R, Baker JR (Eds) Advances in Parasitology 20. Academic Press, London, 1–292. https://doi.org/10.1016/S0065-308X(08)60539-4

Dyk V (1955) Present stage of investigation of the parasites of Slovak fishes. Biologia 10: 162–172.

Eberhard ML, Ruiz-Tiben E (2014) Case report: cutaneous emergence of *Eustrongylides* in two persons from South Sudan. American Journal of Tropical Medicine and Hygiene 90: 315–317. https://doi.org/10.4269/ajtmh.13-0638

Gaglio G, Reina V, Caffara M, Gjurcevic E, Iaria C, Marino F (2016) Risk of introduction of *Clinostomum complanatum* (Digenea: Clinostomidae) to Sicily through use of *Cobitis bilineata* (Canestrini, 1865) as live baits. Bulletin of the European Association of Fish Pathologists 36: 105–110.

Giannetto D, Carosi A, Franchi E, Pedicillo G, Pompei L, Lorenzoni M (2012) Assessing the impact of non-native freshwater fishes on native species using relative weight. Knowledge and Management of Aquatic Ecosystems 404: 03. https://doi.org/10.1051/kmae/2011081

Gibson DI, Jones A, Bray RA (2002) Keys to the Trematoda. Vol 1. CABI Publishing and The Natural History Museum, London, 521 pp. https://doi.org/10.1079/9780851995472.0000

Gustinelli A, Caffara M, Florio D, Otachi EO, Wathuta EM, Fioravanti ML (2010) First description of the adult stage of *Clinostomum cutaneum* Paperna, 1964 (Digenea: Clinostomidae) from grey herons *Ardea cinerea* L. and a redescription of the metacercaria from the Nile tilapia *Oreochromis niloticus niloticus* (L.) in Kenya. Systematic Parasitology 76: 39–51. https://doi.org/10.1007/s11230-010-9231-5

Guti G (1992) The population density of perch, *Perca fluviatilis* L. in the Cikola backwater system of the river Danube, Hungary. Hydrobiologia 242: 195–198. https://doi.org/10.1007/BF00019968

Jursa M (2003) Interesting findings of macrophytes from 3 aquatic biotopes of Bratislava territory. Bulletin Slovenskej botanickej spoločnosti 25: 115–120. [In Slovak]

Kakacheva-Avramova D (1983) Helminths of freshwater fishes in Bulgaria. Bulgarian Academy of Sciences, Sofia, 261 pp. [In Bulgarian]

Kestemont P, Dabrowski K, Summerfelt RC (2015) Biology and culture of percid fishes. Springer, Dordrecht, 901 pp. https://doi.org/10.1007/978-94-017-7227-3

Kim H, Cho S, Oh H, Byeon HK (2019) A case of unexpected *Clinostomum complanatum* infection initially presenting as foreign body in pharynx. Korean Journal of Parasitology 57: 175–177. https://doi.org/10.3347/kjp.2019.57.2.175

Kirin D, Hanzelová V, Shukerova S, Hristov S, Turcekova L, Spakulova M (2013) Helminth communities of fishes from the river Danube and Lake Srebarna, Bulgaria. Scientific papers Series D Animal Science 56: 333–340.

Kuchta R, Scholz T, Brabec J, Bray RA (2008) Suppression of the tapeworm order Pseudophyllidea (Platyhelminthes: Eucestoda) and the proposal of two new orders, Bothriocephalidea and Diphyllobothriidea. International Journal for Parasitology 38: 49–55. https://doi.org/10.1016/j.ijpara.2007.08.005

Liska I (2015) The Danube River Basin. The Handbook of Environmental Chemistry, vol. 39. Springer, Berlin, 523 pp. https://doi.org/10.1007/978-3-662-47739-7

Liška I, Wagner F, Slobodník J (2008) Joint Danube survey 2. Final scientific report. ICPDR – International commission for the protection of the Danube River, Vienna, Austria, 242 pp.

Littlewood DTJ, Olson PD (2001) Small subunit rDNA and the plathelminthes: signal, noise, conflict and compromise. In: Littlewood DTJ, Bray RA (Eds) Interrelationships of the Platyhelminthes. Taylor & Francis, New York, 262–278. https://doi.org/10.1080/106351502753475961

Ljubojevic D, Novakov N, Djordjevic V, Radosavljevic V, Pelic M, Cirkovic M (2015) Potential parasitic hazards for humans in fish meat. Procedia Food Science 5: 172–175. https://doi.org/10.1016/j.profoo.2015.09.049

Measures LN (1988) Revision of the genus *Eustrongylides* Jägerskiöld, 1909 (Nematoda: Dioctophymatoidea) of piscivorous birds. Canadian Journal of Zoology 66: 885–895. https://doi.org/10.1139/z88-131

Moravec F (1994) Parasitic Nematodes of Freshwater Fishes of Europe. Academia, Praha, 470 pp.

Paunovic MM, Jakovcev-Todorovic DG, Simic VM, Stojanovic B, Cakic PD (2007) Macroinvertebrates along the Serbian section of the Danube River (stream km 1429–925). Biologia 62: 214–221. https://doi.org/10.2478/s11756-007-0032-5

Popova OA, Sytina LA (1977) Food and feeding relations of Eurasian perch (*Perca fluviatilis*) and pikeperch (*Stizostedion lucioperca*) in various waters of the USSR. Journal of the Fisheries Research Board of Canada 34: 1559–1570. https://doi.org/10.1139/f77-219

Reiczigel J, Marozzi M, Fábián I, Rózsa L (2019) Biostatistics for parasitologists – a primer to quantitative parasitology. Trends in Parasitology 35: 277–281. https://doi.org/10.1016/j.pt.2019.01.003

Schiemer F, Guti G, Keckeis H, Staras M (2004) Ecological status and problems of the Danube and its fish fauna: a review. In: Welcomme RL, Petr R (Eds) Proceedings of the Second International Symposium on the Management of Large Rivers for Fisheries, Phnom Penh, Cambodia, 11–14 February 2003. Bangkok, Food and Agriculture Organization of the United Nations & The Mekong River Commission, Thailand, 273–299.

Scholz T (1986) Observations on the ecology of five species of intestinal helminths in perch (*Perca fluviatilis*) from Mácha lake fishpond system, Czechoslovakia. Věstník československé společnosti zoologické 50: 300–320.

Scholz T, Hanzelová V (1998) Tapeworms of the Genus *Proteocephalus* Weinland, 1858 (Cestoda: Proteocephalidae), Parasites of Fishes in Europe. Academia, Praha, 118 pp. https://doi.org/10.2307/3285724

Scholz T, de Chambrier A, Shimazu T, Ermolenko A, Waeschenbach A (2017) Proteocephalid tapeworms (Cestoda: Onchoproteocephalidea) of loaches (Cobitoidea): Evidence for monophyly and high endemism of parasites in the Far East. Parasitology International 66: 871–883. https://doi.org/10.1016/j.parint.2016.09.016

Shukerova S, Kirin D, Hanzelová V (2010) Endohelminth communities of the perch, *Perca fluviatilis* (Perciformes, Percidae) from Srebarna Biosphere Reserve, Bulgaria. Helminthologia 47: 99–104. https://doi.org/10.2478/s11687-010-0016-9

Soylu E (2013) Metazoan parasites of perch *Perca fluviatilis* L. from Lake Sığırcı, Ipsala, Turkey. Pakistan Journal of Zoology 45: 47–52.

Tockner K, Schiemer F, Ward JV (1998) Conservation by restoration: the management concept for a river-floodplain system on the Danube river in Austria. Aquatic Conservation 8: 71–86. https://doi.org/10.1002/(SICI)1099-0755(199801/02)8:1%3C71::AID-AQC265%3E3.0.CO;2-D

Wicht B, Limoni C, Peduzzi R, Petrini O (2009) *Diphyllobothrium latum* (Cestoda: Diphyllobothriidea) in perch (*Perca fluviatilis*) in three sub-alpine lakes: influence of biotic and abiotic factors on prevalence. Journal of Limnology 68: 167–173. https://doi.org/10.4081/jlimnol.2009.167

ZooKeys 899: 59–84 (2019)
doi: 10.3897/zookeys.899.38892
http://zookeys.pensoft.net

RESEARCH ARTICLE

A peer-reviewed open-access journal
ZooKeys
Launched to accelerate biodiversity research

Resolving species boundaries in the *Atlanta brunnea* species group (Gastropoda, Pterotracheoidea)

Deborah Wall-Palmer[1], Mona Hegmann[1,2], Erica Goetze[3], Katja T.C.A. Peijnenburg[1,4]

1 *Marine Biodiversity Group, Naturalis Biodiversity Center, P.O. Box 9517, 2300 RA Leiden, The Netherlands* **2** *Institute for Biosciences, University of Rostock, Albert Einstein Straβe 3, 18059 Rostock, Germany* **3** *Department of Oceanography, University of Hawaii at Manoa, 1000 Pope Road, Honolulu, Hawaii, 96822, USA* **4** *Institute for Biodiversity and Ecosystem Dynamics (IBED), University of Amsterdam, P. O. Box 942480 1090 GE Amsterdam, The Netherlands*

Corresponding author: *Deborah Wall-Palmer* (dmwallpalmer@gmail.com)

Academic editor: *E. Neubert* | Received 7 August 2019 | Accepted 29 October 2019 | Published 12 December 2019

http://zoobank.org/E61D98E3-E9E6-49CF-BC7F-2E59AF928100

Citation: Wall-Palmer D, Hegmann M, Goetze E, Peijnenburg KTCA (2019) Resolving species boundaries in the *Atlanta brunnea* species group (Gastropoda, Pterotracheoidea). ZooKeys 899: 59–84. https://doi.org/10.3897/zookeys.899.38892

Abstract

Atlantid heteropods are a family of holoplanktonic marine gastropods that occur primarily in tropical and subtropical latitudes. Atlantids bear a delicate aragonitic shell (<14 mm) and live in the upper ocean, where ocean acidification and ocean warming have a pronounced effect. Therefore, atlantids are likely to be sensitive to these ocean changes. However, we lack sufficiently detailed information on atlantid taxonomy and biogeography, which is needed to gain a deeper understanding of the consequences of a changing ocean. To date, atlantid taxonomy has mainly relied on morphometrics and shell ornamentation, but recent molecular work has highlighted hidden diversity. This study uses an integrated approach in a global analysis of biogeography, variation in shell morphology and molecular phylogenies based on three genes (CO1, 28S and 18S) to resolve the species boundaries within the *Atlanta brunnea* group. Results identify a new species, *Atlanta vanderspoeli*, from the Equatorial and South Pacific Ocean, and suggest that individuals of *A. brunnea* living in the Atlantic Ocean are an incipient species. Our results provide an important advance in atlantid taxonomy and will enable identification of these species in future studies of living and fossil plankton.

Keywords

Atlantidae, biogeography, phylogenetic analysis, shell morphology, South Pacific Ocean

Introduction

The heteropods (Pterotracheoidea) are a superfamily of marine gastropods (Order Littorinimorpha) consisting of three families: Pterotracheidae, Carinariidae and Atlantidae (Lalli and Gilmer 1989; Bouchet et al. 2017). While most marine gastropods are benthic in habitat, heteropods are holoplanktonic and live entirely in the upper water column. This study focuses on the Atlantidae (atlantids), the most species-rich family of heteropods, including more than 60 % of all heteropod species recognised so far (Seapy 1990; Wall-Palmer et al. 2018b). Atlantids are widespread and occur primarily in the epipelagic zone between the surface and 250 m, in tropical and subtropical latitudes (Wall-Palmer et al. 2018a). They are highly modified for life in the open ocean with several striking morphological adaptions such as the development of complex image-forming eyes, a foot that has adapted into a single swimming fin, and the reduction in size (< 14 mm) and weight of the laterally compressed, thin-walled (3–40 μm) shell (Lalli and Gilmer 1989). The entire shell is moved back and forth rapidly during swimming, so that the swimming fin and shell work together as dissimilar paired swimming appendages (Karakas et al. 2018). This locomotory design means that a structurally sound shell is vital for the survival of atlantids because it is necessary for all swimming, including capturing prey and evading predators. The shell of most atlantids is composed of aragonite, an unstable polymorph of calcium carbonate that is 50 % more soluble in the oceans than calcite (Sun et al. 2015). The chemical composition of the shell and persistent exposure to increasingly acidified waters in the upper water column makes atlantids likely to be particularly sensitive to ocean acidification (Wall-Palmer et al. 2016). However, sensitivity to ocean change is known to be species-specific in holoplanktonic marine gastropods. Roberts et al. (2014) found that different forms of the shelled pteropod *Limacina helicina* (Phipps, 1774) show contrasting trends in shell weight when exposed to undersaturation of calcium carbonate. Therefore, to gain deeper understanding of the consequences of a changing ocean, it is extremely important to resolve the species boundaries of holoplanktonic gastropods accurately, so that species-resolved environmental sensitivities can be determined.

To date, the taxonomy of atlantid heteropods has mainly relied on morphometrics and shell ornamentation, even though it is hard to tell some species apart only by use of morphological characteristics (Richter 1973). In particular, identification within the genus *Atlanta* Lesueur, 1817 is difficult, due to the similarities in body and shell forms (Ossenbrügger 2010). Additionally, there can be variation in morphology and ornamentation within a single species (e.g. *Atlanta selvagensis* de Vera & Seapy, 2006, Wall-Palmer et al. 2018b). Consequently, Richter (1973) suggested that morphometrics alone were insufficient to describe a new species, and assumed that as a result the number of heteropod species was largely underestimated. This underestimated diversity was confirmed in the first molecular phylogenetic study to include all atlantid morphospecies which found 30 % more mitochondrial cytochrome *c* oxidase subunit 1 (CO1) clades than there are described morphospecies (Wall-Palmer et al. 2018b). These authors found at least 10 additional atlantid clades that may represent new species in addition to the 23 currently described present-day species. This study, as well

as many others (Goetze 2010; Burridge et al. 2015, 2019; Barco et al. 2016; Bode et al. 2017; Cornils et al. 2017), highlights the importance of combining morphology (morphometrics), biogeography and molecular analyses when exploring species diversity in the open ocean.

Based on morphological characters (shell, eye type, radula, operculum), atlantid heteropods are divided into groups of closely related species (Tesch 1949). The *Atlanta brunnea* group was first described as the *Atlanta turriculata* group by Tesch (1908), and prior to this study contained two species: *A. turriculata* d'Orbigny, 1836 and *A. brunnea* Gray, 1850 (= *Atlanta fusca* Souleyet, 1852). Additional diversity within this group has been recognised in morphological studies (Souleyet 1852; Tesch 1906; Richter 1961; van der Spoel 1972, 1976) and a single molecular study (Wall-Palmer et al. 2018b); however, the taxonomy of this group has not been investigated in sufficient detail. Here we use a combination of the morphological, biological/biogeographical and phylogenetic species concepts (De Queiroz 2007) to investigate the species boundaries within the *A. brunnea* group. We formally describe the previously recognised *A. turriculata* form B (van der Spoel 1972, 1976), also previously named *A. brunnea* form B (Wall-Palmer et al. 2018b) as *Atlanta vanderspoeli* sp. nov. named after Professor Siebrecht van der Spoel who first recognised *A. vanderspoeli* but did not describe it as a new species (Van der Spoel 1972, 1976).

Materials and methods

Specimen collection

A total of 22 *A. brunnea*, 14 *A. vanderspoeli* (based on the descriptions of van der Spoel 1976) and 55 *A. turriculata* were examined in this study. All specimens have biogeographical data and have been analysed in at least one additional way (molecular, morphological or both, Table 1, Figure 1). Specimens were collected during several research cruises (Table 1) using various plankton nets. Collection methods have been described for all research cruises (Schmidt 1932; Hirai et al. 2015; Burridge et al. 2017a; Wall-Palmer et al. 2018b; Wall-Palmer et al. in preparation). Specimens from the DANA cruise of 1921 (two *A. brunnea*, two *A. vanderspoeli*, and two *A. turriculata*) were kindly made available by the Natural History Museum of Denmark (NHMD). All biogeographical data have been visualised using the software QGIS (QGIS Development Team 2016).

Imaging and morphological analysis

Specimens were identified based on the species keys of Richter and Seapy (1999), Seapy et al. (2003) and van der Spoel (1976), and imaged using a Zeiss automated z-stage light microscope at Naturalis Biodiversity Center, Leiden. Specimen shells were destroyed during the process of DNA extraction, so archived images provide the op-

Table 1. Collection information for specimens examined in this study, with inclusion into each type of analysis as indicated at right. Specimens used for the combined gene phylogeny are indicated with +.

Species	BOLD/ GenBank accession number	Museum accession number	Ocean	Cruise	Station	Biogeography Latitude/ Longitude	Morphological analysis	Molecular analysis		
								CO1	28S	18S
Atlanta brunnea	AGD001-17	RMNH.MOL.341299	Atlantic	AMT24	05	34.75, -26.62		✓	✓	✓
	ATCP003-19	RMNH.MOL.341308	Atlantic	AMT27	09	35.30, -26.28		✓	✓	✓
	ATCP008-19	RMNH.MOL.341314	Atlantic	AMT27	11	32.87, -26.91	✓	✓	✓	✓
	ATCP009-19	RMNH.MOL.341315	Atlantic	AMT27	11	32.87, -26.91	✓	✓+	✓+	✓+
	ATCP010-19	RMNH.MOL.341316	Atlantic	AMT27	11	32.87, -26.91		✓+	✓+	✓+
	ATCP004-19	RMNH.MOL.341309	Atlantic	AMT27	37	-6.87, -25.04		✓		
	ATCP006-19	RMNH.MOL.341311	Atlantic	AMT27	41	-12.63, -25.05		✓		✓
	ATCP007-19	RMNH.MOL.341312	Atlantic	AMT27	47	-24.01, -25.05		✓+	✓+	✓+
	ATCP011-19	RMNH.MOL.341317	Atlantic	AMT27	47	-24.01, -25.05		✓+	✓+	✓+
	AGD008-17	RMNH.MOL.341304	Indian	SN105	04	8.02, 67.08		✓+	✓+	✓+
	AGD009-17	RMNH.MOL.341305	Indian	SN105	04	8.02, 67.08		✓		
	AGD010-17	RMNH.MOL.341300	Indian	SN105	08	4.38, 67.00		✓		
	AGD011-17	RMNH.MOL.341301	Indian	SN105	08	4.38, 67.00		✓+	✓+	✓+
	AGD012-17	RMNH.MOL.341302	Indian	SN105	08	4.38, 67.00		✓		
	AGD013-17	RMNH.MOL.341303	Indian	SN105	08	4.38, 67.00		✓		
	–	–	Indian	SN105	08	4.38, 67.00	✓			
	AGD002-17	RMNH.MOL.341313	Pacific	KH1110	05	-23.00, 180.01		✓	✓	
	ATCP001-19	RMNH.MOL.341306	Pacific	KOK1703	07	23.62, -157.61		✓	✓	
	ATCP002-19	RMNH.MOL.341307	Pacific	KOK1703	07	23.62, -157.61		✓	✓	
	ATCP005-19	RMNH.MOL.341310	Pacific	SO255	100	-28.52, 179.59		✓	✓	
	–	NHMD-232129	Pacific	DANA	3556 VIII	2.87, -87.63	✓			
	–	NHMD-232129	Pacific	DANA	3556 VIII	2.87, -87.63	✓			
Atlanta vanderspoeli	AGD003-17	RMNH.MOL.341320	Pacific	KH1110	15	-23.00, -119.27		✓		
	AGD004-17	RMNH.MOL.341321	Pacific	KH1110	15	-23.00, -119.27		✓	✓	✓
	AGD005-17	RMNH.MOL.341322	Pacific	KH1110	15	-23.00, -119.27		✓	✓	✓
	AGD006-17	RMNH.MOL.341323	Pacific	KH1110	21	-23.00, -100.00		✓		✓
	ATCP013-19	RMNH.MOL.341324	Pacific	KH1110	21	-23.00, -100.00		✓	✓	
	AGD007-17	RMNH.MOL.341325	Pacific	KH1110	21	-23.00, -100.00		✓	✓	✓
	ATCP012-19	RMNH.MOL.341319	Pacific	SO255	057	-29.95, -178.73	✓	✓		
	ATCP014-19	RMNH.MOL.341326	Pacific	SO255	057	-29.95, -178.73		✓		
	–	–	Pacific	SO255	073	-28.13, 179.02	✓			
	ATCP015-19	RMNH.MOL.341327	Pacific	SO255	073	-28.13, 179.02	✓	✓+	✓+	✓+
	ATCP016-19	RMNH.MOL.341328	Pacific	SO255	080	-29.10, -179.72	✓	✓+	✓+	✓+
	ATCP017-19	RMNH.MOL.341329	Pacific	SO255	080	-29.10, -179.72	✓	✓		
	–	NHMD-232153	Pacific	DANA	3613 V	-22.72, 166.10	✓			
	–	NHMD-232154	Pacific	DANA	3620 IV	-24.78, 170.31	✓			
Atlanta helicinoidea	ATCP052-19	RMNH.MOL.341459	Pacific	KOK1703	06	23.52, -156.78		✓+	✓+	✓+
	ATCP049-19	RMNH.MOL.341456	Pacific	KOK1703	08	23.62, -157.61		✓+	✓+	✓+
	ATCP047-19	RMNH.MOL.341454	Pacific	KOK1703	08	23.62, -157.61		✓+	✓+	✓+
Atlanta turriculata	AGD372-17	RMNH.MOL.341775	Indian	SN105	01	11.89, 66.97		✓		
	AGD367-17	RMNH.MOL.341779	Indian	SN105	01	11.89, 66.97		✓	✓	✓
	AGD368-17	RMNH.MOL.341780	Indian	SN105	01	11.89, 66.97		✓		
	AGD369-17	RMNH.MOL.341781	Indian	SN105	01	11.89, 66.97		✓		
	AGD370-17	RMNH.MOL.341782	Indian	SN105	01	11.89, 66.97		✓		
	AGD371-17	RMNH.MOL.341783	Indian	SN105	01	11.89, 66.97		✓		
	AGD376-17	RMNH.MOL.341774	Indian	SN105	04	8.02, 67.08		✓		

Species	BOLD/ GenBank accession number	Museum accession number	Ocean	Cruise	Station	Biogeography Latitude/ Longitude	Morphological analysis	Molecular analysis		
								CO1	28S	18S
Atlanta turriculata	AGD375-17	RMNH.MOL.341776	Indian	SN105	04	8.02, 67.08		✓		
	AGD373-17	RMNH.MOL.341784	Indian	SN105	04	8.02, 67.08		✓+	✓+	✓+
	AGD374-17	RMNH.MOL.341785	Indian	SN105	04	8.02, 67.08		✓		
	AGD380-17	RMNH.MOL.341769	Indian	SN105	08	4.38, 67.00		✓		
	AGD378-17	RMNH.MOL.341777	Indian	SN105	08	4.38, 67.00		✓		
	AGD379-17	RMNH.MOL.341778	Indian	SN105	08	4.38, 67.00		✓		
	AGD377-17	RMNH.MOL.341786	Indian	SN105	08	4.38, 67.00		✓		
	ATCP123-19	RMNH.MOL.341814	Indian	SN105	08	4.38, 67.00	✓	✓	✓	✓
	AGD381-17	RMNH.MOL.341770	Indian	SN105	19	-2.95, 66.99		✓+	✓+	✓+
	AGD382-17	RMNH.MOL.341771	Indian	SN105	19	-2.95, 66.99		✓	✓	✓
	AGD383-17	RMNH.MOL.341772	Indian	SN105	19	-2.95, 66.99		✓		
	AGD384-17	RMNH.MOL.341773	Indian	SN105	19	-2.95, 66.99		✓		
	AGD363-17	RMNH.MOL.341797	Pacific	KH1110	05	-23.00, 180.01		✓	✓	✓
	AGD361-17	RMNH.MOL.341801	Pacific	KH1110	05	-23.00, 180.01		✓		
	AGD362-17	RMNH.MOL.341802	Pacific	KH1110	05	-23.00, 180.01		✓	✓	✓
	AGD365-17	RMNH.MOL.341798	Pacific	KH1110	08	-22.79, -158.10		✓		
	AGD364-17	RMNH.MOL.341799	Pacific	KH1110	08	-22.79, -158.10		✓		
	AGD366-17	RMNH.MOL.341800	Pacific	KH1110	08	-22.79, -158.10		✓		
	ATCP103-19	RMNH.MOL.341788	Pacific	KOK1703	01	22.91, -157.72		✓	✓	✓
	ATCP112-19	RMNH.MOL.341803	Pacific	KOK1703	01	22.91, -157.72	✓	✓	✓	
	ATCP102-19	RMNH.MOL.341787	Pacific	KOK1703	03	22.65, -157.69		✓	✓	
	ATCP116-19	RMNH.MOL.341807	Pacific	KOK1703	03	22.65, -157.69	✓	✓	✓	
	ATCP118-19	RMNH.MOL.341809	Pacific	KOK1703	03	22.65, -157.69	✓	✓	✓	
	ATCP120-19	RMNH.MOL.341811	Pacific	KOK1703	03	22.65, -157.69	✓	✓+	✓+	✓+
	ATCP122-19	RMNH.MOL.341813	Pacific	KOK1703	03	22.65, -157.69	✓	✓		
	ATCP124-19	RMNH.MOL.341815	Pacific	KOK1703	03	22.65, -157.69	✓	✓	✓	
	ATCP104-19	RMNH.MOL.341789	Pacific	KOK1703	05	22.65, -157.69		✓	✓	
	ATCP125-19	RMNH.MOL.341816	Pacific	KOK1703	05	22.65, -157.69	✓	✓	✓	✓
	ATCP127-19	RMNH.MOL.341818	Pacific	KOK1703	05	22.65, -157.69	✓	✓	✓	✓
	ATCP129-19	RMNH.MOL.341820	Pacific	KOK1703	05	22.65, -157.69	✓	✓	✓	
	ATCP113-19	RMNH.MOL.341804	Pacific	KOK1703	06	23.52, -156.78	✓	✓		
	ATCP117-19	RMNH.MOL.341808	Pacific	KOK1703	06	23.52, -156.78	✓	✓	✓	✓
	ATCP119-19	RMNH.MOL.341810	Pacific	KOK1703	07	23.62, -157.61	✓	✓	✓	✓
	ATCP115-19	RMNH.MOL.341806	Pacific	KOK1703	08	23.62, -157.61		✓	✓	✓
	ATCP121-19	RMNH.MOL.341812	Pacific	KOK1703	08	23.62, -157.61	✓	✓+	✓+	✓+
	ATCP105-19	RMNH.MOL.341790	Pacific	SO255	057	-29.95, -178.73		✓	✓	✓
	ATCP106-19	RMNH.MOL.341791	Pacific	SO255	073	-28.13, 179.02		✓+	✓+	✓+
	ATCP114-19	RMNH.MOL.341805	Pacific	SO255	073	-28.13, 179.02		✓		✓
	–	–	Pacific	SO255	073	-28.13, 179.02	✓			
	ATCP126-19	RMNH.MOL.341817	Pacific	SO255	073	-28.13, 179.02	✓	✓+	✓+	✓+
	ATCP128-19	RMNH.MOL.341819	Pacific	SO255	073	-28.13, 179.02	✓	✓	✓	✓
	ATCP107-19	RMNH.MOL.341792	Pacific	SO255	080	-29.10, -179.72		✓	✓	✓
	ATCP108-19	RMNH.MOL.341793	Pacific	SO255	080	-29.10, -179.72		✓	✓	✓
	ATCP109-19	RMNH.MOL.341794	Pacific	SO255	080	-29.10, -179.72		✓		✓
	ATCP110-19	RMNH.MOL.341795	Pacific	SO255	080	-29.10, -179.72		✓	✓	✓
	ATCP111-19	RMNH.MOL.341796	Pacific	SO255	100	-28.52, 179.59		✓		
	–	NHMD-232140	Pacific	DANA	3563 IV	-7.76, -131.37	✓			
	–	NHMD-232145	Pacific	DANA	3586 VII	-9.72, -170.67	✓			

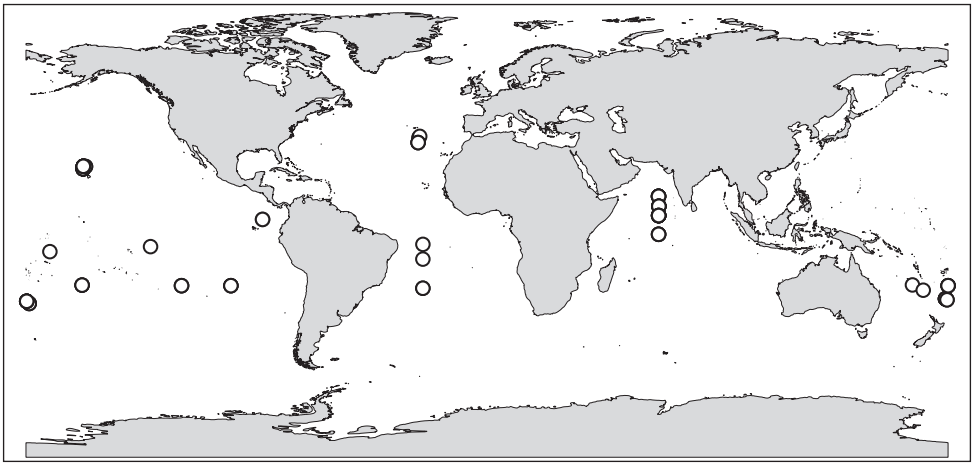

Figure 1. Collection locations for *A. brunnea* group specimens analysed in this study. Members of this species group are known to inhabit all oceans from 40N to 30S (Wall-Palmer et al. 2018b).

portunity to verify in cases of uncertainty between morphologically identified specimens and molecular results. All images are available through the Barcode of Life Data System (BOLD; http://www.boldsystems.org) and are linked to physical DNA extracts at Naturalis Biodiversity Center (Table 1).

Due to the small size of atlantid shells it is difficult to orientate them in a reproducible way for reliable morphometric measurements. Therefore, micro-computed tomography (micro-CT) was used to generate 3D-models for a subset of specimens in order to create 2D-slices through the larval shell for reproducible morphological measurements. A total of five *A. brunnea*, seven *A. vanderspoeli*, and 19 *A. turriculata* were imaged using a SkyScan 1172 high resolution micro-CT scanner. In total 958 images were collected per specimen using the following parameters: no filter, medium resolution camera, an image pixel size of 1.31–2.23 μm, a source voltage of 57 kV, a source current of 177 μA and an exposure time 600–800 ms. The rotation pitch was 0.2°, with averaging frames of 4, and random movement of 10. The software Avizo 9.0 was used to generate a 3D-surface of each shell, and to make 2D-slices perpendicularly through the earliest part of the suture of the protoconch (Figure 2, protoconch pointing upwards) by setting landmarks on the larval shell. Morphological analysis of the 2D-slices was carried out using the software IMAGEJ (Schneider et al. 2012). The apical angle (Figure 2A), maximum larval shell height (Figure 2B), maximum larval shell width measured perpendicular to the spire axis (Figure 2C) and adult shell diameter excluding the keel (Figure 2D) were measured from the 2D-slice three times and the means were calculated. Additionally, the number of whorls in the larval shell and the total number of whorls in the shell were counted using the method of Seapy (1990). For statistical analyses of the morphological data, the software PAST v3.12 was used (Hammer et al. 2001). Normal distributions were tested using the Shapiro-Wilk test (Shapiro 1965). To determine the most important variables, a Principal Component

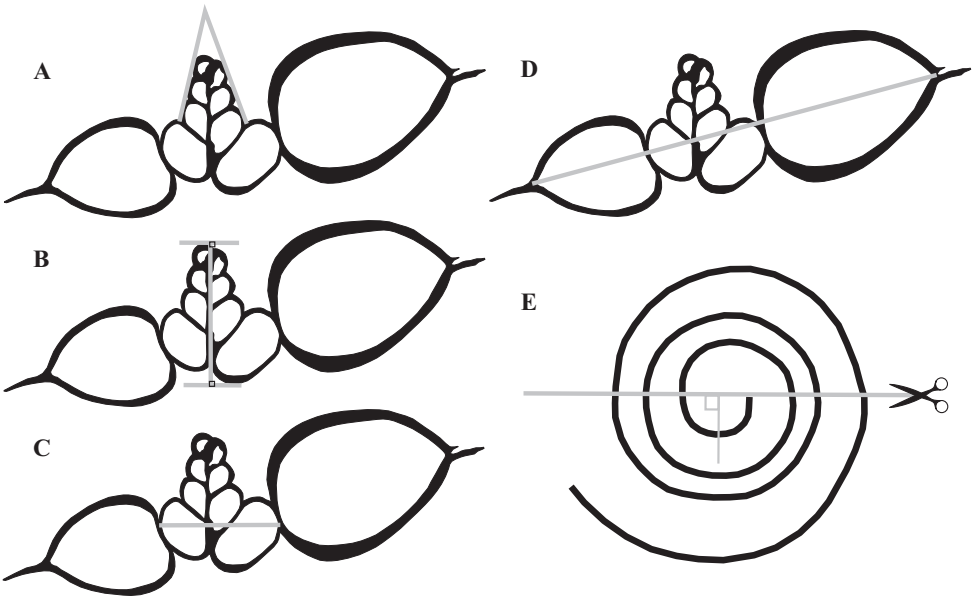

Figure 2. Examples of shell parameters measured from 2D slices of micro-CT scans. Measurements include **A** apical angle **B** larval shell height **C** maximum larval shell width, and **D** maximum adult shell diameter. The position of the slice through the 3D model to create a 2D image is shown in **E** relative to the suture.

Analysis (PCA) was carried out. T-tests were used to detect significant differences between the clades with regards to those informative variables.

Scanning Electron Microscopy (SEM) images were also made on a subset of specimens to investigate the surface shell morphology and ornamentation for each clade. Two specimens of *A. vanderspoeli* and three specimens of *A. turriculata* were scanned using a JEOL JSM-7600F Field Emission SEM. For *A. brunnea*, images of two specimens from Wall-Palmer et al. (2018b) were used.

Molecular methods

DNA extraction was carried out on whole specimens using the NucleoMag 96 Tissue kit on a Thermo Scientific KingFisher Flex magnetic particle processor with a final elution volume of 75 µl. A ~920 bp fragment of the nuclear 18S rRNA gene was amplified using primers 18S-KP-F (Burridge et al. 2017b) and 1800R (Vonnemann et al. 2005). A ~868 bp fragment of the nuclear 28S rRNA gene was amplified using primers C1-F (Dayrat et al. 2001) and D3-R (Vonnemann et al. 2005). Additionally, a ~658 bp fragment of the mitochondrial cytochrome *c* oxidase subunit 1 gene (mtCO1) (Hebert et al. 2003) was amplified using primers jgLCO1490 and jgHCO2198 (Geller et al. 2013). All primers were tailed with M13F and M13R for Sanger sequencing (Messing 1983). PCR reactions contained 17.3 µl ultrapure water (milliQ), 2.5 µl Qiagen 10× PCR buffer CL, 0.5 µl 25 mM $MgCl_2$, 1 µl 10 mg/ml Life BSA, 1.0 µl 10 pMol/

µl of each primer, 0.5 µl 2.5 mM dNTPs, 0.25 µl 5U/µl Qiagen Taq and 1 µl of DNA extract (diluted either 5 or 10 times). For all three genes, PCR was carried out using a BIO-RAD Thermal Cycler and starting with an initial denaturation step of 3 min at 96 °C, followed by 40 cycles of denaturation of 15 s at 96 °C, annealing of 30 s at 50 °C, extension of 40 s at 72 °C and a final extension step of 5 min at 72 °C. PCR products were sequenced by BaseClear (Leiden). All sequences are publicly available through BOLD (see Table 1 for accession numbers). Molecular results have been previously published for some of the specimens (Wall-Palmer et al. 2018b, in preparation).

Phylogenetic analyses

Sequences (forward and reverse strands) were assembled, aligned and verified in Geneious R8 and multiple sequence alignment was performed using MEGA-X (Kumar et al. 2016a). The resulting length of sequence alignments for CO1, 28S and 18S were 658 bp, 868 bp and 920 bp respectively. Phylogenetic relationships were estimated based on single-gene Maximum Likelihood analyses performed in RAxML 8.2.9 (Stamatakis 2014) using the General Time Reversible (GTRCAT) model followed by bootstrap analyses of 1000 replicates (CO1) or 1500 replicates (18S, 28S). Phylogenetic analysis of the three genes combined (2447 bp, GTRCAT, partitioned, 3000 replicates) included) included a subset of 14 specimens (plus three specimens of *A. helicinoidea*), with two specimens per clade per region (in regions where clades are present). All three genes were available for all of the specimens (Table 1). CO1 Genetic distances between and within clades/species were calculated using a Kimura-2-parameter (KP2) substitution model with uniform rates in MEGA-X (Kumar et al. 2016b). Three specimens of *Atlanta helicinoidea* were used as an outgroup in all phylogenetic analyses.

Results

The phylogenetic, morphological and biogeographical analyses produced a congruent result, distinguishing three species within the *A. brunnea* species group. This includes the two previously known species, *A. brunnea* and *A. turriculata.* In addition, the previously described *A. brunnea* form B, (Wall-Palmer et al. 2018b) also known as *A. turriculata* form B (van der Spoel 1972, 1976) is a valid new species and is formally named here *A. vanderspoeli* sp. nov.

Phylogenetic analyses

Phylogenetic analyses of CO1 (Figure 3) and combined genes (Figure 4) recover these three species with moderate to high bootstrap support. The single gene phylogenies of 18S and 28S resolve deeper relationships, but do not resolve the more recent divergences at the species level within the *A. brunnea* species group (Suppl. material 1:

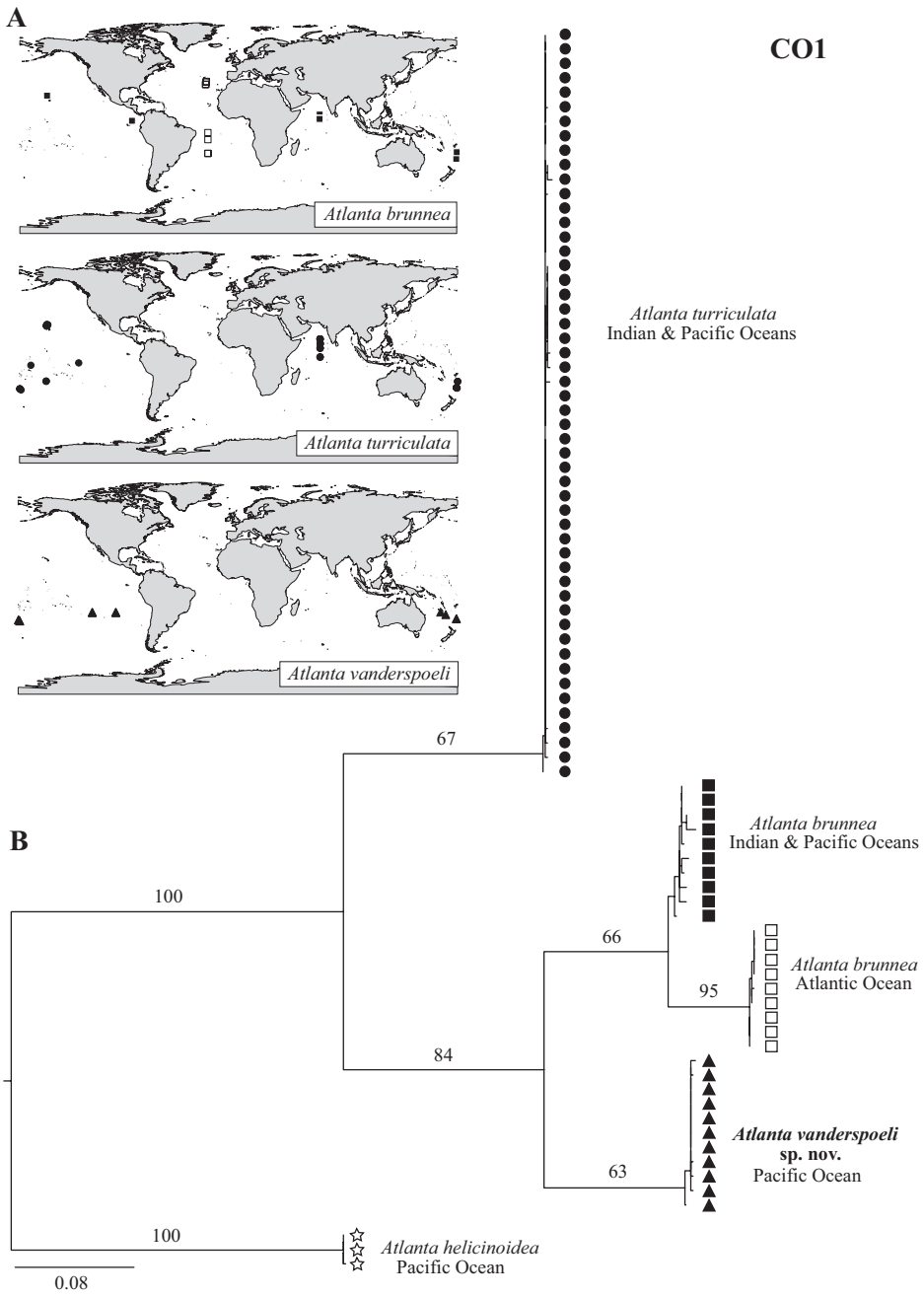

Figure 3.A Distribution maps showing the collection locations for each clade identified in B. The collection location of specimens of *A. turriculata* forma B identified by van der Spoel (1976) from offshore of Ternate Island is marked with a white triangle **B** maximum likelihood phylogeny based on the mitochondrial cytochrome *c* oxidase subunit 1 gene, with strong bootstrap support for four clades within the *A. brunnea* group. *Atlanta vanderspoeli* is supported as a valid species, and *A. brunnea* is formed of two geographically isolated clades. Bootstrap support (%) for nodes is displayed and branch lengths are proportional to the amount of inferred change, as indicated by the scale bar (mean number of nucleotide substitutions per site).

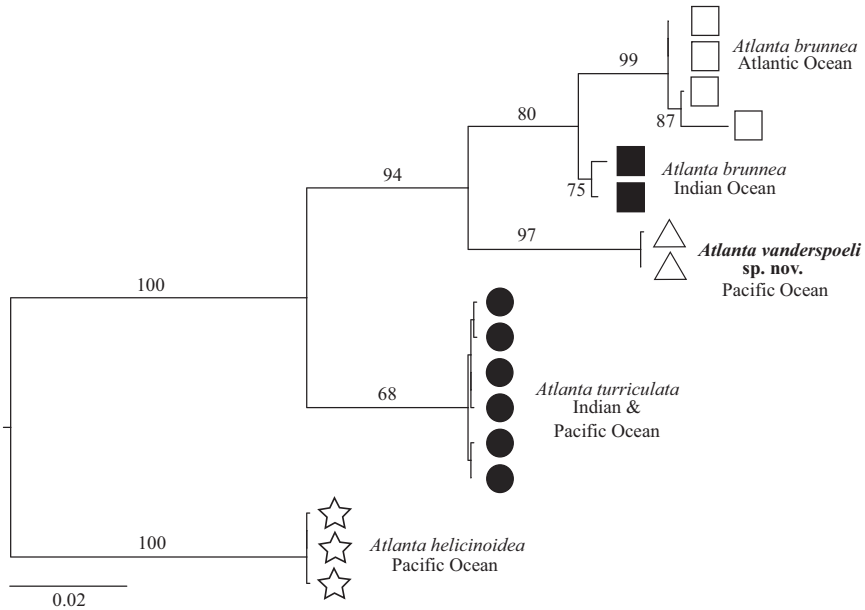

Figure 4. Maximum likelihood phylogeny of the *A. brunnea* species group based on analysis of the combined genes CO1, 28S and 18S with a total alignment of 2447 bp. All four clades within the *A. brunnea* species group are monophyletic with strong bootstrap support. Bootstrap support (%) for nodes is displayed and branch lengths are proportional to the amount of inferred change, as indicated by the scale bar (mean number of nucleotide substitutions per site).

Figures S1–S2). All of the single and combined gene phylogenetic analyses support the *A. brunnea* species group as being monophyletic with 100 % node support. In the combined gene phylogeny (Figure 4), *A. vanderspoeli* forms a monophyletic group with 97% node support, supporting inference that this is a valid species. *Atlanta brunnea* also forms a well-supported (80 % for the combined genes) monophyletic group, but this is further split into two clades. *Atlanta turriculata* forms a monophyletic group (Indian and Pacific Oceans), but this is only moderately supported (68% node support).

Genetic distances for CO1 support the position of *A. vanderspoeli* as a valid new species. *Atlanta brunnea* and *A. vanderspoeli* are separated by a CO1 genetic distance of 13–16% (Table 2). These genetic distances are comparable to the CO1 genetic distances between the previously described species within this species group, *A. brunnea* and *A. turriculata* (18–20 %). CO1 genetic distances between *A. brunnea*, *A. vanderspoeli*, *A. turriculata* and the outgroup species *A. helicinoidea* are 22–25%, 23–24% and 21–22%, respectively (Table 2).

Within *A. brunnea*, the molecular data identify a further separation into two well supported geographic clades, one containing the Indian and Pacific Ocean population and one containing the Atlantic Ocean population (Figure 4, node support of 75% and 99% respectively for the combined genes). There is a CO1 genetic distance of 6–7% between specimens from the Atlantic Ocean and specimens from the Indian and Pacific oceans. This genetic distance is less than distances between other species within

Table 2. Mean values (in bold) and ranges for genetic distances among members of the *A. brunnea* species group, based on a 658 bp fragment of the mitochondrial cytochrome *c* oxidase subunit 1 gene calculated using a Kimura 2-parameter substitution model with uniform rates.

CO1	***A. brunnea*** **Atlantic**	***A. brunnea*** **Indian & Pacific**	***A. vanderspoeli*** **Pacific**	***A. turriculata*** **Indian & Pacific**	***A. helicinoidea*** **Pacific**
A. brunnea Atlantic	**0**				
	0				
A. brunnea Indian & Pacific	**6**	**1**			
	6–7	0–1			
A. vanderspoeli Pacific	**16**	**14**	**0**		
	15 –16	13–15	0–1		
A. turriculata Indian & Pacific	**2**	**19**	**19**	**0**	
	19–20	18–20	18–20	0–1	
A. helicinoidea Pacific	**24**	**23**	**24**	**21**	**0**
	24–25	22–24	23–24	21–22	0

the *A. brunnea* group, and therefore, one of these two populations is likely to be an incipient species. However, the type locality of *A. brunnea* is not known for certain, Gray (1850) having written only '*A. brunnea*, Eydoux' to accompany his drawing of this species. Here we accept the lectotype locality because we assume that Gray illustrated the same specimens that Souleyet (1852) named *A. fusca* (originally given the vernacular name "Atlanta brune"), as they both originated from specimens collected by *Eydoux* on the "Bonite" expedition and the illustrations are almost identical (Suppl. material 1: Figure S3). The type locality for *A. fusca* is the Indian Ocean and so we assume here that the type locality of *A. brunnea* is also the Indian Ocean. Therefore, the newly detected Atlantic Ocean population should be considered as the incipient species.

Shell morphology

Principal Component Analysis (PCA) identifies the apical angle of the protoconch and the number of whorls in the larval shell as the most informative morphological characters to distinguish between *A. brunnea*, *A. vanderspoeli*, and *A. turriculata* (Figure 5). The apical angle of *A. brunnea* is the widest (58.7°–71.0°), followed by *A. vanderspoeli* (35.9°–45.8°) and *A. turriculata* (17.4°–32.2°, Suppl. material 2: Table S1, Figure 6). The difference in apical angle between *A. brunnea* and *A. vanderspoeli*, and between *A. turriculata* and *A. vanderspoeli* is significant (t-test, p=<0.001 for both; Figure 6). Differences in the number of whorls in the larval shell are also identified by the data. *Atlanta brunnea* has 3.75–4.25 whorls, *A. vanderspoeli* has 3.25–4.00 whorls and *A. turriculata* has 4.00–4.50 whorls in the larval shell (Suppl. material 2: Table S1). The height to width ratio of the larval shell, maximum number of whorls (in the whole shell) and adult shell diameter overlap for the three clades and cannot be used as reliable identifying features (Suppl. material 2: Table S1). The low number of specimens does not allow an assessment of morphological differences between the Atlantic Ocean and the Pacific and Indian Ocean specimens of *A. brunnea*.

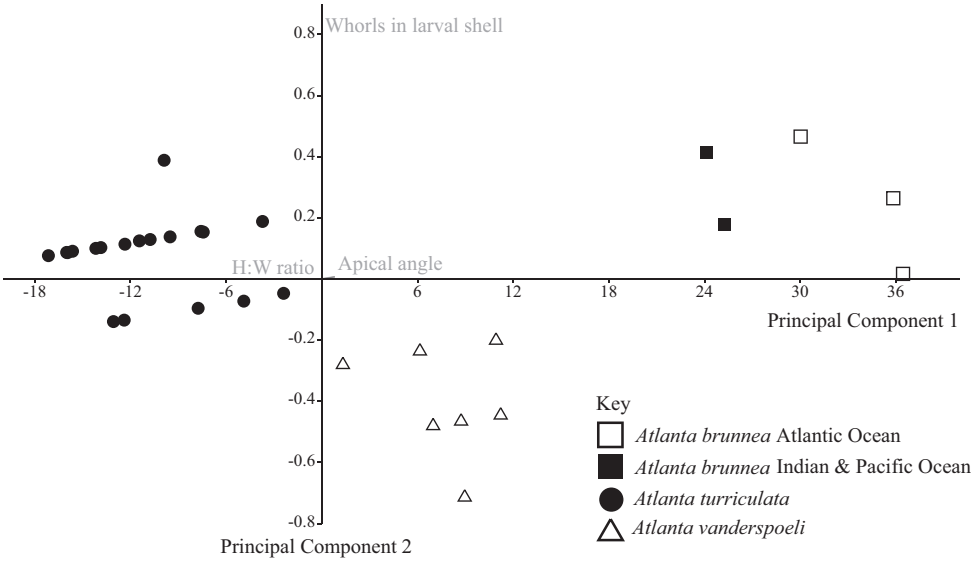

Figure 5. Principal Component Analysis (PCA) performed on apical angle, height: width ratio and the number of whorls in the larval shell. Species identity confirmed for most specimens ($N = 25$) using DNA barcoding (CO1). Two specimens of each species (total $N = 6$) derive from the DANA collection, and could not be DNA barcoded (formalin-fixed). Morphometric data are reported in Suppl. material 2:Table S1.

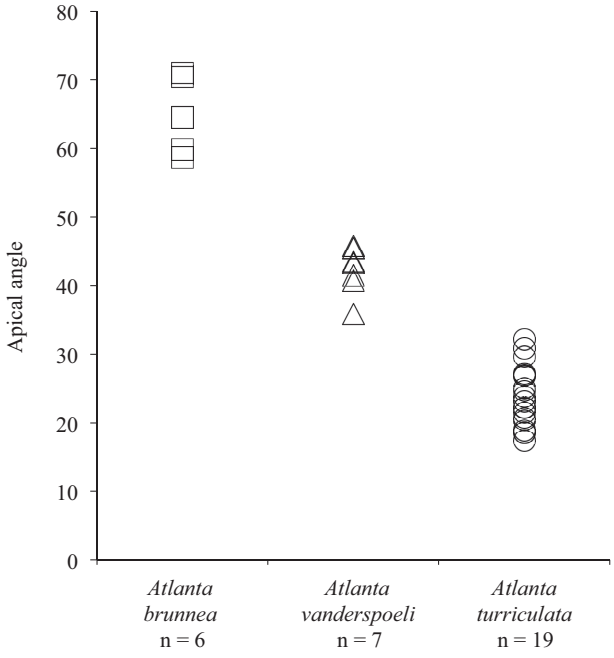

Figure 6. Shell apical angles of *A. brunnea* (Atlantic, Pacific and Indian oceans), *A. vanderspoeli* (Pacific Ocean) and *A. turriculata* (Pacific and Indian oceans) are significantly different and do not overlap.

Ornamentation is limited in its use as an identifying feature for this species group, and the fine micro-ornamentation is only really visible with the use of SEM. All three species have a prominent ridge, or carina that runs slightly above mid-whorl height of the larval shell. The larval shell of *A. brunnea* is easily identified by the heavy zig-zag, and in places, net-like reticulate spiral lines covering the surface (Figure 7B). However, the ornamentation of *A. vanderspoeli* is more difficult to tell apart from *A. turriculata*. In both, the larval shell is more sparsely ornamented than in *A. brunnea*. In *A. vanderspoeli*, interrupted spiral lines and small projections roughly arranged in lines are found above the carina of each whorl, and zig-zag ornamentation is found below the carina of each whorl (Figure 7E, Figure 8). In *A. turriculata*, there is generally little or no ornamentation above the carina of each whorl, but in common with the other two species, zig-zag ornamentation is found below it (Figure 7H).

Biogeography

Data gathered in this study expand the known distribution of the *A. brunnea* group (Wall-Palmer et al. 2016, 2018b). *Atlanta brunnea* was found to have the broadest distribution, in the Atlantic Ocean (north and south subtropical gyres), in the Indian Ocean and in the Pacific Ocean (Figure 3). *Atlanta brunnea* was not found in the central southern Pacific Ocean, although this is based upon limited sampling coverage in this region. Conversely, *A. vanderspoeli* was only found in the equatorial and southern Pacific Ocean (0.80N–29.95S, 127.28E–100.00W). The two species only overlap in the south west and the east Pacific Ocean (Figure 3). The molecular results presented here show that the Atlantic Ocean population of *A. brunnea* is a geographically divergent species. *Atlanta turriculata* was found throughout the Pacific and Indian oceans, overlapping with the distribution of *A. vanderspoeli* in the equatorial and South Pacific Ocean. In agreement with previous studies, *A. turriculata* was not found in the Atlantic Ocean (Figure 3).

Discussion

A note on *Atlanta turriculata* d'Orbigny, 1836

Atlanta turriculata was described by d'Orbigny (1836) from the South Pacific Ocean. This is the region in which the distributions of *A. turriculata* and *A. vanderspoeli* overlap and so it is necessary to check that d'Orbigny described and illustrated specimens of *A. turriculata* and not the morphologically similar *A. vanderspoeli.* Unfortunately, type material of *A. turriculata* could not be found at either the Natural History Museum, London (NHMUK), or the Muséum National d'Histoire Naturelle, Paris (MNHN), where it should be present (syntype material located at NHMUK was discovered to be mislabeled specimens of *Oxygyrus*). In addition, the illustrations of *A. turriculata* made by d'Orbigny are not sufficiently detailed to determine which species he actually drew.

Although the more widely geographically distributed, narrow-turreted spired species is now well known as *A. turriculata*, we find it necessary to solve this potential confusion by depositing a neotype specimen of (what is now widely known as) *A. turriculata* (see Systematics section for details, Figure 9).

The validity of *A. vanderspoeli* sp. nov.

Additional diversity within the *A. brunnea* species group has long been recognised, but, until now, this has not been thoroughly investigated. Van der Spoel (1972) first noticed *A. vanderspoeli* when he remarked on an atlantid form similar to *A. turriculata*, calling it *A. turriculata* forma B. Initially recognised from the soft tissues, van der Spoel described *A. turriculata* forma B as generally having a lack of tubercules on the operculum, which were present in *A. turriculata*. Later, van der Spoel (1976: 146–147) described the shell as having 'whorls in the spire [that] increase more rapidly in width so that the spire in relation to the body whorl is larger than in [*A. turriculata*]'. Van der Spoel deposited specimens of this forma, which are now in the collection of the Naturalis Biodiversity Center, Leiden (Figure 10). More recently, Wall-Palmer et al. (2018b) detected an additional clade within the *A. brunnea* group using a CO1 phylogeny of a global collection of specimens. This clade was more closely related to *A. brunnea*, and was referred to as *A. brunnea* form B. Here we considered three species concepts to determine whether this new clade, referred to in this study as *A. vanderspoeli*, was a valid species; the morphological species concept, the biological isolation (biogeographical) species concept and the phylogenetic species concept (De Queiroz 2007). Under each of these concepts, our results verify that *A. vanderspoeli* is different from the two most closely related species, *A. brunnea* and *A. turriculata*. Although there were only a relatively small number of specimens available for morphological analysis, *A. vanderspoeli* shells were found to be morphologically distinct, having an apical angle that does not overlap with its two closest relatives. The combined three gene phylogeny supports *A. vanderspoeli* to be genetically distinct from *A. brunnea* and *A. turriculata*, with genetic distances comparable to other species within the group. *Atlanta vanderspoeli* also appears to have a relatively restricted distribution, only being found (thus far) in the equatorial and South Pacific Ocean. The pteropod species *Cuvierina tsudai* Burridge, Janssen & Peijnenburg, 2016 has a very similar geographical distribution (Burridge et al. 2015, 2016). The known distribution of *A. vanderspoeli* only overlaps with *A. brunnea* and *A. turriculata* at the very edges of their populations. Relatively poor spatial resolution of molecular data in the Pacific Ocean means it is possible that the distribution of *A. vanderspoeli* is also wider (e.g. in the north Pacific). The species is therefore not strongly geographically isolated from its two most closely related species. However, these results are compatible with the phylogenetic species concept, because even though the species overlap geographically and likely do meet in nature, there must be no interbreeding as evidenced by the combined gene phylogeny (and 28S, Suppl. material 1: Figure S1).

An Atlantic Ocean incipient species

Results of the phylogenetic analysis also highlight a probable incipient species. The morphospecies *A. brunnea* was found to have two genetically different populations, one in the Indian and Pacific Oceans, and one in the Atlantic Ocean. The genetic distance between the two populations is relatively small, but suggests that the populations of *A. brunnea* in the Atlantic Ocean must be isolated and becoming a new species. This result agrees with Wall-Palmer et al. (2018b) who suggested the existence of an additional genetic lineage but due to insufficient data this could not be confirmed as a distinct species. Richter (1961) also noted differences in the Atlantic population of *A. fusca* (= *A. brunnea*), describing them as having smaller, more pigmented shells when compared to specimens in the Indian Ocean. Differences in the operculum and radula were also reported by Richter (1961). We did not detect any morphological differences between the two populations of *A. brunnea*, however, only shell ornamentation and the measurements of the larval shell have been analysed here.

Systematics

Phylum Mollusca
Class Gastropoda Cuvier, 1797
Subclass Caenogastropoda Cox, 1960
Order Littorinimorpha Golikov & Starobogatov, 1975
Superfamily Pterotracheoidea Rafinesque, 1814
Family Atlantidae Rang, 1829
Genus *Atlanta* Lesueur, 1817

***Atlanta vanderspoeli* Wall-Palmer, Hegmann & Peijnenburg, sp. nov.**
http://zoobank.org/10CC5F39-3E0A-4A53-B7D3-74F4DA5BA966
Figures 7, 8

Atlanta turriculata forma B – van der Spoel 1972: 550
Atlanta turriculata forma B – van der Spoel 1976: 146–147
Atlanta brunnea – Quesquén Liza 2017: 265
Atlanta brunnea form B – Wall-Palmer et al. 2018b: 10, Fig. 3

Type locality. DANA expedition (1928–1930) station 3558VII, South Pacific 0.30S, 99.12W. Specimen collected on the 18^{h} September 1928 at 19:00 from 200–300 m water depth.

Holotype. Figure 7D–E, NHMD-232132, Housed at the Natural History Museum of Denmark, Copenhagen.

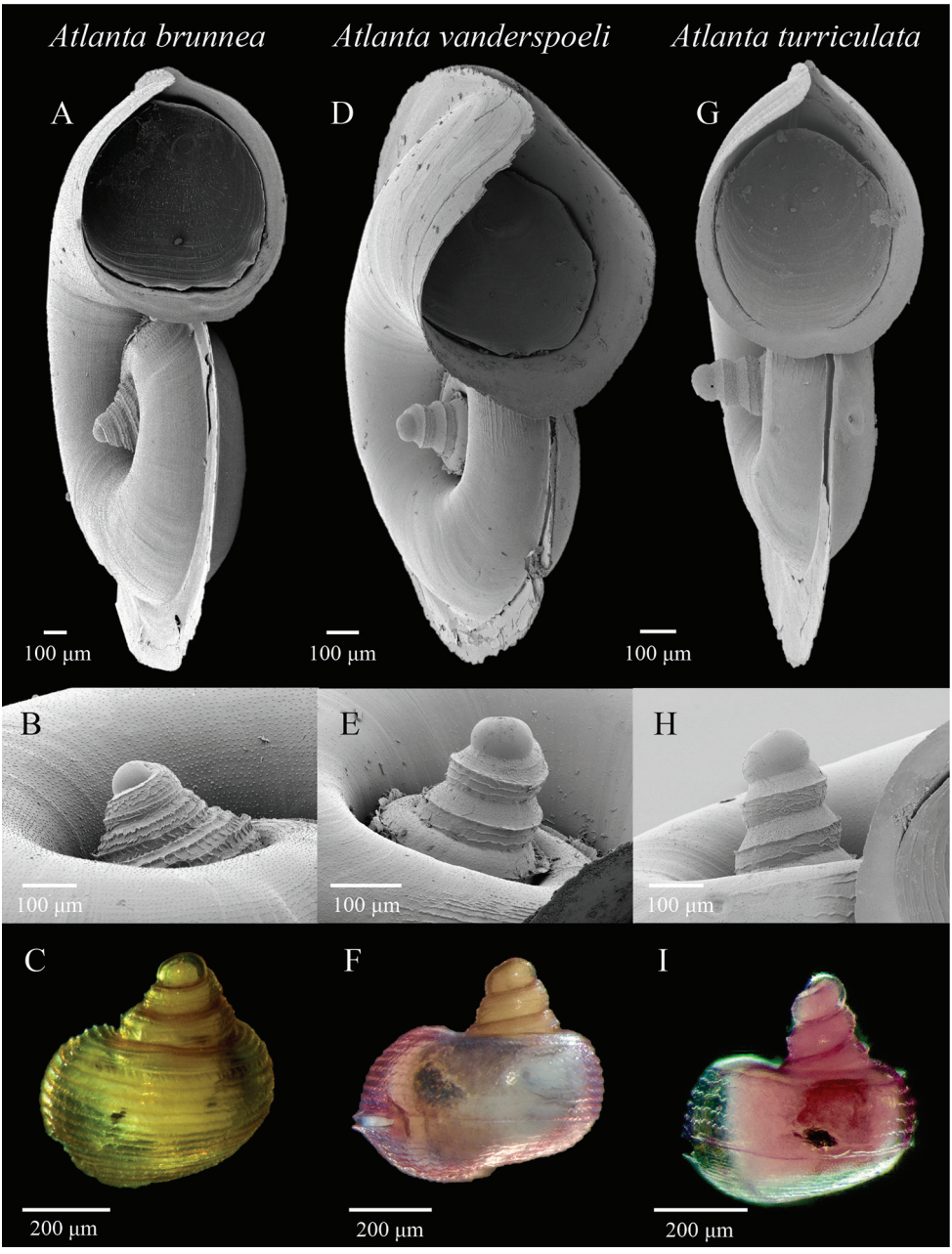

Figure 7. Scanning Electron Microscopy (SEM) and stacked light microscopy images of representative specimens of *A. brunnea*: **A, B** DANA_3929VIII **C** SN105_08, *A. vanderspoeli*: **D–E** DANA_3558VII (Holotype, NHMD-232132) **F** KH1110_15 and *A. turriculata*: **G, H** DANA_3929VIII **I** SN105_19. Apical angle is the most useful morphological feature for distinguishing between the species (**B–C, E–F, H–I**). The shell of *A. brunnea* is always brown (**C**); however, the colour of *A. vanderspoeli* and *A. turriculata* shell and soft tissues (**F, I**) can vary and these are not reliable features for identification.

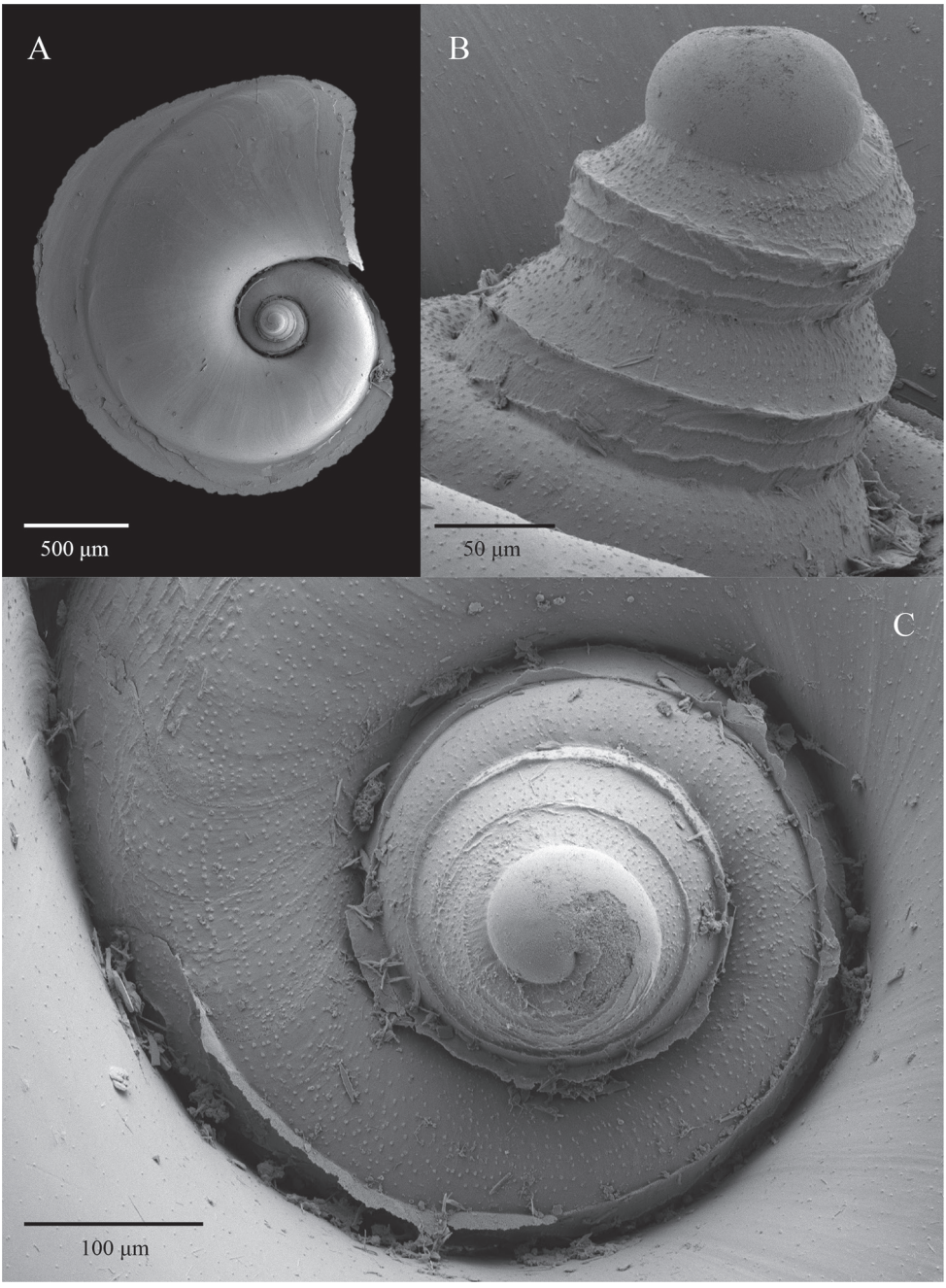

Figure 8. SEM images of the *A. vanderspoeli* holotype from station DANA_3558VII (NHMD-232132) **A** apical view of the entire shell showing the rapid inflation of the shell **B** magnified view of the micro-ornamentation **C** magnified apical view showing the extent of the carina.

Paratypes. NHMD-232153. DANA_3613V, South Pacific 22.72S, 166.10E. Specimen collected on 28 April 1928 at 03:15 from 100–200 m water depth. Housed at the Natural History Museum of Denmark, Copenhagen. RMNH.MOL.342212. Type material of *A. turriculata* forma B (Figure 10) was deposited by van der Spoel in the collections of the Zoological Museum of Amsterdam (now housed at the Naturalis Biodiversity Center, Leiden, RMNH). We designate these specimens as paratypes of *A. vanderspoeli*. They were collected during the "Siboga" Expedition at station 136 in the equatorial Pacific 0.80N, 127.28E.

Diagnosis. *Atlanta* species with a larval shell of 3 ¼ to 4 whorls. The larval shell is much higher than wide, conical with an apical angle of 35–46°. The larval shell has a prominent carina slightly above mid-whorl height. The whorls of the larval shell are further covered in a micro-ornamentation of interrupted spiral lines and small projections roughly arranged in spiral lines (approximately five lines in total) above this carina, and zig-zagged ornamentation below it (Figs 7D–F, 8).

Description. The shell is small and fresh specimens vary in colour from brown to pink-purple. The adult shell is on average 1000 μm in diameter without the keel (Suppl. material 2: Table S1). The shell begins to inflate on the boundary of teleoconch and protoconch at 3¼ to 4 whorls and has a total of 4¾ to 5 whorls in adults. The keel begins after 3¾ to 4 whorls and inserts between the final whorl and the preceding in larger specimens (filling the space between the whorls). The keel is tall (~400 μm), thin and transparent, and gradually truncates towards the aperture (after ca. ¾ of a whorl). The soft tissues of the foot/fin and sucker can be mottled black (see Suppl. material 3: video clip). The last whorl of the larval shell is ca. 262 to 372 μm in diameter (Suppl. material 2: Table S1). The larval shell is high and conical, with heavy ornamentation covering the surface. A prominent carina is situated slightly above mid-whorl height and is visible with light microscopy. The spiral lines and zig-zag ornamentation is more clearly visible using SEM. The operculum is type a (macro-oligogyre) and the eyes are of type a, with no transverse slit (Seapy et al. 2003).

Discussion. The shape of the larval shell, shell size, colouration, operculum and eye type demonstrate that *A. vanderspoeli* belongs within the *A. brunnea* species group. This is supported by the molecular analysis presented within this study and by Wall-Palmer et al. (2018b). Molecular data finds *A. vanderspoeli* to be most closely related to *A. brunnea*, followed by *A. turriculata*. These are also morphologically the most similar species. *Atlanta vanderspoeli* can be distinguished from these two species using the apical angle, which is more narrow than in *A. brunnea*, but wider than in *A. turriculata*. Van der Spoel (1972) noted that the operculum of (*A. turriculata* forma B) *A. vanderspoeli* generally does not have tubercles/spines, or that these are less developed (van der Spoel 1976) compared to the operculum of *A. turriculata*. Due to a lack of adult specimens, we were unable to extract an operculum to confirm this.

Distribution. All specimens were found in the equatorial and south Pacific Ocean from 0.80N to 29.95S, and from 127.28E to 100.00W (Figure 3). Specimens were

collected from the upper 600 m using oblique and vertical plankton tows. During this study we only found specimens of *A. vanderspoeli* in the south Pacific Ocean. However, specimens identified as *A. turriculata* forma B by van der Spoel (1976) were collected at 'Ternate Anchorage' in the Indomalayan Archipelago ("Siboga" Expedition station 136, equatorial Pacific 0.80N, 127.28E. Figure 10).

Etymology. Named after Professor emeritus Siebrecht van der Spoel, who first noticed *A. vanderspoeli*, but described it only as *A. turriculata* forma B due to a lack of specimens (van der Spoel 1976). Professor van der Spoel spent many years working on holoplanktonic gastropods and made important contributions to our understanding of their taxonomy and distributions.

Atlanta turriculata d'Orbigny, 1836

Figure 9

Original type locality. The great Austral Ocean between 30 and 34S.

Holotype. We have been unable to locate any type material for *A. turriculata* (thought to have been deposited in NHMUK or MNHN).

Neotype. RMNH.MOL.342213. SN105_08, Indian Ocean 4.38N, 67.00E. Specimen collected during the SN105 expedition of the ORV *Sagar Nidhi*, on the 10th December 2015 at 04:40 from 67 m water depth. Housed at the Naturalis Biodiversity Center, Leiden.

Two additional specimens have been deposited at the Natural History Museum, London. NHMUK20191155 and NHMUK20191156, from station KOK1703_06, Pacific Ocean 23.52N, 156.77W. Specimens collected during the KOK1703 expedition of the RV "Ka'Imikai-O-Kanaloa" on the 3rd September 2017 at 03:59 from 0–250 m water depth.

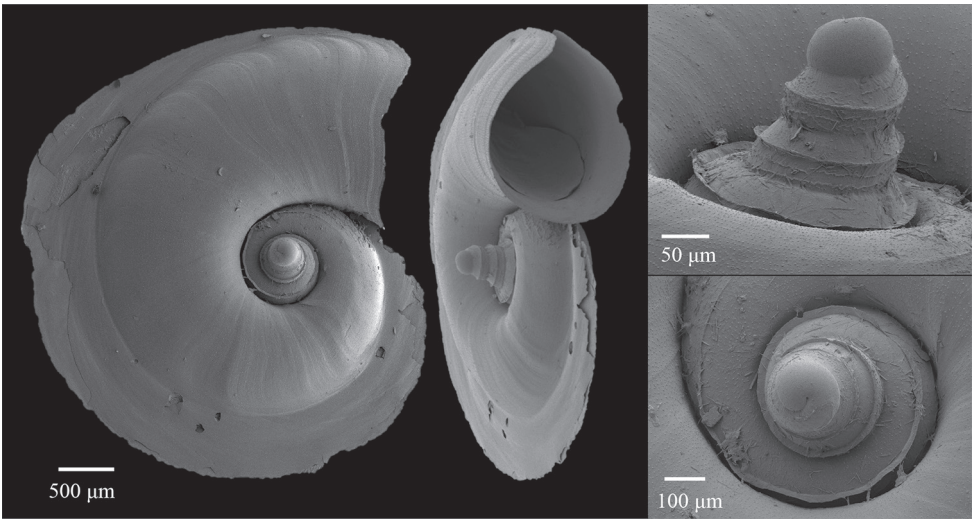

Figure 9. *Atlanta turriculata* neotype RMNH.MOL.342213, housed at the Naturalis Biodiversity Center.

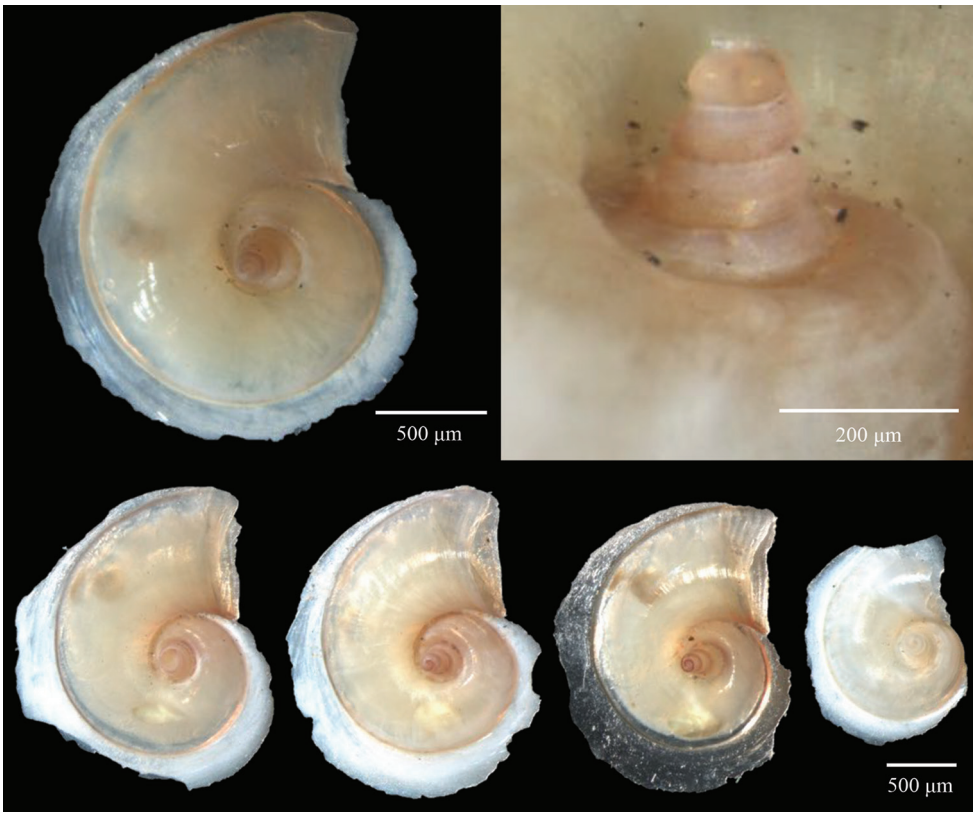

Figure 10. Five specimens of *Atlanta turriculata* forma B identified by van der Spoel and held in the collection at the Naturalis Biodiversity Center. These specimens are now designated as paratypes of *Atlanta vanderspoeli* RMNH.MOL.342212.

The holotype of *Atlanta vanderspoeli* is the property of the Natural History Museum of Denmark, Copenhagen. The neotype of *Atlanta turriculata* is the property of the Naturalis Biodiversity Center, Leiden. Both institutes maintain a research collection with proper facilities for preserving name-bearing types and these types are made accessible for study.

Conclusions

Using an integrated species concept, this study demonstrates that the *A. brunnea* group contains three valid species, *A. brunnea*, *A. turriculata*, and *A. vanderspoeli* sp. nov. A further incipient species that is restricted to the Atlantic Ocean should also be considered in future research, in particular during ecological or experimental studies. We hope that the integrated approach to species validation reported here will facilitate other workers in identifying *A. vanderspoeli* in their studies. Increased spatial coverage is now needed to fully understand the current distributions and environmental toler-

ances of this new species. Only with a larger and more complete dataset, including collection depths and concurrently collected environmental data, will it be possible to understand the responses of these atlantids to a changing ocean.

Acknowledgements

We are grateful to Atsushi Tsuda (University of Tokyo), Alice K. Burridge and Lisette Mekkes (Naturalis Biodiversity Center) for providing specimens and/or helping with specimen collection. We thank Arie W. Janssen and María Moreno-Alcántara for comments and suggestions on our manuscript, and particularly for help with the systematic section. We would also like to thank Yamell Kuen (University of Amsterdam) for sorting specimens from AMT27 material, Dirk van der Marel and Rob Langelaan for assistance with SEM and micro-CT and Tom Schiøtte and Martin Vinther Sørensen (Natural History Museum of Denmark, Copenhagen), Jeroen Goud and Bram van der Bijl (Naturalis Biodiversity Center, Leiden) and Andreia Salvador and Jon Todd (Natural History Museum, London) for facilitating access to collections in their care and for making specimens available to us. We would like to acknowledge the scientists and crew who took part in cruises AMT24, AMT27, DANA 1928–1930, KH1110, SN105, SO255, and KOK1703, and the Atlantic Meridional Transect (AMT) programme. The Atlantic Meridional Transect is funded by the UK Natural Environment Research Council through its National Capability Long-term Single Centre Science Programme, Climate Linked Atlantic Sector Science (grant number NE/R015953/1). This study contributes to the international IMBeR project and is contribution number 334 of the AMT programme. The SN105 expedition is part of IIOE-2 and was funded by the Indian National Centre for Ocean Information Services (INCOIS), Ministry of Earth Sciences, Govt. of India. The RV "Sonne"' cruise SO255 was funded by the German Federal Ministry of Education and Research (BMBF; grant 03G0255A). This project has received funding from the European Union's Horizon 2020 research and innovation programme under the Marie Skłodowska-Curie grant agreement No. 746186 (POSEIDoN, D.W-P.).

References

Barco A, Raupach MJ, Laakmann S, Neumann H, Knebelsberger T (2016) Identification of North Sea molluscs with DNA barcoding. Molecular Ecology Resources 16: 288–297. https://doi.org/10.1111/1755-0998.12440

Bode M, Laakmann S, Kaiser P, Hagen W, Auel H, Cornils A (2017) Unravelling diversity of deep-sea copepods using integrated morphological and molecular techniques. Journal of Plankton Research 39: 600–617. https://doi.org/10.1093/plankt/fbx031

Bouchet P, Rocroi J-P, Hausdorf B, Kaim A, Kano Y, Nützel A, Parkhaev P, Schrödl M, Strong EE (2017) Revised Classification, Nomenclator and Typification of Gastropod and Monoplacophoran Families. Malacologia 61: 1–526. https://doi.org/10.4002/040.061.0201

Burridge AK, Janssen AW, Peijnenburg KTCA (2016) Revision of the genus *Cuvierina* Boas, 1886 based on integrative taxonomic data, including the description of a new species from the Pacific Ocean (Gastropoda, Thecosomata). ZooKeys 619: 1–12. https://doi.org/10.3897/zookeys.619.10043

Burridge AK, Van Der Hulst R, Goetze E, Peijnenburg KTCA (2019) Assessing species boundaries in the open sea: an integrative taxonomic approach to the pteropod genus *Diacavolinia*. Zoological Journal of the Linnean Society 20: 1–25. https://doi.org/10.1093/zoolinnean/zlz049

Burridge AK, Goetze E, Raes N, Huisman J, Peijnenburg KTCA (2015) Global biogeography and evolution of *Cuvierina* pteropods. BMC Evolutionary Biology 15(39): 1–16. https://doi.org/10.1186/s12862-015-0310-8

Burridge AK, Goetze E, Wall-Palmer D, Le Double SL, Huisman J, Peijnenburg KTCA (2017a) Diversity and abundance of pteropods and heteropods along a latitudinal gradient across the Atlantic Ocean. Progress in Oceanography 158: 213–223. https://doi.org/10.1016/j.pocean.2016.10.001

Burridge AK, Hörnlein C, Janssen AW, Hughes M, Bush SL, Marlétaz F, Gasca R, Pierrot-Bults AC, Michel E, Todd JA, Young JR, Osborn KJ, Menken SBJ, Peijnenburg KTCA (2017b) Time-calibrated molecular phylogeny of pteropods. PLoS ONE 12(6): e0177325. https://doi.org/10.1371/journal.pone.0177325

Cornils A, Wend-Heckmann B, Held C (2017) Global phylogeography of *Oithona similis* s.l. (Crustacea, Copepoda, Oithonidae) – A cosmopolitan plankton species or a complex of cryptic lineages? Molecular Phylogenetics and Evolution 107: 473–485. https://doi.org/10.1016/j.ympev.2016.12.019

Cox LR (1960) Thoughts on the classifi cation of the Gastropoda. Proceedings of the Malacological Society of London 33: 239–261.

Cuvier G (1797) Tableau Elementaire de L'histoire Naturelle des Animaux. Baudouin, Paris, 710 pp. https://doi.org/10.5962/bhl.title.45918

Dayrat B, Tillier A, Lecointre G, Tillier S (2001) New Clades of Euthyneuran Gastropods (Mollusca) from 28S rRNA Sequences. Molecular Phylogenetics and Evolution 19: 225–235. https://doi.org/10.1006/mpev.2001.0926

De Queiroz K (2007) Species Concepts and Species Delimitation. Systematic Biology 56: 879–886. https://doi.org/10.1080/10635150701701083

Eydoux JTF, Souleyet LFA (1841) Voyage autour du monde: exécuté pendant les années 1836 et 1837 sur la corvette « La Bonite », commandée par M. Vaillant, capitaine de vaisseau, publié par ordre du Gouvernement sous les auspices du Département de la marine. Histoire Naturelle, Zoologie. Atlas. A. Bertrand, Paris: 8 pp, mammifères pls 1–12, oiseaux pls 1–10, reptiles pls 1–10, poissons pls 1–10, crustacés pls 1–5, insectes pls 1–2, mollusques pls 1–15, 15bis, 16–23, 23bis, 24, 24bis, 24A-E, 25–45, zoophytes pls 1–2, vers pl. 1.

Geller J, Meyer C, Parker M, Hawk H (2013) Redesign of PCR primers for mitochondrial cytochrome c oxidase subunit I for marine invertebrates and application in all-taxa biotic surveys. Molecular Ecology Resources 13: 851–861. https://doi.org/10.1111/1755-0998.12138

Goetze E (2010) Species discovery in marine planktonic invertebrates through global molecular screening. Molecular Ecology 19: 952–967. https://doi.org/10.1111/j.1365-294X.2009.04520.x

Golikov AN, Starobogatov YaI (1975) Systematics of prosobranch gastropods. Malacologia 15: 185–232.

Gray JE (1850) Explanation of Plates. Figures of Molluscous Animals. Longman, Brown, Green and Longmans, London, 124 pp.

Hammer Ø, Harper DAT, Ryan PD (2001) PAST: paleontological statistics software package for education and data analysis. Palaeontologia Electronica 4: 1–9.

Hebert PD, Cywinska A, Ball SL (2003) Biological identifications through DNA barcodes. Proceedings of the Royal Society of London. Series B: Biological Sciences 270: 313–321. https://doi.org/10.1098/rspb.2002.2218

Hirai J, Tsuda A, Goetze E (2015) Extensive genetic diversity and endemism across the global range of the oceanic copepod *Pleuromamma abdominalis*. Progress in Oceanography 138: 77–90. https://doi.org/10.1016/j.pocean.2015.09.002

Karakas F, D'Oliveira D, Maas AE, Murphy DW (2018) Using a shell as a wing: pairing of dissimilar appendages in atlantiid heteropod swimming. The Journal of Experimental Biology 221: jeb192062. https://doi.org/10.1242/jeb.192062

Kumar S, Stecher G, Tamura K (2016a) MEGA7: Molecular Evolutionary Genetics Analysis Version 7.0 for Bigger Datasets. Molecular Biology and Evolution 33: 1870–1874. https://doi.org/10.1093/molbev/msw054

Lalli CM, Gilmer RW (1989) Pelagic snails: the biology of holoplanktonic mollusks. Stanford University Press, California.

Lesueur JA (1817) Mémoire sur deux nouveaux genres de mollusques, Atlante et Atlas. Journal de Physique, de Chimie, d'Histoire Naturelle et des Arts 85: 390–393.

Messing J (1983) New M13 vectors for cloning. Methods in Enzymology 101: 20–78. https://doi.org/10.1016/0076-6879(83)01005-8

Orbigny A d' (1836) Voyage dans l'Amérique méridionale (le Brésil, la république orientale de l'Uruguay, la république Argentine, la Patagonie, la république du Chili, la république de Bolivia, la république du Pérou), exécuté pendant les années 1826, 1827, 1828, 1829, 1830, 1831, 1832 et 1833, 5(3). Mollusques. Bertrand, Paris, 49–184 pp. [atlas (1846)] https://doi.org/10.5962/bhl.title.85973

Ossenbrügger H (2010) Distribution Patterns of Pelagic Gastropods at the Cape Verde Islands. Semester Thesis. Helmholtz Centre for Ocean Research, Kiel.

Phipps CJ (1774) A Voyage Towards the North Pole Undertaken by his Majesty's Command 1773. W. Bowyer & J. Nichols, London, 275 pp.

QGIS Development Team (2016) QGIS Geographical Information System. Open Source Geospatial Foundation Project. http://qgis.osgeo.org

Quesquén Liza RC (2017) Holoplanktonic gastropod mollusks in the Peruvian Sea collected between 1994 and 2005. Boletín Instituto del Mar del Perú 32: 260–308.

Rafinesque CS (1814) Précis des Découvertes et Travaux Somiologiques de Mr. C.S. Rafinesque-Schmalz Entre 1800 et 1814. Palermo, 76 pp. https://doi.org/10.5962/bhl.title.6135

Rang S (1829) Manuel de L'histoire Naturelle des Mollusques et de Leurs Coquilles, Ayant Pour Base de Classification Celle de M. le Baron Cuvier. Roret, Paris, 390 pp. https://doi.org/10.5962/bhl.title.77502

Richter G (1961) Die Radula der Atlantiden (Heteropoda, Prosobranchia) und ihre Bedeutung für die Systematik und Evolution der Familie. Zeitschrift für Morphologie und Ökologie der Tiere 50: 163–238. https://doi.org/10.1007/BF00408284

Richter G (1973) Zur Stammesgeschichte pelagischer Gastropoden. Natur und Museum: 265–275.

Richter G, Seapy RR (1999) Heteropoda. South Atlantic Zooplankton. Backhuys, Leiden, 621–647.

Roberts D, Howard WR, Roberts JL, Bray SG, Moy AD, Trull TW, Hopcroft RR (2014) Diverse trends in shell weight of three Southern Ocean pteropod taxa collected with Polar Frontal Zone sediment traps from 1997 to 2007. Polar Biology 37: 1445–1458. https://doi.org/10.1007/s00300-014-1534-6

Schmidt J (1932) The Carlsberg foundation's oceanographical expedition round the world 1928–30 and previous "Dana"-expeditions, under the leadership of Professor Johannes Schmidt. Dana Report 1.

Schneider CA, Rasband WS, Eliceiri KW (2012) NIH Image to ImageJ: 25 years of image analysis. Nature Methods 9: 1–671. https://doi.org/10.1038/nmeth.2089

Seapy RR (1990) The pelagic family Atlantidae (Gastropoda: Heteropoda) from Hawaiian waters: a faunistic survey. Malacologia 32: 107–130.

Seapy RR, Lalli CM, Wells F (2003) Heteropoda from Western Australian waters. In: Wells FE, Walker DI, Jones DS (Eds) The marine Flora and Fauna of Dampier, Western Australia. Western Australian Museum, Perth, 513–546.

Shapiro SS (1965) Shapiro-Wilk W test. Biometrika 52: 591–611. https://doi.org/10.1093/biomet/52.3-4.591

Souleyet FLA (1852) Hétéropodes. In: Eydoux F, Souleyet FLA, (Eds) Voyage Autour du Monde Exécuté Pendant les Années 1836 et 1837 sur la Corvette "'La Bonite" (Vol. 2) Zoologie. Bertrand, Paris, 289–392.

van der Spoel S (1972) Notes on the identification and speciation of Heteropoda (Gastropoda). Zoologische mededelingen 47: 545–560.

van der Spoel S (1976) Pseudothecosomata. Gymnosomata and Heteropoda. Bohn, Scheltema & Holkema, Utrecht, 484 pp.

Stamatakis A (2014) RAxML version 8: a tool for phylogenetic analysis and post-analysis of large phylogenies. Bioinformatics 30: 1312–1313. https://doi.org/10.1093/bioinformatics/btu033

Sun W, Jayaraman S, Chen W, Persson KA, Ceder G (2015) Nucleation of metastable aragonite $CaCO_3$ in seawater. Proceedings of the National Academy of Sciences 112: 3199–3204. https://doi.org/10.1073/pnas.1423898112

Tesch JJ (1906) Die Heteropoden der "Siboga"-expedition. Siboga Reports: 1–112. https://doi.org/10.5962/bhl.title.11221

Tesch JJ (1908) Systematic Monograph of the Atlantidae (Heteropoda) with enumeration of the species in the Leyden Museum. Notes from the Leyden Museum 30: 1–30.

Tesch JJ (1949) Heteropoda. Dana Report 34.

de Vera A, Seapy RR (2006) Atlanta selvagensis, a new species of heteropod mollusc from the Northeastern Atlantic Ocean (Gastropoda: Carinarioidea). Vieraea 34: 45–54.

Vonnemann V, Schrödl M, Klussmann-Kolb A, Wägele H (2005) Reconstruction of the phylogeny of the Opisthobranchia (Mollusca: Gastropoda) by means of 18S and 28S rRNA gene sequences. Journal of Molluscan Studies 71: 113–125. https://doi.org/10.1093/mollus/eyi014

Wall-Palmer D, Janssen AW, Goetze E, Choo LQ, Mekkes L, Peijnenburg KTCA (in preparation) Time-calibrated molecular phylogeny of atlantid heteropods.

Wall-Palmer D, Smart CW, Kirby R, Hart MB, Peijnenburg KTCA, Janssen AW (2016) A review of the ecology, palaeontology and distribution of atlantid heteropods (Caenogastropoda: Pterotracheoidea: Atlantidae). Journal of Molluscan Studies 82: 221–234. https://doi.org/10.1093/mollus/eyv063

Wall-Palmer D, Metcalfe B, Leng M, Sloane H, Ganssen G, Vinayachandran P, Smart C (2018a) Vertical distribution and diurnal migration of atlantid heteropods. Marine Ecology Progress Series 587: 1–15. https://doi.org/10.3354/meps12464

Wall-Palmer D, Burridge AK, Goetze E, Stokvis FR, Janssen AW, Mekkes L, Moreno-Alcántara M, Bednaršek N, Schiøtte T, Sørensen MV, Smart CW, Peijnenburg KTCA (2018b) Biogeography and genetic diversity of the atlantid heteropods. Progress in Oceanography 160: 1–25. https://doi.org/10.1016/j.pocean.2017.11.004

Supplementary material 1

Figures S1–S3

Authors: Deborah Wall-Palmer, Mona Hegmann, Erica Goetze3 Katja T.C.A. Peijnenburg

Data type: multimedia

Explanation note: **Figure S1.** Maximum likelihood phylogeny of the *A. brunnea* group based on 28S. **Figure S2.** Maximum likelihood phylogeny of the *A. brunnea* group based on 18S. **Figure S3.** The original illustration of (**A**) *Atlanta brunnea* by Gray (1850) is clearly copied from the original illustration by Eydoux and Souleyet (1841) of (**B**) *Atlanta brune* (vernacular name) later formally named *A. fusca* (Souleyet, 1852).

Link: https://doi.org/10.3897/zookeys.899.38892.suppl1

Supplementary material 2

Table S1. Morphometric data for *A. brunnea*, *A. vanderspoeli* and *A. turriculata*

Authors: Deborah Wall-Palmer, Mona Hegmann, Erica Goetze3 Katja T.C.A. Peijnenburg

Data type: measurement

Link: https://doi.org/10.3897/zookeys.899.38892.suppl2

Supplementary material 3

***Atlanta vanderspoeli* video clip**

Authors: Deborah Wall-Palmer, Mona Hegmann, Erica Goetze3 Katja T.C.A. Peijnenburg

Data type: multimedia

Explanation note: *Atlanta vanderspoeli* specimen (male) collected during cruise SO255 station 80 at 29.10S, 179.72W.

Link: https://doi.org/10.3897/zookeys.899.38892.suppl3

ZooKeys 899: 85–107 (2019)
doi: 10.3897/zookeys.899.46933
http://zookeys.pensoft.net

RESEARCH ARTICLE

A peer-reviewed open-access journal
ZooKeys
Launched to accelerate biodiversity research

Review of the *Camponotus kiesenwetteri* group (Hymenoptera, Formicidae) in the Aegean with the description of a new species

Sebastian Salata[1], Ana Carolina Loss[1,2], Celal Karaman[3], Kadri Kiran[3], Lech Borowiec[4]

1 *Department of Entomology, California Academy of Sciences, San Francisco, CA, USA* **2** *National Institute of Atlantic Forest (INMA), Santa Teresa, ES, Brazil* **3** *Trakya University, Faculty of Sciences, Department of Biology, Balkan Campus, Edirne, Turkey* **4** *Department of Biodiversity and Evolutionary Taxonomy, University of Wrocław, Wrocław, Poland*

Corresponding author: *Sebastian Salata* (sdsalata@gmail.com)

Academic editor: *M. Borowiec* | Received 28 September 2019 | Accepted 26 November 2019 | Published 12 December 2019

http://zoobank.org/F7252FAD-3536-4D66-82E1-6284D2327F0F

Citation: Salata S, Loss AC, Karaman C, Kiran K, Borowiec L (2019) Review of the *Camponotus kiesenwetteri* group (Hymenoptera, Formicidae) in the Aegean with the description of a new species. ZooKeys 899: 85–107. https://doi.org/10.3897/zookeys.899.46933

Abstract

Based on recently collected material, the *Camponotus kiesenwetteri* group is redefined, and its members known from the Aegean region are diagnosed. *Camponotus schulzi* **sp. nov.** is described from İzmir Province, Turkey. *Camponotus nadimi* Tohmé, 1969 **syn. nov.** is proposed as a junior synonym of *Camponotus libanicus* André, 1881 and *Camponotus kiesenwetteri cyprius* Emery, 1920 **syn. nov.** as a junior synonym of *Camponotus kiesenwetteri* (Roger, 1859). A key to workers of species of the *C. kiesenwetteri* group is provided. Niche modeling analyses are used to account for species habitat suitability across the Aegean region.

Keywords

Aegean Region, carpenter ants, *Myrmentoma*, new synonym, niche modelling, taxonomy

Introduction

The genus *Camponotus* Mayr, 1861 with 1041 valid species and 454 valid subspecies is one of the most speciose within Formicidae. Members of this genus are distributed throughout the world, including the Arctic. However, unquestionably *Camponotus* reaches the highest diversity in the tropics (Bolton 2019). There are two regions in the Mediterranean (sensu Vigna Taglianti et al. 1999) that can be considered as centers of diversity of this genus. The first one, located on the western part of the Mediterranean, stretches from the Iberian Peninsula to the Atlas Mountains (Cagniant 1996; Fernandez 2019). The second one, located at the north-eastern edge of the Mediterranean, was defined by Fattorini (2000) as Aegean and covers the Balkans, western Turkey, Cyprus, Syria, Lebanon and northern Israel (Radchenko 1996; Tohmé and Tohmé 2000a, b; Ionescu-Hirsch 2010; Karaman 2012; Karaman and Aktaç 2013; Karaman et al. 2017; Salata and Borowiec 2018).

In the two last decades, the majority of studies on Mediterranean *Camponotus* focused on the Aegean region. Several recent publications show that this region is diverse and rich in taxa endemic to some islands (Borowiec and Salata 2014; Csősz et al. 2015; Salata and Borowiec 2015a, b, 2016, 2019; Salata et al. 2018) or mountain massifs (Csősz et al. 2007; Tinaut 2007; Kiran et al. 2008; Karaman and Aktaç 2013; Karaman et al. 2017; Salata and Borowiec 2017).

The *Camponotus kiesenwetteri* group comprises several taxa of the subgenus *Myrmentoma* Forel, 1912 distributed almost exclusively in the Aegean. Only *C. libanicus* André, 1881 and *C. aktaci* Karaman, 2013 extend their distribution range to Asia Minor and the Near East. For the first time, the group was defined by Emery (1925) as a group of taxa with impressed mesosomal dorsum, marginate propodeum, and matt body sculpture. Later Radchenko (1997) complemented the definition and listed the following species as members of the group: *C. aegaeus* Emery, 1915 *C. boghossiani* Forel, 1911, *C. kiesenwetteri* (Roger, 1859), and *C. libanicus*. However, the additional discoveries published in recent years provided a more comprehensive understanding of the diversity of the *kiesenwetteri* group (Karaman and Aktaç 2013, Salata and Borowiec 2018). Below, based on the material collected in the Aegean region, we update the definition of the *Camponotus kiesenwetteri* group, provide taxonomic diagnoses and distribution data for its known members and, based on material recently collected in Turkey, describe a new member of this group: *Camponotus schulzi* sp. nov. We also estimated habitat suitability in the Aegean region for species of the *C. kiesenwetteri* group.

Material and methods

Specimens deposited in the Department of Biodiversity and Evolutionary Taxonomy, University of Wrocław, Poland and the Entomological Museum of Trakya University, Edirne, Turkey were collected between 1991 and 2019 from sites in different parts of the Aegean region. The dominant method was direct sampling (hand collecting).

Individual specimens were collected on the ground and tree trunks and from low vegetation. Nests always were located in the soil, most often under trees. All specimens were preserved in 75% EtOH. The study was also supported by material deposited in the Natural History Museum of Crete (Iraklion, Greece), the Muséum d'Historie Naturelle, Genève, and samples collected by Petr Werner (Prague, Czechia). Photos were taken using a Nikon SMZ 1500 stereomicroscope, Nikon D5200 photo camera, and Helicon Focus software. All given label data are in the original spelling, presented in square brackets; a vertical bar (|) separates data on different rows and double vertical bars (||) separate labels. Type specimens' photographs are available online on AntWeb (https://www.AntWeb.org) and are accessible using the unique CASENT or FOCOL identifying specimen code.

Examined specimens are housed in the following collections:

DBET Department of Biodiversity and Evolutionary Taxonomy, University of Wrocław, Poland;
EMTU Entomological Museum of Trakya University, Edirne, Turkey;
MHNG Muséum d'Historie Naturelle, Genève, Switzerland;
MNHN Muséum National d'Histoire Naturelle, Paris, France;
MSNG Natural History Museum, Genoa, Italy;
NHMC Natural History Museum of Crete, Iraklion;
PW Petr Werner collection, Prague, Czechia;
ZMHB Museum für Naturkunde der Humboldt-Universität, Berlin, Germany.

Pilosity inclination degree follows that used in Wilson (1955). Adpressed (0–5°) hairs run parallel or nearly parallel to the body surface. Decumbent hairs stand 10–40°, subdecumbent hair stands ~45° from the surface, suberect hairs bend about 10–20° from vertical, and erect hairs stand vertical or nearly vertical.

Measurements: all measurements are given in mm.

HL head length; measured in a straight line from mid-point of anterior clypeal margin to mid-point of posterior margin in full-face view;
HW head width; measured in full-face view directly above the eyes;
SL scape length; maximum straight-line length of scape;
PW pronotum width; maximum width of pronotum in dorsal view;
PRL propodeum length; measured in lateral view, from metanotal groove to posterior-most point of propodeum;
PRW propodeal width; maximum width of propodeum in dorsal view;
PTH petiole height; the chord of ventral petiolar profile at node level is the reference line perpendicular to which the maximum height of petiole is measured, measured in lateral view;
PTW petiole width; maximum width of the petiolar node in lateral view;
WL Weber's length; measured as diagonal length from the anterior end of the neck shield to the posterior margin of the propodeal lobe.

Ratios:

CI cephalic index, HL/HW;
SI scape index, SL/HL;
PI petiole index, PTH/PTW.

Habitat suitability for species was estimated by niche modeling using Maxent 3.4.1 (Phillips et al. 2006) implemented in R package dismo (Hijmans et al. 2017). Niche modeling was estimated for all species with at least three distinct occurrence localities. The study region encompassed the Aegean biogeographic region as described by Fattorini (2000) with the addition of the Eastern Anatolian deciduous forest ecoregion, sensu World Wide Fund for Nature (WWF; Olson et al. 2001) (Fig. 36). As predictor variables we used solar radiation data and bioclimatic variables (derived from temperature and precipitation) from WordlClim version 2 (http://worldclim.org/version2) with 30 arc seconds spatial resolution grid. In order to minimize multicollinearity between variables, we ran a Pearson correlation analysis to identify variables with correlation absolute values equals or greater to 0.8. For each set of highly correlated variables, we kept only one variable, keeping the ones we consider more biologically meaningful for ant distribution. From an initial set of 31 variables, we selected 9: solar radiation of July (srad07), isothermality (bio03), temperature seasonality (bio04), maximum temperature of warmest month (bio05), minimum temperature of coldest month (bio06), mean temperature of wettest quarter (bio08), precipitation seasonality (bio15), precipitation of wettest quarter (bio16) and precipitation of warmest quarter (bio18). We used a 4-fold cross-validation test, with 75% of the data used for training and 25% for testing. For each species, all four replicates were averaged to build the final model. Importance of variables to the models were assessed by jackknife test. To avoid models that were no better than random, we only accepted final averaged models with a testing area under the curve (AUC) above 0.6.

Synopsis of species of the *Camponotus kiesenwetteri* group

Camponotus aegaeus Emery, 1915
Camponotus aktaci Karaman, 2013
Camponotus boghossiani Forel, 1911
= *Camponotus boghossiani stenoticus* Emery, 1915 (= *Camponotus kiesenwetteri angustatus* Forel, 1889 not *Camponotus angustata* (Latreille, 1798))
Camponotus kiesenwetteri (Roger, 1859)
= *Camponotus kiesenwetteri cyprius* Emery, 1920 **syn. nov.**
Camponotus libanicus André, 1881
= *Camponotus libanicus sahlbergi* Forel, 1913
= *Camponotus nadimi* Tohmé, 1969 **syn. nov.**
Camponotus nitidescens Forel, 1889
Camponotus schulzi **sp. nov.**

Taxonomy

Camponotus kiesenwetteri group

Diagnosis. Metanotal groove absent or shallow; propodeal dorsum relatively flat, propodeal declivity deeply concave, posterior protrusions absent or weakly to well developed; body densely punctate, appears dull (only *C. nitidescens* and *C. schulzi* have sculpture partially reduced on the lateral sides of mesosoma); the whole body bearing short to long, thick, pale and erect setae, and additional short appressed microsetae; head, mesosoma, and gaster uniformly blackish-brown to black (only *C. aktaci* has gaster yellowish-brown); polymorphic species.

Biology. All known species have similar biological preferences and were most often collected in warm and arid habitats within coniferous forests, especially pine forests. Less frequently they were observed in oak forest, woodland-meadow ecotones, xerothermic meadows, suburban areas with maquis, pastures with shrubs, olive plantations, river bank, orchards, occasionally in rocky gorges with deciduous trees. However, records from open habitats most often were located in the vicinity of trees, especially pine trees. Nests were located in soil, usually sandy, under trees, most often between roots, under small stones, less frequently under big stones. The only observed nest of *C. nitidescens* was located in a cracked rock wall on a roadside in oak forest under a loose piece of rock. Workers were active all day with the highest activity at dusk. Both major and minor workers were most often found on trunks and branches of coniferous trees, less often on the ground or litter.

Most of the records located in the European mainland came from areas below 700 m a.s.l. and only *C. nitidescens* is known exclusively from sites located between 1100 and 1700 m a.s.l. However, on Crete, specimens of *C. kiesenwetteri* were also found in area above 1000 m a.s.l., and the highest record comes from Trocharis peak in Lasithi province (2131 m a.s.l.). Members of the group known from Turkey manifest more alpine preferences. According to label data, the new species *Camponotus schulzi* was collected at the site located at an altitude of 1150–1500 m. Also *C. aktaci* is known almost exclusively from montane habitats located above 1000 m a.s.l.

A key to workers of species of the *Camponotus kiesenwetteri* group

1 Mesosoma in lateral view forms a regular arch; metanotal groove absent (Figs 17–22) **2**

– Mesosoma in lateral view with shallow metanotal groove (Figs 2, 6, 11–16) **4**

2 Legs mostly yellowish to reddish-brown, gaster yellowish-brown. Setation of head, mesosoma, and gaster short and sparse (Figs 21, 22). Eastern, western and central Turkey (Fig. 25) ..... ***C. aktaci* Karaman**

– Legs and gaster mostly brown to black. Setation of head, mesosoma, and gaster long and dense (Figs 17–20) **3**

3 Petiolar scale thin, PI > 1.50 (Figs 17, 18). Northeastern Greece, Eastern Aegean Islands and western Turkey (Fig. 24) ..... ***C. aegaeus*** **Emery**
– Petiolar scale thick, PI < 1.42 (Figs 19, 20). The Middle East (Fig. 32) .... ***C. libanicus*** **André**
4 Posterior margin of propodeum with well developed, lateral dentate protrusions (Figs 13, 14). Base of antennal scape with extension. Northeastern, eastern and southern Greece and western Turkey (Fig. 30)..... ***C. kiesenwetteri*** **(Roger)**
– Posterior margin of propodeum without or with weakly developed, indistinct protrusions (Figs 2, 11, 12, 15, 16). Base of antennal scape without or with indistinct extension **5**
5 Surface of mesosoma more strongly sculptured, reticulate and granulate with more or less dull background; posterior margin of propodeum sometimes with weakly-developed, indistinct protrusion (Figs 11, 12). Base of antennal scape without extension. Peloponnese, Crete, southern and eastern Aegean islands and western Turkey (Fig. 28)..... ***C. boghossiani*** **Forel**
– Surface of mesosoma weaker sculptured, especially sides of mesosoma appear more or less shiny; posterior margin of propodeum without protrusions (Figs 1, 2, 5, 6, 15, 16). Base of antennal scape with or without extension **6**
6 Base of antennal scape with extension (Fig. 3). Petiolar scale thick, PI: 1.26–1.33 (Figs 1, 2, 5, 6). Western Turkey (Fig. 35)..... ***C. schulzi*** **sp. nov.**
– Base of antennal scape without extension (Fig. 4). Petiolar scale thin, PI: 1.54–1.74 (Figs 15, 16). Cephalonia Island, western Sterea Ellas and Peloponnese (Fig. 34)..... ***C. nitidescens*** **Forel**

Camponotus aegaeus **Emery, 1915**

Figs 17, 18, 23, 24

Camponotus (*Orthonotomyrmex*) *libanicus* var. *aegaea* Emery, 1915: 4, figs 1, 2 (s.w.q.m.). Syntype workers, queen, Isola Rodi, Greece (Festa) (MSNG) [Syntype worker images examined, AntWeb, CASENT0905395, photos by Zach Lieberman, available on https://www.AntWeb.org]

Diagnosis. Head, mesosoma, and gaster uniformly blackish-brown to black; metanotal groove absent; propodeum without posterior protrusion; body densely punctate, appears dull; base of scape without extension; whole body bears long, thick, pale, dense and erect setae, and short appressed microsetae; petiolar scale thin (PI > 1.50).

Distribution. Greece: North Aegean Islands, South Aegean Islands (Dodecanese), Central Macedonia, Eastern Macedonia and Thrace; Turkey: Adana, Afyon, Antalya, Aydın, Balıkesir, Bilecik, Bursa, Çanakkale, Denizli, Diyarbakır, Elazığ, İzmir, Kırklareli, Kütahya, Manisa, Muğla, Sakarya, Uşak, and Yalova. The species was also recorded from North Macedonia (Bračko et al. 2014) and Bulgaria (Lapeva-Gjonova 2010).

Comments. Almost completely blackish-brown to black body and regularly arched (in lateral view) mesosoma cluster this species with *Camponotus libanicus*. At first glance both species look extremely similar and the most relevant character distinguishing both taxa is the shape of petiolar scale. *Camponotus aegaeus* has the scale thin (PI > 1.50) with a feebly convex anterior surface, while in *C. libanicus* the scale is thick (PI < 1.42) with a strongly convex anterior surface. Both species appear to be vicariant taxa with a more westerly distribution of *C. aegaeus* and more a easterly distribution of *C. libanicus* (Figs 24, 32). Indeed, niche modeling for both species show similar areas with high suitability, especially along the south coast of Turkey and Cyprus. However, unlike *C. libanicus*, *C. aegaeus* has not been recorded from the island. Solar radiation was the variable that contributed the most to the niche model of *C. aegaeus*.

Camponotus aktaci Karaman, 2013

Figs 21, 22, 25, 26

Camponotus aktaci Karaman, 2013: 37, figs 1, 7 (w.). Holotype worker, Akcatekir Village, (37°21'N, 34°49'E), 1300 m a.s.l., Adana, Turkey (EMTU) [holotype and paratypes personally investigated].

Diagnosis. Head and mesosoma uniformly black, gaster and legs yellowish-brown; metanotal groove absent; propodeum without posterior protrusion; body densely punctate, appears dull; base of scape without extension; whole body bears short, thin, pale, sparse and erect setae, and short appressed microsetae; petiolar scale thick.

Distribution. Turkey: Adana, Bingöl, Diyarbakır, Elazığ, Malatya, Muğla.

Comments. Mostly yellowish-brown gaster and legs and short and sparse setation of head, mesosoma and gaster distinctly separates this species from other members of the *Camponotus kiesenwetteri* group. Temperature seasonality contributed most to the distribution model. Niche modeling showed highly suitable areas matching species known distribution at Eastern Anatolian deciduous forests but also additional areas in the central Anatolian steppe region, where there are no current occurrence records for the species. However, the westernmost record from Muğla Province is located in an area of low habitat suitability.

Camponotus boghossiani Forel, 1911

Figs 11, 12, 27, 28

Camponotus boghossiani Forel, 1911: 357 (s.w.). Syntype workers, Lesbos, Greece (MHNG) [syntypes personally investigated, CASENT0910435 and CASENT0910436].

=*Camponotus boghossiani* var. *stenotica* Emery, 1915: 7 (=*Camponotus kiesenwetteri angustatus* Forel, 1889: 261, not *Camponotus angustata* (Latreille, 1798)); Salata and Borowiec 2018: 7: as a synonym of *C. boghossiani*. Holotype worker, Samos,

Greece (ZMHB) [Holotype worker images examined, AntWeb, FOCOL2488, photos by Christiana Klingenberg, available on AntWeb.org]. Note: specimen from Rethymno, Crete, Greece (MSNG), CASENT0905396 is wrongly noted as syntype of *Camponotus stenoticus*.

Diagnosis. Head, mesosoma, and gaster uniformly black; metanotal groove present, shallow; propodeum without or with indistinct bulge-like protrusions; body densely punctate, appears dull; base of scape without extension; whole body bears long, thick, pale, dense and erect setae, and short appressed microsetae; petiolar scale thick.

Distribution. Greece: North Aegean Islands, Crete (Heraklion), South Aegean Islands (Cyclades, Dodecanese), Peloponnese (Messinia); Turkey: Antalya, Balıkesir, Çanakkale, Denizli, Karaman, Kütahya, Muğla, and Uşak.

Comments. Density of sculpture slightly differs within this species and populations from Peloponnese and Aegean Islands are slightly more sculptured than populations from western Turkey. *Camponotus boghossiani* is most similar to *C. nitidescens* and *C. schulzi* and differs from them in the stronger sculpture of the mesosoma and gaster which, at first glance, appears very dull. While in both relatives the sculpture is slightly diffused and the surface is at least partly shiny. *Camponotus kiesenwetteri* has a similarly sculptured body surface but differs in having the posterior margin of the propodeum more or less excavate and forming well-developed, lateral dentate protrusions while in *C. boghossiani* the posterior margin of the propodeum is straight, without protrusions. Isolated specimens of *C. kiesenwetteri*, with posterior margin of propodeum very shallowly excavate, at first glance look very similar to specimens of *C. boghossiani* but can be easily be separated by having an antennal scape with a distinct basal extension, while in *C. boghossiani* the base of the antennal scape has no extension. Precipitation of the wettest quarter was the variable that contributed the most to the distribution model. High suitable areas are indicated especially along the coast of Turkey, Cyprus and Crete.

***Camponotus kiesenwetteri* (Roger, 1859)**
Figs 13, 14, 29, 30

Formica (*Hypoclinea*) *kiesenwetteri* Roger, 1859: 241 (w.). Syntype workers, Greece (ZMHB) [Syntype workers images of *Formica* (*Hypoclinea*) *kiesenwetteri* examined, AntWeb, FOCOL2486 and FOCOL2487, photos by Christiana Klingenberg, available on https://www.AntWeb.org].

=*Camponotus kiesenwetteri* var. *cypria* Emery, 1920: 26 (w.) **syn. nov.** Syntype worker, Cyprus (MSNG) [Syntype worker images of *Camponotus kiesenwetteri cyprius* examined, AntWeb, CASENT0905397, photos by Zach Lieberman, available on https://www.AntWeb.org]

Diagnosis. Head, mesosoma, and gaster uniformly black; metanotal groove present, shallow; propodeum with distinct dentate protrusions; body densely punctate, appears

dull; base of scape with extension; whole body bears long, thick, pale, dense and erect setae, and short appressed microsetae; petiolar scale thick.

Distribution. Greece: Attica, North Aegean Islands, South Aegean Islands (Cyclades, Dodecanese), Central Greece, Crete (Chania, Heraklion, Lasithi, Rethymno), Ionian Islands, Central Macedonia, Eastern Macedonia and Thrace, Peloponnese; Cyprus; Turkey: Balıkesir, İzmir and Muğla.

Comments. The species can be easily separated by the following combination of characters: strongly sculptured body, mesosoma with metanotal groove and posterior margin of propodeum with distinct dentate protrusions, and antennal scape with distinct basal extension. *Camponotus nitidescens* and *C. schulzi* both differ in having a partly shiny body, and *C. boghossiani* differs in having a propodeum without apical protrusions and an antennal scape without basal extension.

Camponotus kiesenwetteri cyprius was described by Emery (1920) based on four specimens collected from Cyprus (no data indicating a precise location). The subspecies was separated from the typical form based on the following characters: smaller body, wider mesosoma, indistinct metanotal groove, thicker petiole and shape of propodeal protrusions. The investigated type specimen agrees with the mentioned description but some of those characters overlap with intraspecific variability observed within *Camponotus kiesenwetteri*. Thus, we consider this species a junior synonym of *C. kiesenwetteri*. Nonetheless, Cyprus did not appear as a suitable region in niche modelling. Minimum temperature of coldest month was the variable that contributed most to the distribution model.

Camponotus libanicus **André, 1881**

Figs 19, 20, 31, 32

Camponotus (*Orthonotomyrmex*) *libanicus* André, 1881: 54, pl. 3, figs 14, 15 (w.). Syntype worker, Lebanon (MNHN) [Syntype worker images examined, AntWeb, CASENT0913700, photos by Will Ericson, available on https://www.AntWeb.org].

=*Camponotus* (*Orthonotomyrmex*) *libanicus* r. *sahlbergi* Forel, 1913: 435 (s.w.); Radchenko 1996: 1197, as a synonym of *C. libanicus*. Syntype worker, Bolkar Mountains, Turkey (MHNG) [Syntype workers images examined, AntWeb, CASENT0910441, and CASENT0910440, photos by Zach Lieberman, available on https://www.AntWeb.org].

=*Camponotus* (*Myrmentoma*) *nadimi* Tohmé, 1969: 6, figs 3, 4 (s.w.) **syn. nov.** [types unavailable].

Diagnosis. Head, mesosoma, and gaster uniformly black; metanotal groove absent; propodeum without posterior protrusion; body densely punctate, appears dull; base of scape without extension; whole body bears long, thick, pale, dense and erect setae, and short appressed microsetae; petiolar scale thick (PI < 1.42).

Distribution. The species is known from Lebanon (André 1881, Tohmé 1969) and Cyprus: Limassol and Girne. It was also recorded from Adana, Diyarbakır, Elazığ,

Hatay, Karaman, and Mersin provinces in Turkey (Forel 1913; Emery 1915; Bolu and Özgen 2018), Israel (Ionescu-Hirsch 2010) and Iran (Paknia et al. 2010). Record from Greece: Aegean Islands by Legakis (2011) is based on unpublished manuscript (Taylor and Clee 2008) and is likely based on a misidentification. Recent research on the ant fauna of the Aegean Islands has not confirmed the occurrence of this species in Greece. Additionally, the old record from İzmir in Turkey (Forel 1911) is doubtful as it was published before the description of *C. aegaeus* and it is located 500 km West of all the recently known localities of this species.

Comments. *Camponotus libanicus* belongs to the species with mesosoma evenly convex in profile, not interrupted by the metanotal groove. It is very similar to *C. aegaeus* and differs by having a thick petiolar scale with PI < 1.42, which in *C. aegaeus* is thinner at PI > 1.50. See also comments in *C. aegaeus*.

In the description of *C. nadimi* from Lebanon, Tohmé (1969) compared this species with *C. libanicus*. The author noted that *C. nadimi* is distinctly polymorphic, while *C. libanicus* was considered as almost monomorphic. Additionally, *C. nadimi* was differentiated from *C. libanicus* based on the presence of emargination on the anterior margin of the clypeus and a thinner petiole. Ionescu-Hirsch (2010) was the first to suggest that the characters mentioned in the description overlap with intraspecific variability observed within populations of *C. libanicus*. Our observations confirm this and, additionally, samples investigated during our study consisted of distinctly polymorphic specimens. Therefore, we consider *C. nadimi* a junior synonym of *C. libanicus*. Minimum temperature of the coldest month was the variable that contributed most to the distribution model. Highly suitable areas are indicated specially along the coast of Turkey, Cyprus, Crete and Eastern Mediterranean conifer forests.

Camponotus nitidescens Forel, 1889

Figs 4, 15, 16, 33, 34

Camponotus kiesenwetteri nitidescens Forel, 1889: 260 (w.) Syntype workers, Kefalonia, Greece (MHNG) [syntypes personally investigated, CASENT0910437 and CASENT0910438].

Diagnosis. Head, mesosoma, and gaster uniformly brownish-black to black; metanotal groove present, shallow; propodeum without protrusions; body punctate, mesosoma with sculpture reduced and its lateral sides at least partially shiny; base of scape without extension; whole body bears long, thick, pale, dense and erect setae, and short appressed microsetae; petiolar scale thick.

Distribution. Greece: Ionian Islands (Cephalonia) Peloponnese (Lakonia and Messinia), Western Greece (Aetolia-Acarnania).

Comments. *Camponotus nitidescens* together with *C. schulzi* are well distinguished from other species of the *C. kiesenwetteri* group in the partly reduced sculpture of the mesosoma and gaster with, at least, the lateral sides of mesosoma partly shiny. Howev-

er, the sculpture is never as shiny as in members of related members of the *Camponotus lateralis* group. Solar radiation was the variable that contributed the most to the distribution model. Although the known distribution is restricted to the western area of the Aegean region, highly suitable areas are indicated in Crete, northeast coast of Turkey, coast of Syria and Lebanon.

***Camponotus schulzi* sp. nov.**
http://zoobank.org/A9B66F54-26A8-44BE-BD39-4A0BEC973F8E
Figs 1–10, 35

Type material. ***Holotype*:** major worker (CASENT0876000): Turkey |Bozdag Mountain | 38.3277N, 28.1112E || 1150–1500 mH | 10.05.2003 | leg. A. Schulz (DBET); ***paratypes*:** 2 major workers, 5 minor workers (CASENT0876001–CASENT0876007): the same data as holotype (DBET, PW, EMTU).

Diagnosis. Head, mesosoma, and gaster uniformly black; metanotal groove present, shallow; propodeum without protrusions; body punctate, mesosoma with sculpture reduced and its lateral sides at least partially shiny; base of scape with extension; whole body bears long, thick, pale, dense and erect setae, and short appressed microsetae; petiolar scale thick.

Description. ***Measurements*.** Major worker (n = 3): HL: 1.827 (1.78–1.92), HW: 1.72 (1.63–1.82), SL: 1.59 (1.52–1.65), WL: 2.343 (2.27–2.44), PW: 1.22 (1.16–1.27), PRL: 0.657 (0.64–0.68), PRW: 0.43 (0.42–0.44), PTH: 0.40 (0.38–0.41), PTW: 0.293 (0.27–0.32), CI: 1.041 (1.028–1.055), SL/HW: 0.926 (0.889–0.982), PTH/PTW: 1.367 (1.281–1.413); minor worker (n = 5): HL: 1.31 (1.13–1.46), HW: 1.03 (0.94–1.29), SL: 1.297 (1.21–1.41), WL: 1.83 (1.65–2.02), PW: 0.96 (0.86–1.08), PRL: 0.58 (0.52–0.64), PRW: 0.34 (0.32–0.39), PTH: 0.397 (0.35–0.48), PTW: 0.307 (0.27–0.38), CI: 1.192 (1.132–1.241), SI: 1.185 (1.093–1.287), PI: 1.297 (1.263–1.333). ***Body colouration.*** Head, mesosoma and petiolus black, gaster from brownish-black to black. Legs brown to black, trochanters as dark as femora (Figs 1, 2, 4, 5), antennal scape brown, base and apex of scape in some specimens paler than the central part of scape, reddish-brown (Fig. 3). ***Head.*** In major workers large, trapezoidal in outline, the widest at height of eyes, distinctly narrowed anteriorly and rounded posteriorly (Fig. 7). Anterior margin of clypeus in the middle with semicircular emargination. Eyes small, placed distinctly below the mid-length of the head, 0.6 times as long as the length of tempora and 0.47 times as long as the length of genae. Scape short, slightly shorter than the width of head, with well-marked extension, without preapical constriction (Fig. 3). Funicle elongate and thin, 1.3 times as long as scape, first segment elongate, 2.3–2.4 times as long as wide on the apex, 1.4 times as long as the second segment, segments 3–6 equal in length and slightly longer than the second segment, segments 7–11 slightly shorter than the second segment. Surface of scape with fine microsculpture, very short and sparse appressed setae and 2–3 short, erect setae

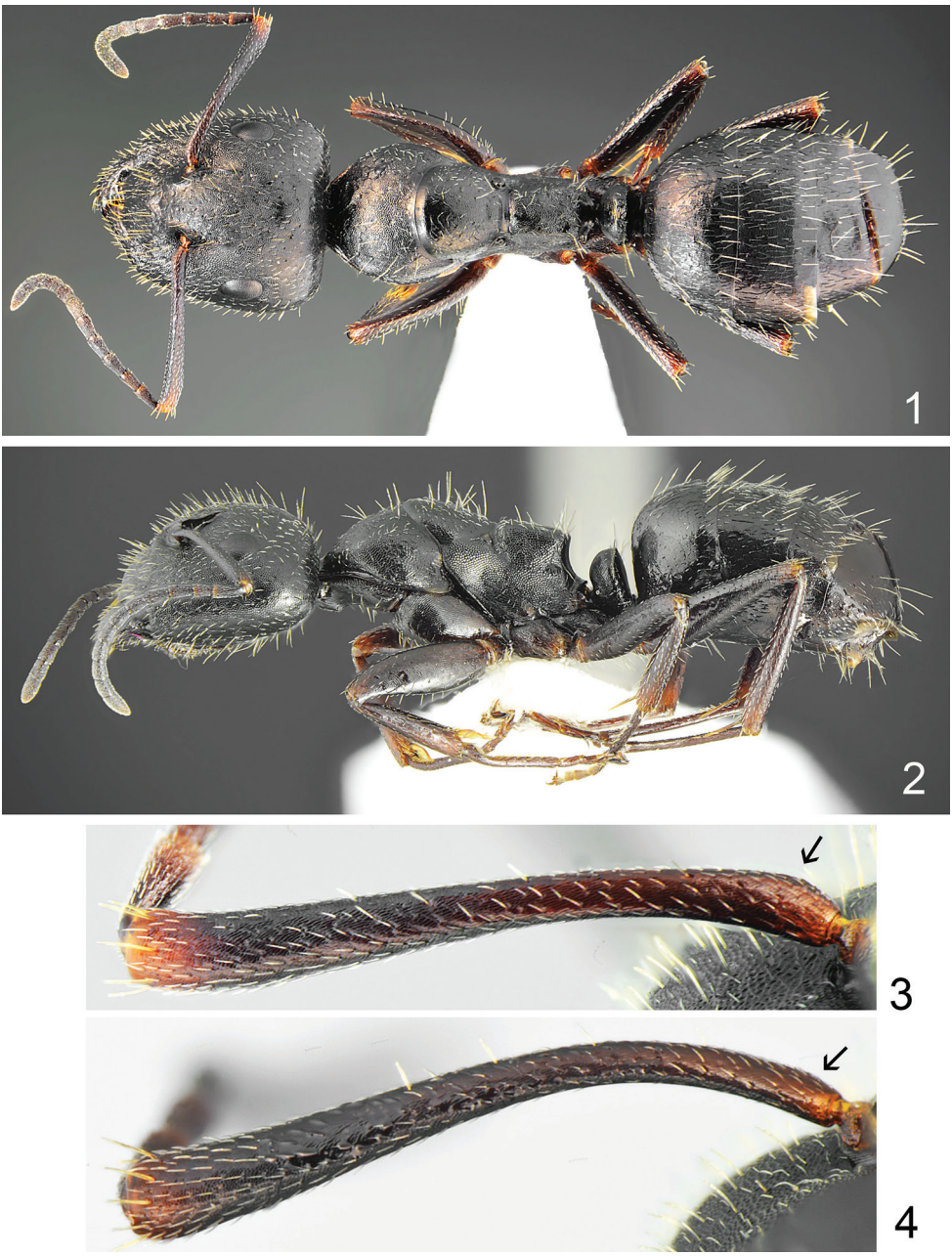

Figures 1–4. 1, 2 *Camponotus schulzi* sp. nov., major worker: **1** dorsal **2** lateral **3, 4** antennal scape **3** *Camponotus schulzi* sp. nov. **4** *Camponotus nitidescens* (arrows indicate the base of scape lacking extension).

(Fig. 7). In minor workers head oval, the widest at height of eyes; slightly narrowed anteriorly and rounded posteriorly (Fig. 8). Anterior margin of clypeus without or with very shallow emargination. Eyes proportionally larger than in major workers;

Figures 5, 6. *Camponotus schulzi* sp. nov., minor worker **5** dorsal **6** lateral.

placed distinctly below the mid-length of the head, small, approximately 0.78 times as long as the length of tempora and 0.56 times as long as the length of genae. Scape short, slimmer than in major workers, 1.2–1.3 times longer than the width of head, with well-marked extension, without preapical constriction. Funicle in shape and ratio of segments similar to major workers. The surface of scape with fine microsculpture, covered with very short and sparse appressed setae, without erect setae. The whole surface of the head, in both major and minor workers, with numerous white, erect setae (Figs 2, 6). Mandibles short, dorsal surface with distinct microreticulation and partly with elongate setose punctures and elongate rugulae, matt, inner margin with one larger and 3–4 smaller teeth. Clypeus on the whole surface microreticulate and with sparse, moderately coarse, setose punctures, matt. Frontal carinae short, extending to the line connecting 1/3 length of eyes, form a regular arch, antennal sockets flat with a thin median line, microreticulate, with sparse setose punctures, dull. The area between eyes and occipital margin of head distinctly microreticulate and appears distinctly dull, microreticulation gradually diffused

Figures 7, 8. *Camponotus schulzi* sp. nov., head and antennae **7** major worker **8** minor worker.

from dorsal to the ventral part of the head. Gena and tempora on the underside of the head with interspaces microreticulate to granulate, shiny. ***Mesosoma.*** Promesonotum regularly convex in profile with distinct metanotal groove, slightly deeper

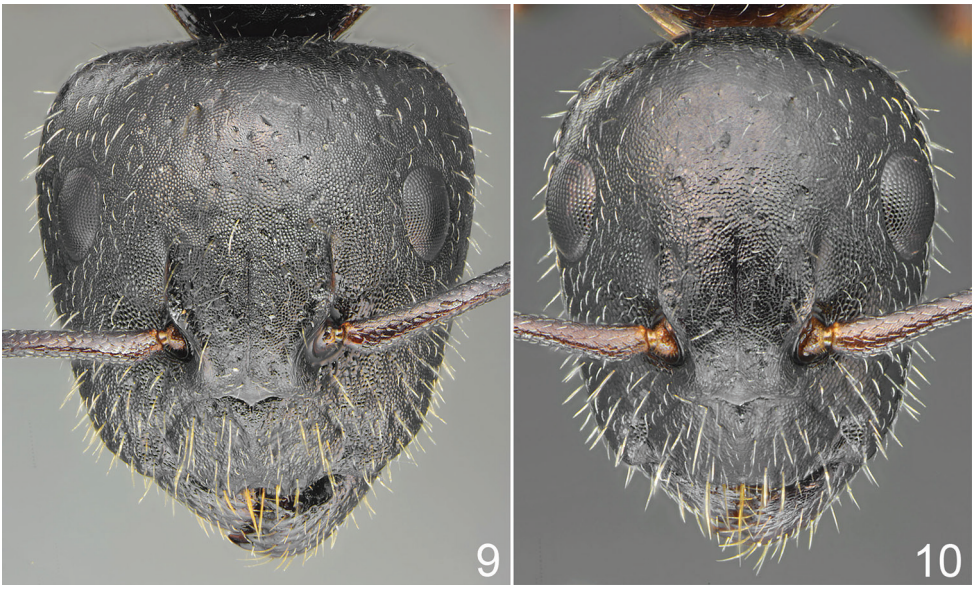

Figures 9, 10. *Camponotus schulzi* sp. nov., head sculpture **9** major worker **10** minor worker.

in major workers than in minor workers (Figs 2, 6). Propodeum elongate, in major workers 1.36–1.40 and in minor worker 1.50–1.60 times as long as wide; dorsal surface flat, posterior margin distinctly concave, posterior corners never forming tooth-like protrusions. The whole surface of pronotum, dorsal part of mesonotum and lateral parts of propodeum with sparse, moderately long, appressed setae, dorsal part of the whole mesosoma with long, white erect setae. Mesosoma on dorsal surface with distinct microreticulation, cells of microsculpture with shiny interspaces. On lateral sides of pronotum, microreticulation tending to form a linear sculpture of slightly shiny interspaces, sides of meso- and metathorax with a regular granulate sculpture of slightly shiny to matt interspaces. ***Petiole.*** Microreticulate but appears shiny. Petiolar squama stout, 1.26–1.33 as high as wide in lateral view, with convex anterior and flat posterior surfaces, margin with row of long, white setae (Figs 2, 6). ***Gaster.*** Tergites with sparse, short appressed setae and numerous long erect setae, with distinct regular microsculpture of transverse cells, on the whole surface more or less shiny. ***Legs.*** Moderately long, hind femora 0.8 times as long as mesosoma, hind tibiae slightly shorter than hind femora, the first segment of hind tarsi 0.8 times as long as hind femora. The whole surface of femora and tibiae with short, sparse, appressed to suberect pubescence, posterior and ventral surface of fore femora, and ventral surface of mid and hind femora with several, long erect setae, the surface of femora and tibiae appear shiny to slightly matt. Hind tibia with one long and two short apical spines and on the inner surface with a row of 3–5 short spines.

Etymology. Named after Andreas Schulz, a German amateur myrmecologist and naturalist, who extensively explored the Aegean region and collected valuable material, including the specimens of *C. schulzi* sp. nov.

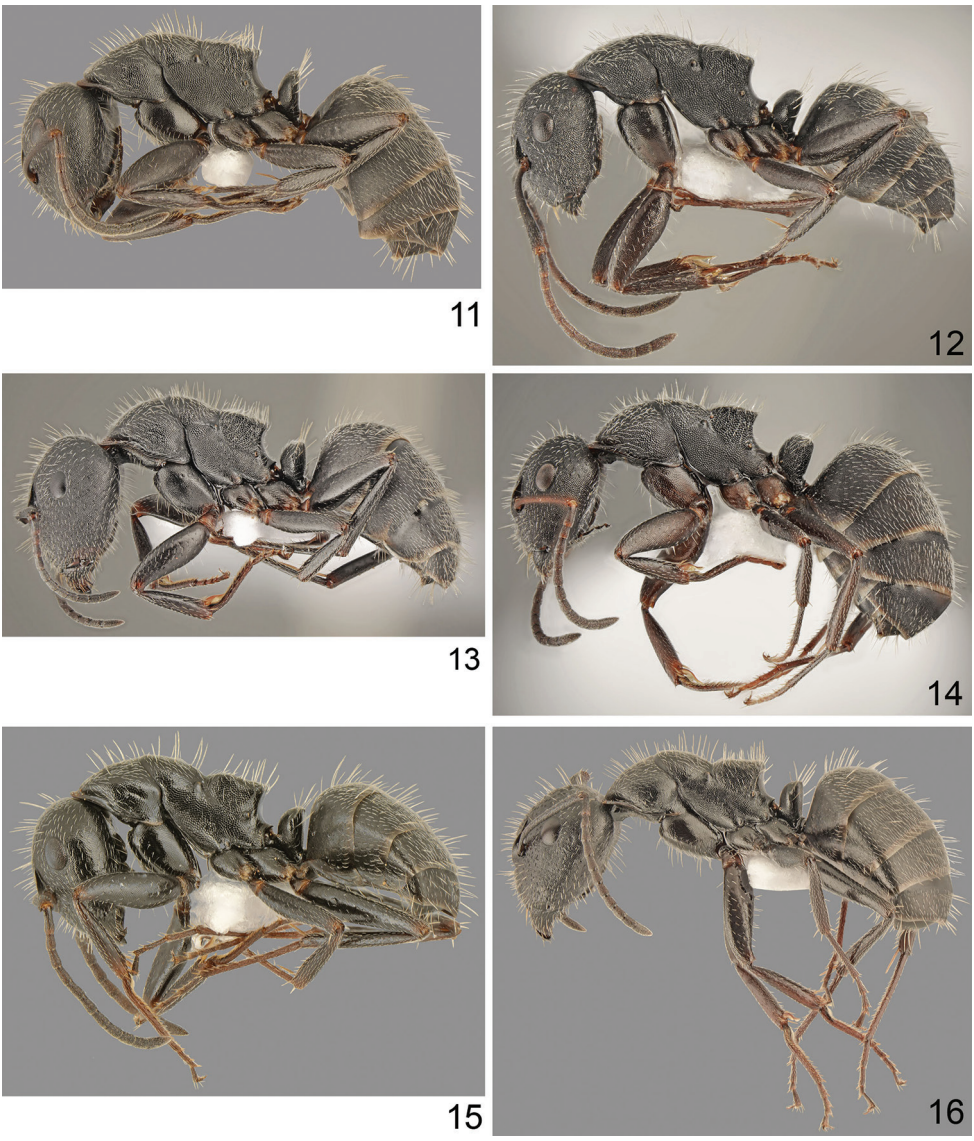

Figures 11–16. Workers in lateral view **11, 13, 15** major **12, 14, 16** minor: **11, 12** *Camponotus boghossiani* Forel **13, 14** *C. kiesenwetteri* (Roger) **15, 16** *C. nitidescens* Forel.

Distribution. Western Turkey: İzmir Province, Bozdağ Mts.

Comments. *Camponotus schulzi* sp. nov. is distinctly polymorphic, the largest major workers 1.5 times longer than the smallest minor workers. Within the *C. kiesenwetteri* group, together with *C. boghossiani*, *C. kiesenwetteri*, and *C. nitidescens*, it forms a distinct complex characterized by a shallow but distinct metanotal groove. *Camponotus boghossiani* and *C. kiesenwetteri* differ from *C. schulzi* in the

Figures 17–22. Workers in lateral view **17, 19, 21** major **18, 20, 22** minor: **17, 18** *Camponotus aegaeus* Emery **19, 20** *C. libanicus* André **21, 22** *C. aktaci* Karaman.

matt body with strong and non-reduced sculpture on the whole head, mesosoma, and gaster (Figs 11–14). Additionally, *C. kiesenwetteri* differs in having well-developed, dentate protrusions on the posterior margin of propodeum, while in *C. schulzi* sp. nov. the posterior margin of the propodeum is lacking such structures; *C. boghossiani* differs also in the base of antennal scape lacking an extension (Fig. 4), while in *C. schulzi* sp. nov. the extension is well marked (Fig. 3). *Camponotus nitidescens* is the most similar to *C. schulzi* sp. nov., because both species have the mesosomal surface partly covered with weaker sculpture and especially the sides of mesosoma appear more or less shiny in both (Figs 15, 16). However, *C.*

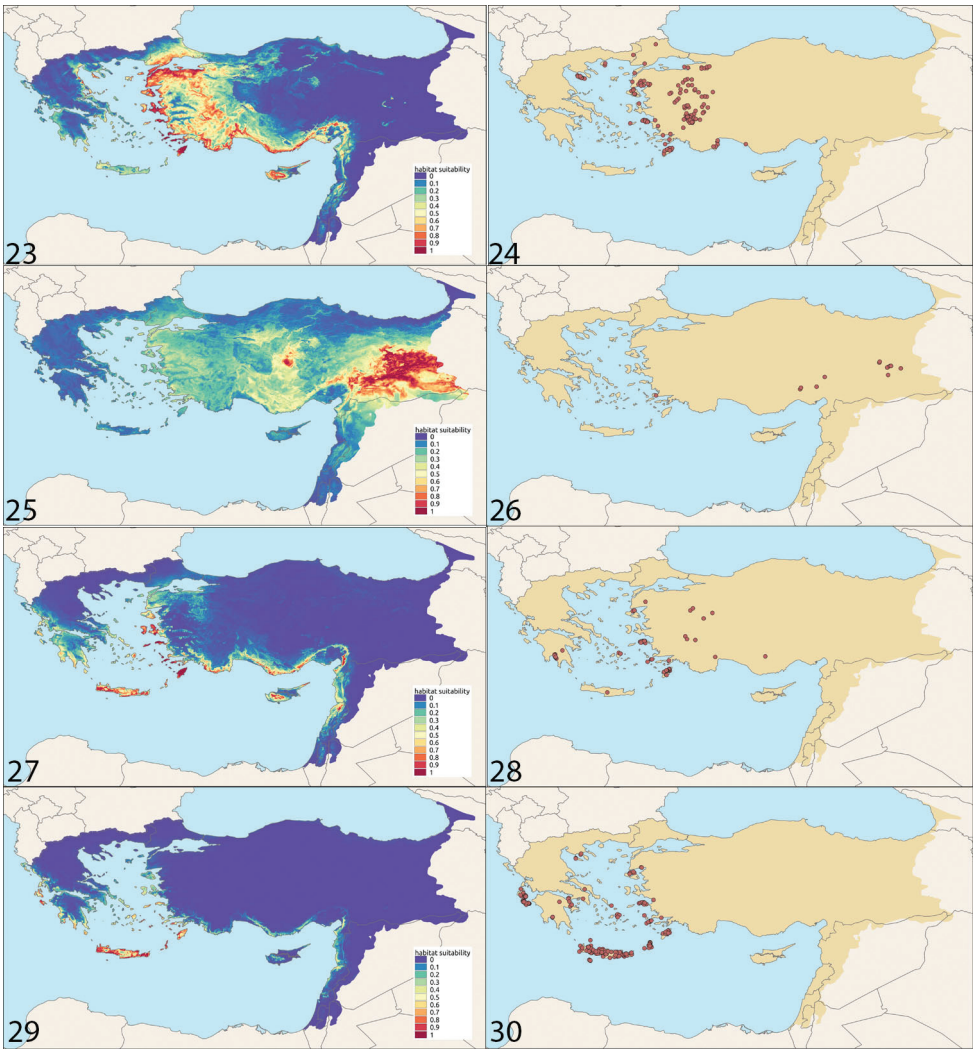

Figures 23–30. Habitat suitability and distribution **23, 24** *Camponotus aegaeus* **25, 26** *Camponotus aktaci* **27, 28** *Camponotus boghossiani* **29, 30** *Camponotus kiesenwettri*.

nitidescens has the base of the antennal scape without extension (Fig. 4) while in *C. schulzi* sp. nov. the extension is well marked (Fig. 3). Both species are also broadly separated geographically. *Camponotus nitidescens* has a narrow distribution range limited to the southern Ionian Islands, western Sterea Ellas, and Peloponnese. While *C. schulzi* sp. nov. was collected in western Turkey (Fig. 26). Species of the *C. piceus* complex of the *Camponotus lateralis* group at first glance can appear similar to *C. schulzi* sp. nov. but they differ in less-sculptured mesosoma and gaster. Especially their gaster is shinier and not as regularly reticulate or granulate as in *C. schulzi* sp. nov.

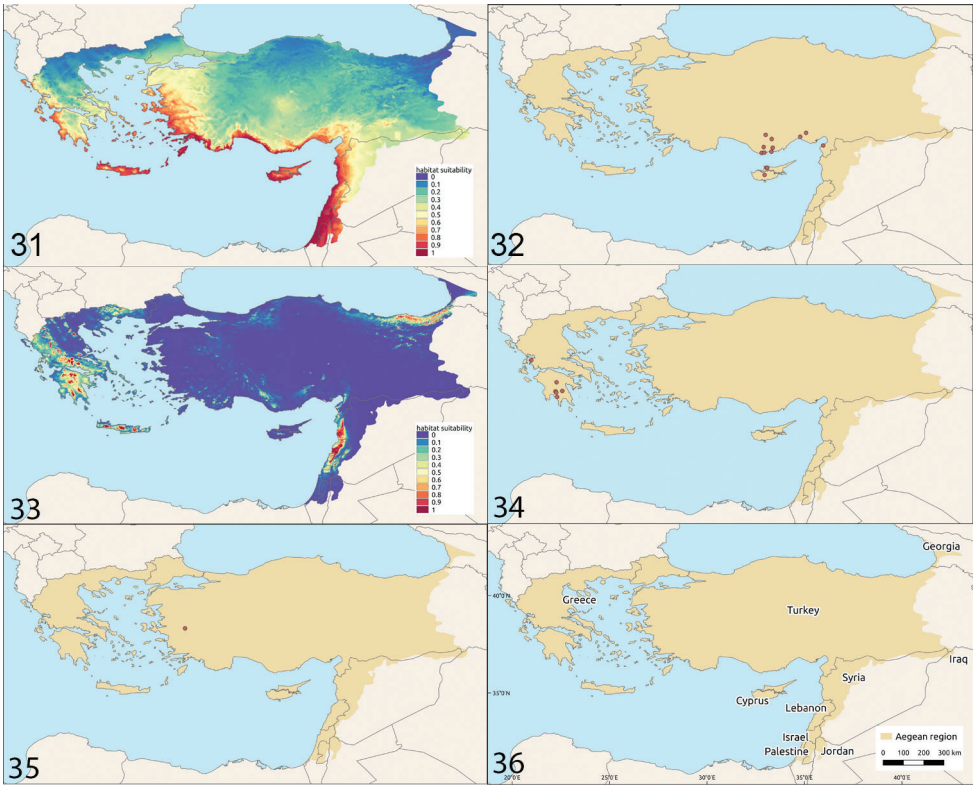

Figures 31–34. Habitat suitability and distribution **31, 32** *Camponotus libanicus* **33, 34** *Camponotus nitidescens* **35** distribution of *Camponotus schulzi* **36** the Aegean with adjacent regions.

Discussion

Camponotus schulzi sp. nov. is a member of the subgenus *Myrmentoma*. Currently, there are 24 species and one subspecies of this subgenus known from the eastern part of the Mediterranean. Emery (1925) and Radchenko (1997) divided members of this subgenus into three groups: *Camponotus lateralis* group, *Camponotus fallax* group, and *Camponotus kiesenwetteri* group.

The *Camponotus lateralis* group is the most speciose and represented by 12 species: *C. anatolicus* Karaman & Aktaç, 2013, *C. atricolor* (Nylander, 1849), *C. candiotes* Emery, 1894, *C. dalmaticus* (Nylander, 1849), *C. ebneri* Finzi, 1930, *C. heidrunvogtae* Seifert, 2019, *C. hirtus* Karaman & Aktaç, 2013, *C. honaziensis* Karaman & Aktaç, 2013, *C. lateralis* (Olivier, 1792), *C. piceus* (Leach, 1825), *C. rebeccae* Forel, 1913, and *C. staryi* Pisarski, 1971. In the most recent revision of the group (Seifert 2019) its members were characterized by small body size, rectangular or trapezoid propodeum in dorsal view, propodeal dorsum clearly delimited laterally by strong longitudinal edges, discontinuous dorsal profile of mesosoma, which is always depressed between mesonotum and propodeum, straight to convex dorsal area of

propodeum which forms a distinct angle with the caudal declivity, shiny gaster, and short and sparse pubescence on gaster. Species of this group occur in Europe, Asia Minor, and the Caucasus.

The *Camponotus fallax* group contains six species and one subspecies – *C. abrahami* Forel, 1913, *C. fallax* (Nylander, 1856), *C. gestroi* Emery, 1878, *C. gestroi creticus* Forel, 1886, *C. kurdistanicus* Emery, 1898, *C. tergestinus* Müller, 1921, and *C. vogti* Forel, 1906. The group is characterized by a small to moderate body size, regularly arched mesosoma sometimes with shallow concavity between mesonotum and propodeum, straight to angular dorsal surface of propodeum, shiny surface of mesosoma and gaster, and short and never dense pubescence hairs on gaster.

The *Camponotus kiesenwetteri* group as defined here comprises seven species and can be divided into two groups. The first one consists of species lacking a metanotal groove and includes *C. aegaeus*, *C. libanicus*, and *C. aktaci*. The second group is created by taxa with shallow but distinct metanotal groove: *C. boghossiani*, *C. kiesenwetteri*, *C. nitidescens*, and *C. schulzi*. Most of the members of the *kiesenwetteri* group have an exclusively Aegean distribution. However, based on the distribution patterns of *C. libanicus*, and *C. aktaci* more records of members of this group are expected from the Near East. In fact, all species but *C. kiesenwetteri* showed large areas of suitable habitats in the east portion of the Aegean region.

Acknowledgments

We would like to thank Dr. Bernard Landry (Genève, Switzerland) for providing access to the collection of ants preserved in Muséum d'Histoire Naturelle, Genève (MHNG). The authors wish to thank the curator of NHMC entomological collection Dr. Apostolos Trichas and the NHMC technician Mrs. Ljubica Kardaki for their support and kind assistance during work on the NHMC ant collection. We also thank P. Werner (Prague, Czechia) for providing material from Turkey for our study. Furthermore, we thank James Trager, Alexander Radchenko and Phil Ward for reviewing and improving a previous version of this manuscript.

References

André E (1881) Catalogue raisonné des Formicides provenant du voyage en Orient de M. Abeille de Perrin et description des espèces nouvelles. Annales de la Société Entomologique de France (6)1: 53–78.

Bolton B (2019) An online new general catalogue of the ants of the world, including a synopsis of taxonomic publications on Formicidae: 1–3345. http://antweb.org. [Accessed 7 March, 2019]

Bolu H, Özgen İ (2018) Some Observation About Formicidae (Hymenoptera) in Almond Agroecosystems in East-Southeast Anatolian Region of Turkey. Munis Entomology & Zoology 13: 495–498.

Borowiec L, Salata S (2014) Review of Mediterranean members of the *Aphaenogaster cecconii* group (Hymenoptera: Formicidae), with description of four new species. Zootaxa 3861: 40–60. https://doi.org/10.11646/zootaxa.3861.1.2

Bračko G, Wagner HC, Schulz A, Gioahim E, Maticic J, Tratnik A (2014) New investigation and a revised checklist of the ants (Hymenoptera: Formicidae) of the Republic of Macedonia. North-Western Journal of Zoology 10(1): 10–24.

Cagniant H (1996) Les *Camponotus* du Maroc (Hymenoptera: Formicidae): clé et catalogue des espèces. Annales de la Société Entomologique de France (N.S.) 32: 87–100.

Csősz S, Radchenko A, Schulz A (2007) Taxonomic revision of the Palaearctic *Tetramorium chefketi* species complex (Hymenoptera: Formicidae). Zootaxa 1405: 1–38.

Csősz S, Heinze J, Mikó I (2015) Taxonomic Synopsis of the Ponto-Mediterranean Ants of *Temnothorax nylanderi* Species-Group. PLoS ONE 10(11): e0140000. https://doi.org/10.1371/journal.pone.0140000

Emery C (1915) Escursioni zoologiche del Dr. Enrico Festa nell'Isola di Rodi. XII. Formiche. Bollettino dei Musei di Zoologia ed Anatomia Comparata della Reale Università di Torino 30(701): 1–7.

Emery C (1920) Studi sui *Camponotus*. Bullettino della Società Entomologica Italiana 52: 3–48.

Fattorini S (2000) Dispersal, vicariance and refuges in the Anatolian Pimeliinae (Coleoptera, Tenebrionidae): remarks on some biogeographical tenets. Biogeographia-The Journal of Integrative Biogeography 21(1): 355–398. https://doi.org/10.21426/B6110103

Emery C (1925) Hymenoptera. Fam. Formicidae. Subfam. Formicinae. Genera Insectorum 183: 1–302.

Fernandez JA (2019) Web page on ants of Spain: https://mirmecologia.jimdo.com/fichas-especies/formicinae/camponotus/

Forel A (1889) Ameisen aus den Sporaden, den Cykladen und Griechenland, gesammelt 1887 von Herrn von Oertzen. Berliner Entomologische Zeitschrift [1888] 32: 255–265. https://doi.org/10.1002/mmnd.47918880404

Forel A (1911) Fourmis nouvelles ou intéressantes. Bulletin de la Société Vaudoise des Sciences Naturelles 47: 331–400.

Forel A (1913) Fourmis de la faune méditerranéenne récoltées par MM. U. et J. Sahlberg. Revue Suisse de Zoologie 21: 427–438. https://doi.org/10.5962/bhl.part.37159

Hijmans RJ, Phillips S, Leathwick J, Elith J (2017) dismo: Species Distribution Modeling. R package version 1.1–4. https://CRAN.R-project.org/package=dismo

Ionescu-Hirsch A (2010) An annotated list of *Camponotus* of Israel (Hymenoptera: Formicidae), with a key and descriptions of new species. Israel Journal of Entomology [2009] 39: 57–98.

Karaman C (2012) *Camponotus ruseni* n. sp. (Hymenoptera: Formicidae) – a putative second parasitic species of the genus *Camponotus* Mayr. Journal of the Kansas Entomological Society 85(4): 309–317. https://doi.org/10.2317/0022-8567-85.4.309

Karaman C, Aktaç N (2013) Descriptions of four new species of *Camponotus* Mayr (Hymenoptera: Formicidae), with a key for the worker caste of the *Camponotus* of Turkey. Journal of the Kansas Entomological Society 86: 36–56. https://doi.org/10.2317/JKES120516.1

Karaman C, Kiran K, Aksoy V, Camlitepe Y (2017) A new species of the genus *Camponotus* (Mayr) (Hymenoptera, Formicidae) from Turkey. Turkish Journal of Zoology 41: 998–1004. https://doi.org/10.3906/zoo-1704-20

Kiran K, Aktaç N, Tezcan S (2008) Three new species of ants (genus *Aphaenogaster*, Hymenoptera: Formicidae) from Turkey. Biológia (Bratislava) 63: 689–695. https://doi.org/10.2478/s11756-008-0123-y

Lapeva-Gjonova A (2010) First records of three ant species (Hymenoptera: Formicidae) from Bulgaria. Myrmecological News 14: 1–3.

Legakis A (2011) Annotated list of the ants (Hymenoptera, Formicidae) of Greece. Hellenic Zoological Archives 7: 1–55.

Olson DM, Dinerstein E, Wikramanayake ED, Burgess ND, Powell GVN, Underwood EC, D'Amico JA, Itoua I, Strand HE, Morrison JC, Loucks CJ, Allnutt TF, Ricketts TH, Kura Y, Lamoreux JF, Wettengel WW, Hedao P, Kassem KR (2001) Terrestrial ecoregions of the world: a new map of life on Earth. Bioscience 51(11): 933–938. https://doi.org/10.1641/0006-3568(2001)051[0933:TEOTWA]2.0.CO;2

Paknia O, Radchenko A, Pfeiffer M (2010) New records of ants (Hymenoptera: Formicidae) from Iran. Asian Myrmecology 3: 29–38.

Phillips SJ, Anderson RP, Schapire RE (2006) Maximum entropy modeling of species geographic distributions. Ecological Modelling 190: 231–259. https://doi.org/10.1016/j.ecolmodel.2005.03.026

Radchenko AG (1996) A key to the ant genus *Camponotus* (Hymenoptera, Formicidae in Palearctic Asia. Zoologicheskii Zhurnal 75: 1195–1203.

Radchenko A (1997) Review of ants of the subgenus *Myrmentoma* genus *Camponotus* (Hymenoptera, Formicidae) of the Asian Palearctic. Entomological Review (Birmingham) 77: 1050–1059.

Roger J (1859) Beiträge zur Kenntniss der Ameisenfauna der Mittelmeerländer. I. Berliner Entomologische Zeitschrift 3: 225–259. https://doi.org/10.1002/mmnd.18590030209

Salata S, Borowiec L (2015a) A taxonomic revision of the genus *Oxyopomyrmex* André, 1881 (Hymenoptera: Formicidae). Zootaxa 4025(1): 1–66. https://doi.org/10.11646/zootaxa.4025.1.1

Salata S, Borowiec L (2015b) Redescription of *Crematogaster cypria* Santschi, 1930, new status, with description of two new related species from Greece and Turkey (Hymenoptera, Formicidae). ZooKeys 505: 59–77. https://doi.org/10.3897/zookeys.505.9566

Salata S, Borowiec L (2016) A new species of the *Aphaenogaster cecconii* group (Hymenoptera: Formicidae) from Rhodes. Zootaxa 4170: 194–200. https://doi.org/10.11646/zootaxa.4170.1.13

Salata S, Borowiec L (2017) Species of *Tetramorium semilaeve* complex from Balkans and western Turkey, with description of two new species of (Hymenoptera: Formicidae: Myrmicinae). Annales Zoologici (Warsaw) 62: 279–313. https://doi.org/10.3161/00034541ANZ2017.67.2.008

Salata S, Borowiec L (2018) Taxonomic and faunistic notes on Greek ants (Hymenoptera: Formicidae). Annals of the Upper Silesian Museum in Bytom Entomology 27(online 008): 1–51. http://doi.org/10.5281/zenodo.2199191

Salata S, Borowiec L (2019) Preliminary contributions toward a revision of Greek *Messor* Forel, 1890 (Hymenoptera: Formicidae). Turkish Journal of Zoology 43: 52–67. https://doi.org/10.3906/zoo-1809-41

Salata S, Borowiec L, Trichas A (2018) Taxonomic Revision of the Cretan Fauna of the Genus *Temnothorax* Mayr, 1861 (Hymenoptera: Formicidae), with Notes on the Endemism of Ant Fauna of Crete. Annales Zoologici (Warsaw) 68(4): 769–808. https://doi.org/10.3161/00034541ANZ2018.68.4.004

Seifert B (2019) A taxonomic revision of the members of the *Camponotus lateralis* species group (Hymenoptera: Formicidae) from Europe, Asia Minor and Caucasia. Soil Organisms 91: 7–32.

Taylor MJ, Clee C (2008) Preliminary Systematic List of Ant Species Recorded from Chios, Greece. Compiled by M.J. Taylor & C. Clee from material collected by M.J. Taylor, C. Clee, C.A. Collingwood & M. Hull. Determinations by C.A.C. (manuscript), 2 pp.

Tinaut A (2007) A new species of the genus *Rossomyrmex* Arnoldi, 1928 from Turkey (Hymenoptera, Formicidae). Graellsia 63: 135–142. https://doi.org/10.3989/graellsia.2007.v63.i1.86

Tohmé G (1969) Description d'espèces nouvelles de fourmis au Liban (Hymenoptera Formicoidea). Publications de l'Université Libanaise. Section des Sciences Naturelles 7: 1–15.

Tohmé G, Tohmé H (2000a) Redescription de *Camponotus festai* Emery, 1894, et description de *C. sannini* n. sp., deux fourmis du Liban at de la Syrie (Hymenoptera, Formicidae). Bulletin de la Société Entomologique de France [1999] 104: 473–480.

Tohmé G, Tohmé H (2000b) Redescription de *Camponotus oasium* Forel, 1890, de *C. fellah* Emery, 1908, de *C. sanctus* Forel, 1904 et description de *C. palmyrensis* n. sp., quatre fourmis du Liban et de la Syrie (Hymenoptera, Formicidae). Bulletin de la Société Entomologique de France 105: 387–394.

Wilson EO (1955) A monographic revision of the ant genus Lasius. Bulletin of the Museum of Comparative Zoology 113: 1–201.

Vigna Taglianti A, Audisio PA, Biondi M, Bologna MA, Carpaneto GM, De Biase A, Fattorini S, Piattella E, Sindaco R, Venchi A, Zapparoli M (1999) A proposal for a chorotype classification of the Near East fauna, in the framework of the Western Palaearctic region. Biogeographia 20: 31–59. https://doi.org/10.21426/B6110172

ZooKeys 899: 109–140 (2019)
doi: 10.3897/zookeys.899.47070
http://zookeys.pensoft.net

RESEARCH ARTICLE

A peer-reviewed open-access journal
ZooKeys
Launched to accelerate biodiversity research

Unloved, paraphyletic or misplaced: new genera and species of small to minute lucinid bivalves and their relationships (Bivalvia, Lucinidae)

John D. Taylor[1], Emily A. Glover[1]

1 *Department of Life Sciences, The Natural History Museum, London, SW7 5BD, UK*

Corresponding author: *John D. Taylor* (j.taylor@nhm.ac.uk)

Academic editor: *G. Oliver* | Received 4 October 2019 | Accepted 22 November 2019 | Published 12 December 2019

http://zoobank.org/9AA5216D-3150-475D-A165-B36EABCB61E2

Citation: Taylor JD, Glover EA (2019) Unloved, paraphyletic or misplaced: new genera and species of small to minute lucinid bivalves and their relationships (Bivalvia, Lucinidae). ZooKeys 899: 109–140. https://doi.org/10.3897/zookeys.899.47070

Abstract

Species identified as *Pillucina* are paraphyletic in molecular analyses and a new generic name, *Rugalucina*, is introduced for a complex of three similar species *Rugalucina angela* from the northern Indian Ocean and Red Sea, *R. vietnamica* from South East Asia, and *R. munda* from northern and north eastern Australia. *Lucina concinna* from the Red Sea, previously synonymised with *P. vietnamica/angela* is recognised as a *Rugalucina*-like species but with a very short anterior adductor scar. *Divaricella cypselis* from Karachi is similarly now recognised as a distinct species, probably related to *Rugalucina* but with oblique commarginal sculpture and a short adductor scar. A group of minute Indo-West Pacific lucinids with highly unusual multi-cuspate lateral teeth and previously classified as *Pillucina* are separated under a new genus *Pusillolucina* **gen. nov.**, with the description of three new species *P. arabica*, *P. africana*, and *P. biritika* from the Arabian Gulf, Mozambique, and Madagascar. Finally, a new genus, *Notocina*, is introduced for the small southern Atlantic species, *Epicodakia falklandica*, shown in molecular analyses to be misplaced at subfamily level and now classified in Lucininae and not Codakiinae with *Epicodakia*.

Keywords

bivalves, chemosymbiosis, taxonomy, Indo-West Pacific, South Atlantic

Introduction

Within the chemosymbiotic bivalve family Lucinidae, genera in the *Loripes* group have been identified as monophyletic (Taylor et al. 2011, 2016) and characterised by a distinctive internally inset ligament. In the eastern Atlantic and Mediterranean *Loripes orbiculatus* is recognised as the most abundant lucinid in shallow water seagrass habitats and its important role in ecosystem function has been much studied (Johnson et al. 2002; Heide et al. 2012; Rossi et al. 2013; Geest et al. 2014). Other genera within the *Loripes* group include *Lucinella* and *Keletistes* in the Atlantic and from the Indo-West Pacific *Pillucina*, *Wallucina*, and *Chavania*. Of these, *Pillucina* is the most diverse with eleven currently recognised species (Glover and Taylor 2001; 2016) distributed from the Red Sea to the Hawaiian Islands. Some species have been recorded with high population densities in seagrass and peri-mangrove habitats (Nakaoka et al. 2002; Uede and Takahashi 2008, Meyer et al. 2008; Rattanachot and Prathep 2015). However, recent and ongoing molecular analyses indicate that *Pillucina* is paraphyletic with *P. vietnamica* Zorina, 1978 and *P. pusilla* Glover & Taylor, 2016 aligning distantly from five other *Pillucin*a species (Taylor et al. 2011, 2016, Glover et al. 2016). Moreover, it is also now apparent that the reportedly widespread *Pillucina vietnamica* is a complex of three similar species with distinct distributional ranges. In view of the paraphyly and the separate status of the *Pillucina vietnamica* species group we propose a new genus and a reappraisal of the constituent species including two names resurrected from synonymy and recognition of an early available name from Australia.

The other lucinid separated by paraphyly and not closely related to the other *Pillucina* species is the minute *Pillucina pusilla* from the Philippines that possesses distinctive multi-cuspate lateral teeth. This extremely unusual character was first recognised in *Pillucina denticula* Glover & Taylor, 2001 from near Durban, South Africa. Recently, we have identified herein other species of minute lucinids with similar dentition from the Arabian Gulf, Mozambique and northern and southern Madagascar. Species with this dentition form a morphologically distinct clade that we recognise with a new generic name.

Additionally, amongst these small lucinids it is apparent that the southern Atlantic species *Epicodakia falklandica* Dell, 1964 is misclassified because molecular results (Taylor et al. 2011, 2016) place it in the large subfamily Lucininae rather than Codakiinae with other *Epicodakia* species. We review the morphology and relationships of this species and place it in a new genus.

During the last 20 years there has been a marked proliferation of generic categories within Lucinidae building on and revising the prior classifications of Chavan (1969) and Bretsky (1976). This is a reflection of increased taxonomic activity following the discovery of chemosymbiosis but also the clear indication from molecular results and more detailed morphological studies that a number of existing genera are paraphyletic or polyphyletic, with some species misclassified even at subfamily level. At species level increased sampling effort, with closer attention to smaller sieve size fractions, has revealed an unexpected range of minute lucinids and this, coupled with greater attention to museum collections and type material, has highlighted previously neglected species.

Institutional abbreviations

AMS	Australian Museum, Sydney
BAS	British Antarctic Survey
MCG	Museo Civico, Genoa
MNHN	Muséum national d'Histoire naturelle, Paris
NHMUK	Natural History Museum, London
NMSA	KwaZulu-Natal Museum, Pietermaritzburg South Africa
NMV	National Museum of Victoria, Melbourne
NMW	National Museum of Wales
UMZC	University Museum of Zoology, Cambridge, UK
WAM	Western Australian Museum, Perth
ZISP	Zoological Institute, St Petersburg, Russia

Other abbreviations

IWP	Indo-West Pacific
L	shell length
LV	left valve
P1	protoconch 1 length
P2	protoconch 2 length
RV	right valve
SEM	scanning electron microscopy
sh	complete shell both valves
v	single valve

Systematics

Family Lucinidae Fleming, 1828
Subfamily Lucininae Fleming, 1828

***Rugalucina* gen. nov.**
http://zoobank.org/09C8B8AD-4DF9-48A5-8D17-EACA3B276B11

Type species. *Lucina* (*Codakia*) *angela* Melvill, 1899. Here designated.

Diagnosis. Small L to 15 mm, sub-circular, sculpture of fine, commarginal lamellae crossed by strong radial ribs more prominent to anterior and posterior, with overall crinkled appearance, ligament largely internal, obliquely inset, anterior adductor muscle scar ventrally detached from pallial line for half of length, inner shell margin crenulate.

Etymology. From Latin *ruga* for wrinkle or crease and *Lucina*, feminine.

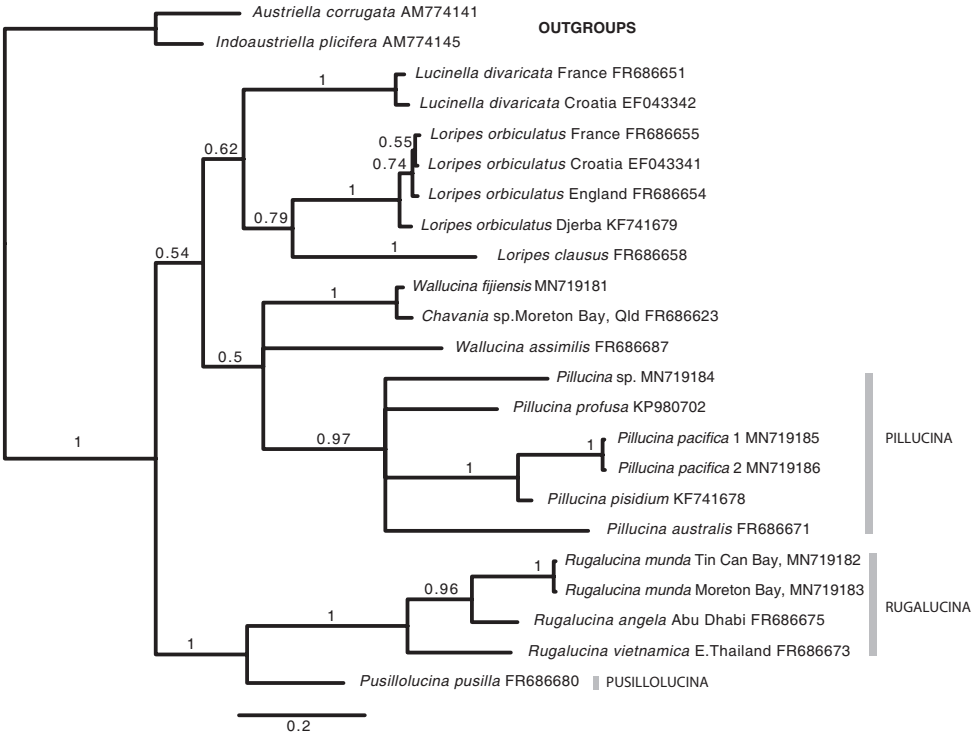

Figure 1. Single gene tree for the *Loripes* group of genera and species based on cytochrome b gene sequences, using Bayesian inference as implemented by MrBayes. Support values are posterior probabilities. Methods as in Taylor et al. (2011, 2016). GenBank numbers are attached to names. Newly sequenced species: *Wallucina fijiensis* Kavieng, Papua New Guinea (MNHN IM- IM-2013-54066), *Pillucina pacifica*, Kavieng, KAV 1 (MNHN IM- IM-2013-54743), KAV 2 (MNHN IM-2013-51690), *Pillucina* sp. Kavieng, PNG (MNHN IM-2013-54590), *Rugalucina munda* North Stradbroke Island, Moreton Bay, Qld, Australia (NHMUK 20191069), *R. munda* Tin Can Bay, Qld, Australia (NHMUK 20191070).

Included species. *Lucina* (*Codakia*) *angela* Melvill, 1899, *Pillucina vietnamica* Zorina, 1978, *Lucina* (*Codakia*) *munda* A. Adams, 1856. Tentatively included: *Divaricella cypselis* Melvill, 1918 and *Lucina concinna* H. Adams, 1871.

Comparison with other genera. *Rugalucina* is part of the broader *Loripes* group within the Lucininae, all having an obliquely inset internal ligament. Other genera within the group are *Pillucina*, *Pusillolucina Wallucina*, *Lucinella*, *Chavania*, and *Keletistes*. Of these only *Pillucina*, *Pusillolucina*, and *Rugalucina* have prominent radial sculpture. In shell characters *Rugalucina* differs from *Pillucina* in the more strongly divergent radial sculpture, the longer anterior adductor muscle scar and the more coarsely crenulate inner shell margin.

In molecular analyses members of the *Loripes* group form a monophyletic subclade of Lucininae. Seven species of putative *Pillucina* have been included in analyses (Taylor et al. 2016), *P. pisidium*, *P. symbolica*, *P. australis*, *P. profusa*, *P. pacifica*, '*P.*' *pusilla*, and '*P.*' *vietnamica*, the latter from Thailand, Abu Dhabi, and Queensland. Although the type species *P. hawaiiensis* has not yet been included, *P. pacifica* is similar in morphol-

ogy and could be regarded as a proxy. The *Pillucina* species are not monophyletic in published trees or in the mitochondrial cytochrome b gene tree (Fig. 1), with those identified as *P. vietnamica* and *P. pusilla* separated from the other species and now classified herein into two new genera with distinct morphological characters. Note: we use the cyt b gene in the analysis of the *Loripes* group shown in Fig. 1 as this best reflects species level relationships within clades of the subfamily Lucininae as shown by previous analyses using three genes (Taylor et al. 2011, 2016).

Previously, we regarded *Pillucina vietnamica* as a wide-ranging species in the northern Indian Ocean through south east Asia to southern China (Glover and Taylor 2001), the name replacing the earlier but preoccupied *Lucina fischeriana* Issel, 1869, with *P. angela* as an possible phenotype from the northern Arabian Sea. Although more comprehensive sampling across the whole range is desirable, evidence from analysis of the cytochrome b gene (Fig. 1) shows that specimens from Tin Can Bay and Moreton Bay, Qld, Australia differ from samples from Kungkraben Bay, Thailand and Abu Dhabi supporting a species level separation. Our evidence suggests that *Pillucina* '*vietnamica*' from Arabia, Thailand and Queensland are distinct. After further study of type material, we use the name *R. angela* for the northern Indian Ocean species, *P. vietnamica* for the southeast Asian species, and *P. munda* for the northern Australian species.

Lucina concinna H. Adams, 1871 previously placed in the synonymy of *P. vietnamica* by Glover and Taylor (2001) is now recognised as having distinct morphological characters and renamed because the original species name is preoccupied. We also resurrect *Divaricella cypselis* Melvill, 1918 from the synonymy of *R. angela* and recognise it as another morphologically distinct species, from the Arabian Sea and southern India.

Rugalucina angela **(Melvill, 1899)**

Figs 2, 3

Lucina fischeriana Issel, 1869: 83–84, pl. 1, fig. 8 (non *L. fischeriana* d'Orbigny, 1845: Jurassic fossil).
Lucina (*Codakia*) *angela* Melvill, 1899: 98, pl. 2, fig. 8.
Loripes fischeriana: Lamy 1916: 151.
Pillucina fischeriana: Oliver 1992: 98, pl. 20, fig. 4.
Pillucina fischeriana: Oliver 1995: 236, fig. 1026.
Pillucina angela: Oliver 1995: 236, fig. 1025.
Pillucina vietnamica (part): Glover and Taylor 2001: 273.
Pillucina angela: Glover and Taylor 2001: 279, figs 9 h, i.
Pillucina angela (part): Huber 2015: 422, figs p. 76.

Type material. *Lucina fischeriana* 5 syntypes (MCG), type locality: Suez, Egypt.

L. angela two syntypes NHMUK1899.12.18.20-21; L 7.9 mm and 6.1 mm; 1 syntype NMW 1955.158.684.

Type locality. Gwadur, Pakistan, 8 fathoms (15 m).

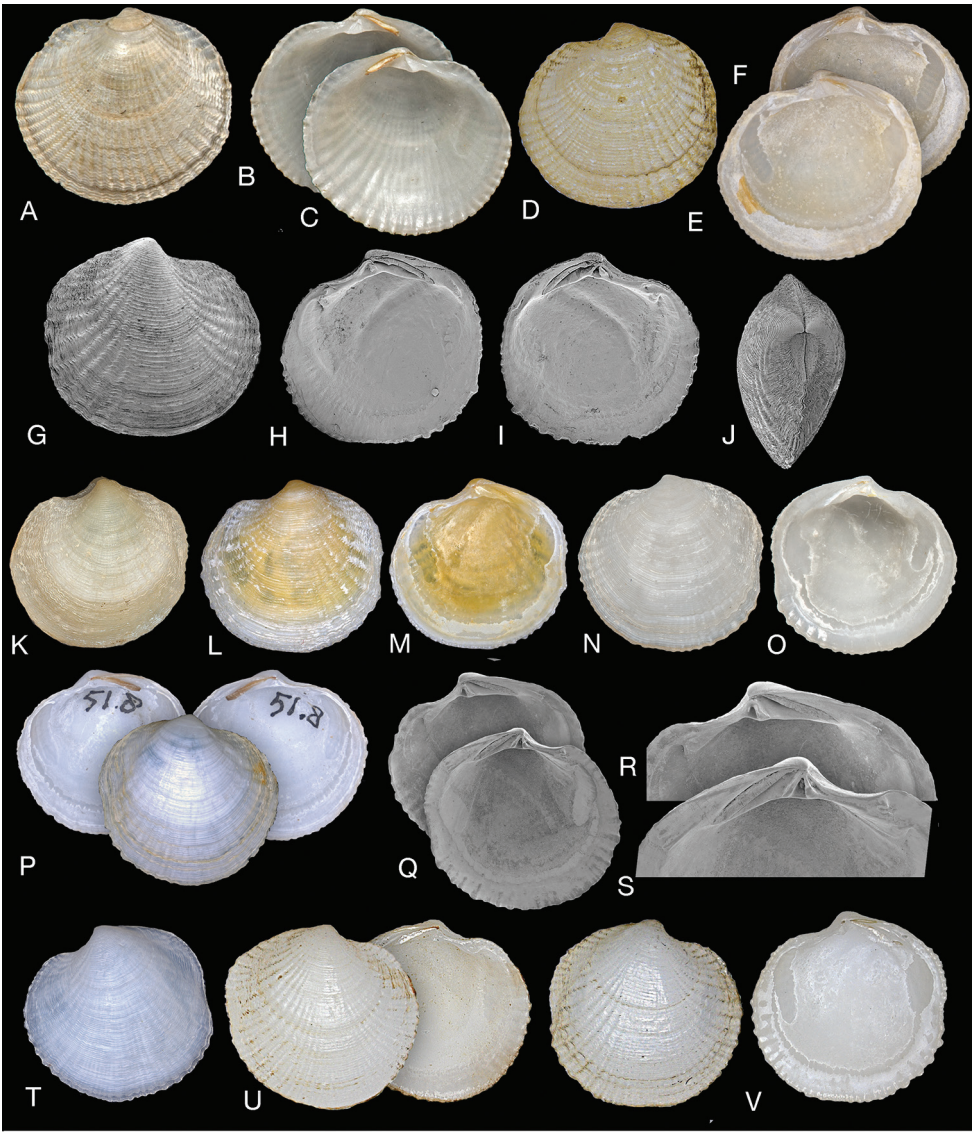

Figure 2. *Rugalucina angela* (Melvill, 1899). **A–C** Syntype of *Lucina* (*Codakia*) *angela* Melvill, 1899 (NHMUK 1899.12.18.20), exterior of left valve and interiors of right and left valves. Gwadur, Pakistan, L 8.1mm **D–F** *L.* (*C.*) *angela* syntype (NHMUK 1899.12.18.20), exterior of left valve and interiors of right and left valves, L 6.1 mm **G–M** *Rugalucina angela* Ras al Khaimah, Arabian Gulf, (NHMUK 20191071) **G** exterior SEM of right valve, L 5.0 mm **H, I** interior SEM of right and left valves, L 7.7 mm **J** dorsal view, L 5.9 mm **K** exterior of left valve, L 7.9 mm **L, M** exterior of left valve, interior of right valve, L 7.6 mm **N, O** *R. angela* exterior and interior of left valve, Gulf of Suez (NHMUK1868.5.29.2), L 13.7 mm **P** *R. angela* exterior of right valve and interior of right and left valves, Egypt, 7km south of Hurgada, H Dekker colln 4569, L 12.8 mm **Q** interior of left and right valves, Egypt, Port Safaga, H Dekker colln 3263, L 9.4 mm **R, S** detail of hinge teeth of **Q**. **T** *R. angela* exterior of left valve. Red Sea, Yemen, Orestes Point, N of Midi, H Dekker colln 4553, L 9.8 mm **U** *R. angela* exterior of right and interior of left valves, Aden (NHMUK 1963340), L 10.6 mm **V** *R. angela* exterior and interior of right valve, Krusadai, India, (NHMUK 1953.1.30.69-76), L 8.4 mm.

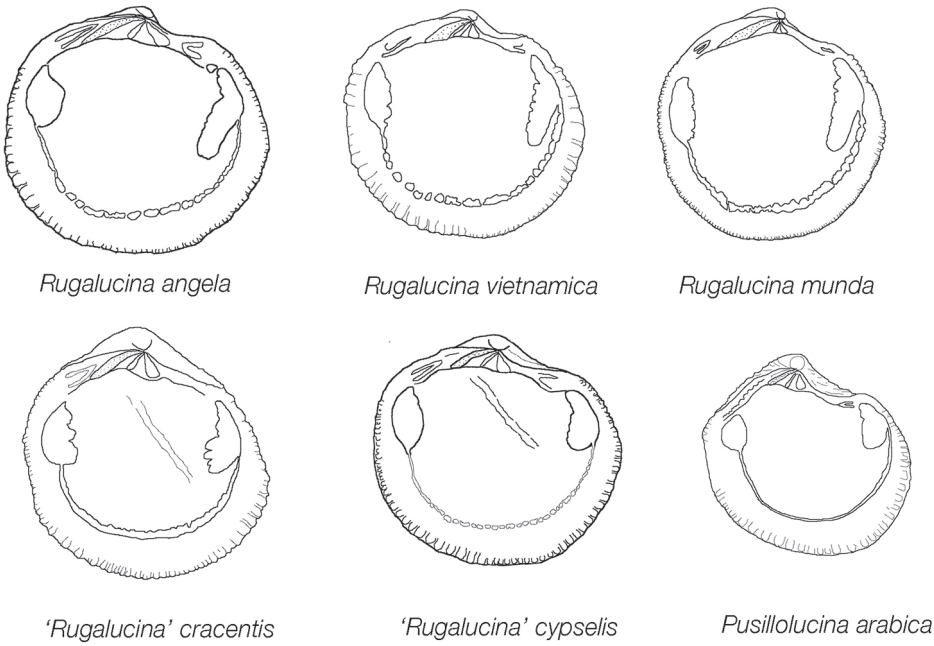

Figure 3. Internal drawings of left valves of *Rugalucina* and *Pusillolucina* species. Not to scale.

Description. Small (L to 15 mm), subcircular, inflated. Colour white, yellow or orange. Waxy appearance. Sculpture of strong diverging radial ribs, broader and more widely spaced to the anterior and posterior. Ribs crossed by fine, closely spaced, commarginal lamellae which curve over ribs producing a roughly scabrous appearance. Central parts of shell generally without ribs. Lunule large, broadly lanceolate, smooth. Ligament internal, obliquely inset. Hinge: RV with single large cardinal tooth and short anterior and posterior lateral teeth, LV with two cardinal teeth, lateral teeth consisting of small sockets. Anterior adductor scar narrow, elongate, detached from pallial line for ca. half of length. Pallial line irregularly lobate, or slightly divided. Inner shell margin coarsely crenulate to anterior and posterior.

Distribution. Red Sea: Great Bitter Lake (Hoffman et al. 2006), Suez Canal, El Ballah (NHMUK 1950.11.10.1), Suez (NHMUK 1968.5.29.2), Safaga, Dongonab Bay (NHMUK), Oreste Point, Yemen (Dekker colln), Aden (NHMUK 1963340). **Arabian Gulf**: Kuwait (NHMUK), Tarut Bay, Qatar (NHMUK), Abu Dhabi (NHMUK), Ras al Khaimah (NHMUK). **Arabian Sea**: Khor Kalba, Sharjah (NHMUK), Karachi, dredged (NHMUK 1953.1.30.85). Oman: Masirah Island (NHMUK). **Indian Ocean**: South India: Chennai (Madras) (NHMUK 1953.1.30.169-73), Krusadai Island (NHMUK 1953.1.30.110), Kundugal Point, Krusadai Island (NHMUK1953.1.30.175-181), Tuticorin (NHMUK 1953.1.30.99-101). Sri Lanka: Trincomalee (NHMUK 1910.9.28.175-178).

Rugalucina angela (as *Pillucina vietnamica*) is recorded as an invasive species off Israel in the eastern Mediterranean (Steger et al. 2018).

Remarks. *Rugalucina angela* shows variation in shell morphology between various localities around the Arabian Peninsula and Red Sea. For example, shells from the Arabian Gulf are usually smaller, while those from the northern Red Sea as on Gulf of Suez shores are generally larger, and the marginal crenulations stronger. We regard these differences as ecophenotypic probably associated with the extreme environmental conditions such as the very high salinities experienced in the southern Arabian Gulf, usually more than 40 psu but in shallow lagoons as high as 52–55 psu (Price 1982) and approximately 40–46 psu at Safaga in the northern Red Sea (Zuschin and Oliver 2003) and probably higher for the habitats occupied by *Rugalucina*.

Rugalucina angela is closely similar in shell morphology to *R. vietnamica* and *R. munda*. The differences are subtle; externally they share diverging radial ribs that are stronger to anterior and posterior, and the fine commarginal lamellae. *Rugalucina angela* has a shorter anterior dorsal area, larger hinge plate and teeth, and a slightly more divergent anterior adductor scar. *Rugalucina vietnamica* is higher, with a longer anterior dorsal area. *Rugalucina munda* is similar but the radial sculpture is much less pronounced with finer margin denticulations and subdued commarginal sculpture.

Rugalucina vietnamica (Zorina, 1978)

Figs 3, 4

Pillucina vietnamica Zorina, 1978:195, figs 3 & 6).
Pillucina vietnamica: Lutaenko 2000: 383, pl. 1, figs 1, 2; pl. 3, fig. 1.
Pillucina vietnamica (part): Glover and Taylor 2001: 273, figs 7a-g.
Pillucina vietnamica: Glover et al. 2016: 553, fig. H, A-M.
Pillucina angela (Melvill, 1899) (part): Huber 2015: 422, figs p. 76.

Type material. *Pillucina vietnamica* syntypes (ZISP), 13 shells and 1 valve, L 5.5–8.9 mm.

Type locality. Intertidal, south coast of Hainan, China.

Description. Small (L to 10 mm), sub-circular, longer than high, posteriorly slightly truncate, moderately inflated. Shell white, slightly translucent and waxy in appearance. Sculpture of many, fine, low, commarginal lamellae and low radial ribs which are broader and more prominent towards the anterior and posterior. Radial ribs are conspicuously fluted where commarginal lamellae cross giving a crinkled appearance. Lunule elongate, lanceolate and impressed, slightly asymmetrical. Ligament internal, short, situated on a broadly triangular resilifer. Hinge: right valve with single, cardinal tooth, anterior and posterior lateral teeth small, posterior tooth elongate. Left valve with two narrow cardinal teeth, a small anterior lateral socket and posterior lateral narrow socket. Anterior adductor muscle scar medium-long, detached for ca. 50 % of length. Posterior scar ovate. Pallial line entire, sometimes partially discontinuous or irregularly lobate. Shell margin crenulate, with crenulations coarser towards anterior and posterior.

Distribution. Singapore: Pulau Semakau (NHMUK), Seringat Bay (NHMUK). **Malaysia**: Langkawi (AMS). **Western Thailand**: Ao Bang Ben, Kapoe (NHMUK), Ban Bang Ben (NHMUK), Tung Nam Dan, Phang Nga Province

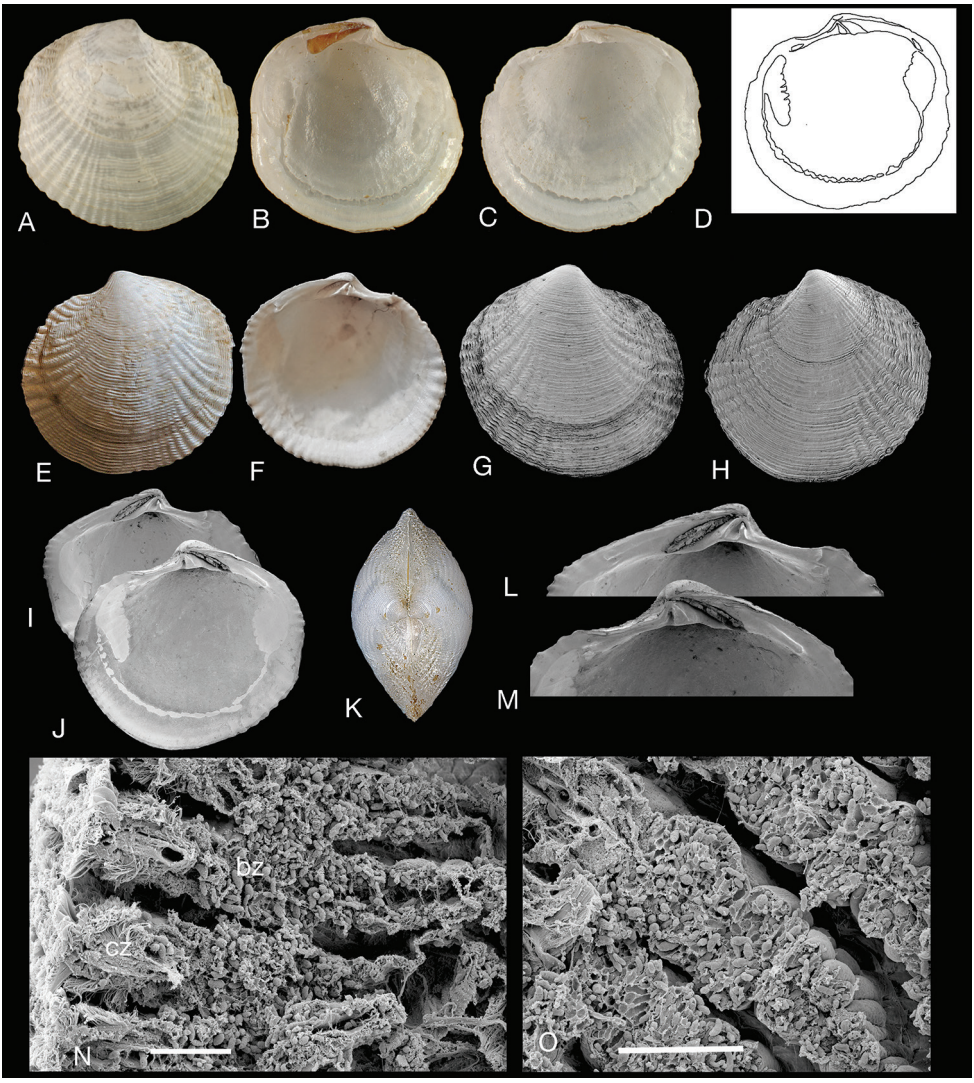

Figure 4. *Rugalucina vietnamica* (Zorina, 1978). **A–C** *Pillucina vietnamica* Zorina, 1978 syntypes (ZISP), exterior of right valve and interior of left and right valves, Hainan, China, L 5.5–8.9 mm **D** internal drawing of **C. E, F** *R. vietnamica* Palau Semaku, Singapore (NHMUK 20150057), L 8.5 mm **G–L** *R. vietnamica* Kungkraben Bay, eastern Thailand (NHMUK 20191072) **G** exterior of right valve, L 7.0 mm. **H** exterior of left valve, L 7.0 mm **I, J** interior of left and right valves, L 7.7 mm **K** dorsal view L 5.6 mm **L, M** detail of hinge of **I** and **J**. **N** Section through gill of *Rugalucina vietnamica* Kungkraben Bay, Thailand showing filaments with ciliary (cz) and bacteriocyte zones (bz). Critical-point dried preparation **O** detail showing abundant bacterial symbionts in bacteriocytes. Scale bars: 20 μm (**N**); 10 μm (**O**).

(NHMUK), **Eastern Thailand**: Kungkraben Bay (NHMUK). **Cambodia**: 5 km E of port, Sihanoukville (NHMUK). **Vietnam**: Dam Bay near Nha Trang (Zvonareva et al. 2019). **China:** Hainan (MNHN), Hong Kong (NHMUK), Daya Bay (NHMUK).

Habitat. Intertidal to shallow sub-tidal seagrass and muddy habitats. Recorded at high densities in muddy seagrass and mangrove fringe habitats of eastern and western Thailand (Meyer et al. 2008; Rattanachot and Prathep 2016). Gill structure and symbiotic bacteria are illustrated in Fig. 4N, O.

Remarks. Although we formerly recorded *Rugalucina vietnamica* with a broad longitudinal range from the northern Red Sea to southern China (Glover and Taylor 2001) we now regard it as having a narrower range along the continental margin of south eastern Asia with few records from islands. Despite intensive sampling by the MNHN Paris Expeditions around Panglao, Philippines (2004, 2005) and Papua New Guinea (2012, 2014) no *R. vietnamica* were recorded (Glover and Taylor 2016 and unpublished data).

Rugalucina munda (A. Adams, 1856)

Figs 3, 5

Lucina (*Codakia*) *munda* A. Adams, 1856: 225 not figured.

Type material. ***Syntypes*:** 3 whole shells NHMUK 20140004. H. Cuming colln, collected by Mr Strange. Shell lengths 11.3 mm, 11.2 mm, 10.4 mm. (Fig. 5A–H).

Type locality. Moreton Bay, Queensland, Australia.

Material examined. Australia: Western Australia: Parry Harbour, Kimberley (WAM). Broome Bay (WAM). Northern Territory: Darwin, East Point. Gove (NMV), Groote Eylandt G. of Carpentaria (AMS). Friday Island, Torres Strait (AMS). Queensland: Somerset, Cape York (AMS), Port Douglas (16°28'48"S, 145°27'41"E) seaward edge of mangroves (NHMUK). Buchan Point, Cairns (AMS), Port Denison, Bowen (AMS), Seaforth, Mackay (AMS), Yeppoon (AMS), Tin Can Bay, Snapper Point (25°54'12.18"S, 153°00'58"E), mangroves, muddy sand. Moreton Bay, Redland Bay (27°37'03"S, 153°19'06"E), muddy seagrass, 1 m. North Stradbroke Island, near Dunwich, seagrass (27°29'44"S, 153°23'57"E).

Description. Small, L to 11 mm, sub-circular, posteriorly slightly truncate in juveniles, shallow posterior sulcus, moderately inflated. Shell colour white, internally often yellowish. Sculpture of fine, low commarginal lamellae crossed by low radial ribs which are broader and more prominent towards the anterior and posterior. Radial ribs are slightly fluted where crossed by commarginal lamellae. Lunule elongate, lanceolate, slightly asymmetrical. Ligament internal, short, situated on a broadly triangular resilifer. Hinge: right valve with single, narrow, cardinal tooth, anterior and posterior lateral teeth small; left valve with two narrow cardinal teeth, small anterior lateral and posterior lateral teeth. Anterior adductor muscle scar medium length, detached for ca. 50 % of length. Posterior scar ovate. Pallial line entire, irregularly lobate. Shell margin finely crenulate, with crenulations coarser towards anterior and posterior.

Distribution. Northern and north eastern Australia.

Habitat. Intertidal and shallow subtidal muddy sand, nearshore seagrass and mangrove fringe.

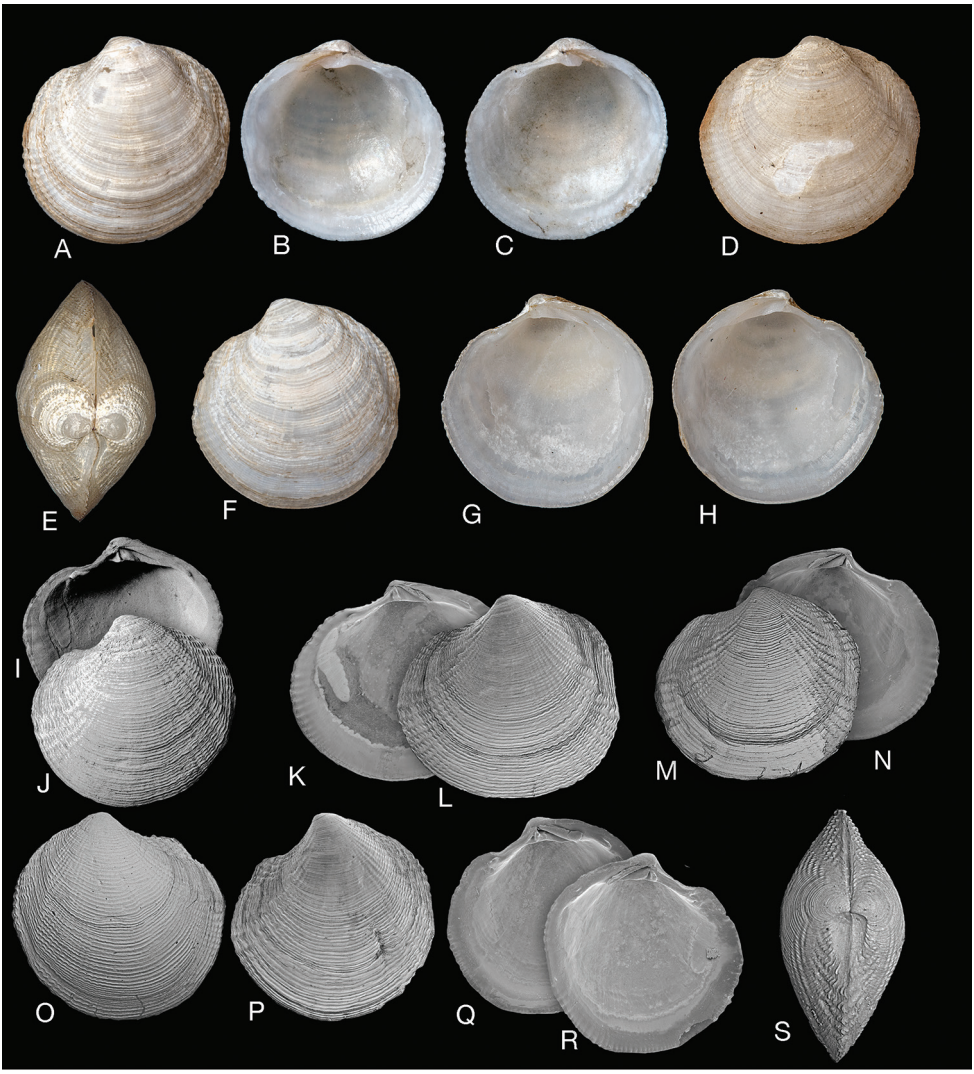

Figure 5. *Rugalucina munda* (Adams 1856). **A–H** Syntypes *Lucina* (*Codakia*) *munda* A. Adams, 1856 (NHMUK 20140004) Moreton Bay, Queensland, Australia **A–C** exterior and interior of left and right valves, syntype A, L 11.3 mm **D, E** exterior of left valve and dorsal view, syntype B, L 11.2 mm **F–H** exterior of left valve and interior of left and right valves, syntype C, L.10.4 mm **I, J** *Rugalucina munda* exterior of left valve and interior of right valve, Redland Bay, Moreton Bay, Queensland (NHMUK 20191073), L 6.8 mm **K–N** *R. munda* Tin Can Bay, Queensland (NHMUK 20191074) **K** Exterior left valve, L 6.9 mm **L** interior of right valve, L 6.3 mm **M** interior of left valve, L 5.5 mm **N** exterior of left valve, L 6.7 mm **O–S** *R. munda* Port Douglas, Queensland (NHMUK 20191085) **O** exterior of right valve, L 6.5 mm **P** exterior of left valve, L 4.8 mm **Q, R** interior of right and left valves, L 7.2 mm **S** dorsal view, L 5.5 mm.

Remarks. *Rugalucina munda* is closely similar in shell morphology to *R. vietnamica* and *R. angela* and we previously confounded the species (Glover and Taylor 2001). In shell morphology the differences are subtle; *R. munda* is more ovoid, the radial ribs

are finer, and the inner shell margin is less coarsely crenulated compared to *R. angela* and *R. vietnamica*. Furthermore, Glover and Taylor (2001: fig. 16) recorded a distributional gap between Australian and Asian records of '*P. vietnamica*'. Features of the anatomy and ctenidial bacteria of *R. munda* from Port Douglas, Qld were described by Glover and Taylor (2001, as *Pillucina vietnamica*).

Hedley (1913: 267) recommended that the name *Lucina munda* be rejected as unrecognisable because at that time type material had not been identified and the original description ambiguous. Later, because the incorrect type material had been isolated in the NHMUK collection the name *Lucina munda* had been regarded (e.g., Lamprell and Whitehead 1992) as a synonym of *Ctena bella* (Conrad, 1837). More recent recognition of the original type material (JDT & EAG) showed that *Lucina (Codakia) munda* (syntypes figured here for the first time from the Cuming collection and collected in Moreton Bay by Mr Strange) is a species similar to *Rugalucina vietnamica* and *R. angela*. In his description Adams (1856) highlights the dichotomously radiating ribs and the radially grooved inner shell margin and the yellowish shell interior. *Rugalucina munda* is thus the earliest name for the Australian species.

Rugalucina sensu lato

Here we include two species from the northern Indian Ocean and Red Sea that are similar externally to *Rugalucina vietnamica* but differ from it and each other in shell sculpture, hinge, and muscle scar characters. No molecular material is available for firmer placement of either species.

'*Rugalucina*' *cypselis* (Melvill, 1918)

Figs 3, 6

Divaricella cypselis Melvill, 1918: 156, pl. 5, fig. 33.

Type material. *D. cypselis* holotype NHMUK 1921.1.28.42. sh, L 5.2 mm.

Type locality. Karachi, Pakistan, 20–30 fathoms (36–55 m).

Other material examined. Pakistan: Karachi, Winckworth collection (NHMUK 20191075) 55 sh, 52 v. **India**: dredged Chennai (Madras), Winckworth Collection (NHMUK 1958.1.30.45) 1 sh. Chennai (Madras) (NHMUK 1953.1.30.169-73 part) 5 v.

Description. Small (L to 5.2 mm), sub-circular, inflated. Colour white or yellowish. Sculpture of diverging, curved, radial ribs prominent to anterior and posterior but are subdued or absent in middle parts of shell. Ribs crossed by closely spaced, narrow, low, commarginal lamellae that are aligned obliquely to the ventral shell margin (Fig. 6M). Radial ribs with small scales where crossed by commarginal lamellae. Early parts of shell relatively smooth. Protoconch P1 ca 88 μm, P2 ca 170 μm with growth

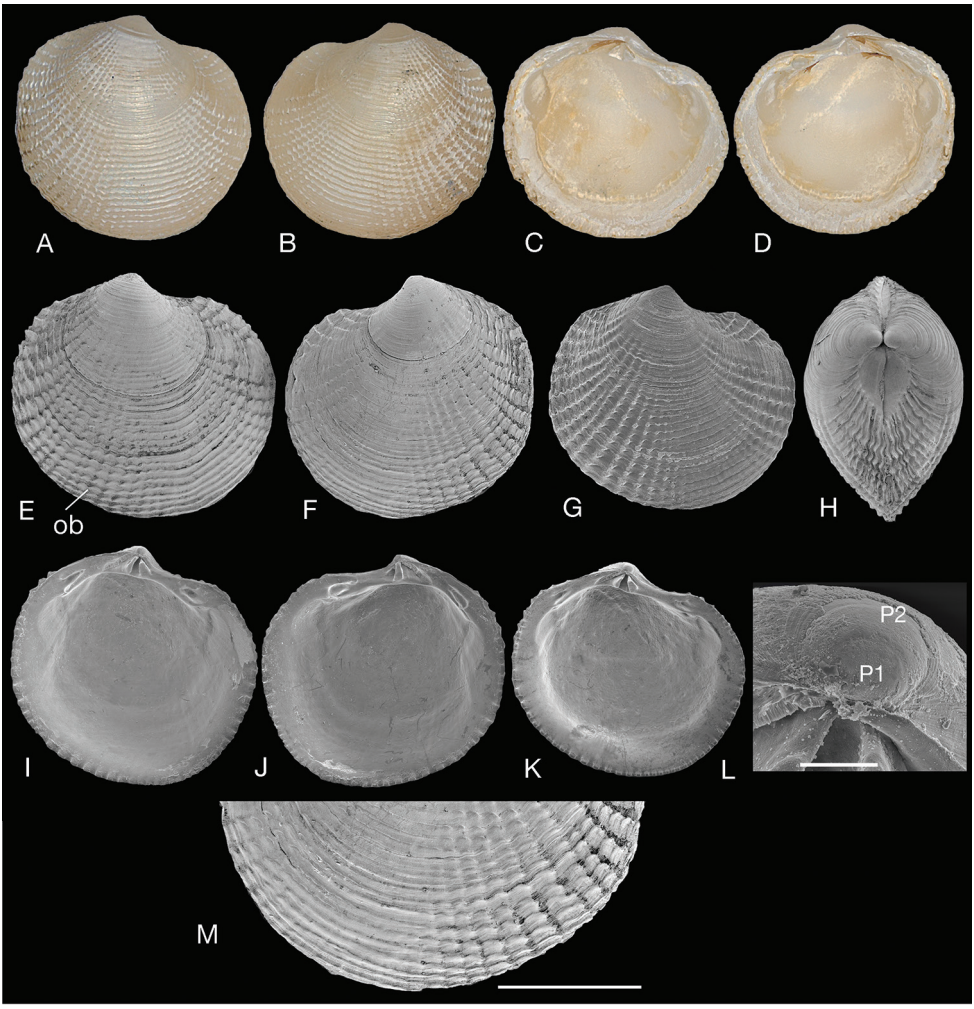

Figure 6. '*Rugalucina*' *cypselis* (Melvill, 1918). **A–D** Holotype *Divaricella cypselis* Melvill, 1918 (NHMUK 1921. 1. 28. 92), Karachi, L 5.2 mm **E–L** '*Rugalucina*' *cypselis* Karachi (NHMUK 20191075) Winckworth collection **E** right valve, L 3.1 mm, ob – oblique commarginal lamellae **F** left valve, L 3.0 mm **G** right valve, L 3.2 mm **H** dorsal view, L 1.9 mm **I** interior left valve, L 3.2 mm **J** interior right valve, L 3.2 mm **K** interior left valve, L 3.0 mm **L** protoconch **M** detail of ventral margin (**F**) showing obliquely aligned commarginal lamellae. Scale bar: 100 µm (**L**); 1 mm (**M**).

increments (Fig 6L). Lunule broadly lanceolate, smooth. Ligament largely internal, short, set on oblique resilifer. Hinge: right valve with single cardinal tooth and prominent anterior and posterior lateral teeth; left valve with two cardinal teeth, the anterior larger and sockets for anterior and posterior lateral teeth. Anterior adductor muscle scar, short, broad, ventrally detached from pallial line for ca. 15 % of length, posterior scar ovoid. Pallial blood vessel scar visible. Pallial line discontinuous in small blocks. Shell margin dentate, coarser towards anterior and posterior.

Distribution. Known from the northern Arabian Sea and southern India. Probably more abundant in the northern Indian Ocean but unrecognised.

Remarks. Dekker and Goud (1995: 6) excluded *D. cypselis* from *Divaricella* more correctly suggesting placement in *Pillucina*. Whereas previously we included *Divaricella cypselis* in the synonymy of *Pillucina angela* because of the similarity of external sculpture (Glover and Taylor 2001) we now recognise it as a morphologically distinct species. The holotype and other specimens from the Karachi area all have a very short anterior adductor muscle scar (Figs 3, 7I–K) that is barely detached from the pallial line compared with the longer and ventrally detached scar of *Rugalucina angela*, *R. vietnamica* and *R. munda*. It also has a distinctive sculpture of oblique commarginal lamellae set at an angle to the ventral shell margin that is not seen in other *Rugalucina*. Similar radial ribs and dentate inner shell margin are present in *Pusillolucina* species, but they have multi-cuspate posterior lateral teeth and lack the oblique commarginal sculpture.

The obliquely inset internal ligament indicates placement in the *Loripes* group of genera and while the external sculpture resembles *Rugalucina* in radial ribbing the obliquely aligned commarginal lamellae are similar to that seen in *Lucinella divaricata* (Linnaeus, 1758) from the eastern Atlantic but that species lacks any radial ribbing.

'*Rugalucina*' *cracentis* sp. nov. (replacement name)
http://zoobank.org/1D3FC94A-5371-40EC-AB78-B85AF858A230
Figs 3, 7

Lucina concinna H. Adams, 1871: 791, pl. 48, fig. 13 (non *Lucina concinna* Deshayes, 1857 an Eocene fossil).
Loripes concinnus: Lamy 1916: 15.
? *Pillucina concinna*: Oliver 1992: 98, pl 20, figs 5a, b.
Pillucina cypselis (Melvill, 1918): Dekker and Orlin 2000: 11.
Pillucina vietnamica: Zuschin and Oliver 2003: pl. 24, figs 24.8-24-13.

Type material. Holotype of *Lucina concinna* UMZC I.100470 Gulf of Suez, Red Sea. L 9.2 mm.

Etymology. *cracentis* Latin, genitive singular of *cracens* meaning neat, graceful. Adjective.

Diagnosis. Ovoid shape, slightly higher than long, diverging radial ribs, ligament short, largely internal, hinge with ventral flexure, right valve with single large cardinal tooth, anterior adductor muscle scar short.

Description. Small, L to 9 mm. ovoid, slightly higher than long (H/L 1.01), inflated, umbones prominent, rounded. Colour white or yellowish. Sculpture of diverging radial ribs, coarser and more widely spaced to anterior and posterior, ribs finer and more subdued in middle parts of shell. Ribs crossed by fine, low, closely spaced, commarginal lamellae. Lunule short, heart shaped. Ligament short, obliquely inset. Hinge line with ventral flexure (Fig. 7R, S), right valve with single, relatively large cardinal tooth and small

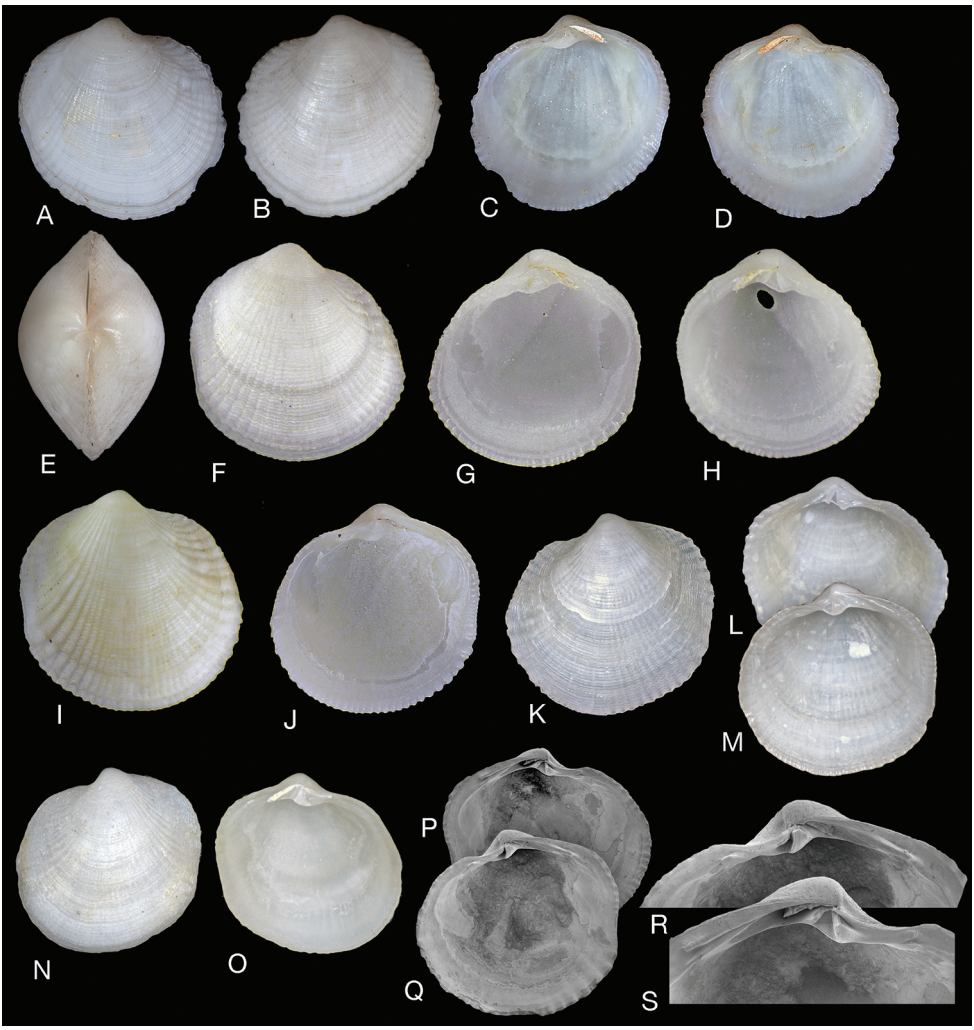

Figure 7. '*Rugalucina*' *cracentis* sp. nov. **A–E** *Lucina concinna* Holotype (ZMC I.100470) Gulf of Suez, exterior and interior of right and left valves and dorsal view, L 9.2 mm **F–H** '*Rugalucina cracentis*' exterior of right valve and interior of right and left valves Egypt, Dahab, Gulf of Aqaba, Red Sea. H. Blatterer colln, L 6.7 mm **I, J** *R. cracentis* exterior and interior of right valve Dahab, Gulf of Aqaba, Red Sea, H. Blatterer colln, L 8.5 mm **K, L** *R cracentis* exterior and interior of left valve Egypt, 4 km north of Port Safaga, H. Dekker colln 6930, L 8.3 mm **M** interior of right valve, L 8.8 mm **N, O** exterior and interior left valve Egypt, 4 km north of Port Safaga, H. Dekker colln 6930, L 7.1 mm **P, Q** interiors of right and left valves, H. Dekker colln 6930, L 8.7 mm **R, S** hinge details of **P** and **Q**.

anterior and posterior lateral teeth, left valve with two cardinal teeth the anterior larger and a central socket, small anterior and posterior lateral teeth. Anterior adductor muscle scar short with lobate posterior dorsal edge, ventrally detached from pallial line for 15% of length; posterior scar ovate. Pallial line largely entire, irregularly lobate. Pallial blood vessel trace visible. Inner shell margin crenulate, more coarsely to anterior and posterior.

Distribution. Red Sea: Egypt: Gulf of Suez (ZMC), Port Safaga (Dekker colln), Ras Baghdadi (Dekker colln), Sharm el Naga (Dekker colln), Makadi Bay (Dekker colln), Gulf of Aqaba: Dahab (Blatterer colln), Yemen -al Durayhimi (Dekker colln), Aden (NHMUK 1902.12.30.749). **Arabian Gulf**: Kuwait (NHMUK), Saudi Arabia, Tarut Bay (NHMUK 20191076).

Remarks. Dekker and Orlin (2000) used *Pillucina cypselis* as a synonym of the preoccupied *Lucina concinna* but, as shown above, the species differ in external morphology. Although Glover and Taylor (2001) included this species in the synonymy of *Pillucina vietnamica* (NW Indian Ocean forms now *Rugalucina angela*) we consider it distinct. Externally, it is similar to *Rugalucina angela* but differs in the ovoid shape, the finer radial ribs, the much shorter anterior adductor scar, the ventral flexure of the hinge line and large cardinal tooth in the right valve.

The ovoid shape and flexured hinge line with the large cardinal tooth in the right valve are features of *Pillucina* s. s. but *Pillucina* species usually have less prominent radial ribbing (Glover and Taylor 2001, 2016). Molecular data are needed to determine placement in either *Pillucina* or *Rugalucina*.

Pusillolucina gen. nov.

http://zoobank.org/EE71DE26-9C58-44AE-9531-39C064CA866A

Type species. *Pillucina pusilla* Glover & Taylor, 2016. Here designated. Philippines.

Diagnosis. Very small, L to 3 mm, sub-circular, higher than long. Umbones prominent. Sculpture of thin commarginal lamellae, elevated to anterior and posterior, crossed by radial ribs that are more prominent to anterior and posterior. Lunule broadly lanceolate, concave. Ligament short, largely internal. Hinge: RV with single cardinal tooth, large anterior lateral tooth and a complex multi-cuspate posterior lateral tooth consisting of up to ten cusps; LV with two cardinal teeth, the anterior larger, posterior lateral tooth formed of sockets for projecting cusps of the right valve. Anterior adductor scar very short, barely detached from pallial line, pallial line irregularly discontinuous. Inner shell margin crenulate.

Etymology. Derived from Latin *pusilla* meaning very small and *Lucina*. Feminine

Comparison with other genera. *Pusillolucina* is similar in many external characters including shape and sculpture to some *Pillucina* (type species *Pillucina spaldingi* Pilsbry, 1921 = *Pillucina hawaiiensis* (Smith, 1885)). By comparison no *Pillucina* species possess the unusual multi-cuspate posterior dentition. Moreover, *Pusillolucina pusilla* is distinct in molecular analyses (Fig. 1 and Taylor et al. 2016) from most *Pillucina* including five common shallow water Indo-West Pacific species but aligns with '*Pillucina vietnamica*'. This latter is now placed in a separate genus, *Rugalucina* (see below), whose species are larger and, significantly, even in minute juveniles, lack the multi-cuspate posterior lateral teeth of *P. pusilla* and its congeners.

Included species. *Pillucina pusilla*, *Pillucina denticula* Glover & Taylor, 2001, *Pusillolucina africana* sp. nov., *Pusillolucina arabica* sp. nov., *Pusillolucina biritika* sp. nov. These species differ mainly in characters of the dentition.

Distribution. Indo-West Pacific, low intertidal to 70 m.

***Pusillolucina pusilla* Glover & Taylor, 2016**
Figs 8 A–F

Pillucina pusilla Glover and Taylor 2016: 159, figs 41D, 44 A–L.

Type material. ***Holotype*:** MNHN-IM-2000-26591. ***Paratypes*:** 6 (MNHN-IM-2000-26592, IM-2009-10362). L 1.2–1.8 mm.

Type locality. Philippines, Bohol Island, Manga, 9°41.1'N, 123°51.4'E, 3–4 m, mud, [PANGLAO 2004: stn S19].

Description. Very small, glossy, L to 1.8 mm, sub-circular, higher than long, inflated. Umbones prominent. Sulci and dorsal areas poorly defined. Sculpture of thin commarginal lamellae elevated to anterior and posterior, with 17–25 low, rounded radial ribs, divaricate in anterior part of shell. Juvenile shell with elevated commarginal lamellae but no radial ribs. Microsculpture of fine growth increments only. Protoconch P1 +P 2 = 134 µm, P2 with numerous growth increments. Lunule broadly lanceolate, depressed, asymmetric, larger part in left valve. Ligament short, internal, oriented

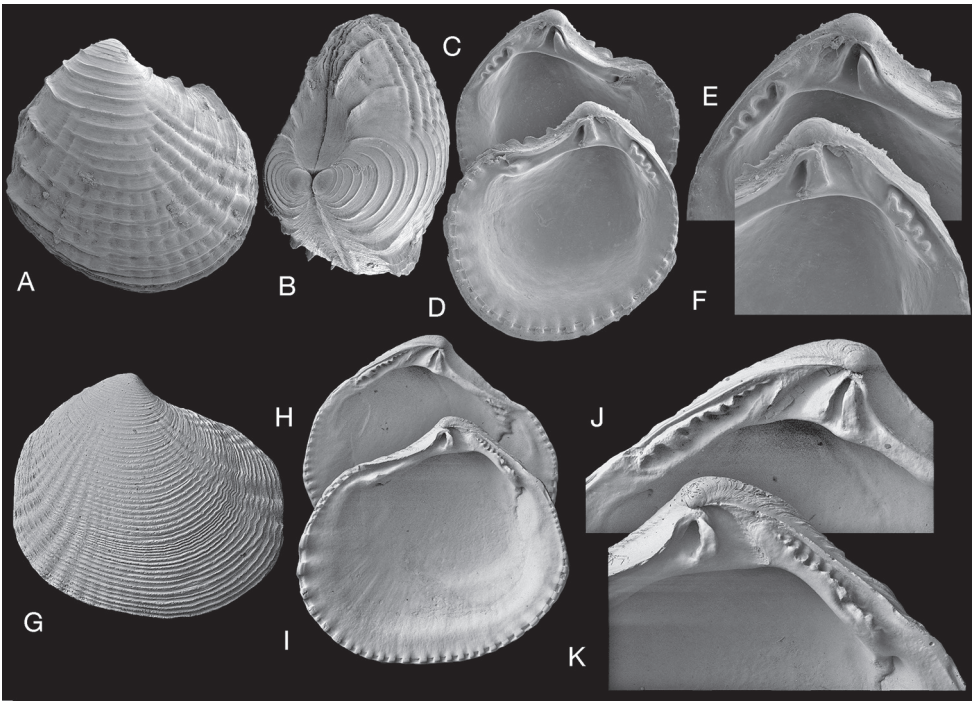

Figure 8. *Pusillolucina pusilla* and *P. denticula.* **A–D** *Pusillolucina pusilla* (Glover & Taylor, 2016) **A** *Pillucina pusilla* Holotype (MNHN IM-2000-26591) Philippines, Bohol Island, L 1.2 mm **B** holotype dorsal view **C, D** *P. pusilla* interior of left and right valves, paratype (MNHN IM-2000-26592), L 1.05 mm **E, F** detail of hinge teeth in **C, D**. **G–K** *Pusillolucina denticula* (Glover & Taylor, 2001) Durban Bay, South Africa **G** exterior of right valve, paratype (NMSA), L 2.9 mm **H, I** interior of left and right valves, holotype (NMSA), L 3.5 mm **J, K** detail of hinge teeth.

parallel to cardinal teeth. Hinge: right valve with single cardinal tooth, large anterior lateral tooth and posterior lateral tooth consisting of four or five cusps, left valve with two cardinal teeth, the anterior larger, anterior lateral socket, posterior lateral with sockets for cusps of the right valve. Anterior adductor scar very short, barely detached from pallial line, pallial line irregularly discontinuous. Inner shell margin coarsely crenulate.

Pusillolucina denticula (Glover & Taylor, 2001)

Figs 8 G–K

Pillucina denticula Glover & Taylor, 2001: 271, figs 7a–g.

Type material. ***Holotype*****:** NMSA B310/T1758, L 3.5 mm; ***Paratypes*****:** NMSA V8402/T1759, L 2.9 mm, 2.8 mm, 3.1 mm, NHMUK 20000377, L 3.5 mm.

Type locality. Durban Bay, South Africa.

Description. Shells small, L to 3.5 mm, robust, sub-circular to ovoid in outline. Sculpture of fine, closely spaced, commarginal lamellae crossed by low, rounded radial ribs that are prominent and broader towards anterior and posterior. Ribs inconspicuous in central part of shell. Lunule long, lanceolate. Ligament internal, short. Right valve with a single cardinal tooth, a prominent anterior lateral tooth and a long posterior lateral tooth divided into 8–10 small cusps. Left valve with two cardinal teeth, a small anterior lateral and a posterior tooth divided into sockets for cusps of the RV. Anterior adductor muscle scar short and barely detached from the pallial line. Inner shell margin crenulate, with crenulations more widely spaced anteriorly.

Pusillolucina arabica sp. nov.

http://zoobank.org/BD3CBB6A-99A1-4F13-9553-BAC006538A64

Figs 3, 9,10

Type material. ***Holotype*****:** NHMUK 20191077 L 2.4 mm. ***Paratypes*****:** figured L 2.1 mm, L 2.0 mm, L 1.9 mm, unfigured 11 sh, 2 v (NHMUK 20191078).

Type locality. Arabian Gulf, Tarut Bay, Saudi Arabia, dredged (17.5.1971) K. Smythe collection.

Material examined. NHMUK consultancy report ECM 5027C/06. Arabian Gulf: station 36 FC, 27°42'38"N, 52°11'16"E 25 m (NHMUK20191080), stn 39 FC, 27°42'05"N, 52°10'50"E 31 m, NHMUK 20191081), stn 41 FC, 27°42'31"N, 52°10'02"E 32 m (NHMUK 20191079), stn 48 FC, 27°45'0.27"N, 52°07'46"E 23 m (NHMUK 20191082).

Etymology. *arabica* from Latin *arabicus*. Used as an adjective.

Diagnosis. *Pusillolucina* with posterior lateral teeth divided into four or five cusps and sockets.

Description. Shell very small, L to 2.4 mm, ovate, umbones prominent, sculpture of closely spaced, narrow, commarginal lamellae, sometimes elevated at posterior and

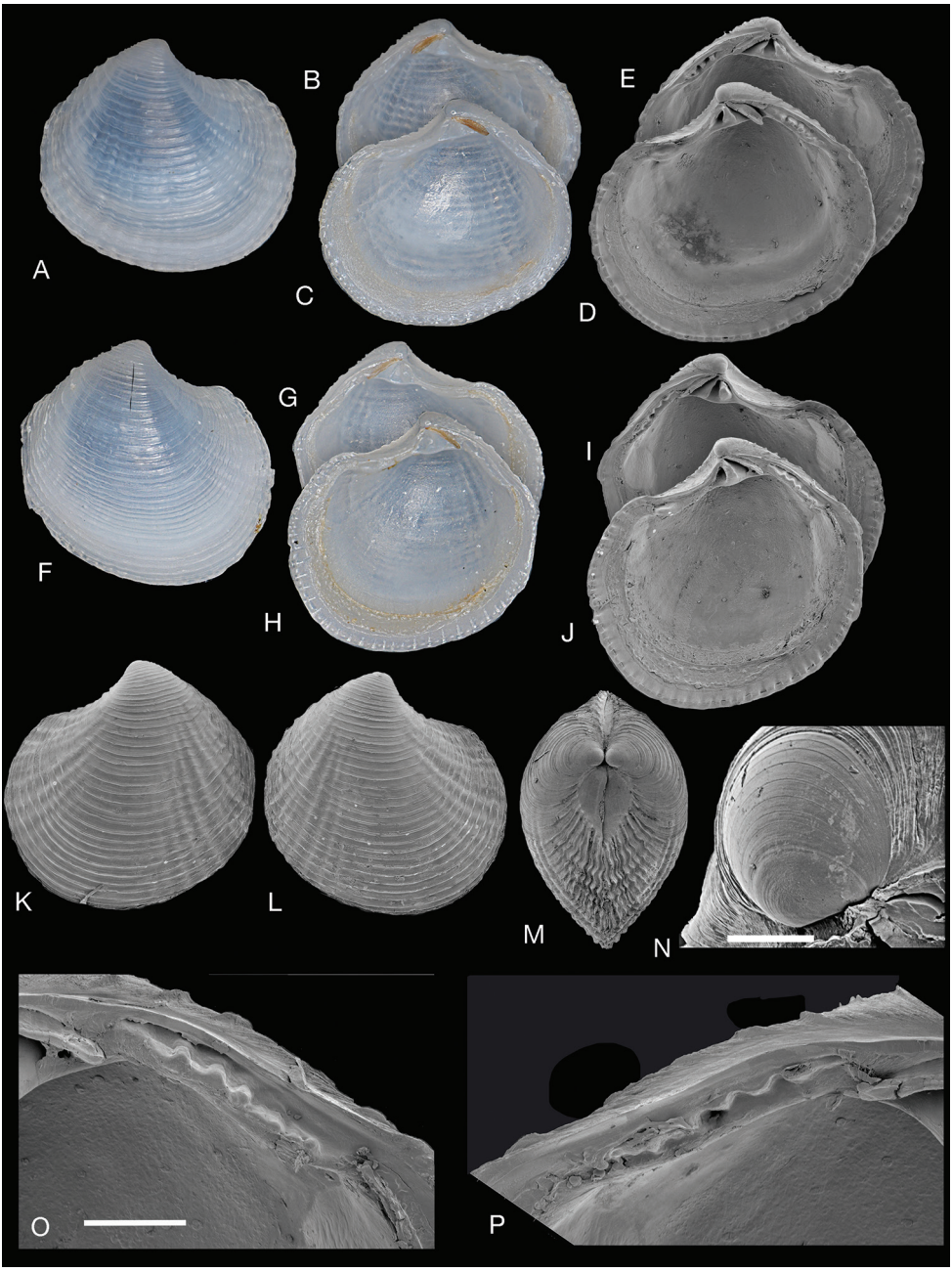

Figure 9. *Pusillolucina arabica* sp. nov. Tarut Bay, Saudi Arabia, Arabian Gulf. **A–C** Holotype (NHMUK 20191077) exterior of right valve and interior of left and right valves, L 2.4 mm **D, E** holotype, interior of left and right valves SEMs **F–H** paratype (NHMUK 20191078) exterior of right valve and interior of left and right valves, L 2.1 mm **I, J** paratype F-H (NHMUK 20191078) interior of left and right valves SEM **K, L** paratype (NHMUK 20191078) exterior of left and right valves, L 2.0 mm **M** paratype (NHMUK 20191078) dorsal view, L 1.9 mm **N** protoconch of holotype, scale bar 50 μm **O, P** paratype **I–J** detail of multi-cuspate posterior lateral hinge teeth. Scale bar: 200 μm.

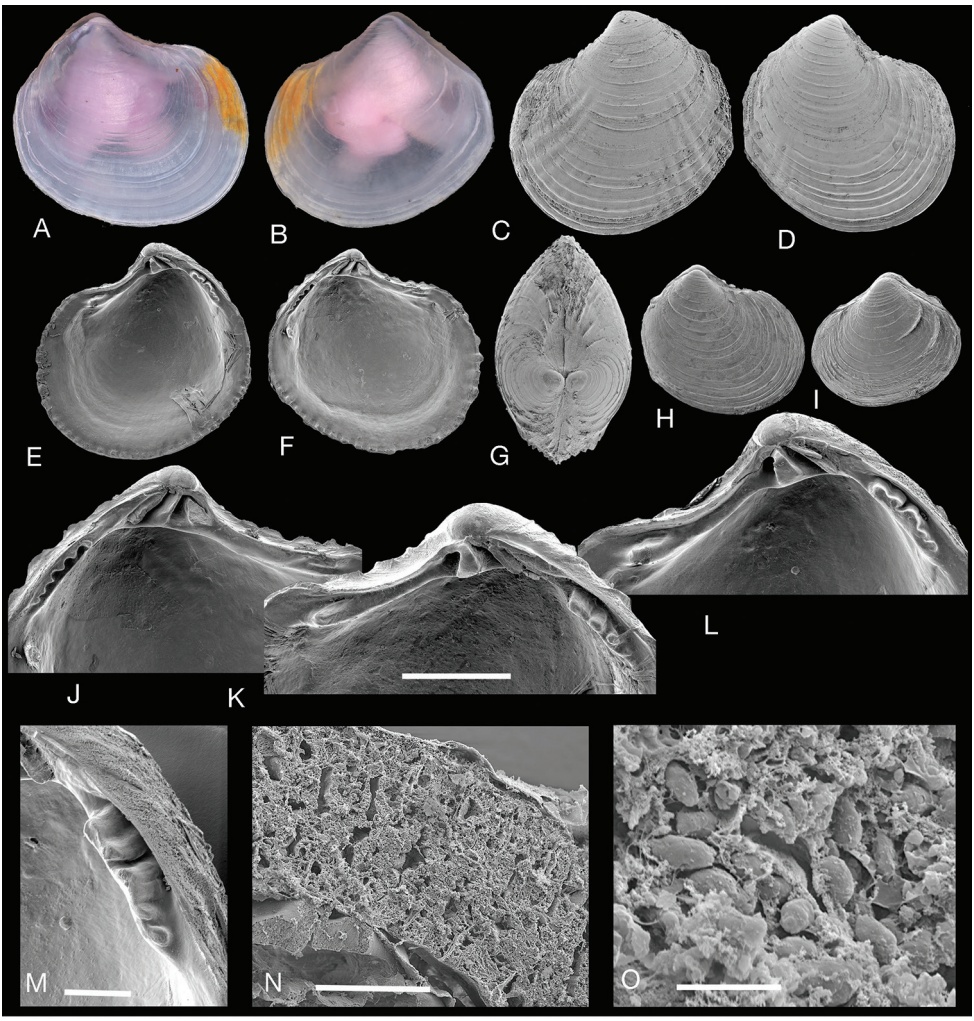

Figure 10. *Pusillolucina arabica* sp. nov. Arabian Gulf NHMUK consultancy samples- see text for details. **A** Lateral view of right valve stn 41C (NHMUK 20191079) stained with Rose Bengal, L 1.3 mm **B** lateral view of left valve stn 41C (NHMUK 20191079), L 1.2 mm **C, D** exterior of left (L 1.5 mm) and right (L 1.3 mm) valves stn 39FC (NHMUK 20191081) **E, F** Interior of right (L 1.4 mm) and left (L 1.5 mm) valves stn 36FC (NHMUK 20191080) **G** dorsal view, stn 39FC (NHMUK 20191081), L 1.3 mm. **H** juvenile shell, stn 48FC (NHMUK 20191082), L 1.1 mm **I** juvenile shell, stn 36FC (NHMUK 20191080), L 0.9 mm **J–L** hinge teeth of left and right valves stn 36FC (NHMUK 20191080) **M** detail of posterior lateral tooth of right valve stn 36FC (NHMUK 20191080) **N** section through a ctenidial demibranch with thickened bacteriocyte zone, critical point dried preparation **O** symbiotic bacteria. Scale bars: 300 μm (**J–L**); 100 μm (**M**); 50 μm (**N**); 4 μm (**O**).

anterior dorsal margins, crossed at anterior and posterior by low radial ribs, juvenile shells with commarginal lamellae only. Colour: white, translucent when wet. Protoconch: P1 84 μm, P1 + P2 = 155 μm, P2 with numerous growth increments. Lunule

broadly lanceolate, smooth. Ligament internal, short, set alongside cardinal teeth. Hinge: right valve with single cardinal tooth, anterior lateral tooth located above anterior adductor muscle. Posterior lateral tooth long, divided into four or five cusps, left valve with two cardinal teeth, the anterior larger, anterior lateral tooth small, posterior lateral tooth divided into four or five sockets for cusps of right valve. Anterior adductor muscle scar short, barely detached from pallial line, posterior scar ovoid. Inner shell margin crenulate, more strongly to anterior and posterior.

Remarks. *Pusillolucina arabica* differs from the Philippine *P. pusilla* by the more ovate outline, and the less prominent commarginal and radial sculpture. By comparison, *P. africana* has finer more closely spaced commarginal sculpture and more cusps (7–8) on the posterior lateral tooth. From South Africa *P. denticula* has much finer commarginal sculpture and up to 10 smaller cusps on the posterior lateral tooth. From Madagascar *P. biritika* sp. nov. has only three cusps on the posterior lateral tooth.

Despite its small size, *P. arabica* has the characteristic, thick inner ctenidial demibranchs with a well-developed bacteriocyte zone packed with symbiotic bacteria ca 3–4 μm (Fig. 10N, O) similar to other lucinids.

***Pusillolucina africana* sp. nov.**

http://zoobank.org/2533482F-2D76-413A-AB4E-1AC96BA998C9

Fig. 11

Type material. *Holotype*: MNHN-IM-2000-35107, sh, L 2.3 mm; ***Paratypes*:** 10 v, L 1.9–2.2 mm MNHN-IM-2000-35108, 3 v NHMUK 20191083.

Type locality. Mozambique, Inhaca Island, Baia Campessuane, 3–4 m, INHACA stn MD1, 26°03.6'S, 32°56.6'E. 25NOV2011.

Etymology. Named for Africa, used as an adjective.

Diagnosis. *Pusillolucina* with posterior lateral teeth divided into seven or eight cusps and sockets.

Description. Shell very small, L to 2.4 mm, ovate, umbones prominent, sculpture of closely spaced, narrow, commarginal lamellae, sometimes slightly elevated at posterior and anterior dorsal margins, crossed at anterior and posterior by low radial ribs, juvenile shells with commarginal lamellae only. Protoconch: P1 ca 75 μm, P1 + P2 = 140 μm, P2 with numerous growth increments. Lunule long, broadly lanceolate, smooth. Ligament internal, short, set on triangular resilifer alongside cardinal teeth. Hinge: right valve with single cardinal tooth, anterior lateral tooth located above anterior adductor muscle. Posterior lateral tooth long, divided into seven or eight cusps, left valve with two cardinal teeth, the anterior larger, anterior lateral tooth small, posterior lateral tooth with seven or eight sockets for cusps of right valve. Anterior adductor muscle scar short, barely detached from pallial line, posterior scar ovoid. Pallial line continuous. Inner shell margin crenulate, more strongly to anterior.

Remarks. For comparison with other species see *P. arabica* above.

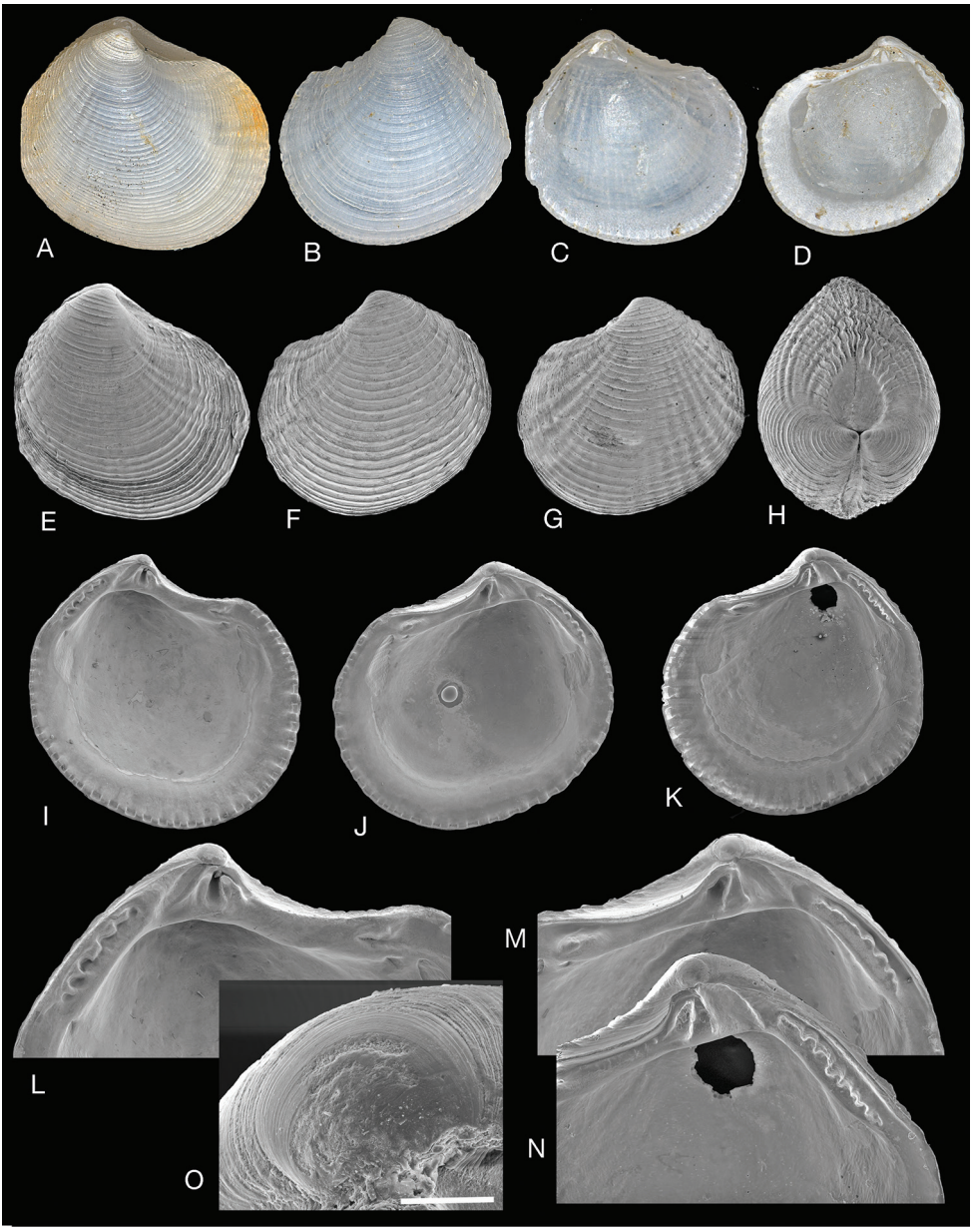

Figure 11. *Pusillolucina africana* sp. nov. Mozambique, Inhaca Island, Baia Campessuane, 3–4 m, INHACA stn MD1. **B–O** Paratypes (MNHN-IM-2000-35108). **A** Holotype (MNHN-IM-2000-35107), L 2.3 mm **B** paratype exterior left valve, L 2.1 mm **C** interior of left valve, L 2.1 mm **D** interior right valve, L 1.9 mm **E** exterior right valve, L 2.2 mm **F** exterior left valve, L 2.2 mm **G** exterior of left valve, L 2.2 mm **H** dorsal view, L 2.4 mm **I** interior of left valve, L 2.1 mm **J** interior of right valve, L 2.1 mm **K** interior of right valve, L 2.1 mm **L–N** detail of hinges of **I, J, K**. **O** Protoconch. Scale bar: 50 μm (**O**).

***Pusillolucina biritika* sp. nov.**
http://zoobank.org/FBD2E714-389D-4B91-BE1A-8BCB5820ACE9
Fig. 12

Type material. *Holotype*: MNHN-IM-2000-35109 1.1 mm, ***Paratypes*:** MNHN-IM-2000-35110, MNHN-IM-2000-35111, MNHN-IM-2000-35181, NHMUK 20191084 lengths 1.1–1.5 mm.

Type locality. *Holotype*: South Madagascar east of Cap Antsirabe, 49–52 m, ATIMO-VATAE stn TP11, 25°02.8'S, 47°01.3'E. 06MAY2010 (MNHN-IM-2000-35109).

***Paratypes*:** South Madagascar east of Cap Antsirabe, 49–52 m, ATIMO-VATAE stn TP11, 25°02.8'S, 47°01.3'E. 06MAY2010 (MNHN-IM-2000-35181 5 v).

South Madagascar off Baie Fort-Dauphin 54–56 m, ATIMO-VATAE stn TP18, 25°02.4'S, 47°03.2.6'E, 11MAY2010 (MNHN-IM-2000-35110 6 sh, 9 v. NHMUK 20191084 1 sh, 2 v).

Northwest Madagascar, S of Cap St Sébastien, 42–44 m, MIRIKY stn DW3202, 12°35.6'S, 48°49.9'E, 29JUN2009 (MNHN-IM-2000-35111 6 v).

Etymology. Biritika, meaning extremely small in Malagasy. Used as a noun in apposition.

Diagnosis. *Pusillolucina* with posterior lateral teeth divided into three cusps and sockets.

Description. Very small, L 1.5 mm, sub-ovate, longer than high, umbones prominent. Sculpture of fine commarginal lamellae crossed at anterior and posterior by low, rounded, radial ribs, juvenile shells with commarginal lamellae only. Some lamellae extended as scales along posterior dorsal margin. Lunule long, lanceolate. Ligament short internal on short resilifer. Hinge: RV with single cardinal tooth and single anterior lateral tooth, posterior lateral tooth short, divided into three cusps, LV with two cardinal teeth the posterior-most thin, posterior lateral tooth with three sockets for cusps of the right valve. Anterior adductor muscle scar short, barely detached from pallial line, posterior scar ovate. Pallial line entire. Shell margin coarsely crenulate, more strongly to anterior and posterior.

***Notocina* gen. nov.**
http://zoobank.org/50070A53-D987-4091-958E-35BB99DE91A4

Type species. *Epicodakia falklandica* Dell, 1964. Here designated.

Diagnosis. Small (L to 3 mm), sub-ovoid, slightly longer than high. Umbones prominent. Posterior dorsal margin straight. Sculpture of low, rounded, commarginal lamellae with poorly defined fine radial ribs to anterior and posterior. Microsculpture densely punctate. Ligament short, protrudes above dorsal margin. Lunule broadly lanceolate. Hinge line narrow, left valve with two small cardinal teeth and anterior and posterior lateral teeth. Right valve with single, slightly bifid cardinal tooth and anterior and posterior lateral teeth. Anterior adductor muscle scar short, slightly detached from pallial line, inner shell margin finely denticulate.

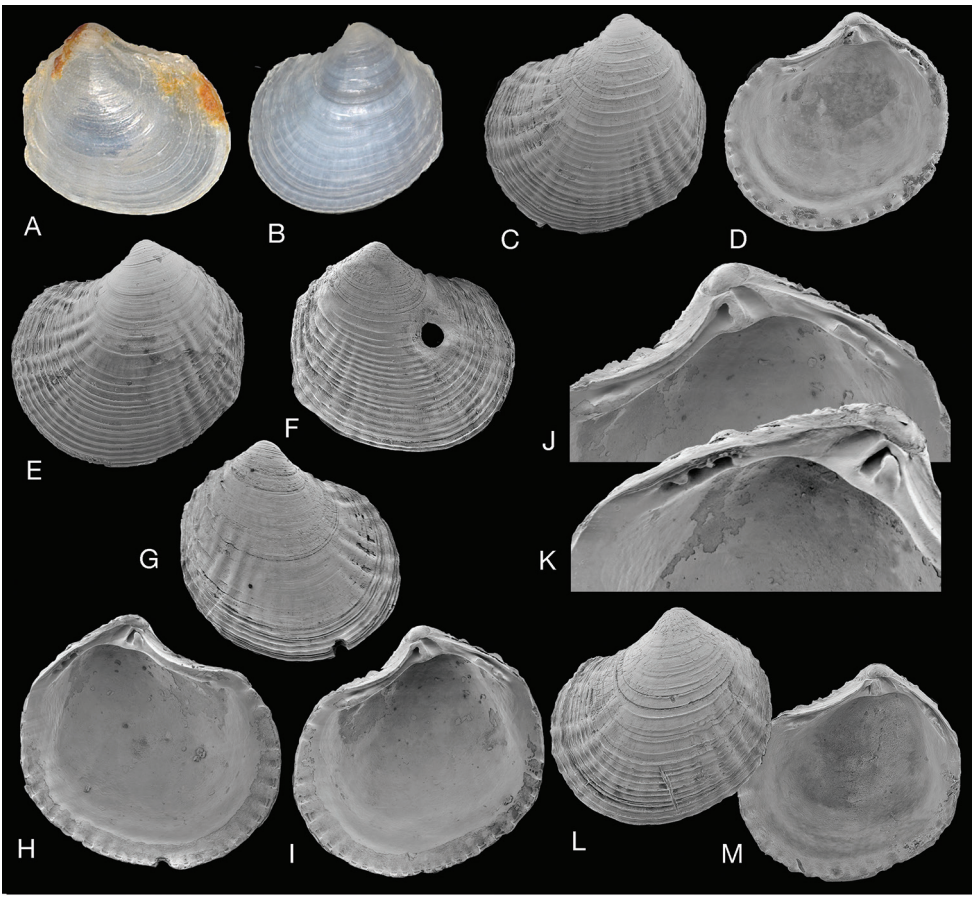

Figure 12. *Pusillolucina biritika* sp. nov. **A, B** South Madagascar east of Cap Antsirabe, 49–52 m, ATIMO-VATAE stn TP11, 25°02.8'S, 47°01.3'E. (MNHN) **C–E, L, M** South Madagascar off Baie Fort-Dauphin 54–56 m, ATIMO-VATAE stn TP18, 25°02.45'S, 47°03.26'E (MNHN) **F–K** Northwest Madagascar, S of Cap St Sébastien, 42–44 m, MIRIKY stn DW3202, 12°35.6'S, 48°49.9'E (MNHN). **A** Holotype, stn TP11 (MNHN-IM-2000-35109), L 1.1 mm **B** paratype stn TP11 (MNHN-IM-2000-35181) L 1.5 mm **C** paratype stn TP18 (MNHN-IM-2000-35110) exterior of left valve, L 1.3 mm **D** paratype stn TP18 (MNHN-IM-2000-35110) interior of right valve, L 1.3 mm **E** paratype stn TP18 (MNHN-IM-2000-35110) exterior of left valve L 1.5 mm **F** paratype stn DW3202 (MNHN-IM-2000-35111). exterior of right valve L 1.4 mm **G** paratype stn DW3202 (MNHN-IM-2000-35111). exterior of right valve L 1.1 mm **H** paratype stn DW3202 (MNHN-IM-2000-35111) interior of left valve L1.4 mm **I** paratype stn DW3202 (MNHN-IM-2000-35111) interior of right valve L 1.3 mm **J, K** detail of hinge teeth of **H** and **I**. **L, M** Paratype TP18 (MNHN-IM-2000-35110) exterior of left valve and interior of right valve L 1.2 mm.

Etymology. *notos* in Greek meaning south, *-cina* as an abbreviation of *Lucina*. In reference to the southern Atlantic distribution. Female gender.

Remarks. Dell (1964) placed *N. falklandica* in *Epicodakia* (type species *E. consettiana* Iredale, 1930) because of some similarity of hinge teeth and sculpture. He remarked that only two species of *Epicodakia* were known (*E. consettiana* Iredale, 1930

and *E. neozelanica* Powell, 1937) but since then a number of other species from the Indo-West Pacific, Western Atlantic and Eastern Pacific have been classified in the genus (Glover and Taylor 2007; 2016; Taylor et al. 2016; MolluscaBase). Molecular analyses place *Epicodakia* in the subfamily Codakiinae, close to *Ctena* species (Taylor et al. 2016). Inclusion of '*Epicodakia*' *falklandica* indicates it belongs in the subfamily Lucininae in a well-supported position as a sister species to *Troendleina suluensis* Glover & Taylor, 2106 from 150–600 m in the Sulu Sea. *Troendleina* includes three described species, all from deeper water; *T. marquesana* Cosel & Bouchet, 2008 from the Marquesas Islands, *T. musculator* Cosel & Bouchet, 2008 from the Solomon Islands and *T. suluensis* Glover & Taylor, 2016 from the Philippines and we are aware of further undescribed species. There is no close similarity of *Troendleina* to *E. falklandica* in shell characters: species of the former are larger with lengths of 30–40 mm, a sculpture of growth increments with fine radial threads, small cardinal teeth, obscure or absent lateral teeth, and a finely dentate inner shell margin. *Notocina falklandica* has some similarity to *Parvilucina* species in size and shell characters but is not closely aligned in molecular trees. Another unusual small species *Guyanella clenchi* from the southern Caribbean (Taylor et al. 2016) is similar to *Notocina falklandica* in size but differs in having a distinctive internal ligament and lacks any radial sculpture. Neither *Troendleina*, *Parvilucina* nor *Guyanella* species possess the punctate microsculpture that occurs in *N. falklandica* and sporadically amongst other Lucinidae including species of Myrteinae, some *Ctena*, *Epicodakia* and *Codakia* species (Codakiinae) and *Funafutia levukana* (Lucininae) (Glover and Taylor 2016).

***Notocina falklandica* (Dell, 1964)**
Fig. 13

Epicodakia falklandica Dell, 1964: 206, fig. 4 (17, 18, 19).

Type material. ***Holotype*:** NHMUK 1962857/1; ***Paratypes*:** NHMUK 1962858/1; 1962859/1; 1962860/1; 1962861/2; 1962862/2.

Type locality. Off Falkland Islands, Discovery station WS 766. 44°58'S, 60°05'30"W, 545 m. Paratype depth range 105–219 m.

Material examined. South Georgia, 53.561108S, 37.88494W, 221 m BIOPEARL cruise 1, 05.04.2006 sample B-06-1167. GenBank numbers: 18S KF741615, 28S KF741644, cyt b KF741675.

Description. Shells small, L 2–3 mm, ovoid, slightly longer than high. Umbones prominent. Posterior dorsal margin straight. Sculpture of low rounded commarginal lamellae with narrow interspaces. Faint radial ribs visible to anterior and posterior. Microsculpture of dense fine punctae (2–3 μm in diameter). Protoconch: P1 = 188 μm, P1 + P2 = 242 μm, P2 with fine growth increments (South Georgia shell). Ligament short, protruding above posterior dorsal margin (Fig. 13J), set in shallow nymph. Escutcheon well defined, smooth. Lunule slightly impressed, broadly

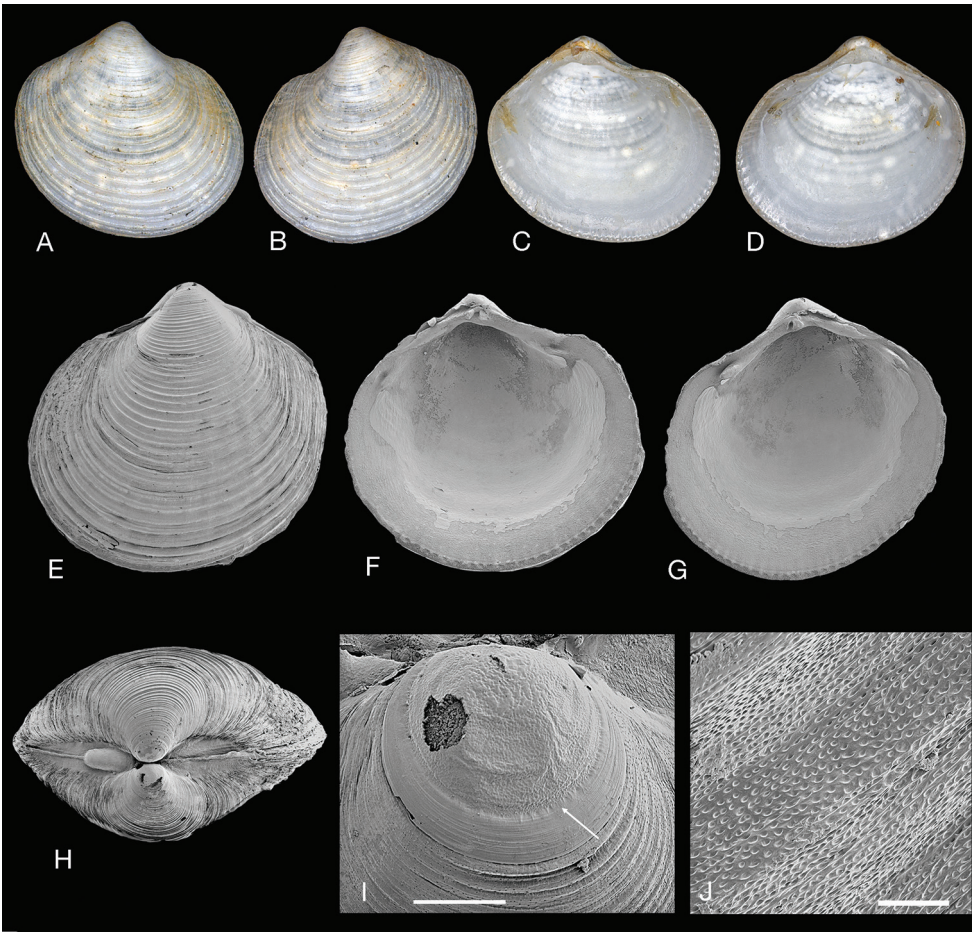

Figure 13. *Notocina falklandica* (Dell, 1964). **A–D** Holotype of *Epicodakia falklandica* (NHMUK 1962857/1) exterior and interior views of both valves, L 2.5 mm **E–J** *N. falklandica* paratype (NHMUK 1962858) Falkland Islands, Discovery stn WS 214, 208 m **E** exterior of left valve, L 1.9 mm **F, G** interior of left and right valves, L 2.3 mm **H** dorsal view, L 1.9 mm **I** protoconch, arrow indicates boundary of P1 and P2 **J** detail of **E** showing punctate microsculpture. Scale bar: 100 μm (**I**); 20 μm (**J**).

lanceolate. Hinge line narrow, left valve with two small cardinal teeth and anterior and posterior lateral teeth. Right valve with single, slightly bifid cardinal tooth and anterior and posterior lateral teeth. Anterior adductor muscle scar short, barely detached from pallial line, posterior adductor scar ovoid. Pallial line entire. Inner shell margin finely denticulate.

Distribution. South Atlantic: around Falkland Islands (Dell 1964), Argentina, outer continental shelf off Buenos Aires (Roux et al. 1993); Patagonia shelf, South Georgia, South Orkney Islands (Zelaya 2005). Depth range 100–545 m (distribution map at https://www.gbif.org/species/6523387).

Discussion

There is a general perception that bivalves having chemosymbiosis with thiotrophic or methanotrophic bacteria are large, as exemplified by Vesicomyidae (*Calyptogena magnifica* Boss & Turner, 1980, 263 mm), Modiolinae (*Bathymodiolus boomerang* Cosel & Olu, 1998, 360 mm), Solemyidae (*Acharax bartschi* (Dall, 1908), 210 mm) that live at hydrothermal vents and hydrocarbon seeps. Among the several bivalve families with chemosymbiotic life habits Lucinidae is by far the most diverse with more than 400 species occupying a wide range of habitats from the intertidal to bathyal depths and spanning a wide size range from 1.5 to 170 mm. The largest living species are *Meganodontia acetabulum* Bouchet & Cosel, 2004 with shell lengths up to 170 mm and *Codakia distinguenda* (Tryon, 1872) at 160 mm, while the Eocene fossil, *Superlucina megameris* (Dall, 1901), attained a shell height of 310 mm (Taylor and Glover 2009). Nevertheless, most species of Lucinidae are much smaller, with recent studies revealing minute species as small as 1.5 mm (Glover and Taylor 2016, Taylor et al. 2016). Additionally, with availability of molecular phylogenies, paraphyly is increasingly being recognised in genera and families previously classified by morphological characters. Such paraphyly has been found in the small lucinids previously assigned to *Pillucina*; one group consists of several species similar to the genotype of *Pillucina* and the other includes species some previously neglected but now assigned to the new genera, *Rugalucina* and *Pusillolucina*, that are also distinctive in morphology.

One of the foci of this paper has been the recognition of some very small lucinid species within the new genus *Pusillolucina* with adult shell lengths of 1–3 mm. All the species in this genus have a very unusual multi-cuspate lateral dentition not seen in any other lucinids. The recognition of these minute lucinids extends the morphological and functional range of Lucinidae. Even the smallest have chemosymbiosis with thickened ctenidial demibranchs occupied by symbiotic bacteria. Other minute lucinids include *Guyanella clenchi* (Altena, 1968) 1–2 mm and *Parvilucina latens* Taylor & Glover, 2016, 2–3 mm, both documented from Guadeloupe but likely occur more widely in the western Atlantic (Taylor et al. 2016). The latter species was first detected in molecular analyses having initially been confounded with *Parvilucina pectinella* (C.B. Adams, 1852). Additionally, most species of *Liralucina*, have shell lengths less than 5 mm (Glover and Taylor 2007), they are little recorded but common in some coral reef associated habitats (Glover and Taylor 2007).

Another small species that has been phylogenetically misplaced is *Notocina falklandica* widely recorded from outer shelf and bathyal depths around the Falkland Islands, Argentina and Uruguay. Since the original description by Dell (1964) its placement in *Epicodakia* (Codakiinae) had been problematic but molecular data now shows that it should be classified in the subfamily Lucininae in a monospecific genus close to *Troendleina* from the Indo-West Pacific with no comparable taxa known from the southern Atlantic.

Two species described here, *Rugalucina angela* and '*R.*' *cracentis*, are abundant in the northern Red Sea where a surprising number of other lucinids have been recorded. From intensive sampling around Safaga Bay (Zuschin and Oliver 2003; 2005) lucinids were amongst the most abundant bivalves with 15 species comprising nearly 40 % of the shells recovered, most frequently *Cardiolucina semperiana* (Issel, 1869), *Wallucina erythraea* (Issel, 1869) and '*Pillucina fischeriana*'. With taxonomic refinements 19 species are now recognised from the Safaga area (Taylor and Glover 2005, herein). The northern Red Sea is a highly oligotrophic environment and, with a nutritional strategy of chemosymbiosis utilising sulphides from the benthic substrate, lucinids can survive in nutrient poor habitats where food availability for suspension feeding bivalves is limited.

Acknowledgements

Special thanks are due to Suzanne Williams (NHMUK) for the molecular analysis of Figure 1 and Vassia Koutsouveli for help with sequencing. Katrin Linse (BAS) kindly provided molecular samples of *Notocina falklandica.* Kevin Webb and Richard Turney (NHMUK) provided much expert help with macro- and microphotography. We are very grateful to Henk Dekker for the generous loan of Red Sea samples of *Rugalucina* species that contributed to the figures and distribution data. Richard Preece and Matthew Lowe (ZMC) provided images of the holotype of *Lucina concinna* and Hubert Blatterer kindly allowed us to use his images of *Pillucina concinna* (= *R. cracentis* sp. nov.).

We are grateful to colleagues at the MNHN Paris (Philippe Bouchet, Virginie Héros, Barbara Buge, Philippe Maestrati), for help and the opportunity to work on samples from INHACA, ATIMO VATAE, MIRIKY, and KAVIENG expeditions. The ATIMO VATAE and MIRIKY expeditions to Madagascar (Principal Investigator, Philippe Bouchet) were part of a cluster of 2009–2010 Mozambique-Madagascar expeditions funded by the Total Foundation, Prince Albert II of Monaco Foundation, and Stavros Niarchos Foundation under "Our Planet Reviewed", a joint initiative of Muséum national d'Histoire naturelle and Pro Natura International in partnership with Institut d'Halieutique et des Sciences Marines, University of Toliara and the Madagascar bureau of Wildlife Conservation Society. The INHACA expedition to Mozambique took place in 2011 at Estaçao de Biologia Marina de Inhaca as part of a collaboration between MNHN and Universidade Eduardo Mondlane in Maputo, through the good office of Jose Rosado.

Finally, we thank two reviewers and the editors of ZooKeys for helpful suggestions.

References

Adams A (1856) Descriptions of twenty-five new species of shells from the collections of Hugh Cuming, Esq. Proceedings of the Zoological Society of London 1855: 221–226.

Adams CB (1852) Catalogue of species of *Lucina*, which inhabit the West Indian Seas. Contributions to Conchology 1: 1–17.

Adams H (1871) Descriptions of twenty-six new species of shells collected by Robert McAndrew, Esq., in the Red Sea. Proceedings of the Zoological Society of London 1870: 788–793.

Altena CO van (1968) The Holocene and Recent marine bivalve Mollusca of Surinam. Studies on the Fauna of Suriname and other Guyanas 42(10): 153–179.

Boss KJ, Turner RD (1980) The giant white clam from the Galapagos Rift, *Calyptogena magnifica* species novum. Malacologia 20: 161–194.

Bouchet P, Cosel R von (2004) The world's largest lucinid is an undescribed species from Taiwan (Mollusca: Bivalvia). Zoological Studies 43: 704–711.

Bretsky SS (1976) Evolution and classification of the Lucinidae (Mollusca; Bivalvia). Palaeontographica Americana 8(50): 219–337.

Chavan A (1969) Superfamily Lucinacea Fleming, 1828. In: Moore RC (Ed.) Treatise on invertebrate paleontology, Part N, Mollusca 6, Bivalvia, vol. 2. Geological Society of America and University of Kansas Press, Boulder, Colorado, N491–N518.

Conrad TA (1837) Descriptions of new marine shells, from Upper California. Collected by Thomas Nutall Esq. Journal Academy of Natural Sciences, Philadelphia 7: 227–268.

Cosel R von, Bouchet P (2008) Tropical deep-water lucinids (Mollusca: Bivalvia) from the Indo-Pacific: essentially unknown, but diverse and occasionally gigantic. In: Héros V, Cowie RH, Bouchet P (Eds) Tropical Deep Sea Benthos 25. Mémoires du Muséum national d'Histoire naturelle 196: 115–213.

Cosel R von, Olu K (1998) Gigantism in Mytilidae. A new *Bathymodiolus* from cold seep areas on the Barbados accretionary Prism. Comptes Rendus de l'Académie des Sciences ser. 3 – Science de la Vie 321: 655–663. https://doi.org/10.1016/S0764-4469(98)80005-X

Dall WH (1901) A gigantic fossil *Lucina*. The Nautilus 15: 40–42.

Dell RK (1964) Antarctic and sub Antarctic Mollusca: Amphineura, Scaphopoda and Bivalvia. Discovery Reports 33: 93–250.

Dekker H, Goud J (1995) Review of the Indo-West Pacific species of *Divaricella* sensu auct. with descriptions of two new species and a summary of the species from other regions. Vita Marina 43: 1–12.

Dekker H, Orlin Z (2000) Check-list of Red Sea Mollusca. Spirula 47 supplement: 2–46.

Fleming J (1828) A history of British animals, exhibiting the descriptive characters and systematical arrangement of the genera and species of quadrupeds, birds, reptiles, fishes, Mollusca and Radiata of the United Kingdom; including the indigenous, extirpated and extinct kinds; together with periodical and occasional visitants. Bell & Bradfute, Edinburgh, 565 pp. https://doi.org/10.5962/bhl.title.12859

Geest M van der, Sall AA, Ely SO, Nauta RW, Gils JA van, Piersma T (2014) Nutritional and reproductive strategies in a chemosymbiotic bivalve living in a tropical intertidal seagrass bed. Marine Ecology Progress Series 501: 113–126. https://doi.org/10.3354/meps10702

Glover EA, Taylor JD (2001) Systematic revision of Australian and Indo-Pacific Lucinidae (Mollusca: Bivalvia): *Pillucina*, *Wallucina* and descriptions of two new genera and four new species. Records of the Australian Museum 53: 263–292. https://doi.org/10.3853/j.0067-1975.53.2001.1349

Glover EA, Taylor JD (2007) Diversity of chemosymbiotic bivalves on coral reefs: Lucinidae of New Caledonia and Lifou (Mollusca, Bivalvia). Zoosystema 29: 109–181.

Glover EA, Taylor JD (2016) Lucinidae of the Philippines: highest known diversity and ubiquity of chemosymbiotic bivalves from intertidal to bathyal depths (Mollusca: Bivalvia). In: Héros V, Strong E, Bouchet P (Eds) Tropical Deep-Sea Benthos, volume 29. Mémoires du Muséum national d'Histoire naturelle 20: 865– 234.

Glover EA, Williams ST, Taylor JD (2016) Lucinid bivalves of Singapore and their relationships (Bivalvia: Lucinidae). Raffles Bulletin of Zoology, supplement 34: 539–565.

Hedley C (1913) Studies on Australian Mollusca. Part XI. Proceedings of the Linnean Society of New South Wales 38: 258–339. https://doi.org/10.5962/bhl.part.13561

Heide T van der, Govers LL, Fouw J de, Olff H, Geest M van der, Katwijk MM van, Piersma T, Koppel J van de, Silliman BR, Smolders AJP, Gils JA van (2012) A three-stage symbiosis forms the foundation of seagrass ecosystems. Science 336: 1432−1434. https://doi.org/10.1126/science.1219973

Huber M (2015) Compendium of bivalves 2. ConchBooks, Harxheim, Germany, 907 pp.

Iredale T (1930) More notes on the marine Mollusca of New South Wales. Records of the Australian Museum 17: 384–407. https://doi.org/10.3853/j.0067-1975.17.1930.773

Issel A (1869) Malacologia del Mare Rosso, richerche zoologiche e paleontologiche. Pisa, Italy. https://doi.org/10.5962/bhl.title.11638

Johnson MA, Fernandez C, Pergent G (2002) The ecological importance of an invertebrate chemoautotrophic symbiosis to phanerogam seagrass beds. Bulletin of Marine Science 71: 1343–1351.

Lamprell K, Whitehead T (1992) Bivalves of Australia, Crawford House Press, Bathurst, Australia, 182 pp.

Lamy E (1916) Les Lucines et les Diplodontes de la Mer Rouge (d'après les matériaux recueillis par M. de Dr Jousseaume). Bulletin du Muséum national d'Histoire naturelle, Paris 22: 145–155, 183–190.

Lutaenko K (2000) Russian contributions to studies of Vietnamese bivalves Part 2. List of species recorded by Russian authors or stored in Museums. Phuket Marine Biological Center Special Publication 21: 361–390.

Melvill JC (1899) Notes on Mollusca from the Arabian Sea, Persian Gulf, and Gulf of Oman, mostly dredged by Mr. F.W. Townsend, with descriptions of twenty-seven species. Annals and Magazine of Natural History series 7(4): 81–101. https://doi.org/10.1080/00222939908678167

Melvill JC (1918) Descriptions of thirty-four species of marine Mollusca from the Persian Gulf, Gulf of Oman and Arabian Sea, collected by Mr. F.W. Townsend. Annals and Magazine of Natural History series 9(1): 137–158. https://doi.org/10.1080/00222931808562296

Meyer E, Nilkerd B, Glover EA, Taylor JD (2008) Ecological importance of chemoautotrophic lucinid bivalves in a peri-mangrove community in Eastern Thailand. Raffles Museum Bulletin of Zoology, supplement 18: 41–55.

MolluscaBase (2019) MolluscaBase. Lucinidae J. Fleming, 1828. World Register of Marine Species. http://www.marinespecies.org/aphia.php?p=taxdetails&id=218 on 2019-10-01

Nakaoka M, Mukai H, Chunhabundit S (2002) Impacts of dugong foraging on benthic animal communities in a Thailand seagrass bed. Ecological Research 17: 625–638. https://doi.org/10.1046/j.1440-1703.2002.00520.x

Oliver PG (1992) Bivalved seashells of the Red Sea. Verlag Christa Hemmen & National Museum of Wales, Wiesbaden & Cardiff, 330 pp.

Oliver PG (1995) Bivalvia. In: Dance SP (Ed.) Seashells of Eastern Arabia Motivate Publishing, Dubai, 194–281.

Pilsbry HA (1921) Marine mollusks of Hawaii-XIV, XV. Proceedings of the Academy of Natural Sciences of Philadelphia 72: 360–382.

Powell AWB (1937) New species of marine Mollusca from New Zealand. Discovery Reports 26: 1153–222.

Price ARG (1982) Western Arabian Gulf echinoderms in high salinity waters and the occurrence of dwarfism. Journal of Natural History 16: 519–527. https://doi.org/10.1080/00222938200770421

Rattanachot E, Prathep A (2015) Species-specific effects of seagrass on below ground biomass, redox potential and *Pillucina vietnamica* (Lucinidae). Journal of the Marine Biological Association of the United Kingdom 95: 1693–1704. https://doi.org/10.1017/S0025315415000934

Rossi F, Colao E, Martinez MJ, Klein JC, Carcaillet F, Callier MD, de Wit, R, Caro A (2013) Spatial distribution and nutritional requirements of the endosymbiont-bearing bivalve *Loripes lacteus* (sensu Poli, 1791) in a Mediterranean *Nanozostera noltii* (Hornemann) meadow. Journal of Experimental Marine Biology and Ecology 440: 108–115. https://doi.org/10.1016/j.jembe.2012.12.010

Roux A, Bastida R, Bremec C (1993) Comunidades bentónicas de la plataforma continental Argentina, campaiías transección BIP "0ca Balda" 1987/88/89. Boletim do Instituto Oceanográfico, Sao Paulo 41: 81–94. https://doi.org/10.1590/S0373-55241993000100007

Smith EA (1885) Report on the Lamellibranchiata collected by H.M.S. Challenger during the years 1873–76. Report of the Scientific Results of the Voyage of H.M.S. Challenger 1873–76 13: 1–341.

Steger J, Stockinger M, Ivkić A, Galil BS, Albano PG (2018) New records of non-indigenous molluscs from the eastern Mediterranean Sea. Bioinvasions Records 7: 245–257. https://doi.org/10.3391/bir.2018.7.3.05

Taylor JD, Glover EA (2009) The giant lucinid bivalve from the Eocene of Jamaica – systematics, life habits and chemosymbiosis (Mollusca: Bivalvia: Lucinidae). Palaeontology 52: 95–109. https://doi.org/10.1111/j.1475-4983.2008.00839.x

Taylor JD, Glover EA (2013) New lucinid bivalves from shallow and deeper water of the Indo-West Pacific Oceans (Mollusca: Bivalvia: Lucinidae). ZooKeys 326: 69–90. https://doi.org/10.3897/zookeys.326.5786

Taylor JD, Glover EA, Smith L, Dyal P, Williams ST (2011) Molecular phylogeny and classification of the chemosymbiotic bivalve family Lucinidae (Mollusca: Bivalvia). Zoological Journal of the Linnean Society 163: 15–49. https://doi.org/10.1111/j.1096-3642.2011.00700.x

Taylor JD, Glover EA, Williams ST (2014) Diversification of chemosymbiotic bivalves: origins and relationships of deeper water Lucinidae. Biological Journal of the Linnean Society 111: 401–420. https://doi.org/10.1111/bij.12208

Taylor JD, Glover EA, Smith L, Ikebe C, Williams ST (2016) New molecular phylogeny of Lucinidae: increased taxon base with focus on tropical western Atlantic species (Mollusca: Bivalvia). Zootaxa 4196: 381. https://doi.org/10.11646/zootaxa.4196.3.2

Tryon GW (1872) Catalogue and synonymy of the Recent species of the family Lucinidae. Proceedings of the Academy of Natural Sciences of Philadelphia 24: 82–96.

Uede T, Takahashi Y (2008) Benthos communities of the *Zostera japonica* meadows in the intertidal zone of Takinai and Uchinoura, Tanabe Bay, Wakayama Prefecture, Japan. Japanese Journal of Benthology 63: 42–55. https://doi.org/10.5179/benthos.63.42

Zelaya DG (2005) The bivalves from the Scotia Arc islands: species richness and faunistic affinities. Scientia Marina 69 (supplement 2): 113–122. https://doi.org/10.3989/scimar.2005.69s2113

Zorina IP (1978) New species of bivalve molluscs (Bivalvia) of the Gulf of Tonkin (South China Sea). Trudy Zoological Institut, Leningrad 61: 193–203. [in Russian]

Zuschin M, Oliver PG (2003) Bivalves and bivalve habitats in the northern Red Sea. The northern Bay of Safaga (Red Sea, Egypt): an actuopalaeontological approach. VI. Bivalvia. Naturhistorisches Museum, Vienna, 304 pp.

Zuschin M, Oliver PG (2005) Diversity patterns of bivalves in a coral dominated shallow-water bay in the northern Red Sea high species richness on a local scale. Marine Biology Research 1: 396–410. https://doi.org/10.1080/17451000500456262

Zvonareva SS, Mekhova ES, Hà Võ T, Kantor YI (2019) Checklist of bivalve molluscs in mangroves of Khánh Hòa Province, Vietnam. Molluscan Research 39: 296–312. https://doi.org/10.1080/13235818.2019.1638567

ZooKeys 899: 141–149 (2019)
doi: 10.3897/zookeys.899.39442
http://zookeys.pensoft.net

RESEARCH ARTICLE

A peer-reviewed open-access journal
ZooKeys
Launched to accelerate biodiversity research

Description of *Seba longimera* sp. nov. from hydrothermal vents in the Okinawa Trough, Northwest Pacific (Amphipoda, Amphilochoidea, Sebidae)

Yanrong Wang[1,2,5], Chaodong Zhu[1,5], Zhongli Sha[2,3,4,5], Xianqiu Ren[2]

1 *Key Laboratory of Zoological Systematics and Evolution, Institute of Zoology, Chinese Academy of Sciences, Beijing 100101, China* **2** *Institute of Oceanology, Chinese Academy of Sciences, Qingdao 266071, China* **3** *Laboratory for Marine Biology and Biotechnology, Qingdao National Laboratory for Marine Science and Technology, Qingdao, China* **4** *Center for Ocean Mega-Science, Chinese Academy of Sciences, Qingdao 266071, China* **5** *College of Biological Sciences, University of Chinese Academy of Sciences, Beijing 100049, China*

Corresponding author: *Zhongli Sha* (shazl@qdio.ac.cn)

Academic editor: *C. O. Coleman* | Received 26 August 2019 | Accepted 31 October 2019 | Published 12 December 2019

http://zoobank.org/375EE7B2-38CF-4D9F-81D0-20A40DDD2711

Citation: Wang Y, Zhu C, Sha Z, Ren X (2019) Description of *Seba longimera* sp. nov. from hydrothermal vents in the Okinawa Trough, Northwest Pacific (Amphipoda, Amphilochoidea, Sebidae). ZooKeys 899: 141–149. https://doi.org/10.3897/zookeys.899.39442

Abstract

Seba longimera **sp. nov.**, of the family Sebidae Walker, 1908, is described from hydrothermal vents in Okinawa Trough. Other two congenic species, *S. bathybia* Larsen, 2007 and *S. profundus* Shaw, 1989, are also reported from these hydrothermal vents, but the new species can be readily distinguished from them in having the merus of pereopods 5 and 6 extending beyond distal margin of carpus, coxa 4 smaller than coxae 2 and 3, and coxa 5 with the posterior lobe larger than the anterior one, rather than equilobate.

Keywords

Taxonomy, Sebidae, new species, hydrothermal vents, Okinawa Trough

Introduction

The genus *Seba* Spence Bate, 1862 currently contains 24 species (updated by Köppen and Coleman 2011), and occurs in the Mediterranean Sea, Eastern and Southern Atlantic Ocean, southern United States, Hawaiian Islands, Indian Ocean, Antarctica,

Japan, Eastern Pacific, and Australia from shallow to deep waters (Larsen 2007; Ariyama 2009; Yerman and Coleman 2009). When the Chinese research vessel "KEXUE" surveyed the biodiversity of hydrothermal vents in Okinawa Trough in the western Pacific in 2014, some individuals referred to *Seba* were collected. After careful examination, those specimens exhibited some distinctive characters differentiating them from the other described *Seba* species. The new species is most similar to *S. bathybia* Larsen, 2007 and *S. profundus* Shaw, 1989, which are also reported from hydrothermal vents. However, *Seba longimera* sp. nov. differs from above two species in having pereopods 5 and 6 with the merus extending beyond the distal margin of carpus, coxa 4 smaller than coxae 2 and 3, and coxa 5 having the posterior lobe larger than the anterior one, rather than equilobate. The present work describes this new species and compares it with closely related species.

Material and methods

The present material was collected by ROV "FAXIAN" during expeditions to the Okinawa Trough hydrothermal vents by the Institute of Oceanology, Chinese Academy of Sciences (**IOCAS**) in April 2014. All the specimens examined are deposited in the Marine Biological Museum, Chinese Academy of Sciences (**MBMCAS**), Qingdao, China. Specimens were examined and dissected under a dissecting microscope (ZEISS Discovery V20). Line drawings were prepared with a graphics tablet using Adobe Photoshop CS6 software. Length measurements are made along the outline of the animals, beginning from the anterior margin of head to the end of the telson.

The following abbreviations are used in Figures 1–4: A, antenna; E, epimeron; G, gnathopod; L, Left; LL, lower lip; Md, mandible; Mx1, maxilla 1; Mx2; maxilla 2; Mxp, maxilliped; P, pereopod; R, right; T, telson; U, uropod; UL, upper lip.

Systematics

Order Amphipoda Latreille, 1816
Suborder Amphilochidea Boeck, 1871
Superfamily Amphilochoidea Boeck, 1871
Family Sebidae Walker, 1907
Subfamily Sebinae Holsinger & Longley, 1980

Genus *Seba* Spence Bate, 1862

Diagnosis. See Ariyama (2009).

***Seba longimera* sp. nov.**
http://zoobank.org/BE6D0C6C-3BBE-46FB-9D21-21ECD4E39801
Figures 1–4

Material examined. ***Holotype***: male (6.1 mm) (MBM 286557), dissected, Okinawa Trough, 27°32'N, 126°58'E, RY0067, ROV-3, depth 1243 m, 16 Apr. 2014. ***Paratype***: female (4.4 mm), dissected, same data as holotype.

Additional materials. 1 female (4.5 mm), 3 males (4.2–5.5 mm) (MBM 286557), Okinawa Trough, 27°32'N, 126°58'E, RY0067, ROV-3, depth 1243 m, 16 Apr. 2014. 1 female (3.3 mm) 1 male (4.1 mm) (MBM 286560), Okinawa Trough, 27°33'N, 126°58'E, RY0051, ROV-3, depth 1243 m, 16 Apr. 2014. 15 females and males (<5.5 mm) (MBM 286565), Okinawa Trough, 27°33'N, 126°58'E, RY0069, ROV-3, depth 1243 m, 16 Apr. 2014.

Description of male holotype. ***Head.*** Eyes not visible in ethanol material. *Antenna 1* subequal in length to antenna 2; peduncular article 1 shorter than article 2 (0.8×); article 2 elongate, length 4.1× width; article 3 less than half the length of article 1; primary flagellum 5-articulate, not setose; accessory flagellum hardly reaching to end of 1st flagellar article, 2-articulate, distal article tiny. *Antenna 2* with peduncular article 4 1.7× longer than article 5; peduncular article 5 much narrower than article 4; flagellum 3-articulate, not setose.

Mouthparts. Epistome separate, upper lip rounded. *Right mandible* incisor well developed, with blunt denticles; palp 3-articulate, article 2 1.2× longer than article 3, bearing one long seta, article 3 bearing apical long seta; left mandible with dentate lacinia mobilis. *Lower lip* with inner lobes absent; mandibular lobes weak. *Maxilla 1* with inner plate rounded, bearing single robust apical seta; outer plate broadly truncate, bearing five robust apical setae; palp 1-articulate, with two apical setae. *Maxilla 2* with inner plate wider and shorter than outer plate, with 3 apical setae; outer plate with four apical setae. *Maxilliped* with very short inner plates, reduced to small lobes; outer plates short, slightly beyond distal margin of 1st palp article, rounded, bearing few marginal and apical setae; palp 4-articulate, inner margins of article 2 and 3 bearing setae, dactylus elongate, slender.

Pereon. *Coxae 1–4* longer than broad, overlapping. *Gnathopod 1* parachelate, stouter than gnathopod 2; coxa with a small seta at posteroventral corner; basis linear, with 1 long seta on posterior margin; ischium subquadrate; merus subequal in length to ischium, posterior margin bearing three long setae; carpus shorter than palm, distally expanded, posterior margin lobate, bearing patch of long setae distally; palm slightly longer than deep, ventral margin fringed with long setae, with five bumps and few setae; dactylus curved, tapering. *Gnathopod 2* elongate, chelate; coxa oval; basis linear, naked; ischium longer than menus, naked; merus subequal in length to carpus; carpus distally expanded; propodus slender, narrowing distally, more than 4× longer than carpus. Lower finger of chela straight, bearing row of short setae on palmar edge;

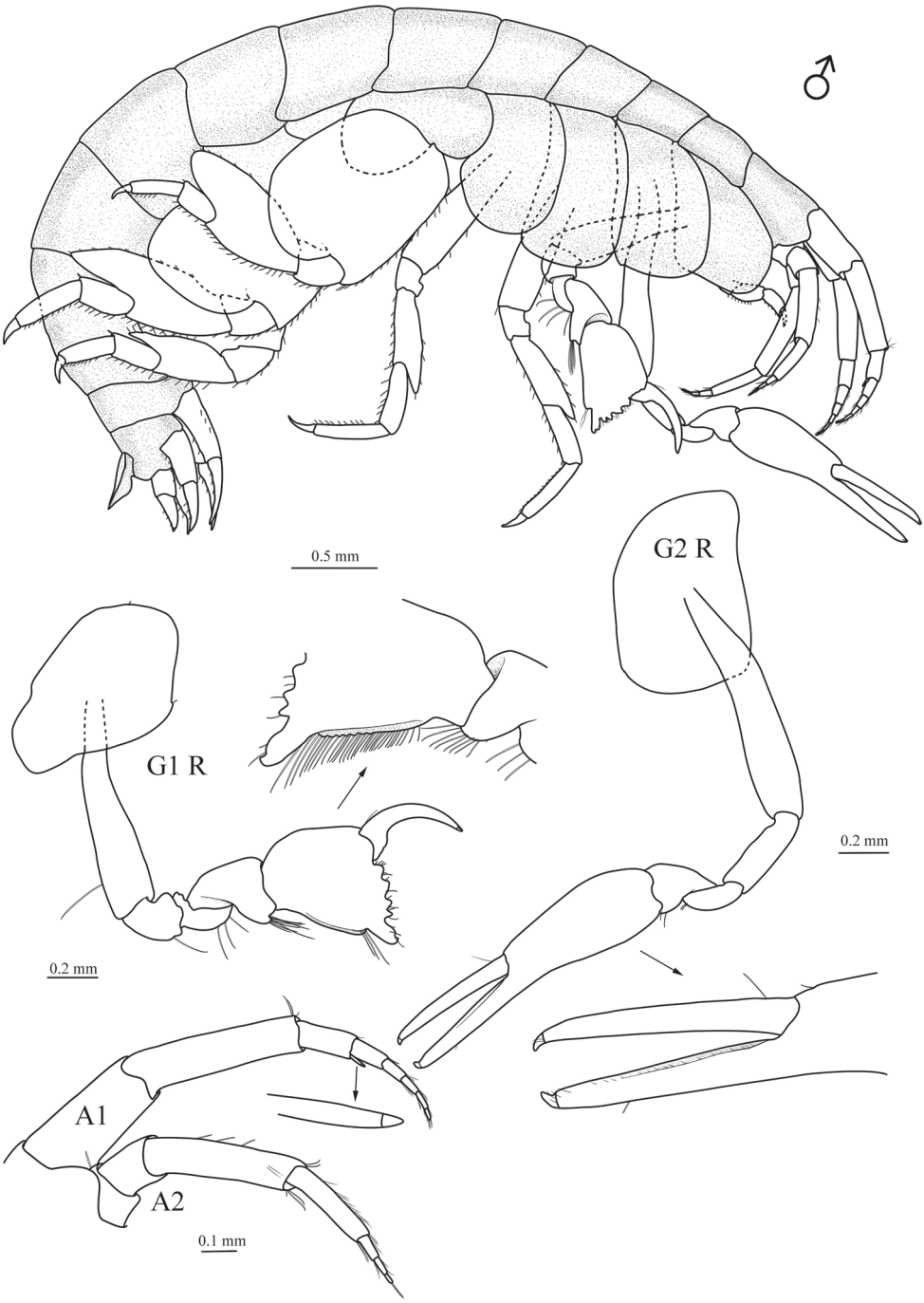

Figure 1. *Seba longimera* sp. nov., male holotype (6.1 mm) (MBM 286557), Okinawa Trough. G1 R, right gnathopod 1; G2 R, right gnathopod 2; A1, antenna 1 (with accessory flagellum enlarged); A2, antenna 2.

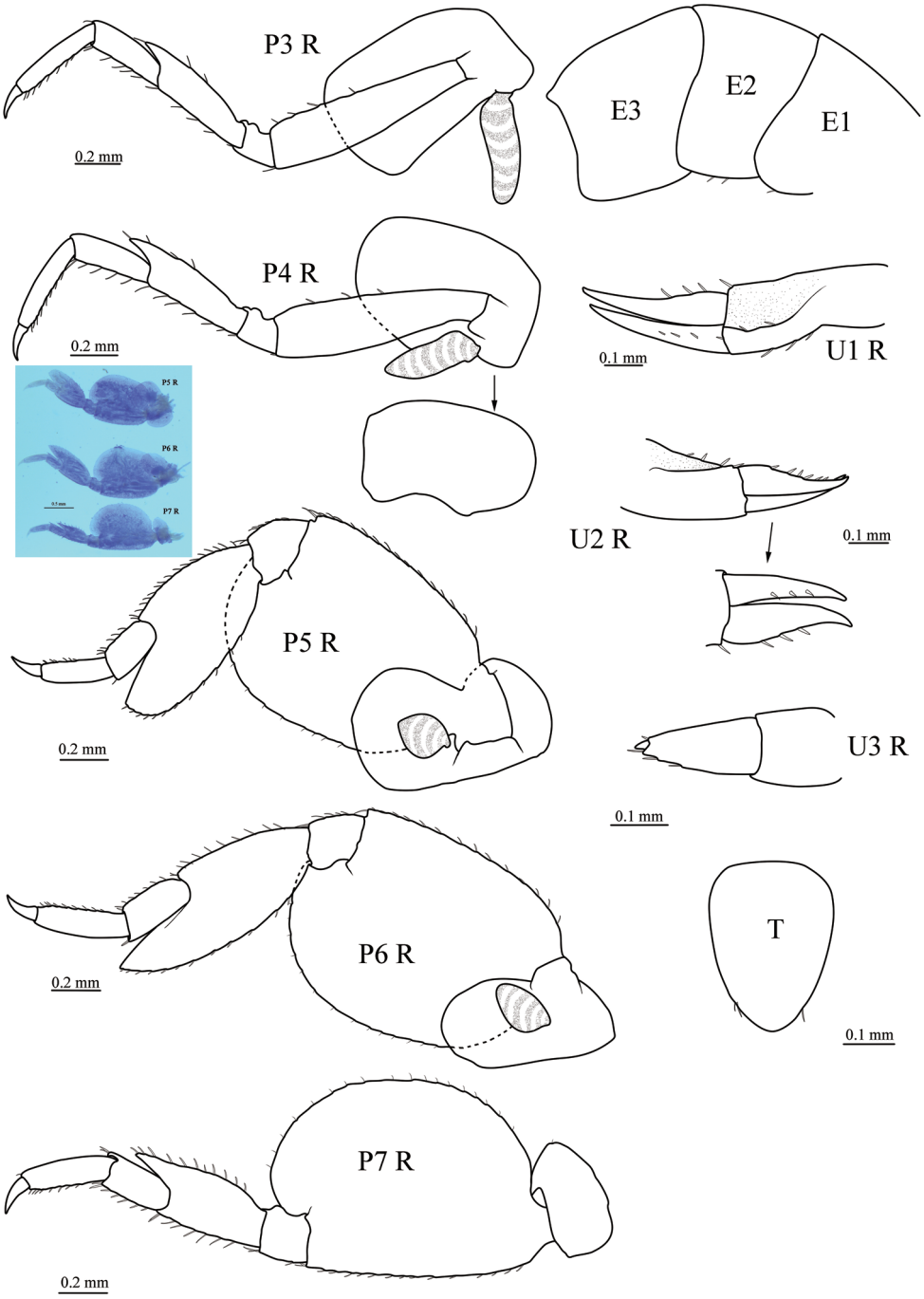

Figure 2. *Seba longimera* sp. nov., male holotype (6.1 mm) (MBM 286557), Okinawa Trough. P3 R, right pereopod 3; P4 R, right pereopod 4; P5 R, right pereopod 5; P6 R, right pereopod 6; P7 R, right pereopod 7; U1 R, right uropod 1; U2 R, right uropod 2; U3 R, right uropod 3; T, telson; E1–3, epimeron 1–3.

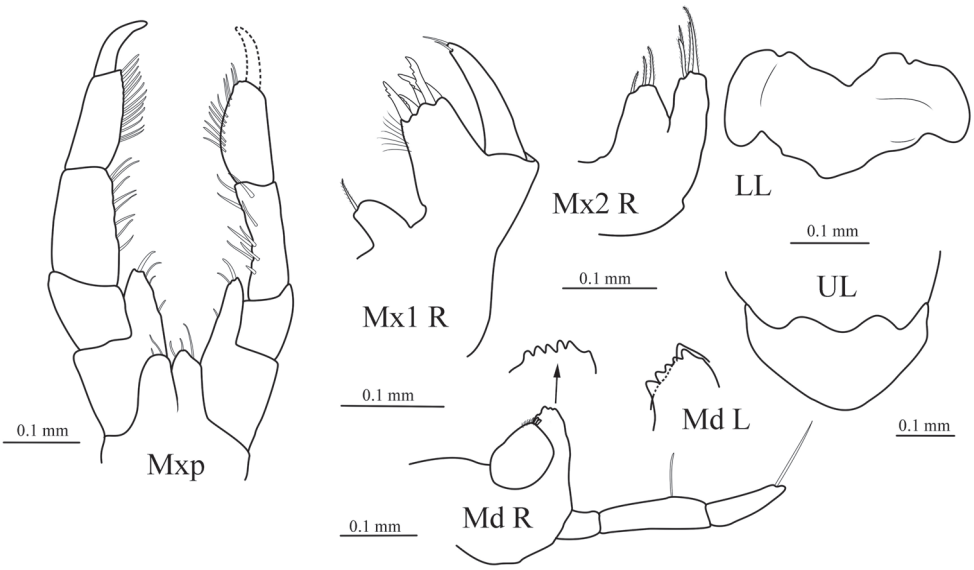

Figure 3. *Seba longimera* sp. nov., male holotype (6.1 mm) (MBM 286557), Okinawa Trough. UL, upper lip; LL, lower lip; Md R, right mandible (with incisor process enlarged); Md L, incisor process and lacinia mobilis of left mandible enlarged; Mx1 R, right maxilla 1; Mx2 R, right maxilla 2; Mxp, pair of maxillipeds.

dactylus slender, straight, fitting palm, distally with few short setae. *Pereopod 3* with coxa slightly longer than coxa 2; basis not expanded posteriorly, anterior margin bearing four shorter setae in distal half length; ischium subrectangular, anterior margin notched; merus anterodistally drawn out, pointed, both anterior and posterior margins bearing few robust setae; carpus shorter than merus; propodus slightly longer than carpus; dactylus curved, tapering. *Pereopod 4* slightly larger than pereopod 3, but of similar appearance; coxa smaller than coxa 3, posterior margin excavated. *Pereopod 5* coxa bilobed, posterior lobe longer and larger than anterior lobe; basis evenly expanded, posteroproximal margin overlaps posterior coxal lobe; merus expanded, produced posteroventrally, well overreaching distal margin of carpus; carpus shorter than propodus; dactylus curved. *Pereopod 6* larger than pereopods 5 and 7, of similar appearance with pereopod 5, coxa unilobate. *Pereopod 7* smaller than pereiopod 5, coxa unilobate, much smaller than coxa 6; merus expanded, but smaller than that of pereopods 5 and 6, not extending past distal margin of carpus; carpus shorter than propodus.

Gills present on coxae 3–6, small, not pleated.

Pleon. *Epimeron 1–3* smooth, posteroventral margin rounded. *Uropod 1* peduncle subequal in length to rami, with two distal, two lateral, and three medial robust setae; outer ramus slightly shorter than inner ramus, both outer and inner ramus with three robust setae. *Uropod 2* extending as far as uropod 1, peduncle slightly longer than rami, with one distal and five marginal setae; outer ramus slightly shorter than inner ramus; outer and inner ramus each with three marginal robust setae. *Uropod 3* uniramous,

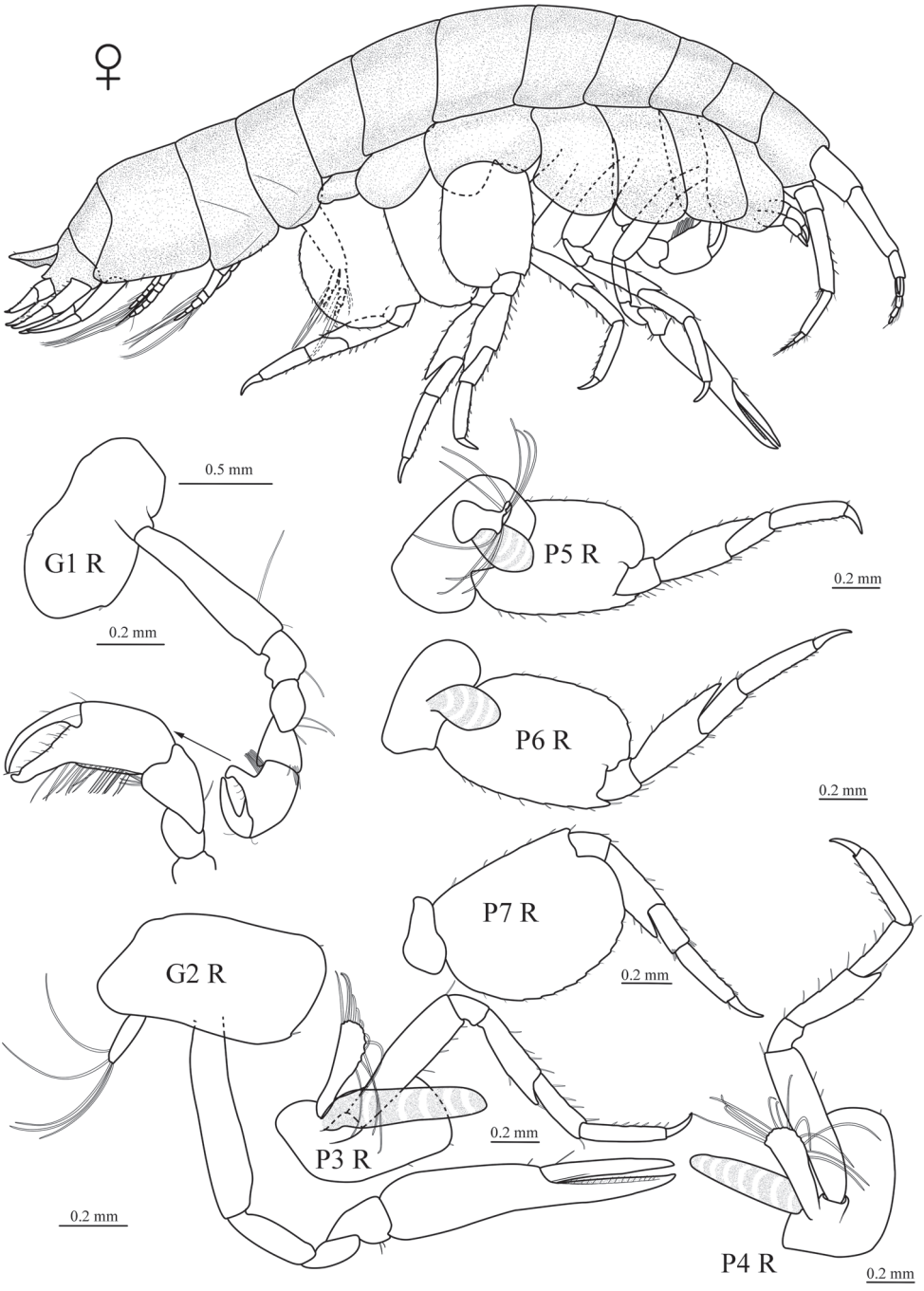

Figure 4. *Seba longimera* sp. nov., female paratype (4.5 mm) (MBM 286557), Okinawa Trough. G1 R, right gnathopod 1; G2 R, right gnathopod 2; P3 R, right pereopod 3; P4 R, right pereopod 4; P5 R, right pereopod 5; P6 R, right pereopod 6; P7 R, right pereopod 7.

peduncle naked; ramus longer than peduncle, with two marginal setae and two setae at base of minute terminal article. *Telson* entire, laminar, tapering distally, smoothly rounded, distinctly overreaching end of uropod 3 peduncle, with one or two distolateral setae on each margin.

Sexually dimorphic characters. Based on female paratype, 4.5 mm.

Gnathopod 1 parachelate, but tending to chelate; propodus much narrower than that of male; palm nearly straight, only bearing few setae. Pereopods 5 and 6 with basis not as expanded as in male, narrower than that of pereopod 7; merus not as expanded as in male, and not extending to distal margin of carpus.

Variation. In one small male specimen (4.2 mm), the merus of pereopods 5 and 6 does not overreaching distal margin of carpus.

Etymology. From the Latin *longus* (= long), referring to the merus of pereopods 5 and 6 overreaching the distal margin of carpus.

Distribution. Northwest Pacific, Okinawa Trough, the hydrothermal vents at a depth of 1243 m.

Remarks. The new species, reaching a length of 6 mm, is larger than all described *Seba* species that are usually less than 4 mm (Shaw 1989). *Seba longimera* sp. nov. is most similar to *S. bathybia* and *S. profundus*, which also are associated with hydrothermal vents, but it differs from these two species in the following characters. It differs from *S. bathybia* by having: the denticulate palm of gnathopod 1; coxa 2 lacking a notch, and coxa 4 smaller than coxae 2 and 3; the posterior lobe of the bilobed coxa 5 larger than the anterior lobe, and the expanded merus of pereopods 5 and 6 distinctly overreaching the distal margin of the carpus in male. Similarly, the new species differs from *S. profundus* by having coxa 4 smaller and the posterior lobe of coxa 5 larger than the anterior one; pereopod 6 larger than pereopods 5 and 7, rather than smaller than them as shown in Shaw (1989: fig. 3A); and the merus of pereopods 5 and 6 expanded beyond the distal margin of the carpus in male.

Acknowledgements

This work was funded by the Strategic Priority Research Program of the Chinese Academy of Sciences (XDA22050302), the Key Research Program of Frontier Sciences, Chinese Academy of Sciences (QYZDB-SSWDQC036), the National Key R&D Program of China (2018YFC0310702; 2018YFC0310802), the National Natural Science Foundation of China (31625024), and the Senior User Project of RV KEXUE (KEXUE2018G21).

References

Ariyama H (2009) Four species of the genus *Seba* from Japan, with descriptions of two new species (Crustacea: Amphipoda: Sebidae). Zootaxa 2159: 44–68. https://doi.org/10.11646/zootaxa.2159.1.2

Bate CS (1862) Catalogue of the specimens of amphipodous Crustacea in the collection of the British Museum. British Museum of Natural History, London, 399 pp. [58 pls.] https://doi.org/10.5962/bhl.title.20901

Boeck A (1871) Crustacea Amphipoda Borealia et Arctica. Forhandlinger fra Videnskabernes Selskab, Christiania 1871: 83–280. https://doi.org/10.5962/bhl.title.2056

Holsinger JR, Longley G (1980) The subterranean amphipod crustacean fauna of an artesian well in Texas. Smithsonian Contributions to Zoology 308: 1–62. https://doi.org/10.5479/si.00810282.308

Köppen K, Coleman CO (2011) *Seba henriki*, a new amphipod (Crustacea, Sebidae) from Norfolk Island, Australia. Zoosystematics and Evolution 87 (2): 319–326. https://doi.org/10.1002/zoos.201100009

Larsen K (2007) Amphipoda (Crustacea; Peracarida) from the hydrothermal vent system of the Juan de Fuca Ridge, Escabana Trough and Gorda Ridge, Northeast Pacific. Part I. Lysianassidae and Sebidae. Zootaxa 1445: 1–26. https://doi.org/10.11646/zootaxa.1445.1.1

Latreille PA (1816) Amphipoda. Nouveau Dictionaire d'Histoire naturelle, appliquée aux Arts, à l'Agriculture, à l'Économie rurale et domestique, à la Médecine, etc. Par une société de Naturalistes et d'Agriculteurs (2nd ed.) Tome 1. Deterville, Paris, 467–469. https://doi.org/10.5962/bhl.title.20211

Shaw P (1989) New amphipods from geothermal vent sites off the west of Vancouver Island British Columbia, with a reappraisal of the amphipod family Sebidae. Canadian Journal of Zoology 67: 1882–1890. https://doi.org/10.1139/z89-269

Walker AO (1907) Amphipoda from the Auckland Islands. Annals and Magazine of Natural History (Series 8) 2: 33–39. https://doi.org/10.1080/00222930808692451

Yerman MN, Coleman CO (2009) Sebidae. Zootaxa 2260: 861–871. https://doi.org/10.11646/zootaxa.2260.1.48